



REFERENCE ONLY

UNIVERSITY OF LONDON THESIS

Degree **PhD**

Year **2006**

Name of Author **EVANS, B.R.**

COPYRIGHT

This is a thesis accepted for a Higher Degree of the University of London. It is an unpublished typescript and the copyright is held by the author. All persons consulting the thesis must read and abide by the Copyright Declaration below.

COPYRIGHT DECLARATION

I recognise that the copyright of the above-described thesis rests with the author and that no quotation from it or information derived from it may be published without the prior written consent of the author.

LOANS

Theses may not be lent to individuals, but the Senate House Library may lend a copy to approved libraries within the United Kingdom, for consultation solely on the premises of those libraries. Application should be made to: Inter-Library Loans, Senate House Library, Senate House, Malet Street, London WC1E 7HU.

REPRODUCTION

University of London theses may not be reproduced without explicit written permission from the Senate House Library. Enquiries should be addressed to the Theses Section of the Library. Regulations concerning reproduction vary according to the date of acceptance of the thesis and are listed below as guidelines.

- A. Before 1962. Permission granted only upon the prior written consent of the author. (The Senate House Library will provide addresses where possible).
- B. 1962 - 1974. In many cases the author has agreed to permit copying upon completion of a Copyright Declaration.
- C. 1975 - 1988. Most theses may be copied upon completion of a Copyright Declaration.
- D. 1989 onwards. Most theses may be copied.

This thesis comes within category D.



This copy has been deposited in the Library of UCL



This copy has been deposited in the Senate House Library, Senate House, Malet Street, London WC1E 7HU.

USH1C: Expression and interactions in the retina

Bronwen Rebecca Evans

The Institute of Child Health and Great Ormond Street Hospital for Sick
Children
University College London.

A thesis submitted to the University of London for the degree of
Doctor of Philosophy
2006

UMI Number: U592795

All rights reserved

INFORMATION TO ALL USERS

The quality of this reproduction is dependent upon the quality of the copy submitted.

In the unlikely event that the author did not send a complete manuscript and there are missing pages, these will be noted. Also, if material had to be removed, a note will indicate the deletion.



UMI U592795

Published by ProQuest LLC 2013. Copyright in the Dissertation held by the Author.
Microform Edition © ProQuest LLC.

All rights reserved. This work is protected against unauthorized copying under Title 17, United States Code.



ProQuest LLC
789 East Eisenhower Parkway
P.O. Box 1346
Ann Arbor, MI 48106-1346

ABSTRACT

Usher syndrome is an autosomal recessive disease, displaying pathology of the auditory and visual systems. The three clinical phenotypes are linked to eleven different loci, and differ in the severity and age of onset of sensorineural hearing loss, vestibular areflexia and Retinitis Pigmentosa. The expression pattern of *Ush1c* which encodes a PDZ domain containing protein (Harmonin) has been established in the murine ear. This study examined the localisation of the protein in the murine eye, detecting *Ush1c* mRNA from E12.5 and localising the protein to the newborn photoreceptors from P2.

In the developed retina, harmonin was localised to the photoreceptor outer segments. Further immunoreactivity was noted in unfixed tissue, showing harmonin colocalising with the USH1B and 1D proteins to the photoreceptor inner segments and outer plexiform layer. The USH1B and USH1D proteins are known to interact with and be involved in the correct localisation of harmonin in the ear. Yet in the eye, harmonin localisation in fixed tissue was maintained in the outer segments in the absence of either USH1 protein.

To further examine the protein interactions of harmonin, a Yeast Two-Hybrid study was undertaken using a bovine retinal library. Six possible interacting proteins were identified and confirmed by yeast mating. Several of these positive interactors, although interacting with the whole harmonin protein, did not interact with any of its PDZ binding domains. One such protein was phosducin, a small acidic cytosolic protein. Its potential as a binding partner

for harmonin in the retina was confirmed by a pull down assay and immunolocalisation studies. Phosducin is known to interact with proteins associated with glutamate receptors at the photoreceptor ribbon synapses. Its interaction with harmonin would suggest a role for harmonin in the outer plexiform layer and more specifically at the ribbon synapses of the retina.

ACKNOWLEDGEMENTS

Firstly I would like to thank my two supervisors Dr Maria Bitner-Glindzicz and Dr Jane Sowden for their support, guidance and patience throughout this research. I would also like to thank the Child Health Research Appeal Trust, the MRC, Defeating Deafness and Fight for Sight, UK for funding this work.

I would particularly like to thank the following people for their kind donations of time, expertise and materials, without which this research would not have been possible. Thank you to Drs I Kobayashi (Department of Pediatrics, Hokkaido University Graduate School of Medicine and University Hospital, Japan) and M Scanlan (Ludwig Institute for Cancer Research, NY USA), for their invaluable gifts of the anti-USH1C polyclonal and monoclonal antibodies respectively. Thanks also to Dr U. Müller (Scripps Research Institute, CA USA) for his donation of the anti-cadherin 23 antibody and to Dr Arshavsky (Department of Ophthalmology, Harvard Medical School and the Massachusetts Eye and Ear Infirmary, MA USA.), for the donation of the anti-phosducin antibody.

With regards to the Yeast Two-hybrid study, special thanks go to Dr CH. Sung (Department of Ophthalmology, Weill Medical College of Cornell University, NY USA), for the donation of the bovine retinal library and pACT2 vector; to Drs L. Lin and J. Achermann (Institute of Child Health and Great Ormond Street Hospital for Sick Children, London UK) for the donation of the

MATCHMAKER GAL4 Two-Hybrid System III vectors and yeast strains and to thank Miss K Pearce for her in-house sequencing service.

Furthermore I would like to thank Prof Karen Steel and Dr Ralph Holme, (MRC Institute of Hearing Research, Nottingham, UK), for their generous gift of the *waltzer* and *shaker-1* mice, and also Dr Gail M Seigel (Department of Ophthalmology, University at Buffalo, NY USA) for the gift of the R28 cell line. Thank you to Dr S. Cassalotti (Institute of Laryngology and Otology, London, UK) for the mouse inner ear RNA samples and to Mr. Graham Nevill, (Institute of Laryngology and Otology, London, UK) for technical assistance with the semithin sectioning and tissue preparation. Also thank yous must go to Dr J. Clohessy, Miss N. Dhomen, Dr Pearson and Mr. P. Rutland for their technical advice on different aspects of this work, and to the members of the Clinical and Molecular Genetics department for the friendship and scientific insights throughout the period of this research. I would especially like to thank Dr Elene Haralambous from the department, for her friendship and excellent advice on writing a thesis.

Lastly I must thank my family: my parents and my sister for their continuing love and support in any endeavor I undertake, and especially for proof reading this. My husband Jason: I love him for many reasons, not least of which for his unending supply of love, patience and cups of tea.

Table of Contents

Abstract	2	
Acknowledgements	4	
List of Tables	14	
List of Figures	16	
List of Figures	16	
List of Appendices	19	
List of Appendices	19	
Abbreviations	20	
1	INTRODUCTION.....	25
1.1	<i>Hearing loss, vision loss and combined sensory loss: Epidemiology</i> ..	25
1.1.1	Usher syndrome.....	26
1.2	<i>The vertebrate ear and eye</i>	28
1.2.1	The vertebrate ear.....	28
1.2.1.1	Anatomy of the ear.....	28
1.2.1.2	Auditory transduction	30
1.2.2	The vertebrate eye	33
1.2.2.1	Anatomy of the eye	33
1.2.2.2	Development of the eye	40
1.2.2.3	Phototransduction	44
1.3	<i>Usher syndrome</i>	46
1.3.1	The clinical phenotype	46
1.3.1.1	The auditory phenotype: sensorineural hearing loss	46
1.3.1.2	The visual phenotype: Retinitis Pigmentosa	47
1.3.1.3	Atypical Usher syndrome	50
1.3.1.4	Additional associated clinical characteristics	51
1.3.2	The genetics of Usher syndrome.....	52
1.3.3	Usher syndrome proteins: their structure and localisation within the normal ear and eye	55
1.3.3.1	Myosin VIIA.....	55
1.3.3.2	Harmonin – the USH1C protein.....	60
1.3.3.3	Cadherin 23	62
1.3.3.4	Protcadherin 15.....	64
1.3.3.5	Sans.....	65
1.3.3.6	Usherin	66
1.3.3.7	NBC3	67

1.3.3.8	Very large G-coupled receptor protein b (Vlgr1b)	68
1.3.3.9	Clarin-1	70
1.3.4	Usher syndrome proteins: their interactions in the normal ear and eye ..	
	71
1.3.4.1	Usher protein complexes formed in the normal ear	71
1.3.4.2	Postulated Usher protein complexes formed in the normal eye	73
1.3.5	Mouse models of Usher syndrome	73
1.4	<i>Research aims</i>	75
1.5	<i>Background to research methodology</i>	76
1.5.1	Methods for determining gene expression and protein localization patterns	76
1.5.1.1	Reverse Transcription Polymerase Chain Reaction (RT-PCR).....	76
1.5.1.2	Immunostaining.....	77
1.5.1.2.1	Synthesis of antibodies	78
1.5.1.2.1.1	Selection of epitopes	78
1.5.1.2.1.2	Polyclonal antisera production protocol	80
1.5.1.2.2	Techniques for the validation of synthesised antibodies	80
1.5.2	Techniques for investigating protein interactions	81
1.5.2.1	The yeast two-hybrid system.....	81
1.5.2.2	Confirmation and further characterization of positive interactors	87
1.5.2.2.1	Sequencing of candidate interacting proteins	87
1.5.2.2.2	Yeast mating	88
1.5.2.2.3	Co-immunoprecipitation (CO-IP)	88
2	METHODOLOGY	90
2.1	<i>Materials: Solutions</i>	90
2.2	<i>Materials: Technical</i>	91
2.3	<i>Determination of the temporal and spatial expression of Ush1c and harmonin within the normal murine eye</i>	91
2.3.1	Methodology: Identification of the pattern of protein localisation of harmonin in the adult murine retina	91
2.3.1.1	Tissue preparation	91
2.3.1.1.1	Tissue collection	91
2.3.1.1.2	Tissue fixation and cryopreservation	92
2.3.1.1.3	TESPA coating of slides	92
2.3.1.1.4	Cryosectioning sectioning	93
2.3.1.1.5	Processing and UV light curing of LR gold resin	93
2.3.1.1.6	Semithin sectioning	94

2.3.1.2	Harmonin localisation in the adult murine retina	94
2.3.1.2.1	Single antibody staining of fixed tissues	95
2.3.1.2.2	Double antibody staining of fixed tissues.....	96
2.3.1.3	Methodology: Investigation into the effects of fixation upon harmonin localisation	97
2.3.2	Methodology: Examination of the protein localisation of harmonin in the absence of myosin VIIA and cadherin 23	97
2.3.3	Methodology: Determination of the age of onset of <i>Ush1c</i> gene expression.....	97
2.3.3.1	Harmonin localisation in the postnatal murine retina	97
2.3.3.2	<i>Ush1c</i> expression in the prenatal murine retina.....	98
2.3.3.2.1	Isolation of total RNA	98
2.3.3.2.2	Two-step Reverse Transcription Polymerase Chain Reaction (RT-PCR)	99
2.3.3.2.2.1	Agarose gel electrophoresis.....	101
2.4	<i>Generation of polyclonal antibodies to harmonin isoforms.....</i>	102
2.4.1	Selection of the antigenic peptides for anti-harmonin antibody synthesis	102
2.4.2	Methodology: Analysis of the anti-harmonin antibodies by ELISA	103
2.4.3	Methodology: Analysis of the anti-harmonin antibodies by immunolabelling of murine retinas	105
2.4.4	Methodology: Analysis of the anti-harmonin antibodies by immunoblotting analysis	106
2.4.4.1	Preparation of protein samples.....	106
2.4.4.1.1	Protein extraction from cells	106
2.4.4.1.1.1	Cryostorage and recovery of mammalian cell lines	106
2.4.4.1.1.2	Maintenance of R28 cells and trypsinisation.....	107
2.4.4.1.1.3	Protein extraction from cells	108
2.4.4.1.2	Protein extraction from tissue	108
2.4.4.1.3	Calculation of protein concentration by the Bradford method	109
2.4.4.2	SDS-PAGE and electrotransfer of proteins onto nitrocellulose membranes	110
2.4.4.3	Western blotting with monoclonal and polyclonal anti-harmonin.....	112
2.4.4.4	Western blotting with anti-LTPR serum	113
2.4.4.5	Protein purification from serum.....	113
2.4.4.5.1	Isolation of immunoglobulins from serum	113
2.4.4.5.2	Column regeneration.....	115

2.4.4.6	Western blotting with purified anti-LTPR IgGs and unpurified anti-LTPR serum	115
2.4.4.7	Western blotting with pre-absorbed purified anti-LTPR IgGs and unpurified anti-LTPR serum	116
2.4.5	Methodology: Analysis of antigenic peptide hydrophobicity.....	117
2.4.6	Methodology: Investigation into the presence of anti-harmonin IgGs in the anti-LTPR antibody sera	117
2.5	<i>Investigation into candidate harmonin-interacting proteins within the normal eye.....</i>	119
2.5.1	Methodology: A Yeast Two-hybrid screen of a bovine retinal library to find harmonin-interacting proteins	119
2.5.1.1	Confirmation of yeast strain phenotypes	119
2.5.1.1.1	Long term storage of yeast	119
2.5.1.1.2	Recovery of yeast from frozen stocks	119
2.5.1.1.3	Preparation of liquid yeast cultures	120
2.5.1.1.4	Confirmation of the phenotype of the yeast strains	120
2.5.1.2	Generation of bait and control fusion proteins.....	121
2.5.1.2.1	Digestion of DNA with restriction endonucleases.....	121
2.5.1.2.2	Isolation of DNA from agarose gels	122
2.5.1.2.3	Spectrophotometric quantification of DNA concentration	123
2.5.1.2.4	Ligation of DNA into plasmid vectors	123
2.5.1.2.5	Transformation of DNA into bacterial cells	125
2.5.1.2.5.1	Preparation of liquid cultures	125
2.5.1.2.5.2	Long term storage of E.coli and recovery of frozen stocks	125
2.5.1.2.5.3	Preparation of chemically competent E.coli.....	126
2.5.1.2.5.4	Transformation of plasmid DNA into chemically competent E.coli....	126
2.5.1.2.6	Polymerase Chain Reaction (PCR).....	127
2.5.1.2.6.1	Identification of positive recombinants	129
2.5.1.2.7	DNA sequencing.....	129
2.5.1.2.7.1	Sequencing of positive recombinants.....	131
2.5.1.2.8	Isolation and purification of plasmid DNA.....	131
2.5.1.2.8.1	Small scale plasmid purification	131
2.5.1.2.8.2	Large scale plasmid purification.....	132
2.5.1.2.9	Transformation of yeast cells with cloned DNA plasmid.....	133
2.5.2	Validation of bait and control proteins	134
2.5.2.1	Plasmid extraction from yeast.....	134
2.5.2.1.1	Bait sequence analysis	135
2.5.2.2	Protein extraction from yeast	136

2.5.2.2.1	Confirmation of fusion protein identity	137
2.5.2.3	Toxicity effects of the fusion proteins on the host yeast cells.....	139
2.5.2.4	Autonomous activation of the reporter genes	139
2.5.2.4.1	Nutritional reporter gene activation.....	139
2.5.2.4.2	β -galactosidase assay.....	140
2.5.2.5	Yeast mating	141
2.5.2.5.1	Control mating experiments	141
2.5.3	Bovine retinal library screening by sequential transformation into AH109 yeast	142
2.5.3.1	Amplification of the retinal cDNA library	142
2.5.3.2	Sequential co-transformation of baits and preys.....	144
2.5.3.3	Library screening.....	145
2.5.3.4	Segregation of multiple library plasmids with a diploid and repeat analysis of activation of reporter genes	146
2.5.4	Characterisation of candidate interactors	146
2.5.4.1	PCR amplification of library inserts.....	146
2.5.4.2	Transformation of library inserts in DH5 α and KC8 cells	147
2.5.4.3	DNA sequence analysis of library inserts	149
2.5.5	Confirmation and further characterization of positive interacting preys...	149
2.5.5.1	Confirmation of prey-harmonin interaction by yeast mating	149
2.5.5.1.1	Segregation of yeast plasmids	149
2.5.5.1.2	Transformation of bait and control plasmids into strain Y187	150
2.5.5.1.3	Yeast mating	150
2.5.5.2	Further characterization of prey-harmonin interaction through yeast mating with the PDZ domain baits.....	151
2.5.5.3	Futher analysis of the candidate interactor – Phosducin.....	151
2.5.5.3.1	Identification of the ORF of phosducin and confirmation of its interaction with harmonin by mating analysis	151
2.5.5.3.2	Analysis of Phosducin protein sequence	151
2.5.6	Methodology: Confirmation of an interaction between harmonin and phosducin by co-immunoprecipitation (CO-IP)	152
2.5.6.1	Synthesis of c-myc tagged harmonin and identification of phosducin in whole eye homogenate	152
2.5.6.1.1	Protein synthesis by <i>in vitro</i> transcription and translation	152
2.5.6.1.1.1	Introduction of the HA tag and the T7 promoter sequence to the MCC2 positive control	153
2.5.6.1.1.2	Purification of PCR products	154

2.5.6.1.2	Simultaneous detection of phosducin and harmonin on Western blots...	154
2.5.6.2	CO-IP assay.....	155
2.5.6.2.1	Assay and bait control CO-IP reactions.....	155
2.5.6.2.2	pGBKT7-USH1C and Phd.....	158
2.5.7	Methodology: Validation of candidate interactor through protein localisation and gene expression analysis.....	159
2.5.7.1	Comparison of Phd and harmonin protein localisation in the normal adult retina	159
2.5.7.2	Comparison of Phd and harmonin protein localisation in the normal developing retina.....	160
2.5.7.3	Comparison of Pdc and Ush1c gene expression in the adult and developing ear	160
3	RESULTS CHAPTER: Identification of the temporal and spatial expression of <i>Ush1c</i> and harmonin within the normal murine eye	162
3.1	<i>Identification of the pattern of protein localisation of harmonin in the adult murine retina</i>	163
3.1.1	Harmonin localisation in the adult murine retina	163
3.1.2	The effects of fixation upon harmonin, myosin VIIA and cadherin 23 localisation	167
3.2	<i>Examination of harmonin localisation in fixed retinal tissue in the absence of myosin VIIA or cadherin 23</i>	169
3.3	<i>Determination of the age of onset of <i>Ush1c</i> gene expression</i>	171
3.3.1	Harmonin localisation in the postnatal murine retina	171
3.3.2	<i>Ush1c</i> expression in the prenatal murine retina.....	173
3.4	<i>Conclusions</i>	175
4	RESULTS CHAPTER: Generation of polyclonal antibodies to harmonin isoforms	176
4.1	<i>Analysis of the anti-harmonin antibodies by ELISA</i>	177
4.2	<i>Analysis of the anti-harmonin antibodies by immunolabelling of murine retinas</i>	182
4.3	<i>Analysis of the anti-harmonin antibodies by immunoblotting analysis</i>	184
4.4	<i>Analysis of antigenic peptide hydrophobicity</i>	192

4.5	<i>Investigation into the presence of anti-harmonin IgGs in the anti-LTPR antibody sera</i>	195
4.6	<i>Conclusions</i>	198
5	RESULTS CHAPTER: Identification of candidate harmonin-interacting proteins in the eye.	199
5.1	<i>A Yeast Two-hybrid screen of a bovine retinal library to find harmonin-interacting proteins</i>	200
5.1.1	Confirmation of yeast strain phenotypes	200
5.1.2	Generation of bait and control fusion proteins	202
5.1.2.1	Production of bait and control fusion protein constructs	202
5.1.2.2	Transformation of bait and control constructs into yeast.....	203
5.1.3	Validation of bait and control fusion proteins	205
5.1.3.1	Analysis of the DNA sequence of the baits.....	205
5.1.3.2	Confirmation that the bait fusion protein is harmonin.....	206
5.1.3.3	Toxicity effects of the bait fusion protein on host yeast cells.....	210
5.1.3.4	Verification that neither the bait fusion protein nor the DNA-BD alone is able to autonomously activate the reporter genes	211
5.1.3.5	Control yeast mating experiments	215
5.1.4	Bovine retinal library screening by sequential transformation into AH109 yeast	216
5.1.4.1	Prey library amplification	216
5.1.4.2	Sequential co-transformation of bait and preys	218
5.1.4.3	Library screening	219
5.1.4.4	Segregation of multiple library plasmids with a diploid and repeat analysis of activation of reporter genes	221
5.1.5	Characterisation of candidate interactors	223
5.1.5.1	DNA sequence analysis of library inserts	223
5.1.6	Confirmation and further characterization of positive interacting preys...	223
5.1.6.1	Confirmation of prey-harmonin interaction by yeast mating	224
5.1.6.2	Further characterization of prey-harmonin interaction through yeast mating with the PDZ domain baits.....	228
5.1.6.3	Analysis of possible PBI sequences within prey protein sequences ..	229
5.1.6.4	Further analysis of the candidate interactor – phosducin.....	233
5.1.6.4.1	Identification of the ORF of phosducin and confirmation of its interaction with harmonin by mating analysis.	233
5.1.6.4.2	Analysis of phosducin protein sequence	235

5.2	<i>Confirmation of an interaction between harmonin and phosducin by co-immunoprecipitation (CO-IP).....</i>	237
5.2.1	Synthesis of c-myc tagged harmonin and identification of phosducin in whole eye homogenate	237
5.2.2	CO-IP assay	239
5.3	<i>Validation of candidate interactor through protein localisation and gene expression analysis.....</i>	241
5.3.1	Comparison of phosducin and harmonin protein localisation in the normal adult retina	241
5.3.2	Comparison of phosducin and harmonin protein localisation in the normal developing retina	242
5.3.3	Comparison of Pdc and Ush1c gene expression in the adult and developing ear by RT-PCR	244
5.4	<i>Conclusions</i>	245
6	DISCUSSION.....	246
6.1	<i>Determination of the temporal and spatial expression of Ush1c and harmonin within the normal murine eye.....</i>	246
6.2	<i>Investigation into candidate harmonin-interacting proteins within the normal eye</i>	251
6.3	<i>Possible pathogenic mechanisms in Usher syndrome.....</i>	257
REFERENCES.....		270
APPENDICES		282

LIST OF TABLES

Table 1.1 Additional clinical features thought to be associated with the Usher syndrome phenotype	51
Table 1.2 Usher syndrome	54
Table 1.3 PDZ domain classes	62
Table 2.1 Index to Materials: Solutions data	90
Table 2.2 Index to Materials: Technical data.....	91
Table 2.3 Separation ranges of proteins in different percentages of denaturing SDS-PAGE Gels	111
Table 2.4 Calculation of the ng of vector and insert DNA required for a 2:1 and 5:1 insert:vector ligation reaction	124
Table 2.5 Definitions of the PCR reaction and thermocycler program used in PCR reactions throughout the following chapters.....	128
Table 2.6 A comparison of the sequencing reaction components and thermocycler programs employed by the Big Dye and DYEnamic ET terminator sequencing systems.....	130
Table 2.7 Pull down assay control reactions	157
Table 4.1 Examination of the antigenicity of peptide 1 by ELISA.	179
Table 4.2 Examination of the antigenicity of peptide 2 by ELISA.	180
Table 4.3 Elution readings from the purification of anti-LTPR IgGs from the antibody serum	187
Table 5.1 Analysis of the phenotype of the yeast host strains.....	201
Table 5.2 Calculation of the transformation efficiency of control and bait plasmids into the host yeast strains	204
Table 5.3 Comparison of the toxicity effects of the control and bait fusion proteins to the empty vectors on yeast culture growth.....	210
Table 5.4 Comparison of the ability of the bait and control proteins to autonomously activate transcription of nutritional reporter genes.....	212
Table 5.5 Determination of the concentration of 3-AT required to inhibit the ability of baits pGBK7-USH1C (12-6&8) to autonomously activate transcription of the HIS3 and LacZ reporter genes	213
Table 5.6 Comparison of the ability of the bait and control proteins to autonomously activate transcription of the <i>Lac Z</i> reporter gene.....	214
Table 5.7 Results of Control Mating Analysis.....	215
Table 5.8 Initial colony numbers resulting from the Yeast Two-hybrid screen after seven days incubation at 30°C.	220

Table 5.9 Summary of Appendix 16, showing the elimination of diploid and false positive colonies from further analysis	223
Table 5.10 Examination of the strength of bait-prey interactions as a measure of the speed of their activation of <i>LacZ</i> in comparison to pCL1	223
Table 5.11 A summary of the sequence data produced from the sequenced preys listed in Appendix 19.	224
Table 5.12 Confirmation of interactions between prey proteins and harmonin <i>in vivo</i> by yeast mating analysis.....	226
Table 5.13 A summary of the reasons for excluding individual interactors from further analysis.....	227
Table 5.14 A brief description of the six high priority sequenced interacting proteins	228
Table 5.15 Characterisation of the interactions between pGBK7-USH1C and the prey proteins through yeast mating with PDZ domain bait constructs.....	229

LIST OF FIGURES

Figure 1.1 The structure of the vertebrate ear.....	29
Figure 1.2 Hair cell structure and auditory transduction	32
Figure 1.3 The anatomy of the vertebrate eye	33
Figure 1.4 Specialised features of the vertebrate photoreceptor	36
Figure 1.5 A schematic showing the differences in structure of the hair cell and photoreceptor ribbon synapses.....	39
Figure 1.6 Development of the human eye	41
Figure 1.7 The neural retina.....	43
Figure 1.8 Phototransduction and photopigment recycling.....	45
Figure 1.9 The pattern of cell death during the progression of retinitis pigmentosa.	48
Figure 1.10 Features of retinitis pigmentosa seen by fundus examination	50
Figure 1.11 The structure of myosin VIIA.....	55
Figure 1.12 Localisation patterns of the Usher proteins within the normal ear	58
Figure 1.13 Localisation patterns of the Usher proteins within the normal eye	59
Figure 1.14 The structure of the three isoform classes of harmonin.....	61
Figure 1.15 The structure of cadherin 23	63
Figure 1.16 The structure of protocadherin 15	65
Figure 1.17 The structure of sans	66
Figure 1.18 The structure of usherin	67
Figure 1.19 The structure of NBC3	68
Figure 1.20 The structure of Vlgr1b	69
Figure 1.21 The structure of Clarin-1	70
Figure 1.22 Scanning electron microscope images comparing the organisation of hair cell stereocilia in the USH1 mutant model mice	74
Figure 1.23 A schematic showing the basic steps involved in a yeast two-hybrid reaction	82
Figure 2.1 Selection of Peptide 1 and 2.....	103
Equation 2.1 Calculation of the appropriate concentrations of insert and vector DNA required for 'sticky ended' ligation reactions.	124
Figure 3.1 Localisation of harmonin in the adult murine retina	164
Figure 3.2 Colocalisation of harmonin and rhodopsin in the photoreceptor outer segments.....	166
Figure 3.3 Immunolocalisation of USH1 proteins in unfixed and fixed murine retinas	168
Figure 3.4 Immunolocalisation of harmonin in normal and mutant murine retinas.	170
Figure 3.5 Harmonin localisation in the developing (P2-P12) murine retina	172

Figure 3.6 Usher type 1 gene expression during prenatal murine eye development	174
Figure 4.1 Analysis of the immune response produced to the separate harmonin peptides	181
Figure 4.2 Comparative immunolocalisation of harmonin using the polyclonal anti-harmonin antibody, the anti-LTPR sera and the anti-PADH sera	183
Figure 4.3 Validation of protein aliquots as sources of the harmonin protein	185
Figure 4.4 Harmonin detection on western blots using anti-LTPR antibody sera	186
Figure 4.5 A comparison of the ability of purified anti-LTPR IgGs to recognise harmonin, compared to that of the unpurified anti-LTPR antibody sera	189
Figure 4.6 Examination of the specificity of the anti-LTPR antibody sera and purified anti-LTPR IgGs for harmonin	191
Figure 4.7 Kyte-Doolittle analysis of the hydrophobicity of the peptides	193
Figure 4.8 A hydrophobicity plot of the complete murine harmonin isoform a amino acid sequence	194
Figure 4.9 Ouchterlony analysis investigating the presence of anti-rabbit IgGs in the sera collected from the peptide 1 host	196
Figure 4.10 Ouchterlony analysis investigating the presence of anti-harmonin IgGs in the sera collected from the peptide 1 host	197
Figure 5.1 Schematic showing the structure of harmonin isoform 'a' and the peptides used to construct the bait fusion proteins	202
Equation 5.1 Transformation efficiency formula	204
Figure 5.2 The sequencing electropherogram of pGBK7-USH1C(12)	205
Figure 5.3 Expression of the GAL4BD-bait fusion proteins from the pGBK7-bait constructs by transformed AH109 yeast cells	207
Figure 5.4 Expression of the GAL4AD-bait fusion proteins from the pACT2-positive control constructs by transformed Y187 yeast cells	208
Figure 5.5 Analysis of the pGBK7-USH1C bait fusion protein with tag-specific and protein-specific antibodies	209
Equation 5.2 Calculation of the transformation efficiency during library amplification	216
Figure 5.6 Examination of the bovine retinal library post-amplification amplification	217
Equation 5.3 Calculation of the bovine retinal library titre	217
Figure 5.7 Calculation of the co-transformation efficiency and number of library clones screened	218
Figure 5.8 The amount of library cDNA required to screen 10^6 independent clones	219

Figure 5.9 CLUSTALW alignments of possible harmonin interacting proteins against the PBI region of cadherin 23	229
Figure 5.10 Results of the direct mating analysis between phosducin and bait/control constructs.....	232
Figure 5.11 Schematic of the library cDNA clone extracted from yeast colonies #1.3/1.7/1.9, containing the open reading frame of phosducin.....	233
Figure 5.12 An alignment of the protein sequence of phosducin from various species to examine protein homology and areas of conservation.....	235
Figure 5.13 Western blots showing the presence of phosducin in murine retinal homogenate	237
Figure 5.14 Interaction of harmonin and phosducin confirmed <i>in vitro</i> through pull down analysis.....	239
Figure 5.15 Immunolocalisation of phosducin and harmonin in the adult murine retina.....	240
Figure 5.16 Localisation of phosducin and harmonin in the developing retina.	242
Figure 5.17 Investigation of <i>Pdc</i> expression in developing and adult murine ear..	243
Figure 6.1 Interaction of the USH1 and USH2 proteins via harmonin	260
Figure 6.2 A summary of the localisation of phosducin and the Usher proteins in the murine retina	263
Figure A1 Interaction of c-Myc tagged p53 with HA tagged SV40 T-antigen by pull down analysis.....	331

LIST OF APPENDICES

Appendix 1 Suppliers.....	282
Appendix 2 Media.....	286
Appendix 3 Buffers and solutions	289
Appendix 4 Antibiotics	297
Appendix 5 Fixatives and cryopreservation buffers.....	298
Appendix 6 Agarose and SDS-PAGE gel recipes	299
Appendix 7 Antibodies and cell labelling solutions.....	301
Appendix 8 Genotype and phenotype details of E.coli strains.....	303
Appendix 9 Genotypes of yeast strains used in the Yeast Two-hybrid screen	304
Appendix 10 Plasmids used in the Yeast Two-hybrid screen and associated experiments.....	305
Appendix 11 Equipment.....	306
Appendix 12 Software.....	307
Appendix 13 List of primers used/ Sequence of oligonucleotide primers.....	308
Appendix 14 Semi-quantitative PCR raw data examining the expression of the USH1 genes during embryonic eye developmental stages and in the adult eye. ..	310
Appendix 15 Yeast Two-hybrid Vector Information	312
Appendix 16 Yeast 2 Hybrid Harmonin screening results	313
Appendix 17 Calculation of the transformation efficiency of control and bait plasmids into Y187 yeast.....	321
Appendix 18 Colony Exclusion Data.....	322
Appendix 19 Colony identity	323
Appendix 20 Control CO-IP assay	330

ABBREVIATIONS

3-AT	3-amino-1,2,4-triazole
AD	Activation domain
Ade	Adenine
AMD	Age-related macular degeneration
APS	Ammonium persulphate
AZOOR	Acute Zonal Occult Outer Retinopathy
bp	Base pairs
BSA	Bovine serum albumin
cDNA	Complementary DNA
CFU	Colony forming units
CNS	Central Nervous System
CV	Column volume
ddH ₂ O	Double distilled H ₂ O
DEPC	Diethylpyrocarbonate
DFNA	Autosomal dominant forms of deafness
DFNB	Autosomal recessive forms of deafness
DMEM	Dulbecco's modified eagle's medium
DMF	N,N-dimethylformamide
DMSO	Dimethyl sulfoxide
DNA	Deoxyribonucleic acid
DNA-BD	DNA binding domain
dNTPs	Deoxyribonucleotide triphosphates
DO	Dropout (supplement or solution)
DTT	Dithiothreitol

CAD	Extracellular cadherin repeat domain
ECL	Enhanced chemiluminescent substrate
EDTA	Ethylenediammetra acetic acid
ELM	External limiting membrane
ERG	Electroretinogram
Exo1	Exonuclease1
FERM	Band 4.1/ezrin/radixin/moesin-homology domain
FITC	Fluorescein isothiocyanate
FN3	Fibronectin type 3 repeats
GCL	Ganglion Cell Layer
GDP	Guanosine diphosphate
GPS	G-protein coupled proteolysis site
GTP	Guanosine triphosphate
HA	Heamaggultatin tag
His	Histidine
HPLC	Performance Liquid Chromatography
IHC	Inner hair cells
ILM	Inner limiting membrane
INL	Inner Nuclear Layer
IPL	Inner Plexiform Layer
IS	Inner Segments
IVT	<i>In vitro</i> translation
kb	Kilo base pairs
kDa	Kilo Dalton
KLH	Keyhole limpet hemocyanin
LamG	Laminin G domain

LamGL	Laminin G-like domain
LamNT	Laminin N-terminal domain
LE	Laminin-EGF-like modules domains
Leu	Leucine
LiAc	Lithium acetate
MCS	Multiple Cloning Site
MEM	Minimum essential medium
Met	Methionine
mRNA	Messenger Ribonucleic acid
MyTH4	Myosin tail homology domain
NFL	Nerve Fiber Layer
OCT	Optimal Cutting Temperature compound
ODx	Absorbance of ultra violet light at Xnm
OHC	Outer hair cells
ONL	Outer Nuclear Layer
OPL	Outer Plexiform Layer
OS	Outer Segments
PBI	PDZ Binding Interface
PBS	Phosphate Buffered Saline
PCR	Polymerase Chain Reaction
PDE	Phosphodiesterase
PDZ	Protein-protein interaction domain named after the first three proteins it was discovered in PSD-95/Dlg/ZO-1
PEG	Polyethylene glycol
PFA	Paraformaldehyde
PMSF	Phenylmethyl-sulfonyl fluoride

PNPP	p-Nitrophenyl phosphate
PTX	Pentaxin
RP	Retinitis pigmentosa
RPE	Retinal Pigmented Epithelium
RS	Ribbon Synapses
RT-PCR	Reverse transcriptase polymerase chain reaction
SAM	Sterile alpha motif
SAP	Shrimp Alkaline Phosphatase
SD medium	Minimal <u>Synthetic Dropout</u> medium
SDS	Sodium Dodecyl Sulfate
SDS-PAGE	Sodium Dodecyl Sulfate Polyacrylamide Gel Electrophoresis
TBS-T	Tris Buffer of Sodium with Tween
TE	Tris and EDTA
TEM	Transmission Electron Microscopy
TEMED	N ,N ,N 'N' -tetramethyl ethylenedi amine
TESPA	3- aminopropyltriethoxsilane
TM	Transmembrane domain
Trp	Tryptophan
TSPN	Thrombospondin N-terminal-like domain
TWEEN 20	Polyoxyethylenesorbitan monolaurate
UAS	Upstream activation sequence
Ura	Uracil
USH	Usher syndrome type
UV	Ultra violet
X-gal	5-bromo-4-indolyl-p-D-galactopyranoside
YPD	Yeast Peptone Difco

YPDA Yeast Peptone Difco supplemented with adenine

β -gal assay β -galactosidase assay

1 INTRODUCTION

1.1 ***Hearing loss, vision loss and combined sensory loss:***

Epidemiology

Hearing impairment can develop at any age with varying degrees of severity.

Age-related hearing loss affects ~25% of people aged 65 to 75 and 70%-80% of those aged over 75 (<http://www.nlm.nih.gov/medlineplus/>). Hearing loss in children is rarer and has many causes: some are environmental (i.e. acoustic trauma, ototoxic drugs, certain infections in the mother during pregnancy, or infections in the newborn baby), and some are genetic. Of the disorders attributable to genetic causes, ~30% are syndromic, many of which have been documented and the genes in question identified. The remaining 70% are classed as nonsyndromic with a variety of inheritance patterns involved – autosomal recessive (DFNB loci), autosomal dominant (DFNA loci), X-linked and mitochondrial (reviewed in Resendes, B L et al, 2001). In each case, the hearing impairment is classified according to the degree of severity and by the site of the defect. Conductive hearing loss refers to defects of the external and/or middle ear, whilst sensorineural hearing loss commonly refers to the inner ear but also stretches to the cortical auditory centres of the brain. Approximately 840 babies are born each year in the UK with significant deafness (www.RNID.org.uk). It is estimated that 50% percent of deaf children in the USA have an hereditary form of hearing loss and of these, one third have a syndrome associated with their hearing loss (http://www.pediatric-ent.com/learning/problems/hearing_loss.htm).

Hereditary retinal diseases are also characterized by the severity of vision loss. These diseases are further characterized by the age of onset of the disease, the topographic pattern of visual loss, rod verses cone involvement, ophthalmoscopic findings, and family history. In the developed world, the most common retinal diseases are diabetic retinopathy, glaucoma, and age-related macular degeneration (AMD), which together affect several percent of the population and have both genetic and non-genetic components. Monogenic Mendelian retinal diseases, for example Retinitis Pigmentosa (RP), affect ~1: 2000 people (Rattner, A et al, 1999). RP, like deafness can be inherited both as syndromes and as nonsyndromic RP, in an autosomal recessive mode (84%), an autosomal dominant mode (10%), or as an X-linked recessive disease (6%) and in a few rare cases it is inherited in a digenic mode. The overall frequency of RP in the white US population was estimated at about 1 in 3,700, with no evidence for ethnic heterogeneity (Boughman, J A et al, 1980).

Currently in the UK, it is estimated that there are 23000 individuals affected with both types of defects (www.RNID.org.uk), either as isolated retina-cochlea disorders or associated with other organs in a multisystem disorder e.g. Bardet-Biedl syndrome.

1.1.1 Usher syndrome

Usher syndrome is an example of an isolated retina-cochlea disorder, named after the British ophthalmologist, Charles Usher and with an estimated prevalence of 2-6.2 per 100,000 (Keats, B J et al, 1999). This is an autosomal recessive disease, defined by bilateral sensorineural deafness

combined with a progressive loss of vision due to RP and sometimes associated with vestibular dysfunction (Usher CH., 1914). It is estimated to account for 50% of deaf-blind individuals (Vernon, M, 1969), 18% of Retinitis Pigmentosa sufferers and 3-6% of children born with profound hearing loss (Boughman, J A et al, 1983).

Usher syndrome is both clinically and genetically heterogeneous, with three recognised clinical types (type 1-3) linked to eleven different genes. It is estimated that in the United States and Northern Europe the type 1 phenotype (definitions of type 1-3 are found in section 1.3.1) accounts for 33-44% of all Usher syndrome patients and type 2 accounts for 56-67%. Type 3, whilst accounting for only 2% of all Usher syndrome cases, accounts for 40% of all Finnish Usher syndrome cases due to the presence of a founder mutation in the population (Plantinga, R F et al, 2005 and references therein). It is also thought to account for 20% of the Usher cases seen in Birmingham in the UK (Hope, C I et al, 1997) and for a large percentage of New York Ashkenazi Jewish subjects with Usher syndrome, who displayed a wide range of phenotypic severities, all of which were homozygous for a particular mutation (Ness, S L et al, 2003).

This study examines the role of *USH1C* and its encoded protein in Usher syndrome.

1.2 ***The vertebrate ear and eye***

An understanding of normal ear and eye anatomy is necessary in order to discuss the clinical phenotype of Usher syndrome further.

1.2.1 *The vertebrate ear*

1.2.1.1 Anatomy of the ear

The human ear is made up of three compartments: the external ear, middle ear (Figure 1.1A) and inner ear (Figure 1.1B). Genetic defects may affect any part of the system, but most genetic hearing impairment in the population affects the inner ear. The inner ear is a complex membranous labyrinth in a cavity of the temporal bone consisting of the cochlea which contains the auditory receptors (the hair cells), and the vestibular part containing the balance and gravity receptors. The cochlea consists of a bony tube spiralling around a central core which is divided along its length by the basilar membrane. Two types of hair cells run along the length of the basilar membrane: a single row of 3,500 inner hair cells (IHC) that act as the primary receptor cells, and a triple row of 15,000 outer hair cells (OHC) acting as motor cells to amplify the auditory stimulus, all in contact with the tectorial membrane (Figure 1.1B). Together, the hair cells and their supporting cells on the basilar membrane are called the organ of Corti. On the apical surface of each hair cell are 30-300 stereocilia, stiff actin-filled microvilli that act as the mechanoreceptive structure of the hair cell. The stereocilia are arranged into staircase arrays, where each stereociliar tip is connected to the next-taller stereocilium by a tip link, thus forming a characteristic "V" shape (Figure

1.2 *The vertebrate ear and eye*

An understanding of normal ear and eye anatomy is necessary in order to discuss the clinical phenotype of Usher syndrome further.

1.2.1 *The vertebrate ear*

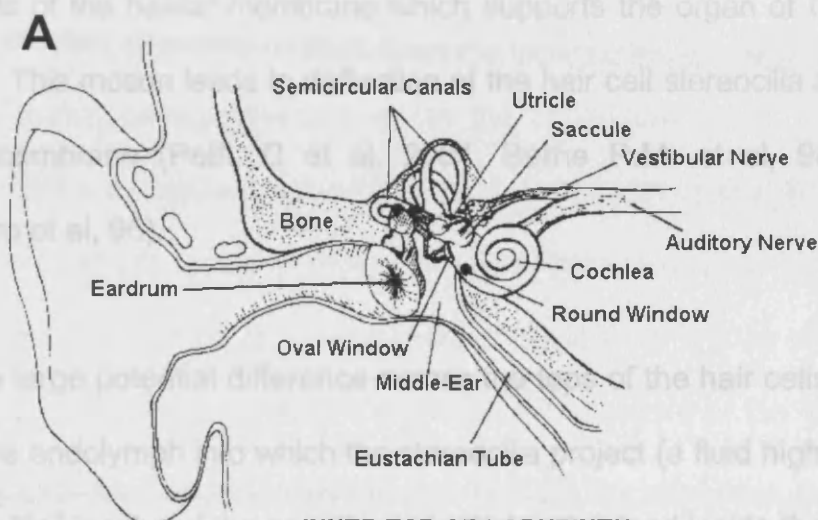
1.2.1.1 Anatomy of the ear

The human ear is made up of three compartments: the external ear, middle ear (Figure 1.1A) and inner ear (Figure 1.1B). Genetic defects may affect any part of the system, but most genetic hearing impairment in the population affects the inner ear. The inner ear is a complex membranous labyrinth in a cavity of the temporal bone consisting of: the cochlea which contains the auditory receptors (the hair cells), and the vestibular part containing the balance and gravity receptors. The cochlea consists of a bony tube spiralling around a central core which is divided along its length by the basilar membrane. Two types of hair cells run along the length of the basilar membrane: a single row of 3,500 inner hair cells (IHC) that act as the primary receptor cells, and a triple row of 15,000 outer hair cells (OHC) acting as motor cells to amplify the auditory stimulus, all in contact with the tectorial membrane (Figure 1.1B). Together, the hair cells and their supporting cells on the basilar membrane are called the organ of Corti. On the apical surface of each hair cell are 30-300 stereocilia, stiff actin-filled microvilli that act as the mechanoreceptive structure of the hair cell. The stereocilia are arranged into staircase arrays, where each stereociliar tip is connected to the next-taller stereocilium by a tip link, thus forming a characteristic "V" shape (Figure

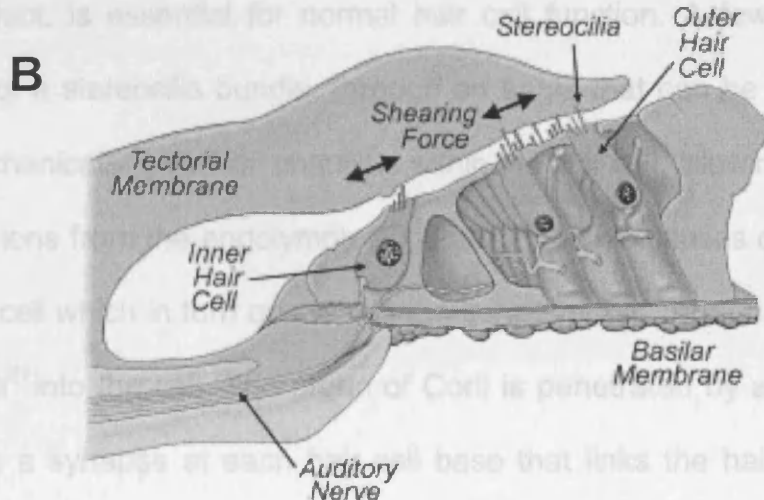
1.2A and Figure 1.22 wildtype) (Petit, C et al, 2001; Berne R.M. et al, 98; Martini, Alessandro et al, 96).

The detection of sound results from channelling of the sound wave through the external and middle ear to the hair cells of the inner ear. The action of the sound wave on the osseous and tympanic membranes of the middle ear causes displacement of the perilymph within the cochlea. This in turn results in wave

Figure 1.1 The structure of the vertebrate ear



INNER EAR OR LABYRINTH



The vertebrate ear is divided into three sections: the external, middle and inner ear. The main structural features and functional elements of the external and middle ear are shown in (A) (<http://www.neurophys.wisc.edu/www/aud/johc.html>). The arrangement of the Organ of Corti of the inner ear is shown in (B) (<http://www.vestibular.org/gallery.html>), highlighting the two different kinds of auditory hair cells, topped by the tectorial membrane.

1.2.1.2 Auditory transduction

The detection of sound results from channelling of the sound wave through the external and middle ear to the hair cells of the inner ear. The action of the sound wave on the ossicles and tympanic membrane of the middle ear causes displacement of the perilymph within the cochlea. This in turn results in wave movements of the basilar membrane which supports the organ of Corti in the inner ear. This motion leads to deflection of the hair cell stereocilia against the tectorial membrane (Petit, C et al, 2001; Berne R.M. et al, 98; Martini, Alessandro et al, 96).

There is a large potential difference across the tops of the hair cells, between the positive endolymph into which the stereocilia project (a fluid high in K^+ ions and low in Na^+ ions) and the negative potential maintained inside the hair cells. This large potential gradient, generated by ion pumps in the lateral wall of the cochlear duct, is essential for normal hair cell function. A few nanometers deflection of a stereocilia bundle, through an angle that can be less than 1°, opens mechanically-gated ion channels within the hair cell, allowing an influx of potassium ions from the endolymph (Figure 1.2B). This causes depolarization of the hair cell which in turn opens voltage-sensitive Ca^{2+} channels that allow entry of Ca^{2+} into the cell. The organ of Corti is penetrated by afferent nerve fibres, with a synapse at each hair cell base that links the hair cells to the bipolar neurones at the centre of the cochlea (Figure 1.2A). An increase in Ca^{2+} concentration triggers neurotransmitter release at the hair cell synapses (Figure 1.2B), thereby converting sound to an electrical stimulus for transmission through the central nervous system (CNS) (Friedman, T et al, 2000).

Signal transduction in the auditory system is different to that of other sensory systems e.g. the visual and olfactory systems, as it does not use a second messenger cascade system to amplify and transmit the signal (Martini, Alessandro et al, 96). Instead it employs direct gating of the transducer channel since it requires responses up to 100 kHz or more, too fast for a second messenger cascade to function. An adaptation motor in the stereocilia regulates the ion channel through a gating-spring which, together with the adaptation motor, controls the tension on the transduction channel. Little is known about the molecular basis of hair cell transduction or the identity of the proteins that form this spring or motor. However there is some evidence that a myosin plays a role in long term adjustment of the tension of links between the stereocilia which are thought to be involved in modulation of the stereocilia bundle as a whole. The stereocilia of hair cells in the vestibular system also function by deflection, this time involving the otolithic membrane, similar to the tectorial membrane, which moves in response to changes in gravity as the head moves (reviewed in Friedman, T et al, 2000; Willems, P J, 2000).

Figure 1.2 Hair cell structure and auditory transduction

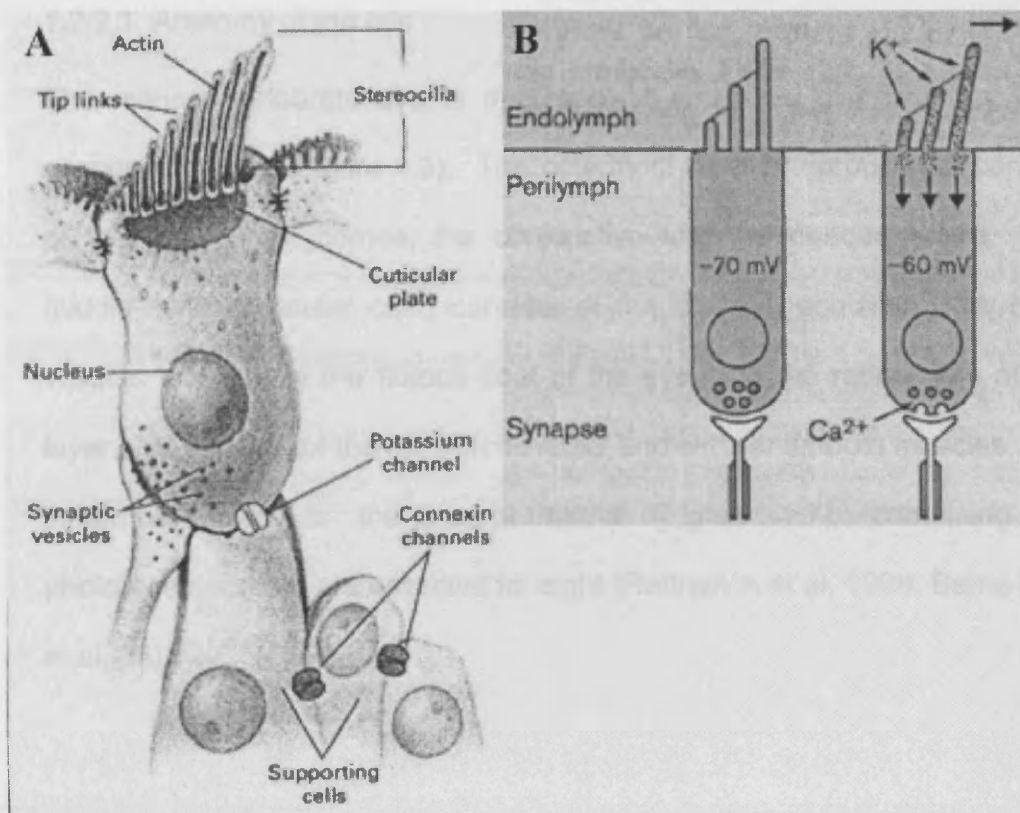


Figure 1.3 The anatomy of the vertebrate eye

(A) The structure of a vertebrate hair cell, showing the actin-rich stereocilia on its apical surface, the ion channels controlling intracellular ion concentrations and the synaptic vesicles of the ribbon synapses at its base. (B) The auditory transduction reaction. Deflection of the stereocilia in response to sound alters intracellular K^+ and Ca^{2+} levels, leading to neurotransmitter release at the hair cell synapse.

(Figure adapted from (A) Willems, P J, 2000 and (B) Friedman, T et al, 2000)

The main structural features of the vertebrate eye are shown above, with a more detailed description of the inner layer, the retina, in Figure 1.7.

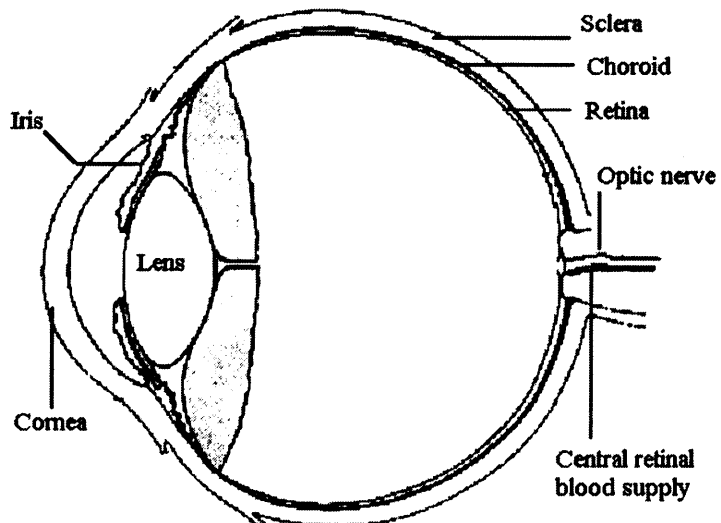
(Picture adapted from National Eye Institute, National Institutes of Health.)

1.2.2 The vertebrate eye

1.2.2.1 Anatomy of the eye

The mature vertebrate eye is a composite structure, composed of three concentric layers (Figure 1.3). The outermost layer or fibrous coat consists of the transparent cornea, the conjunctiva and the opaque sclera. The middle layer (vascular coat) consists of the choroid, containing the blood vessels that supply the fibrous coat of the eye, and the retina. The middle layer also consists of the iris with its radial and circular smooth muscles. The innermost layer is the neural retina (Figure 1.7), containing the photoreceptors that are essential for sight (Rattner, A et al, 1999; Berne R.M. et al, 98).

Figure 1.3 The anatomy of the vertebrate eye



The main structural features of the vertebrate eye are shown above, with a more detailed illustration of the inner layer, the retina, in Figure 1.7.

(Figure adapted from National Eye Institute, National Institutes of Health).

The photoreceptors are the visual equivalent of the auditory hair cells. There are two types of photoreceptor cells (Figure 1.4A), 95% of human photoreceptors are rods (97.2% in mice) and 5% are cones (2.8% in mice) (Jeon, C J et al, 1998). Three types of cone photoreceptor exist in humans, dependent upon which of the light-sensing visual pigments (opsins) is present (red, blue or green). Cones are found throughout the retina but are most concentrated within a small central region, the fovea, where they mediate colour vision and high visual acuity. Rods have low thresholds for detecting light, thus operating well under conditions of reduced lighting. They do not contribute to providing well-defined images or colour vision. Rods also have greater pigment content, accounting for their greater sensitivity to light and thus their role in night vision and in sensitivity to brightness.

Each photoreceptor cell is composed of a synaptic terminal, a cell body, an inner segment (IS), followed by the connecting cilium leading to the highly membranous outer segment (OS). The OS of rods are longer than those of cones and the discs are free floating, whilst cone discs consist of infoldings of the surface membrane (Figure 1.4A) (Rattner, A et al, 1999; Berne R.M. et al, 98).

Transport between the IS and the OS occurs through the connecting cilium. Like all other cilia, the connecting cilium has a microtubule based cytoskeleton, the axoneme, which originates at the basal body in the IS. In the region of the connecting cilium, the axoneme consists of nine pairs of microtubules (each composed of an α and β tubule) but lacks the two central pairs of microtubules, that are often seen in other nonmotile primary cilium

e.g. kidney tubule epithelium (Schwartz, E A et al, 1997). Beyond the connecting cilium itself, the axoneme loses this organization. However the microtubules clearly extend for some distance into the OS (Figure 1.4B).

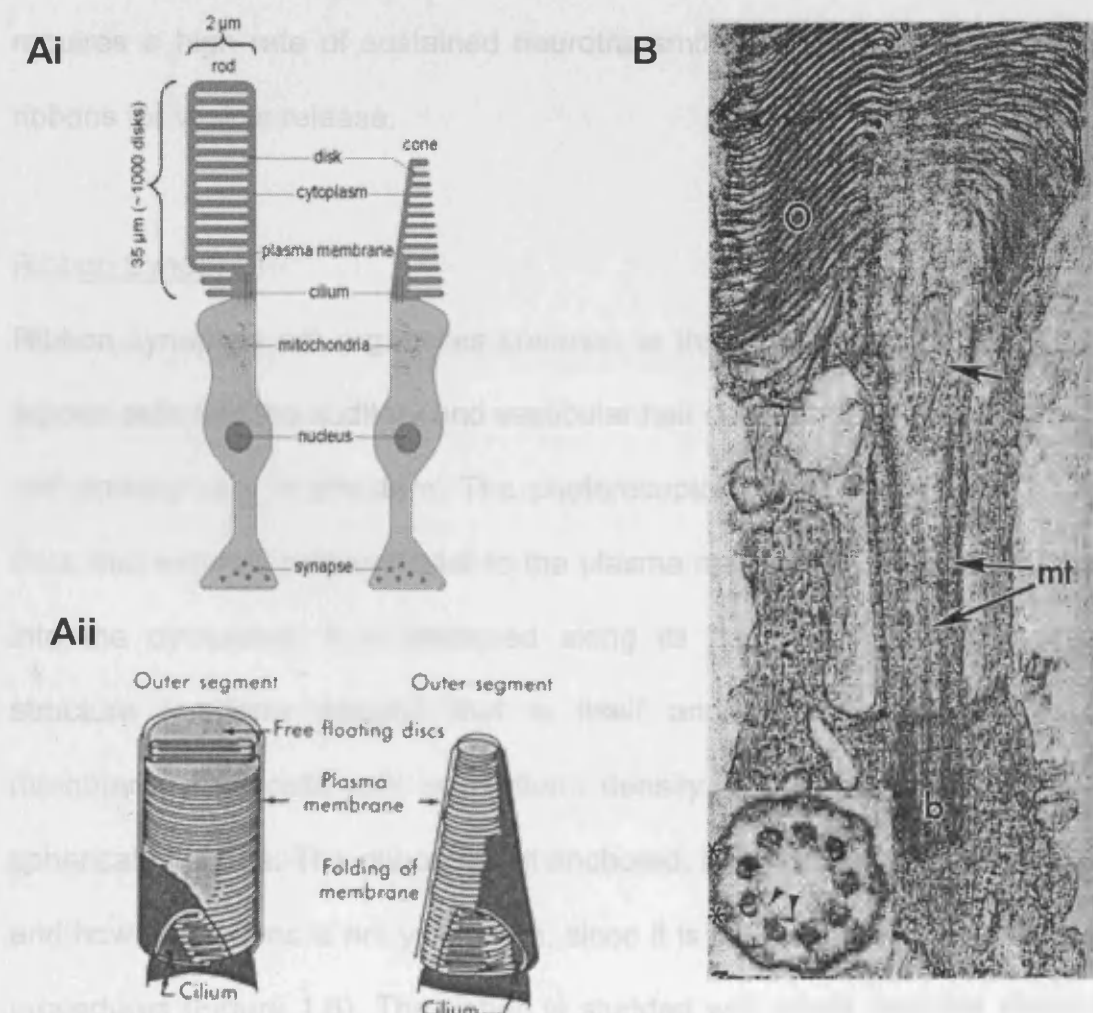
Since the photoreceptor appears to contain several similar proteins to those used by green algae for intraflagellar transport, it has been postulated that this or a similar transport system is employed in the photoreceptors. This postulate is further supported by the abnormal OS assembly (followed by cell death), phenotype seen in retinas of mice with mutations in the gene encoding IFT88 (a protein of the intraflagellar transport system). The cargo carried by this transport system is not well known, but thought to include components of the axoneme, opsins and proteins responsible for OS disc morphogenesis including Peripherin and ROM1 (Besharse, J C et al, 2003). Rhodopsin is directly transported up the connecting cilium using a cytoplasmic dynein that traverses the microtubule network. Also during its passage through the connecting cilium, rhodopsin colocalises with myosin VIIA. Myosin VIIA employs the actin cytoskeleton for movement through the connecting cilium (Wolfrum, U et al, 2000), suggesting that multiple transport systems may exist in the connecting cilium.

Figure 1.4 Specialised features of the vertebrate photoreceptor

(Ai) A schematic of the general features of rod and cone photoreceptors (adapted from <http://www.fz-juelich.de/ibi/ibi-1/datapool/page/24/Figure2.jpg>). (Aii) A more detailed examination of the photoreceptor outer segments (adapted from Berne R.M. et al, 98).

(B) An electron micrograph of the connecting cilium of a human photoreceptor in longitudinal section (figure adapted from Barrong, S D et al, 1992).

O, outer segment. B, basal body. mt →, ciliary microtubules. Single arrow, a tubulovesicular structure within the cilium. Original magnification $\times 65\,006$. The insert is a cross section of the connecting cilium showing the 9 peripheral microtubule doublets (arrowhead) interconnected by a nexin link and joined to the surface membrane by Y shaped linker proteins (*)



The synaptic terminals of the photoreceptors form chemical synapses with the retinal interneurons/second order neurons in the OPL. Synapses consist of a presynaptic active zone, a synaptic cleft and a postsynaptic density. The presynaptic active zone is filled with vesicles containing neurotransmitter, that are released from the presynaptic active zone to dock with the ion channel-rich postsynaptic density membrane, that then passes on the stimulatory signal through the cell layers (Garner, C C et al, 2000). Synapses where exocytosis is evoked by graded depolarization and where signalling requires a high rate of sustained neurotransmitter release, use specialized ribbons for vesicle release.

Ribbon Synapses

Ribbon synapses are organelles common to the vertebrate photoreceptors, bipolar cells and the auditory and vestibular hair cells. Photoreceptor and hair cell ribbons vary in structure. The photoreceptor ribbon is a plate ~30 nm thick that extends perpendicular to the plasma membrane and juts ~200 nm into the cytoplasm. It is anchored along its base to an electron-dense structure (arciform density) that is itself anchored to the presynaptic membrane. Hair cells lack an arciform density, and the ribbons are more spherical in shape. The ribbon is still anchored, but the identity of the anchor and how it functions is not yet known, since it is not visible by standard TEM procedures (Figure 1.6). The ribbon is studded with small particles ~5nm in diameter, along its surface, which tether the synaptic vesicles into dense but not touching clusters, via several fine filaments. Those vesicles tethered along the base of the ribbon make direct contact with the presynaptic membrane and are classed as 'docked' vesicles. There are approximately

5:1, tethered: docked vesicles for plate-like ribbons and 10:1 for spherical ones. The space between spherical ribbons and the membrane is occupied by docked synaptic vesicles which may be the sphere's anchoring element (Sterling, P et al, 2005).

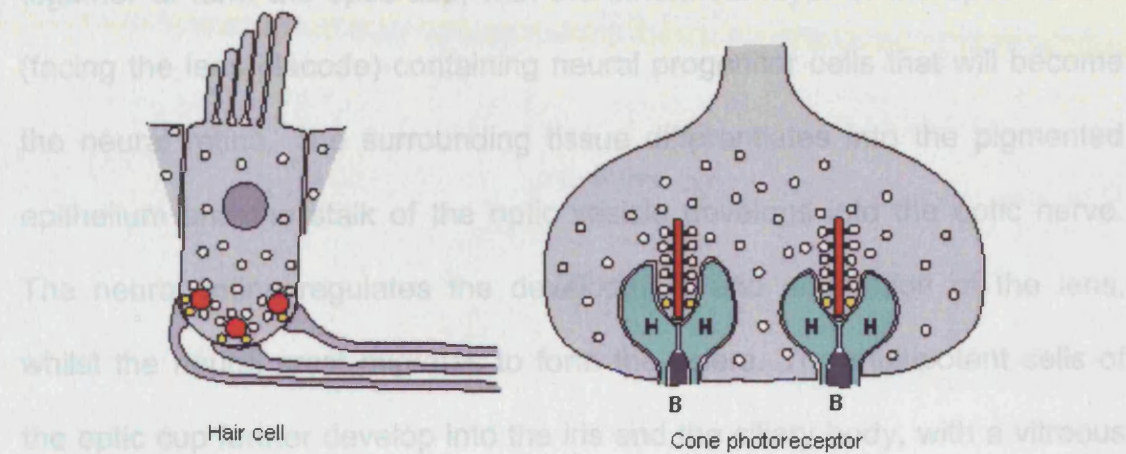
Ribbon synapses vary in their postsynaptic configurations but all the synapses invariably employ glutamate as the primary neurotransmitter. In hair cells, each ribbon supplies a single postsynaptic process (also known as a bouton) across a 20 nm cleft. One released vesicle can depolarize the bouton sufficiently to evoke an action potential, but often there is multivesicular release from a single ribbon onto a single bouton, possibly to enhance signal reliability (Glowatzki, E et al, 2002). The postsynaptic region of the cone photoreceptor ribbon synapses is a triad, formed from the lateral processes of two horizontal cells and the central processes of a bipolar cell. In the rod photoreceptor, the postsynaptic region is only a dyad, formed from the two horizontal cells. In this case, each ribbon supplies glutamate to multiple postsynaptic processes, each expressing a different and characteristic type of glutamate receptor that is located at different distances from the release sites. On average, each vesicle released from a cone synaptic ribbon contributes glutamate to postsynaptic processes at five, progressively more distant locations.

Exocytosis at the ribbon synapses involves the opening of Ca^{2+} channels to release all the vesicles promptly across the ribbon. The level of free Ca^{2+} required for vesicle release varies between ribbon synapses. Hair cells exhibit a steep dependence on Ca^{2+} concentration, whilst exocytosis at

photoreceptor synapses is less steeply dependent on Ca^{2+} levels and is stimulated by much lower levels of free Ca^{2+} (Sterling, P et al, 2005).

The natural vertebrate eye arises from two different and independent types of primordial cells (Figure 1.5). The neural plate folds to give the optic sulcus which enlarges into the optic vesicle, whilst the lens placode originates from the surface ectoderm of the head. The two types of cells are brought

Figure 1.5 A schematic showing the differences in structure of the hair cell and photoreceptor ribbon synapses



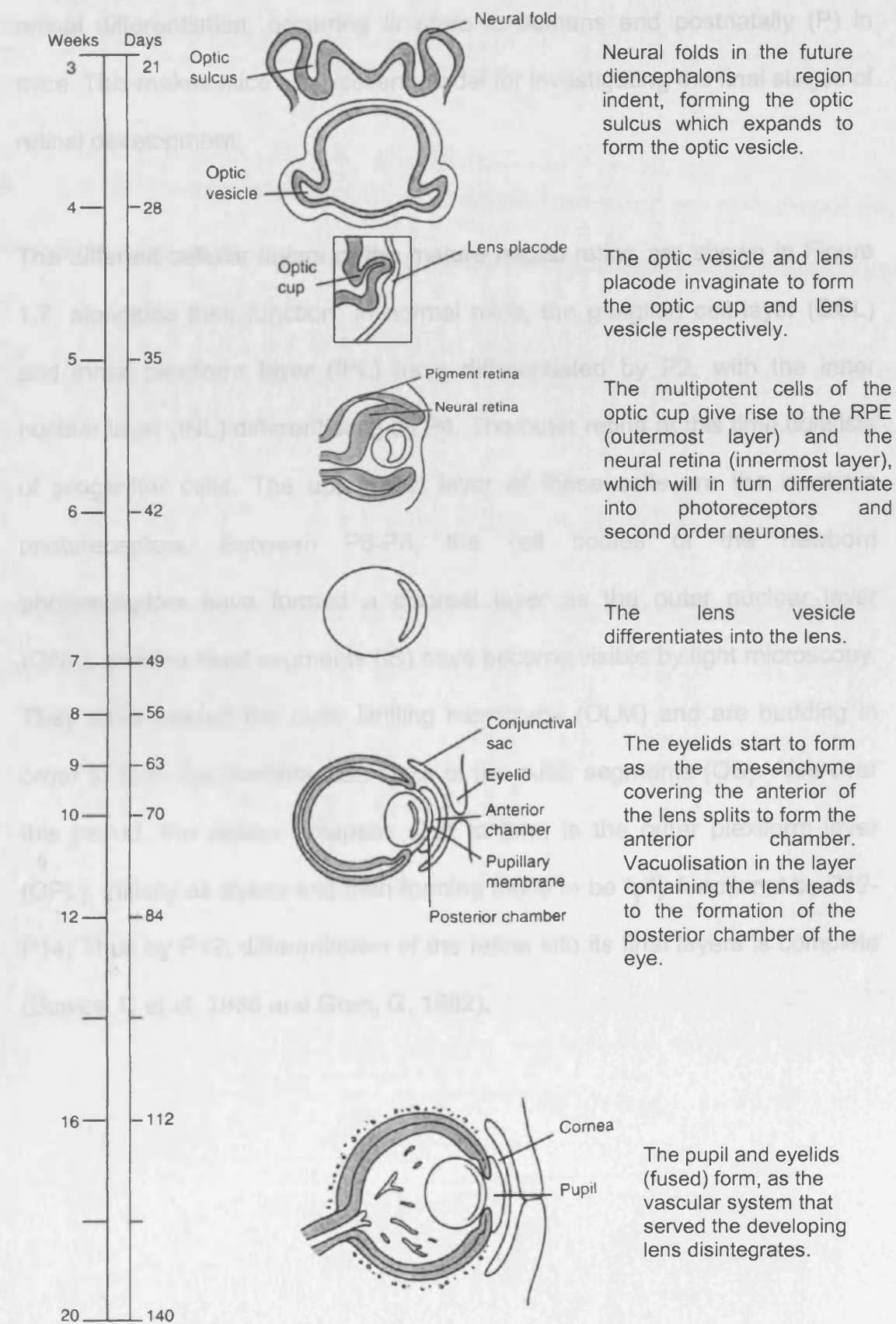
At the basal pole of the hair cell, the spherical ribbons (red) tether the vesicles (white – free vesicles; yellow – docked vesicles) near the presynaptic membrane. Each ribbon supplies one postsynaptic process with 10-20 ribbons per hair cell. In photoreceptors, the ribbons (red) are located at the apex of an invagination formed with three postsynaptic processes (two horizontal cells, H and one bipolar dendrite, B). Each cone forms ~20–50 triads (figure adapted from Sterling, P et al, 2005).

1.2.2.2 Development of the eye

The mature vertebrate eye arises from two different and independent types of primordial cells (Figure 1.6). The neural plate folds to give the optic sulcus which enlarges into the optic vesicle, whilst the lens placode originates from the surface ectoderm of the head. The two types of cells are brought together to form the optic cup, with the innermost layer of the optic vesicle (facing the lens placode) containing neural progenitor cells that will become the neural retina. The surrounding tissue differentiates into the pigmented epithelium and the stalk of the optic vesicle develops into the optic nerve. The neural retina regulates the development and orientation of the lens, whilst the neural crest migrates to form the sclera. The multipotent cells of the optic cup further develop into the iris and the ciliary body, with a vitreous cavity forming between lens and the retina. The pupil then forms, followed by the eyelids from folds in surface ectoderm and its associated mesenchyme (Larsen, William J., 2001), whilst the cells of the retina differentiate into their specific layers and types (Traboulsi, Elias. I, 1999).

Figure 1.6 Development of the human eye

A timeline showing the main stages of eye development in the human embryo (adapted from Larsen, William J., 2001).

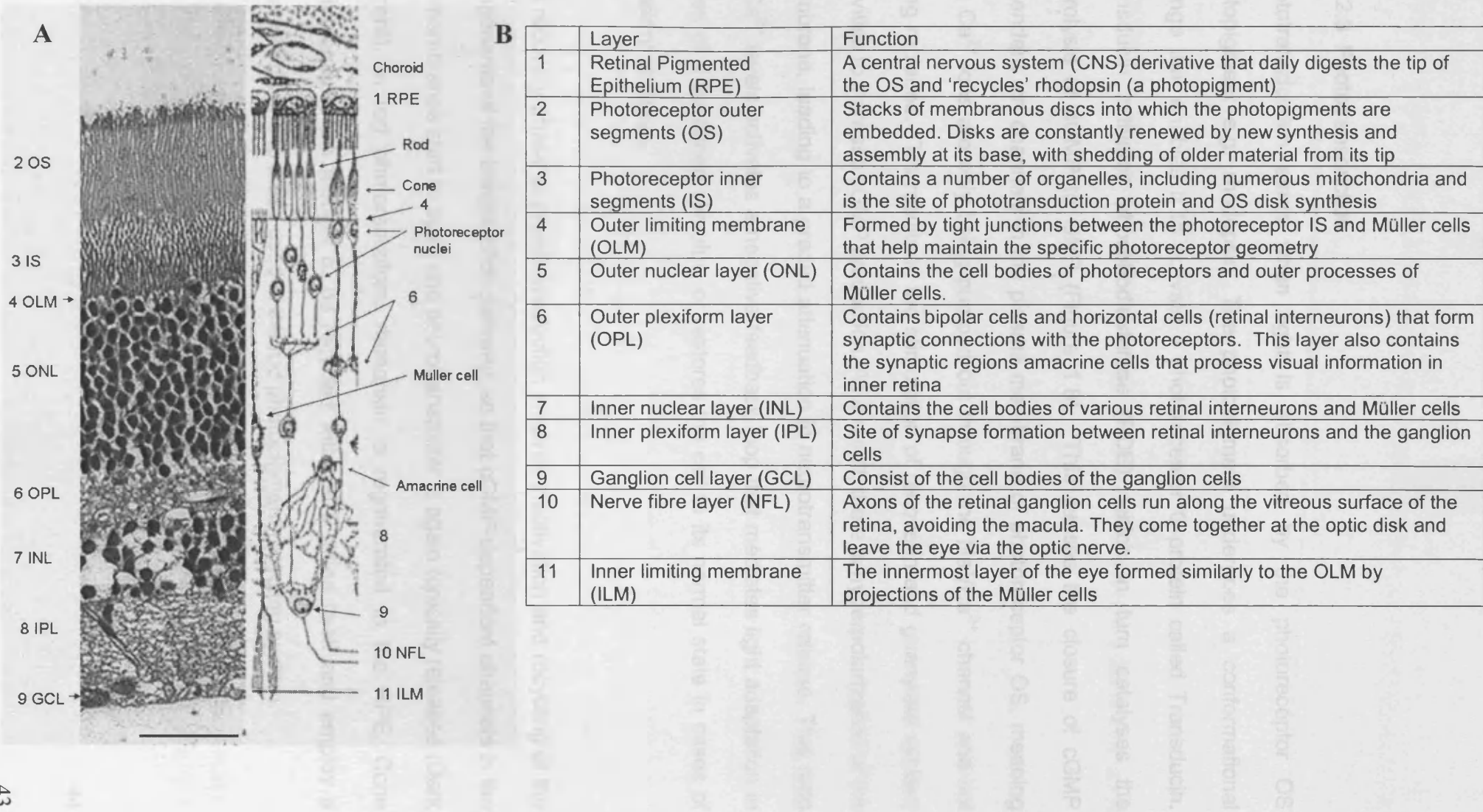


This pattern of development is very similar for most vertebrates, including mice. However, humans and mice do differ in the timing of the final stages of retinal differentiation, occurring *in utero* in humans and postnatally (P) in mice. This makes mice an excellent model for investigating the final stages of retinal development.

The different cellular layers of the mature neural retina are shown in Figure 1.7, alongside their function. In normal mice, the ganglion cell layer (GCL) and inner plexiform layer (IPL) have differentiated by P2, with the inner nuclear layer (INL) differentiating by P4. The outer retina at this time consists of progenitor cells. The uppermost layer of these cells are the newborn photoreceptors. Between P6-P8, the cell bodies of the newborn photoreceptors have formed a discreet layer as the outer nuclear layer (ONL), and the inner segments (IS) have become visible by light microscopy. They have passed the outer limiting membrane (OLM) and are budding in order to form the membranous disks of the outer segments (OS). Also over this period, the ribbon synapses start to form in the outer plexiform layer (OPL), initially as dyads and then forming triads to be fully functional by P12-P14. Thus by P12, differentiation of the retina into its final layers is complete (Bowes, C et al, 1988 and Grun, G, 1982).

Figure 1.7 The neural retina

(A) A semithin section of an adult murine retina (scale bar 50µm), aligned to the relevant layers in a schematic showing the individual cells of the neural retina (figure adapted from Fiore, Mariano et al, 74). (B) A table listing the main features and functions of the retinal layers (Rattner, A et al, 1999; Berne R.M. et al, 98).

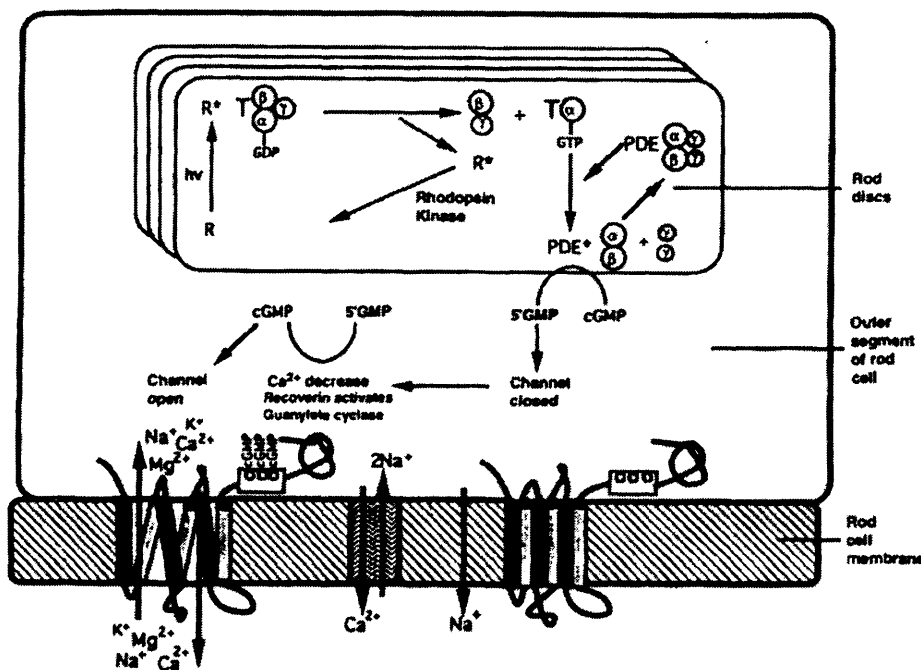


1.2.2.3 Phototransduction

Phototransduction starts when light is absorbed by the photoreceptor OS photopigment e.g. rhodopsin. The photopigment undergoes a conformational change that enables it to activate a photoreceptor G-protein called Transducin. Transducin activates phosphodiesterase (PDE), which in turn catalyses the hydrolysis of cGMP to GMP (Figure 1.8). This causes the closure of cGMP dependent ion channels in the plasma membrane of photoreceptor OS, meaning that Ca^{2+} ions are only being pumped out through the $\text{Na}^+/\text{Ca}^{2+}$ channel and not being replaced. This results in the stimulation of recoverin and guanylate cyclase activities to increase cGMP production. As a result, there is hyperpolarization of the membrane, leading to a graded attenuation in neurotransmitter release. This drop in Ca^{2+} levels activates a negative feedback loop that mediates light adaptation in cases of a sustained stimulus, or restores the cell to its normal state in cases of transient stimulus.

The recovery phase of phototransduction involves inactivation and recycling of the components of the transduction pathway, so that cGMP-dependent channels in the OS membranes start to open and neurotransmitter is again tonically released (Dark Current). In rod photoreceptors, rhodopsin is regenerated in the RPE. Cone photopigments are thought to be recycled within the retina itself and employ a different proteins to those used in the rod photopigment recycling system.

Figure 1.8 Phototransduction and photopigment recycling⁰



Photoactivated rhodopsin (R) molecules stimulate transducin (T), which in turn activates cGMP phosphodiesterase ($\text{PDE} \rightarrow \text{PDE}^*$), leading to reduced cytoplasmic cGMP concentrations and hence closure of cGMP-gated channels. This means that Ca^{2+} ions are only being pumped out through the $\text{Na}^+/\text{Ca}^{2+}$ channel and not being replaced, resulting in stimulation of recoverin and guanylate cyclase activities to increase cGMP production. The rod cell is returned to the "unexcited" state, with the 'used' disk recycled in the RPE (although the recovery reaction is shown here in the OS) (Humphries, P et al, 1992).

⁰Figure reprinted (abstracted/excerpted) with permission from Humphries, P., Kenna, P., and Farrar, G. J. (1992) *On the molecular genetics of retinitis pigmentosa*. Science.256, 804-8. Copyright 1992 AAAS.

1.3 ***Usher syndrome***

1.3.1 *The clinical phenotype*

1.3.1.1 The auditory phenotype: sensorineural hearing loss

Of the three clinical subtypes, type 1 is the severest form of Usher syndrome. It is defined by profound bilateral hearing loss from birth. These children do not develop speech in the absence of intervention, nor do they benefit significantly from the use of hearing aids. They also suffer from vestibular areflexia, the symptoms of which include a difficulty in lifting the head during infancy, delayed motor skill development, an inability to sense gravity and absence of nystagmus in response to ice-water caloric stimulation (Smith, R J et al, 1994). In contrast, individuals with type 2 have normal vestibular activity, and the congenital hearing loss is predominantly in the higher frequencies, with speech development benefiting from hearing aids and speech therapy (Smith, R J et al, 1994).

Usher syndrome type 3 displays the most range in phenotype. Patients show a highly variable type and degree of *progressive* sensorineural hearing loss, which also varies in age of onset. Hearing loss can range from normal, to USH2-like hearing impairment at younger ages, to profound or even USH1-like hearing impairment at more advanced ages (Ness, S L et al, 2003). Patients also show wide variability in vestibular function, ranging from normal to decreased but function is never absent (reviewed by Gorlin, R J et al, 1979).

1.3.1.2 The visual phenotype: Retinitis Pigmentosa

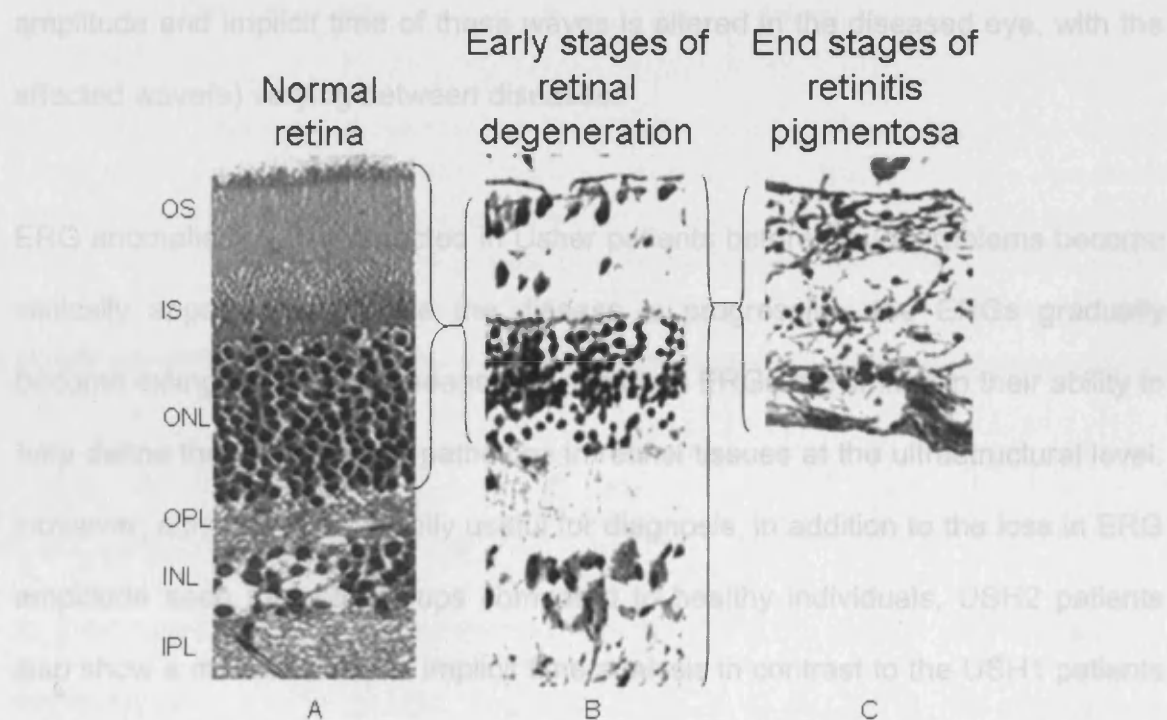
The progressive bilateral retinal degeneration displayed in Usher syndrome is caused by Retinitis Pigmentosa, a condition which can be inherited as an isolated disorder or as part of a syndromic condition. At the cellular level, the progression of RP starts with the degeneration of the photoreceptor layer (Figure 1.9). This is thought to occur by apoptosis, with diseased or dying photoreceptor cells inducing cell death in adjacent photoreceptor cells. The actual mechanism involved is as yet unknown but photoreceptor degeneration spreads through the rods of the midperiphery, to the cones in the midperiphery and then onto the photoreceptors of the fovea (Dryja, T P, 2001). Patients initially experience normal vision, with the development of night blindness as the rod photoreceptors die. This is followed by constriction of the visual fields and tunnel vision, as photoreceptor loss continues in the peripheral retina and onto the central photoreceptors. As the rest of the retinal layers degenerate, impairment in visual acuity increases and rapidly progresses to clinical blindness, although some patients maintain some residual but highly restricted vision (Smith, R J et al, 1994).

In all Usher patients, children are born with normal vision. In type 1 (USH1) patients, retinal degeneration starts in childhood/adolescence, whilst in USH2 patients degeneration occurs slightly later, in adolescence or in early adulthood (Smith, R J et al, 1994). The onset of RP in USH3 patients is also in early adulthood. It had previously been thought that hearing loss occurred prior to retinal degeneration in Usher syndrome but in some type 3 cases, onset of retinal

degeneration was prior to the onset of hearing loss (reviewed by Gorlin, R J et al, 1979).

which measures the functionality of the different layers of the retina by analysing the waves produced in response to: light absorption by the photoreceptors (a-wave), synaptic transmission from the photoreceptors to the second order retinal neurons (b-wave), and interactions between the RPE and

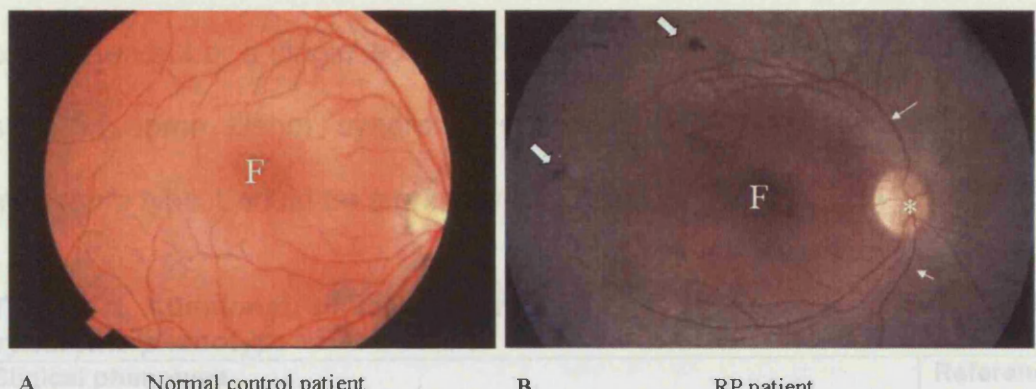
Figure 1.9 The pattern of cell death during the progression of retinitis pigmentosa.



(A) The layers of the neural retina are clearly discernable in the healthy eye. (B) In the early stages of RP, the photoreceptor layer is reduced in thickness where the photoreceptors have lost their outer segments and the number of photoreceptor nuclei is reduced. (C) In end-stage RP, there are no recognisable cell layers and the retina is reduced in both overall thickness and cell number (figure adapted from Dryja, T P, 2001).

1.3.1.4 Additional associated clinical characteristics

Figure 1.10 Features of retinitis pigmentosa seen by fundus examination



Aside from ERG abnormalities, patients with Usher syndrome or retinitis pigmentosa also develop fundus abnormalities. A normal healthy fundus (A) is compared to that of a retinitis pigmentosa patient (B) (National Eye Institute, National Institutes of Health). The fovea is located in the centre of each image (F). As the disease progresses, patients develop abnormal pigment deposits around the mid-periphery of the retina (block arrow). The optic-disk appears paler (*) and the retinal blood vessels are attenuated (→).

1.3.1.3 Atypical Usher syndrome

Atypical forms of Usher syndrome also exists, where the clinical phenotype does not correspond to the genetic diagnosis (Bolz, H et al, 2001). For example, a patient may have a mutation in an USH1 gene but displays a phenotype resembling USH3. Furthermore, cases of USH1D have been found where patients display the characteristic visual and auditory phenotype but have normal vestibular function (Otterstedde, C R et al, 2001).

1.3.1.4 Additional associated clinical characteristics

Other clinical features thought to be associated with Usher syndrome but seen in only a handful or a single isolated case are listed in Table 1.1. The cilia anomalies seen in some Usher syndrome sufferers, led to the suggestion that Usher syndrome type 1 could be a primary cilia disorder (Hunter, D G et al, 1986).

Table 1.1 Additional clinical features thought to be associated with the Usher syndrome phenotype

Clinical phenotype	References
Olfactory loss due to structural abnormalities of the nasal cilia	Marietta, J et al, 1997
Decreased sperm motility and reduced fertility	Hunter, D G et al, 1986
Abnormal axonemes of the retinal photoreceptor cells	Hunter, D G et al, 1986
Abnormal connecting cilia of the retinal photoreceptor cells	Hunter, D G et al, 1986
Profound hearing loss similar to USH1 individuals, but with normal peripheral vestibular function	Otterstedde, C R et al, 2001
Degeneration or atrophy of both the organ of Corti and the stria vascularis, accompanied by loss of the spiral ganglion in all USH types	Takasaki, K et al, 2000
Widespread loss of supporting cell elements of the organ of Corti and damage to the cochlea nerve in USH3 patients	Takasaki, K et al, 2000
Association with bronchiectasis	Bonneau, D et al, 1993
A drop in long chain polyunsaturated fatty acid levels in USH1 patients	Maude, M B et al, 1998
Adnexal tumours found on the lips	Began, D M et al, 2001
Decrease in intracranial volume and in the size of the brain and cerebellum	Keats, B J et al, 1999
Associated mental instability and/or learning defects = Hallgren's syndrome (connection between Usher and Hallgren's not yet known)	Gilbert, P., 0000

1.3.2 The genetics of Usher syndrome

The three clinical forms of Usher syndrome have been linked to eleven different loci (Table 1.2). Type I has been mapped to seven loci so far, labelled A-G, type 2 to three loci, A-C, and type 3 to one locus. At present, nine of the Usher genes have been cloned (*MYO7A*, *USH1C*, *CDH23*, *PCDH15*, *USH1G*, *USH2A*, *USH2B*, *USH2C* & *USH3A*), and it has been suggested that their USH1 proteins are involved in the same signalling pathway or multi protein complex (section 1.3.4.1 & Adato, A et al, 2005b, Boeda, B et al, 2002, Petit, C, 2001). It is thought that mutations in *MYO7A* are responsible for 29-60 % of the cases of USH1, whilst mutations in *USH2A* account for 41-80% of patients suffering from USH2 (Maubaret, C et al, 2005 and references therein).

Some genes underlying nonsyndromic hearing loss have been shown to be allelic with genes causing Usher syndrome e.g. *USH1B/DFNB2/DFNA11* (Weil, D et al, 1997); *USH1C/DFNB18*; *USH1D/DFNB12* and *USH1F/DFNB23* (Ahmed, Z M et al, 2002). Research suggests a genotype-phenotype correlation for some of the Usher genes e.g. *USH1C* and *CDH23*. In these cases, hypomorphic alleles are associated with nonsyndromic hearing loss, whilst more severe mutations result in Usher syndrome. This would suggest that residual function associated with some missense allele products is sufficient for normal vision but not for hearing (Ouyang, X M et al, 2002; Ahmed, Z M et al, 2002; Ahmed, Z M et al, 2003). Meanwhile, mutations in *USH2A* have been associated with nonsyndromic RP but not with isolated hearing loss. Mutations in this gene are thought to account for 70% of all

Usher type 2 patients and about 4.5% of nonsyndromic autosomal recessive RP (Seyedahmadi, B J et al, 2004).

Cases of digenic inheritance have been proven for *PCDH15* & *CDH23* (Zheng, Q Y et al, 2005) and suggested by linkage analysis for *USH3A* & *MYO7A* (Adato, A et al, 1999). This further highlights the genetically heterogenous nature of Usher syndrome and suggests that the Usher proteins may directly interact.

Table 1.2 Usher syndrome

Chromosomal location of the different Usher regions, the gene symbols, encoded protein and corresponding mouse model. Further references are given in the text of sections 1.3.3 and 1.3.5.

Usher type	Gene	Location	Protein	Mouse model
USH1A	<i>USH1A</i> (Kaplan, J et al, 1992)	14q32		
USH1B	<i>MYO7A</i> (Kimberling, W J et al, 1992; Smith, R J et al, 1992)	11q13.5	Myosin VIIA	<i>Shaker-1</i> (Gibson, F et al, 1995; Self, T et al, 1998; Kros, C J et al, 2002; Liu, X et al, 1999; Liu, X et al, 1998; Libby, R T et al, 2001)
USH1C	<i>USH1C</i> (Smith, R J et al, 1992; Saouda, M et al, 1998; Bitner-Glindzicz, M et al, 2000; Verpy, E et al, 2000)	11p15.1	Harmonin (Kobayashi, I et al, 1999; Scanlan, M J et al, 1999)	<i>Deaf circler</i> (Johnson, K R et al, 2003)
USH1D	<i>CDH23</i> (Bork, J M et al, 2001)	10q22.1	Cadherin 23	<i>Waltzer</i> (Di Palma, F et al, 2001a; Libby, R T et al, 2003)
USH1E	<i>USH1E</i> (Chaib, H et al, 1997)	21q21		
USH1F	<i>PCDH15</i> (Ahmed, Z M et al, 2001)	10q21.1	Protocadherin 15	<i>Ames Waltzer</i> (Alagramam, K N et al, 2001a; Ball, S L et al, 2003)
USH1G	<i>USH1G</i> (Mustapha, M et al, 2002)	17q24-25	Sans	<i>Jackson shaker</i> (Kikkawa, Y et al, 2003)
USH2A	<i>USH2A</i> (Eudy, J D et al, 1998a; Weston, M D et al, 2000; Van Wijk, E et al, 2004)	1q41	Usherin	
USH2B	PROPOSED GENE - <i>USH2B</i>	3p23-24.2	NBC3	<i>Sic4a7^{-/-}</i> (Bok, D et al, 2003)
USH2C	<i>USH2C</i> (Pieke-Dahl, S et al, 2000; Weston, M D et al, 2004)	5q14.3-21.3	Vlgr1b	<i>Vlgr1^{-/-}</i> (Johnson, K R et al, 2005; McMillan, D R et al, 2004; Weston, M D et al, 2004); Johnson, K R et al, 2005)
USH3	<i>USH3A</i> (Joensuu, T et al, 2001; Fields, R R et al, 2002)	3q25.1	Clarin-1	

1.3.3 *Usher syndrome proteins: their structure and localisation within the normal ear and eye* (ochlea, photoreceptors, RPE cells, testes and kidney (interestingly no kidney phenotype is seen in Usher syndrome patients) (Haszon, T et al, 1995).

1.3.3.1 Myosin VIIA

The USH1B protein of 2215 amino acids (Weil, D et al, 1996) is an unconventional myosin. Myosins consist of both heavy and light chain polypeptides, although the light chains of unconventional myosins are normally substituted for calmodulin molecules (Redowicz, M J, 2002 and references therein). The structure of the heavy chain of Myosin VIIA is shown in Figure 1.11. Studies have shown that mutations in the conserved IQ motifs disrupt interactions between myosin VIIAa and calmodulin (Bolz, H et al, 2004). Analysis of the effects of different mutations on the structure/function of the other Usher proteins is limited.

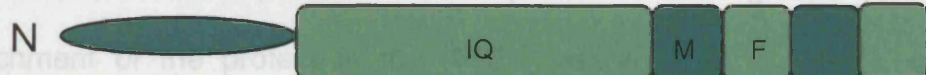


Figure 1.11 The structure of myosin VIIA

Myosin VIIA heavy chain consists of a motor domain typical to most myosins, followed by a neck region of five IQ motifs (IQ). These motifs normally bind the light chain. This is followed by a short coiled coil region which would suggest that myosin VIIA may function as a dimer. The protein ends with a tail region consisting of two large repeats, each comprising a MyTH4 (myosin tail homology) (M) domain and a FERM domain (band 4.1/ezrin/radixin/moesin-homology) (F) (Weil, D et al, 1996).

observed difference in retinal phenotypes between Usher type 1B and the shaker-1 mouse model (section 1.3.5). Finally it was confirmed that the protein was localised to the RPE and the connecting cilia of photoreceptor cells in both humans and

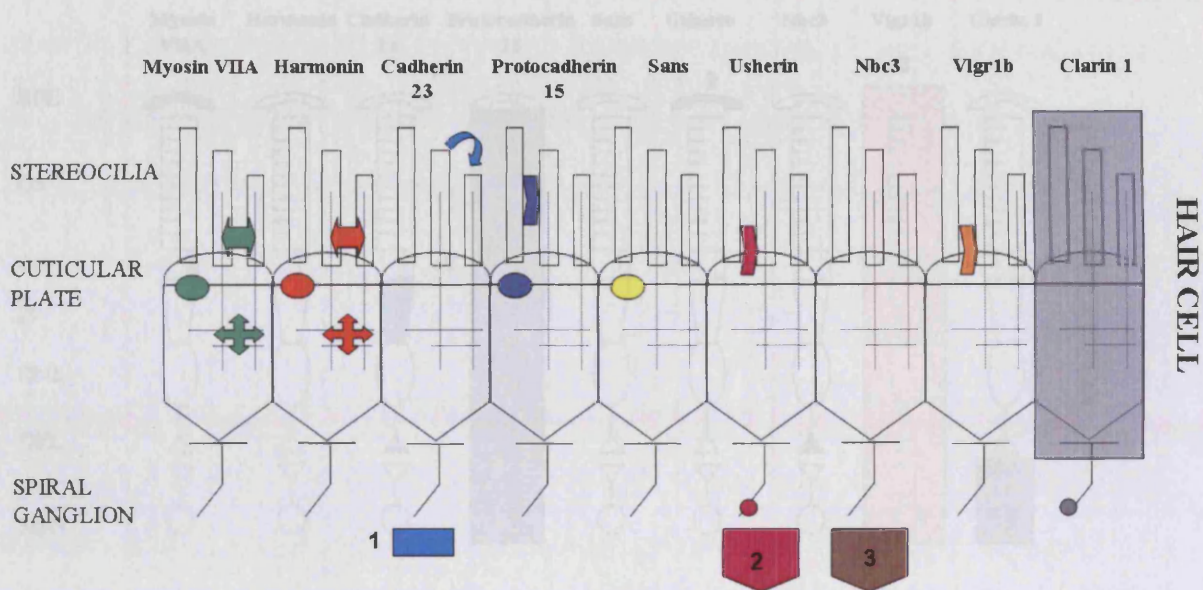
Myosin VIIA is expressed in the olfactory receptor sensory neurons (Weil, D et al, 1996), in the cochlea, photoreceptors, RPE cells, testes and kidney (interestingly, no kidney phenotype is seen in Usher syndrome patients) (Hasson, T et al, 1995). Within the cochlea the protein was localised to the hair cell stereocilia (first E12, Sahly, I et al, 1997), cuticular plate and cytoplasm of both inner and outer hair cells of guinea pig cochlea, and in the sensory epithelium of the bullfrog vestibular system (Hasson, T et al, 1995; Figure 1.12). The protein localisation data and the phenotype of the myosin VIIA null mice (*shaker-1*), led to the postulate that myosin VIIA may be responsible for organising the developing array of haircell stereocilia (Wolfrum, U et al, 1998). This postulate was supported by the null rat model *tornado* (Smits, B M et al, 2005) and the *Drosophila* model (Todi, S V et al, 2005), which showed similar auditory phenotypes and disorganization of the stereocilia of the hair cells (Johnston's Organ in the fly).

Studies on the retina proved more complex, with some groups claiming isolated enrichment of the protein to the RPE (Hasson, T et al, 1995), whilst others localised it to the RPE during development but showed that it was confined to the photoreceptor cells in the mature eye (Weil, D et al, 1996). Furthermore, some claimed that myosin VIIA was restricted to the RPE in mice but was seen in both the RPE and photoreceptor cells in humans (El-Amraoui, A et al, 1996). It was thought that this difference between rodents and humans would account for the observed difference in retinal phenotypes between Usher type 1B and the *shaker-1* mouse model (section 1.3.5). Finally it was confirmed that the protein was localised to the RPE and the connecting cilia of photoreceptor cells in both humans and

rodents (Figure 1.13), where it was thought to be involved in the transport of newly synthesised OS proteins to the site of disk membrane assembly (Liu, X et al, 1997). The difference in previous staining results of Hasson, T et al, 1995, Weil, D et al, 1996 and El-Amraoui, A et al, 1996, was explained through different tissue preparations and the use of different antibodies.

Figure 1.12 Localisation patterns of the Usher proteins within the normal ear

A schematic comparing and summarizing the localisation of the Usher proteins discussed in section 1.3.3 (all relevant references are included therein). The Usher proteins are thought to be involved in the different kinds of links that interlink the stereocilia or connect the stereocilia to the cytoskeleton. These different types of links are denoted by different kinds of arrows on the schematic. Coloured boxes around regions of the haircell highlights situations where expression of the Usher gene has been shown by *in situ* hybridisation. The exact pattern of protein localisation in these cases has yet to be confirmed. Localisation of the Usher proteins in addition to or other regions than the hair cells are denoted by numbers.

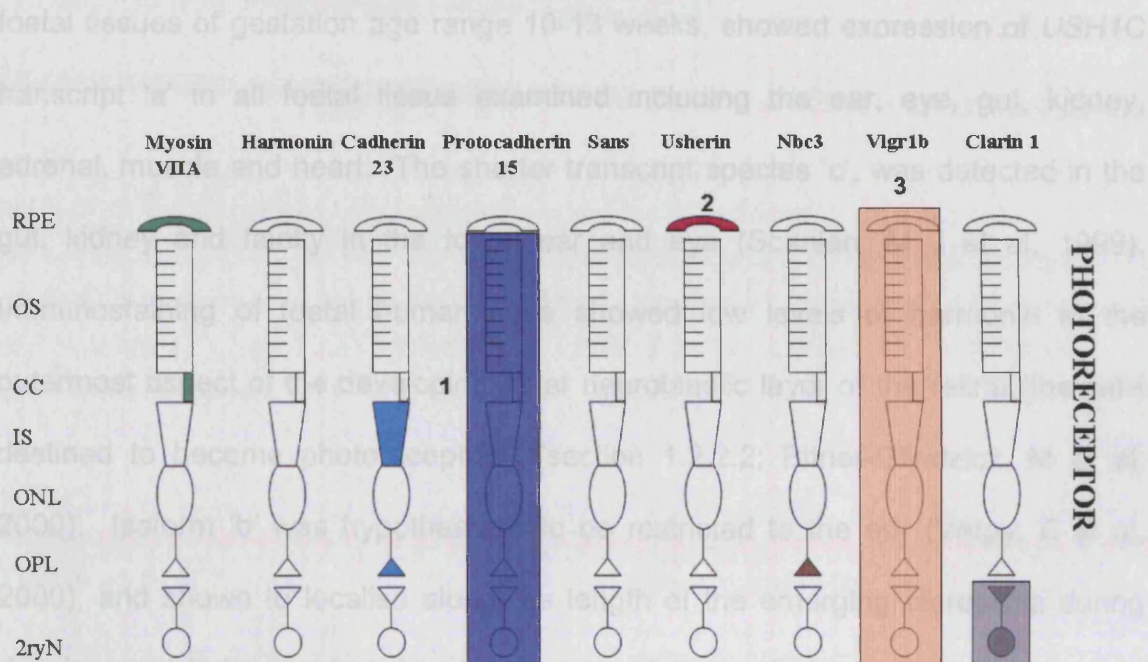


(1) Cadherin 23 is also localised to the Kinocilium, centrosomes and Reisners membrane. (2) Usherin is localised to the stria capillary basement membranes of the cochlea. (3) NBC3 is localised to the spiral ligament, beneath the stria vascularis, beneath the spiral prominence and in the suprastrial region of the cochlea. The exact subcellular localisations of Vlgr1b and Clarin-1 have not been confirmed but *in situ* hybridization has shown gene expression of both in the hair cells.

Tip link, (↗ curved arrow). Stereocilia-stereocilia links (↗ wide arrow head). Stereocilia-cytoskeletal links (↔ double ended arrow). Internal cytoskeletal links (⇋ four way arrow).

Figure 1.13 Localisation patterns of the Usher proteins within the normal eye

A schematic comparing and summarizing the localisation patterns of the Usher proteins in the eye, at the start/early stages of this research (section 1.3.3, all relevant references are included therein). Coloured boxes around regions of the photoreceptor highlights situations where expression of the Usher gene has been shown by *in situ* hybridisation. The exact pattern of protein localisation in these cases has yet to be confirmed. Localisation of the Usher proteins in addition to or other regions than the photoreceptor are denoted by numbers.



(1) The exact pattern of protocadherin 15 localisation in the photoreceptor has yet to be confirmed (section 1.3.3.4). (2) Usherin is localised to the Bruch's membrane adjacent to the RPE. (3) *Vlgr1b* mRNA has been detected in neural retina, RPE and hair cell progenitors.

2ryN, retinal interneurons. OPL, outer plexiform layer. ONL, outer nuclear layer. IS, photoreceptor inner segments. CC, connecting cilium. OS, photoreceptor outer segments. RPE, retinal pigmented epithelium.

1.3.3.2 Harmonin – the *USH1C* protein

Three isoform classes of harmonin (a, b, c) exist (Figure 1.14) produced by alternative splicing of 8 of the 28 exons of the *USH1C*. RT-PCR of various human foetal tissues of gestation age range 10-13 weeks, showed expression of *USH1C* transcript 'a' in all foetal tissue examined including the ear, eye, gut, kidney, adrenal, muscle and heart. The shorter transcript species 'c', was detected in the gut, kidney and faintly in the foetal ear and eye (Scanlan, M J et al, 1999). Immunostaining of foetal human eyes showed low levels of harmonin in the outermost aspect of the developing outer neuroblastic layer of the retina (the cells destined to become photoreceptors) (section 1.2.2.2; Bitner-Glindzicz, M et al, 2000). Isoform 'b' was hypothesized to be restricted to the ear (Verpy, E et al, 2000), and shown to localise along the length of the emerging stereocilia during development but was absent in the developed hair cell. In contrast, isoforms 'a' and 'c' were localised to the cuticular plate and stereocilia during development, and in the mature hair cell (Figure 1.12; Boeda, B et al, 2002).

downstream effectors (Hung, A Y et al, 2002; Harris, B Z et al, 2001a; Harris, B Z et al, 2001b; Huber, A, 2001; Cheng, et al, 2001).

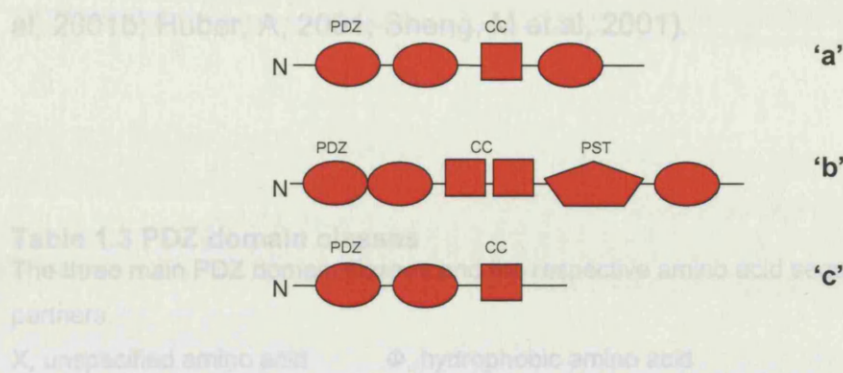


Figure 1.14 The structure of the three isoform classes of harmonin

Isoform class 'a' consists of 3 PDZ domains (**PDZ**) with 1 coiled coil (**CC**) region and corresponds to AIE75/PDZ-73. Class 'b' proteins have 3 PDZ domains, 2 coiled coil regions and a PST domain (rich in proline 27%, serine 13% & threonine 8%) (**PST**). Class 'c' isoforms have 2 PDZ domains and 1 coiled coil region.

All three harmonin isoform classes contain protein-protein recognition modules, known as PDZ domains (PSD-95/Dlg/ZO-1). These global folds form a pocket that specifically recognises short C terminal peptide motifs in their ligands, but can also recognise internal sequences within their binding partners, known as PBIs (PDZ binding interface), which structurally mimic the C terminus. The four C terminal amino acids of the ligand that make up the binding motif have different preferences for particular classes of amino acid, particularly P_0 , and P_{-2} , and can be divided into three classes based on these specificities (Table 1.3). PDZ domains are commonly seen in proteins involved in transporting and targeting appropriate proteins to sites of cellular signalling, in proteins that organise multiprotein signalling complexes, in proteins affecting the establishment and maintenance of cell polarity, in proteins that organize polar sites of cell-cell communication or in protein receptors and their

downstream effectors (Hung, A Y et al, 2002; Harris, B Z et al, 2001a; Harris, B Z et al, 2001b; Huber, A, 2001; Sheng, M et al, 2001).

Table 1.3 PDZ domain classes

The three main PDZ domain classes and the respective amino acid sequences of their binding partners.

X, unspecified amino acid Φ , hydrophobic amino acid

PDZ domain classification	Preferred amino acid sequence of P_{-3} , P_{-2} , P_{-1} , P_0
I	-X -S/T- X- Φ
II	-X- Φ - X- Φ
III	-X -D/E- X- Φ

1.3.3.3 Cadherin 23

CDH23 encodes a novel cadherin-like protein of 3354 amino acids (Bolz, H et al, 2001), expressed in the heart, brain, liver, lung, kidney, ear and eye (Bolz et al 2001). It consists of an N-terminal signal peptide, followed by an extracellular domain of 27 cadherin repeat (CAD) domains, a single transmembrane region (TM) and cytoplasmic tail that showed no homology to any known protein (Figure 1.15; Bolz, H et al, 2001). Within the retina, cadherin 23 is localised to two distinct compartments of the photoreceptor cells, at the OPL and IS, where it may have a role within the ribbon synapses (Figure 1.13). Numerous cadherins localise to synapses and N-cadherin has been shown to be required for axonal outgrowth and

guidance in the retina, suggesting a role for cadherin 23 in synapse plasticity and/or modulation of synapse activity (Bolz, H et al, 2002). The finding of cadherin

23 in the cochlea and vestibular apparatus of the null V^{21} (nonsense mutation) *Waltzer* mice, would suggest that not all isoforms of *Cdh23* are affected by this mutation. The *Waltzer* phenotype and is vital for correct hair bundle organization during development, whilst alternative

Figure 1.15 The structure of cadherin 23

CAD, cadherin repeat domains. TM, transmembrane region

In the ear two splice forms of *CDH23* exist (now known as isoform 'a'), with and without exon 68 as part of the mature mRNA. The + exon 68 transcript is prominent in the cochlear hair cell bundle but absent from other tissues (Siemens, J et al, 2002), whilst the – exon 68 species is detected in Reisners membrane and the developing hair bundle in immature hair cells. In the developed hair cells, cadherin 23 is restricted to the stereocilia tips in both cochlear and vestibular hair cells, where there are ongoing arguments as to its presence as a component of the tip link (Figure 1.12; Siemens, J et al, 2004; Lagziel, A et al, 2005). The tip link controls opening of mechanotransduction channels in the hair cell upon deflection of the stereocilia. Myosin-1C is the only known component of the mechanotransduction apparatus so far and has been shown to interact with the cytoplasmic domain of both isoforms of cadherin 23. Cadherin 23 was also seen to form links between the tallest stereocilia and the kinocilium during development (Siemens, J et al, 2004 and references therein).

A further two isoforms of cadherin 23 (isoforms 'b' and 'c') have recently been shown to be expressed in the murine retina and inner ear. The finding of cadherin 23 in the cochlea and vestibular apparatus of the null v^{6J} (nonsense mutation) *waltzer* mice, would suggest that not all isoforms of *Cdh23* are affected by this mutation. It would appear that isoform 'a' is coupled to the *waltzer* phenotype and is vital for correct hair bundle organization during development, whilst alternative roles for isoforms 'b' and 'c' exist (Lagziel, A et al, 2005).

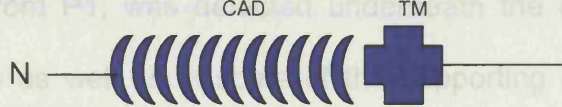
1.3.3.4 Protcadherin 15

In the ear, protocadherin 15 (Figure 1.16) was localised to the IHC and OHC stereocilia, concentrated at the cuticular plate level but also found along the length of the stereocilia. Protein levels along the stereocilia varied between bundles and between stereocilia of the same bundle (Figure 1.12). A similar pattern of staining was seen in the vestibular apparatus (Ahmed, Z M et al, 2003). Protein localisation data and the disorganization of hair cell stereocilia in protocadherin 15 mutant mice, led to the postulate that protocadherin 15 played a role in the maintenance of the links between the stereocilia to correctly organise the bundle (Ahmed, Z M et al, 2003).

et al, 2003). Sans, unlike the other USH1 proteins, is not found along the length of the stereocilia but from P1, was localised under the cuticular plate of the developing hair cells between the supporting cells (Aldao, A et al, 2005b) (Figure 1.12). High levels of Sans immunoreactivity were also seen in

Figure 1.16 The structure of protocadherin 15

The 1955 amino acid protocadherin 15 protein, has an N terminal signal peptide, 11 extracellular calcium binding domains (CAD), a transmembrane domain (TM) and a unique cytoplasmic domain (Ahmed, Z M et al, 2001).



Localisation of protocadherin 15 in the eye is disputed, with one group localizing the protein to the IPL, OPL and NFL in adult and foetal retinas (Alagramam, K N et al, 2001b) and another to the photoreceptor OS, with strongest immunoreactivity in the cones (Figure 1.13) (Ahmed, Z M et al, 2003). In the USH1F zebrafish model, *orbiter*, there are two closely related *Pcdh15* genes 'a' and 'b' that are differentially expressed in the ear and eye respectively. *Pcdh15a* morphants display a similar auditory phenotype to the mouse models but no retinal phenotype. Meanwhile the *Pcdh15b* morphants showed a decrease in b-wave ERG amplitude (although the a-wave was present, it could not easily be measured), with a reduction in correctly positioned melanosomes and a tilting of the photoreceptor OS, but no auditory phenotype. Protocadherin 15 was therefore postulated to be essential in OS alignment and interdigitation with the RPE (Seiler, C et al, 2005).

short protein isoform was localised to virtually every basement membrane in the

1.3.3.5 Sans

The USH1G protein, sans (Figure 1.17), was localised to the hair cells, where it did not directly interact with either actin, microtubules or immediate filaments (Weil, D

et al, 2003). Sans, unlike the other USH1 proteins, is not found along the length of the stereocilia but from P1, was detected underneath the cuticular plate of the developing hair cells as well as in some of the supporting cells (Adato, A et al, 2005b) (Figure 1.12). High levels of Sans immunoreactivity were also seen in cochlea ribbon synapses (Adato, A et al, 2005b). Gene expression has been seen in the eye but the pattern of protein localisation has not yet been determined (Weil, D et al, 2003).

Figure 1.16 The structure of usherin
The long isoform of usherin in a schematic diagram showing a domain homologous to a thrombospondin N-terminal-like domain (TSL), a laminin G-like domain (LGL), a pentapeptide (P), and a PDZ-binding motif (SAM).

Figure 1.17 The structure of sans

Sans is a novel 460 amino acid protein that contains three ankyrin-like domains (**AK**) involved in protein-protein interactions) at the N terminal end, a central region, a SAM (sterile alpha motif) domain (thought to be involved in homo- or heterodimerisation) (**SAM**) and has a PDZ binding motif at its C terminus.

1.3.3.6 Usherin

The USH2A gene encodes two protein isoforms of Usherin (Figure 1.18), both of which are expressed in the foetal cochlea, eye, brain, kidney, and in adult retina, brain, lung, bone marrow, adrenal gland, trachea, spinal cord, and thyroid gland (Eudy, J D et al, 1998b). Semi quantitative RT-PCR showed that transcription levels were low in all tissues except the eye (Van Wijk, E et al, 2004), where the short protein isoform was localised to virtually every basement membrane in the cochlea (Figure 1.12), and to the lens capsule and the Bruch's layer (found between the RPE and the choroids) in the eye (Bhattacharya, G et al, 2002; Figure 1.13). The long isoform has been localised to the base of the differentiating

cochlea and vestibular hair cell stereocilia (possibly acting as a component of the ankle links between stereocilia), but is only maintained in the stereocilia of mature vestibular hair cells (Adato, A et al, 2005a).

the supraline region (Figure 1.12). These findings suggested that in the ear, the stereocilia themselves may be involved in cochlear fluid homeostasis, which is

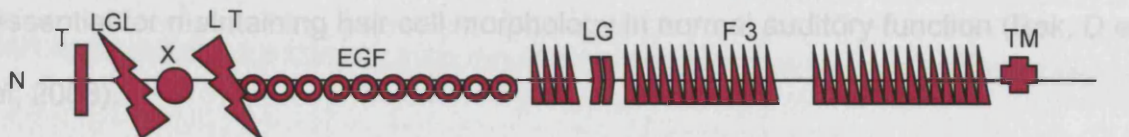


Figure 1.18 The structure of usherin

The long isoform of usherin is 5202 amino acids, containing the following: a domain homologous to a thrombospondin N-terminal-like domain (T), a laminin G-like domain (LGL), a pentaxin (X) domain, a laminin N-terminal (LT) domain, 10 laminin-type EGF-like repeats, four fibronectin type 3 (F3) repeats, 2 laminin G (LG), 28 F3 repeats, a transmembrane domain (TM) and a C terminal class 1 PBI. Between F3 repeats 13 and 14 there is a partial F3 domain and a stretch of ~350 amino acids with no significant homology to any known domain (Van Wijk, E et al, 2004).

1.3.3.7 NBC3

NBC3 is proposed to be the protein involved in Usher type 2B, although no mutations in the gene in humans have been detected to date. The visual and auditory systems have a special requirement for H^+ disposal during sensory transduction, mediated by the sodium bicarbonate cotransporter, NBC3 (SLC4A7) (Figure 1.19). In wildtype mice the transporter is localised to the photoreceptor synaptic terminals of the OPL (Figure 1.13). The plasma membrane ATPase - Ca^{2+} transporters found at the photoreceptor synaptic terminals, extrude Ca^{2+} in exchange for H^+ . It is postulated that NBC3-mediated bicarbonate flux in the

maintaining normal rates of Ca^{2+} efflux. In the cochlea it is localised to the spiral ligament and to fibrocytes beneath the stria vascularis, spiral prominence and in the supralabyrinthine region (Figure 1.12). These findings suggested that in the ear, the fibrocytes themselves may be involved in cochlear fluid homeostasis, which is essential for maintaining hair cell morphology in normal auditory function (Bok, D et al, 2003).

that isoform 'b' acts as a calcium ion receptor whilst isoforms 'd' and 'e' are secreted as extracellular proteins whose function is related to extracellular Ca^{2+} distribution (Yagi, H et al, 2005).



Figure 1.19 The structure of NBC3

This 12 transmembrane domain (TM) protein has *N*-linked glycosylation sites on two of its extracellular loops (LOOP); protein kinases A and C, casein kinase II, and ATP/GTP-binding consensus phosphorylation sites and potential sites for myristylation and amidation on other loops. Both its N and C termini are cytoplasmic and it has a C terminal PBI (Pushkin, A et al, 1999).

Figure 1.20 The structure of Vlgr1b

The 6300 amino acids of VLGR1b produce a large ectodomain of 35 Calyx domains (CAL) (consists of which bind calcium ions and other cations), 1 LamG/Teph/TPTX homology domain

1.3.3.8 Very large G-coupled receptor protein b (Vlgr1b)

Multiple isoforms of Vlgr1 exist (a-c, Weston, M D et al, 2004; McMillan, D R et al, 2002 and d-e, Yagi, H et al, 2005) that vary in structure, showing different

expression patterns within species and between species. All the mutations associated with Usher syndrome have been found in *VLGR1b*, expressed by neural retinal precursors and by cells destined to become the RPE (Figure 1.13).

Transcript expression continues at low levels in adulthood, implying a function for the protein (Figure 1.20) in neural development and/or maintenance (McMillan, D R et al, 2002; Schwartz, S B et al, 2005). The EPTP domain has been postulated to be an epilepsy-associated repeat that when mutated, results in autosomal

dominant lateral temporal lobe epilepsy which increases susceptibility to audiogenic seizures in mice. This postulate is supported by the finding that *frings* mice that express a truncated Vlgr1b protein (lacks the EPTP repeat) experience audiogenic seizures. Other proteins that possess Calx- β domains have been shown to act as calcium dependent aggregating molecules. Therefore it has been postulated that isoform 'b' acts as a calcium ion receptor whilst isoforms 'd' and 'e' are secreted as extracellular proteins whose function is related to extracellular Ca^{2+} distribution (Yagi, H et al, 2005).

reproducible in either the rat or human (Geller, S.F. et al 2004; Figure 1.12).

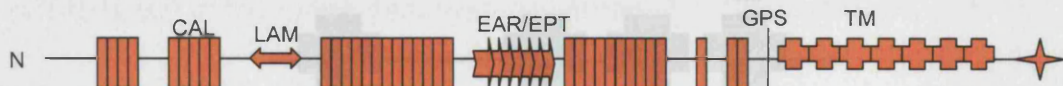


Figure 1.20 The structure of Vlgr1b

The 6300 amino acids of VLGR1b produce: a large ectodomain of 35 Calx- β domains (**CAL**) (portions of which bind calcium ions and other cations), 1 LamG/TspN/PTX homology domain (**LAM**), 7 EAR/EPTP repeats forming a putative β -propeller folding domain (a protein interaction domain that acts as a highly specific receptor (**EAR/EPT**), with possible ligands including extracellular or cell adhesion proteins), a GPS (G-protein coupled proteolysis site) (**GPS**), a B-family 7 transmembrane region (**TM**), a putative intracellular tail with potential serine phosphorylation sites, and a C terminal class 1 PBI (Weston, M D et al, 2004).

Vlgr1b shows similar localisation in the inner ear, to the long isoform of Usherin. It too is localised at the base of the stereocilia in developing vestibular and cochlea hair cells but is absent in the stereocilia of mature cochlea hair cells (Adato, A et al, 2005a; figure 1.12).

1.3.4 Usher syndrome proteins: their interactions in the normal ear and eye

1.3.3.9 Clarin-1

The USH3A protein, Clarin-1 (Fields, R R et al, 2002) (Figure 1.21), belongs to a large family of small integral membrane glycoproteins. PCR amplification showed *USH3A* transcripts in the human retina, inner ear, testes, skeletal muscle and olfactory epithelium (Joensuu, T et al, 2001). *In situ* hybridisation showed gene expression in the IHC and OHC of the organ of Corti and in the spiral ganglion cells (Figure 1.12; Adato, A et al, 2002). Immunohistochemistry labelled Clarin-1 in the horizontal cells and the Müller cells of the inner retina, but this was not reproducible in either the rat or human (Geller, S.F. et al 2004; Figure 1.13).



Figure 1.21 The structure of Clarin-1

Clarin-1 consists of 204 amino acids forming four transmembrane domains (TM) (Fields, R R et al, 2002).

1.3.4 Usher syndrome proteins: their interactions in the normal ear and eye

1.3.4.1 Usher protein complexes formed in the normal ear

Yeast two-hybrid and other interaction studies on the Usher proteins, initially discovered novel or non-Usher protein binding partners for harmonin, including MCC2 (Ishikawa, S et al, 2001); β -catenin (Johnston, A M et al, 2004); PP2AC- α , PP2AC- β or PPP6C (Hirai, A et al, 2004) and Harp (Johnston, A M et al, 2004). Yet because of the similar phenotypes of all the USH1 patients and USH1 mouse models, it was hypothesised that all the type 1 proteins interacted, forming a multi-protein functional complex. The absence of any one of the USH1 proteins would therefore result in the same deafness-blindness phenotype (Boeda, B et al, 2002).

Harmonin has the ability to form dimers or long chains of protein, through interaction of its own PDZ1 and C terminus (Siemens, J et al, 2002). It is also able to interact with the actin cytoskeleton, using the C terminus of isoform 'b' (Boeda, B et al, 2002). Siemens *et al* (2002) and Boeda *et al* (2002) went onto show that myosin VIIA which does not have the classic C terminal sequences usually required for PDZ interactions, binds PDZ1 of harmonin isoform 'b' and that cadherin 23 interacts with PDZ2 of the same isoform. The fact that harmonin isoform 'b' was seen along the entire length of the developing stereocilia and that it was mislocalised in the *shaker-1* mice, suggested that in the ear, myosin VIIA functions to convey harmonin isoform 'b' to its site of action in the stereocilia. The distribution of isoform 'b' in the stereocilia overlaps with that of cadherin 23, which is thought to interlink the stereocilia and organize the stereocilia bundle until it

reaches maturity. Therefore harmonin isoform 'b', once correctly localised by myosin VIIA, may function to link cadherin 23 to the actin filaments of the growing stereocilia, during hair cell bundle development (Boeda, B et al, 2002). Whether this complex is found in adults is not yet certain due to the argument surrounding the localisation of cadherin 23 to the stereocilia tip links (section 1.3.3.3).

Siemens *et al* (2002) also noted that cadherin 23 had two PBIs: the C terminal PBI interacts with PDZ2 of harmonin, whilst an internal PBI interacts with PDZ1. The presence of exon 68 in the ear isoform of cadherin 23, perturbs the internal PBI resulting in harmonin-cadherin 23 interactions through PDZ2 only. In the eye using the -68 cadherin 23 isoforms, there is the possibility that one harmonin molecule is able to interact with two cadherin 23 molecules at the same time, through both PDZ1 and PDZ2 (Siemens, J et al, 2002). This raises questions as to whether myosin VIIA is necessary to correctly localise harmonin within the eye and whether it competes with cadherin 23 for interaction with PDZ1. Different kinds of mutations in these genes may alter the proteins binding ability, giving one of the proteins a greater binding advantage over the other. This may explain why particular mutations affect the ears only, giving nonsyndromic deafness phenotypes rather than Usher syndrome. Another theory is that the alternatively spliced isoforms for both cadherin 23 and harmonin that are differentially expressed between the retina and cochlea, and could result in differing USH1 protein complexes forming in the two organs.

1.3.4.2 Postulated Usher protein complexes formed in the normal eye

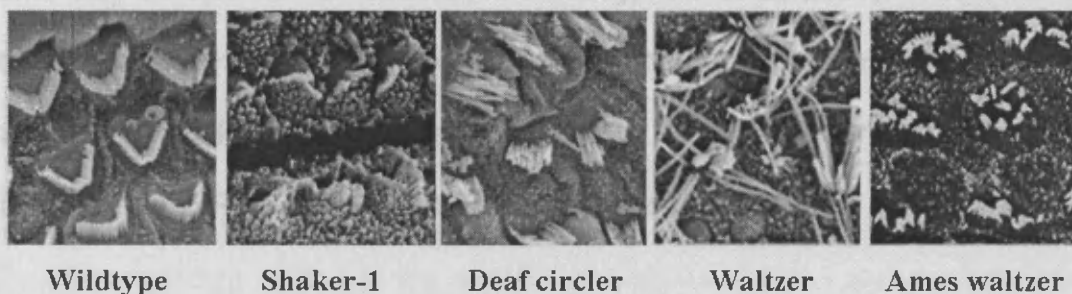
Very little is known about the interactions of harmonin or any of the Usher proteins in the eye. It has been suggested that the USH1 proteins form a similar complex in the retina, as in the ear as discussed previously. Yet the fact that the USH1 patients have normal vision at birth would suggest that if this complex did form, it has a different function to that seen in the ear where it is essential for correctly organising the developing hair cell bundle and therefore for hearing at birth.

1.3.5 *Mouse models of Usher syndrome*

All the USH1 mouse models display similar degrees of hyperactivity, head tossing, circling and profound deafness (references listed in Table 1.2). This is thought to be caused by disorganization or degeneration of auditory and vestibular hair cell stereocilia (Figure 1.22). In contrast, the USH1 mutants show little, if any, retinal abnormalities and certainly nothing comparable to the human phenotype.

The *shaker-1* (USH1B) and *waltzer* (USH1D) mice models used in this research, have normal vision throughout their lifespan and show only minor reductions in ERG a- and/or b- wave amplitudes (Libby, R T et al, 2001; Libby, R T et al, 2003). The *deaf circler* (USH1C) mouse has a normal ERG, with only a slight degeneration in peripheral region of the retina seen in a small sample of mice (Johnson, K R et al, 2003).

Figure 1.22 Scanning electron microscope images comparing the organisation of hair cell stereocilia in the USH1 mutant model mice



The auditory hair cells are arranged in a single row of IHC and a triple row of OHC. On the apical surface of each hair cell, the stereocilia are arranged in a characteristic "V" shape, with each stereociliary tip connected to its taller neighbour. This organized formation is seen in the wildtype mouse but is lost in all the null mouse models for USH1.

Figure adapted from: wildtype, Johnson, K R et al, 2003. *shaker-1*, Self, T et al, 1998. *deaf circler*, Johnson, K R et al, 2003. *waltzer*, Di Palma, F et al, 2001. *ames waltzer*, Alagramam, K N et al, 2001a.

The reason for the differences in retinal phenotypes between humans and mice is as yet unknown. It has been suggested that genetic background may be a cause, or that mutations found in humans resulting in Usher may be different from those found in mice, or that there is a degree of redundancy in mice not seen in humans. A further hypothesis is that there are just intrinsic differences between the two species, one of the main differences being that the first sign of retinal degeneration in human patients generally occurs after several years of age, well beyond the lifespan of a mouse. Several mutant mouse strains e.g. the model for Oguchi disease (Chen, J et al, 1999), developed retinal degeneration after a certain amount of exposure to light. So it has been suggested that the retinas of Usher

mutant mice do not degenerate because they have not been exposed to light in the same way as their human counterparts (Libby, R T et al, 2001). Yet it has been argued, for the *waltzer* mice in particular, that the decreases in implicit time in the murine ERG could be an important observation of the very early retinal pathology of USH1 (Libby, R T et al, 2003; Seeliger, M W et al, 2001).

1.4 *Research aims*

Mutations in *USH1C* are known to cause Usher syndrome and its function in the ear has been postulated. However very little was known about harmonin's localisation and function in the eye. Therefore the aims of this research were to:

- Determine the temporal and spatial expression of *Ush1c* and harmonin within the normal murine eye.
- Investigate potential harmonin-interacting proteins within the normal eye.
- Infer possible pathogenic mechanisms in Usher syndrome.

1.5 *Background to research methodology*

1.5.1 Methods for determining gene expression and protein localization patterns

Gene expression can be analysed on a small scale using the reverse transcription polymerase chain reaction technique, or on a larger scale with cDNA microarrays. Gene expression patterns on tissue sections can be analysed by *in-situ* hybridization, whilst protein localisation is examined by immunostaining techniques.

1.5.1.1 Reverse Transcription Polymerase Chain Reaction (RT-PCR)

RT-PCR-based assays are the most common method for characterising or confirming gene expression patterns and comparing mRNA levels in different sample populations. As RNA cannot serve as a template for PCR, the first step in an RT-PCR assay is the reverse transcription of the RNA template into cDNA, followed by its amplification in a PCR reaction. Gene expression levels can be compared in a semi-quantitative fashion if housekeeping genes e.g. *3-phosphate-dehydrogenase (GAPDH)*, are amplified simultaneously with the target, to act as an internal reference against which other RNA values can be normalised. Real-time RT-PCR is a fully quantitative approach that uses fluorescent reporter molecules to monitor the production of amplification products during each cycle of the PCR reaction (reviewed in Bustin, S A, 2000).

1.5.1.2 Immunostaining

Protein localization by immunostaining, involves the binding of antibodies to target proteins which may be detected directly or indirectly. Direct detection systems, use an antibody that is directly labelled with a reporter molecule e.g. a fluorophore. Alternatively there is the indirect system, which uses the primary antibody as an intermediate unlabelled molecule, which once bound to its target, is in turn detected and bound by a secondary reagent (e.g. a secondary antibody). This secondary molecule is conjugated to a reporter which may be a fluorophore or an enzyme (e.g. alkaline phosphatase). This system allows for amplification of low level signals through the use of multiple specific antibodies and the use of readily available commercial affinity-purified secondary antibodies. The secondary labelling can be varied to allow for investigation of a single protein under different conditions whilst using only the single primary antibody e.g. immunofluorescence and Western blotting. It also allows for double labelling of cells and tissue for more than one protein at a time.

The difficulties associated with the use of antibodies in experiments, include the fact that their immunoreactivity can be affected by the fixation conditions required to maintain tissue architecture. Furthermore, the use of secondary antibodies can result in high levels of non-specific background labeling. This can be reduced using the direct labeling system but this has the disadvantage that a large variety of primary antibodies need to be produced and this is expensive. There are also issues of

cross reactivity between species, where an antibody raised to a mouse protein may detect a different protein in rabbits, giving false positives (Strachan, T et al, 1999).

1.5.1.2.1 Synthesis of antibodies

1.5.1.2.1.1 Selection of epitopes

Traditionally, antibodies have been isolated by immunising suitable animals (e.g. rodents, rabbits, goats, etc.) with a suitable immunogen/antigen. Two types of immunogen are commonly used:

- **Synthetic peptides.** A synthetic peptide of 12-50 amino acids long is chosen from the amino acid sequence and conjugated to a suitable carrier molecule (e.g. keyhole limpet hemocyanin (KLH)), allowing the peptide to adopt a conformation that resembles that of its native state. Although technically simple, the success of this approach is limited due to the reduced number of amino acids with which to form an epitope. Furthermore the use of a short peptide increases the chance of finding homology with other proteins, resulting in cross-reactivity.
- **Fusion proteins.** A cDNA sequence is cloned into an appropriate expression cloning vector for expression in bacteria. The expression vector can confer properties such as the ability to be secreted into the extracellular medium or protection from degradation. This method has a higher success rate as the fusion protein contains most/all of the desired amino acid sequence (Strachan, T et al, 1999).

If immunization is successful, the animal's immune system secretes the protein-specific antibodies into the serum. The serum also contains antibodies to the carrier protein and any other antigens to which the animal had been exposed. Thus the serum is a heterogeneous mixture of antibodies, each produced by a different B lymphocyte. Different antibodies recognize different epitopes of the immunogen, and so the serum is classed as a polyclonal antibody source. Monoclonal antibodies are produced by propagating a clone of cells from a single immortalized B lymphocyte (Strachan, T et al, 1999).

Whether using synthetic peptides or fusion proteins to generate an antibody, it is important that the peptide is hydrophobic. There are two main scales for examining the hydrophobic nature of a peptide: the Kyte-Doolittle scale and the Hopp-Woods scale (<http://arbl.cvmbs.colostate.edu/molkit/hydrophathy/>). With the Kyte-Doolittle scale, peptide regions with values above 0 are said to be hydrophobic in character. For the Hopp-Woods scale, values greater than 0 are said to be hydrophilic. Both scales employ window sizes, referring to the number of amino acids examined at the time, when calculating antigen hydrophobicity. Window sizes can vary from 5 to 25 and should be of a magnitude appropriate for the expected size of the structural motif under investigation:

- Window size of 5-7 is good for determining hydrophilic regions.
- Window size of 19-21 makes hydrophobic, membrane-spanning domains stand out clearly (typically > 1.6 on the Kyte-Doolittle scale).

1.5.1.2.1.2 Polyclonal antisera production protocol

The polyclonal antisera production protocol is a multi-step process that in rabbits takes 77 days. On day zero a pre-bleed was taken from the animal, prior to injection with the antigenic peptide. The primary immune response results in low level production of predominantly IgM antibodies. A booster antigen inoculation was performed on day 14 and then again on day 28, with a test bleed/blood sample taken from the animal on day 35. The secondary immune response is much quicker, producing IgGs at a far greater level and for a longer period than that seen for the primary response (Roitt, I et al, 2001). Further booster antigen injections were given to the animal on days 42, 56 and 70 with test bleed recovery on days 49, 63, and the final harvest bleed on day 77. The antibody was not initially purified from the sera sample as this process can damage the antibody.

1.5.1.2.2 Techniques for the validation of synthesised antibodies

- ELISA analysis

Unconjugated peptides are bound to ELISA plates and the preimmune bleed, individual test bleeds and harvest bleed are analysed at a variety of dilutions, to see if IgGs to the antigenic peptides have been produced.

- Ouchterlony test

To detect whether any IgGs are produced during the synthesis protocol, antigenic proteins/immunoglobulins are placed in wells radial to the central antibody well, and allowed to diffuse through agarose and come into physical contact. If the

antibody serum contains IgGs to an antigen in one of the radial wells, a visible precipitate is formed.

- Immunolabelling and Western blotting

In order to determine whether the antibody can detect and is specific for the protein it was raised against, tissue sections can be immunolabelled and protein extracts blotted.

1.5.2 Techniques for investigating protein interactions

Protein interactions techniques that use libraries or large numbers of candidate interacting-proteins, include mass spectroscopy, phage display and the yeast two-hybrid system. Individual possible interactions between proteins can then be further analysed using FRET (Fluorescence Resonance Energy Transfer), yeast mating and co-immunoprecipitation.

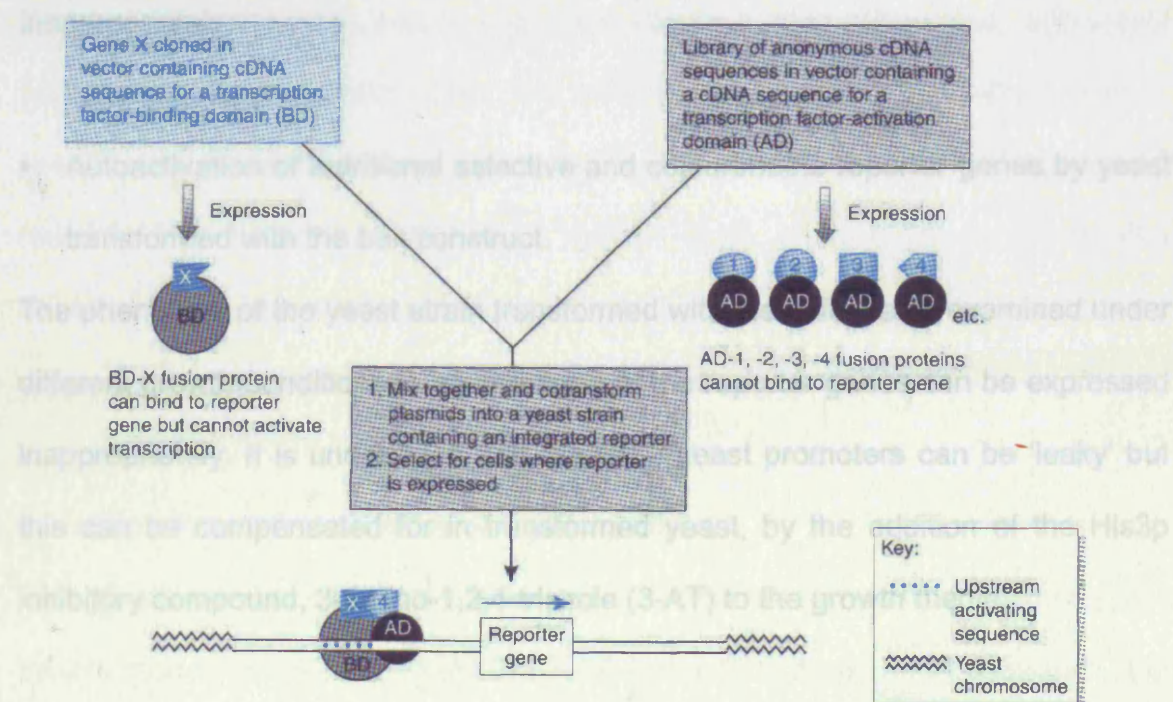
1.5.2.1 The yeast two-hybrid system

The yeast two-hybrid system employs yeast transcriptional activators, such as GAL4, that contain two distinct functional domains: a DNA-BD (binding domain) that binds to an upstream activation site (UAS) of the yeast genes and a transcriptional activation domain (AD) to drive the gene's transcription. Yeast, unlike bacteria, can support the propagation of more than one plasmid having the same replication

origin, i.e. there is no plasmid incompatibility issue in yeast. Therefore when these domains are expressed as spatially distinct fusions with candidate interacting proteins in yeast, these subunits may be brought into sufficiently close proximity to reconstitute normal function. This interaction can be measured as the activation of expression of specific reporter genes (Figure 1.23; Toby, G G et al, 2001). Since the test interaction happens within the nucleus of *S.cerevisiae*, it may produce some false positives for nuclear or membrane proteins, so any candidate positive interactors must be confirmed by alternative methods. The yeast strains themselves contain the reporter genes *HIS3* and *ADE2* which are only expressed when a protein-protein interaction occurs. *LacZ* a colourimetric reporter gene is also only expressed when a protein-protein interaction occurs. Prior to transformation

Figure 1.23 A schematic showing the basic steps involved in a yeast two-hybrid reaction.

(Figure adapted from Strachan, T et al, 1999)



The yeast two-hybrid system is subject to a number of false positives and false negatives which must be detected during the screening process.

False Positives

- Autoactivation of nutritional selective reporter genes by the untransformed yeast strains.

In the MATCHMAKER two-hybrid system, the bait and prey vectors carry nutritional reporter genes *TRP1* and *LEU2* respectively. The yeast strains themselves contain the reporter genes *HIS3* and *ADE2* which are only expressed when a protein-protein interaction occurs. *LacZ* a colourmetric reporter gene is also only expressed when a protein-protein interaction occurs. Prior to transformation and screening, the phenotypes of the yeast strains are examined under different growth conditions to ensure that none of the reporter genes can be expressed inappropriately.

- Autoactivation of nutritional selective and colourimetric reporter genes by yeast transformed with the bait construct.

The phenotype of the yeast strain transformed with the bait is also examined under different growth conditions to ensure none of the reporter genes can be expressed inappropriately. It is understood that the *HIS3* yeast promoters can be 'leaky' but this can be compensated for in transformed yeast, by the addition of the His3p inhibitory compound, 3-amino-1,2,4-triazole (3-AT) to the growth media.

- Inappropriate yeast mating

Yeast mating is the process by which multiple plasmids are introduced into a single yeast cell. One yeast strain of cassette type MAT α expressing one plasmid, is incubated with a MAT α cassette strain containing the other plasmid. At this point, one strain transfers its DNA to the other strain, allowing expression of both plasmids in one cell. Yeast mating control experiments are set up using the empty MATCHMAKER III vectors to ensure that the reporter genes will only express if an interaction occurs between bait and prey.

False Negatives

- Incorrect production of bait fusion proteins

Interactions can be missed or false interactions found (false positives), if the fusion protein produced in the yeast is not the desired bait protein. Therefore the bait construct is sequenced before and after transformation into yeast, and yeast protein extracts on western blots are probed with tag-specific and bait protein-specific antibodies. The use of yeast protein extracts and/or certain antibodies can result in high background levels on western blots. In such cases, an *in vitro* translated (IVT) bait protein using the inbuilt T7 promoter in the bait vector, can be used as the bait protein source to try and minimise background levels.

- Bait proteins are toxic to the host yeast cells

The growth rates of yeast transformed with the bait is compared to that of yeast transformed with the empty MATCHAKER III vectors. A reduction in growth rate

would suggest that the bait fusion protein is toxic to the yeast and therefore inappropriate for screening.

- Failure of yeast mating reactions

Yeast mating control experiments are set up using positive controls/known interactors to ensure that the reporter genes will express if an interaction does occur.

- Non-representative amplification of prey library cDNA

The prey library to be screened must contain at least 10^6 independent clones to maximise the number of different protein interactions examined. Amplification of aliquots with insufficient volume must be representational, such that the same range and proportion of transcripts in the original cDNA library aliquot are maintained. Libraries in the pACT2 vector (Appendix 15), are known to be poor amplifiers in comparison to other GAL4 libraries (expected yields of plasmid DNA per 1×10^6 cfu: pACT2 Libraries = ~0.25 mg; all other MATCHMAKER GAL4 Libraries = ~1 mg, (Y2H Protocols, Clontech)) and require maximum efficiency cells for transformation. The library titre (the number of independent clones per ml) is determined after amplification and must be $>10^8$ cfu/ml for plasmid libraries to ensure continued representation during screening.

- Reduced transformation efficiency during bait generation and library screening.

Library screening by co-transformation, can be accomplished either through the simultaneous transformation of both bait and prey plasmids into one cell, or

through sequential transformation. Simultaneous co-transformation is generally preferred because it is simpler than sequential transformation. There is also the risk that expression of proteins encoded by the first plasmid may be toxic to the cells, thus should spontaneous deletion mutants arise that have a growth advantage, they will accumulate at the expense of true clones containing intact plasmids. On the other hand, if there is no selective disadvantage to cells expressing the first cloned protein, then sequential transformation may be preferred because it uses significantly less plasmid DNA than simultaneous co-transformation.

The overall transformation efficiency for transformation with a single plasmid and for sequential co-transformations should be at least 1×10^4 cfu/ μ g. Simultaneous co-transformation usually results in an efficiency an order of magnitude lower, due to the lower probability that a particular yeast cell will take up both plasmids. A low transformation efficiency would suggest that the bait construct is not optimal and during co-transformation, can reduce the number of library proteins screened and so possible interactions may be missed. Reduced transformation efficiency may be due to suboptimal carrier DNA; suboptimal yeast competent cells; a contaminant in the water that can affect transformation efficiency and/or cell growth; and suboptimal plasmid preparation (Yeast Protocols Handbook, Clontech). ~

- Species incompatibility

Possible interactions may be missed if the prey library is screened with a bait protein of a different species. Alternatively this may lead to false positives.

Therefore any possible interactions must be assessed further, using additional techniques.

1.5.2.2 Confirmation and further characterization of positive interactors

1.5.2.2.1 Sequencing of candidate interacting proteins

Once identified by the activation of the reporter genes, the identity of the preys must be determined by sequencing and database homology searches. PCR products can be produced using the yeast colony directly as template, extracting the yeast plasmid DNA first for use as PCR template or by transforming the plasmid in *E.coli* and using this amplified product as template.

Transformation of yeast plasmid DNA into bacteria can be problematic since the plasmid may be toxic to *E. coli*; may have integrated into the yeast genome and is therefore unable to replicate autonomously; or plasmid DNA may be absent from the extracted yeast DNA aliquot and may be contaminated with yeast chromosomal DNA. Furthermore there may have been insufficient lysis of the yeast cell during plasmid preparation or the yeast may have cannibalized their plasmids due to inhibitory growth pressures i.e. lack of aeration.

1.5.2.2.2 Yeast mating

One of the main features of the yeast two-hybrid assay, aside from the fact that yeast are able to take up more than one plasmid at a time, is that each colony is able to shed plasmids that are not selected for. In order to confirm the protein-protein interactions *in vivo* by yeast mating, prey plasmids (-leu/+amp) can be segregated from the bait plasmids (-trp/+kan) in AH109 cells. The interactions are then confirmed through mating analysis.

1.5.2.2.3 Co-immunoprecipitation (CO-IP)

Immunoprecipitation is an *in vitro* technique that can be used to confirm and further characterize the nature of the interaction between suspected binding partners. An antigen is isolated from a sample e.g. cell lysate, through the formation of an immune complex with an antigen-specific antibody. The immune complex is then captured/precipitated on a solid support e.g. Protein A (a system that binds the antibody but not the antigen). Both of the components of the bound immune complex are then eluted from the support and analyzed by SDS-PAGE and Western blotting to identify the antigen. Co-immunoprecipitation is conducted in essentially the same manner as immunoprecipitation, however in this case the target antigen precipitated by the antibody “co-precipitates” a binding partner/protein complex from the lysate.

Problems associated with immunoprecipitations most commonly involve interference from antibody bands in gel analysis. In those cases where several proteins may be co-precipitated with the target, presence of the co-eluted antibody heavy and light chains (25 and 50 kDa bands in reducing SDS-PAGE gel) in the preparation can obscure the results. The use of fusion tags incorporated into the primary target protein for immobilization of the protein complex or for Western blotting purposes is thought to help minimise this background (<http://www.piercenet.com/>).

The following chapters use the techniques discussed in section 1.5 to investigate harmonin localisation and interactions in the retina, in order to infer possible protein functions in the normal eye, and pathogenic mechanisms in Usher syndrome.

2 METHODOLOGY

The methods and techniques discussed in this chapter are adaptations of standard protocols used within this laboratory unless otherwise stated. Yeast two-hybrid techniques are adapted from the Yeast Protocols Handbook and Y2H MATCHMAKER III Protocols from Clontech. The pull down assay was adapted from methods supplied with the Pro-Found kit (Pierce).

2.1 *Materials: Solutions*

Detailed information on suppliers, solution recipes and strains used in this work can be found in the relevant appendices (Table 2.1).

Table 2.1 Index to Materials: Solutions data

Suppliers	Appendix 1
Media	Appendix 2
Buffers and solutions	Appendix 3
Fixatives and cryopreservation buffers	Appendix 4
Antibodies and cell labeling solutions	Appendix 5
Agarose and SDS-PAGE gels	Appendix 6
Escherichia coli (<i>E.coli</i>) strains	Appendix 7
Yeast (<i>Saccharomyces cerevisiae</i>) strains	Appendix 8
Plasmids	Appendix 9

2.2 **Materials: Technical**

Detailed information on technical resources used can be found in the relevant appendices (Table 2.2).

Table 2.2 Index to Materials: Technical data

Equipment	Appendix 10
Software	Appendix 11

2.3 ***Determination of the temporal and spatial expression of Ush1c and harmonin within the normal murine eye***

2.3.1 *Methodology: Identification of the pattern of protein localisation of harmonin in the adult murine retina*

2.3.1.1 Tissue preparation

2.3.1.1.1 Tissue collection

CD1, SV129, *shaker-1* and *waltzer* mice were culled by cervical dislocation. Whole eyes from fetal, postnatal and adult mice were removed immediately after death and transferred to cold Phosphate Buffered Saline (PBS). Tissue for immunofluorescence studies was either embedding directly in Optimal Cutting Temperature compound (OCT) (Raymond A Lamb) on dry ice, or was fixed and cryoprotected prior to embedding (section 2.3.1.1.2). The lens was removed from tissue designated for Western blot analysis (section 2.4.4.2 - 2.4.4.3) or semithin

sectioning (section 2.3.1.1.6). Fetal eyes were frozen in TRIZOL (Invitrogen) (0.5ml/10mg tissue) at -70°C overnight prior to use (section 2.3.3.2.1). All research involving animal tissue was carried out in accordance with EC directives and the Institute of Child Health Research Ethics Committee.

2.3.1.1.2 Tissue fixation and cryopreservation

Tissue was dissected and fixed in fresh 4% paraformaldehyde (Appendix 5) at 4° overnight. Tissue was washed in Phosphate Buffered Saline (PBS) for 5 minutes, and then transferred to the cryoprotectant sucrose solution for overnight incubation or storage for up to one month at 4°C. Tissue was washed in PBS prior to positioning in the cryomould (L.I.P equipment services), covered in OCT and quick frozen on dry ice and isopentane. Tissue was then stored at -80°C.

2.3.1.1.3 TESPA coating of slides

Coating of slides was carried out in a fume hood. Superfrost glass slides (BDH) were loaded into glass holders, then each was dipped for a minimum of 30 seconds into successive 400ml glass troughs, containing 10%HCl/70% ethanol, diethylpyrocarbonate (DEPC)-water and 95% ethanol. Slides were then covered and dried in an oven overnight at 65°C. Holders were then dipped into glass troughs containing cold 2%TESPA (3-aminopropyltriethoxysilane) in acetone (BDH), acetone wash one, acetone wash two and finally in DEPC-water, each for

30 seconds. Slides were covered again and dried in a 45°C oven overnight. Coated slides were stored covered at room temperature.

2.3.1.1.4 Cryosectioning sectioning

Tissue was removed from the cryomold and affixed to the specimen holder of the OFT Cryostat with a 5040 microtome (Bright) using OCT. The blade and cryostat were precooled to -15 and -20°C respectively, with a knife angle of 15°. 10µm sections were cut and placed on TESPA coated superfrost slides (2.3.1.1.3). Sections were allowed to dry overnight at room temperature and then frozen at -80°C.

2.3.1.1.5 Processing and UV light curing of LR gold resin

Freshly dissected eyes minus the lens (section 2.3.1.1.1), were fixed in 2% PFA in PBS for 1 hr at room temperature. Tissue underwent three, 5 minute washes, in PBS and then was dehydrated for 10 minutes periods in graded alcohols of 30%, 50%, 70%, 95%, and 100%. Tissue was transferred to 50% London Resin (LR) gold (Agar Scientific): 50% absolute alcohol for 1hour, then to 100% LR gold for a further 1 hour. Tissue was incubated over night in 100% LR gold + 0.2% Benzoin methyl ether (which acts as an initiator for the polymerization reaction), then transferred to gelatin capsules fully filled with resin mixture and polymerized in the freeze substitution polymerization apparatus (RMC) at -30°C by overnight UV irradiation.

2.3.1.1.6 Semithin sectioning

The tissue specimen, embedded in the polymerized resin, was locked into the specimen holder and locked in the upright horizontal position of an ultracut E microtome (Reichert). Thin layers of resin were removed manually using a scalpel until the tissue was reached. The specimen holder was returned to its original stand and positioned parallel to the fresh glass knife surface (produced by user). A wax boat was added to the knife, sealed with wax and filled with water. Semithin sections of 1µm were cut until the surface of the specimen was flat and the sections produced, even and complete. A fresh ribbon of semithin sections was then cut and retrieved from the boat using human eyelashes (provided by user). Sections were mounted on uncoated glass slides (BDH) using water, dried on a hot plate for 30 secs and then stained using a 2% methyl blue solution in borax.

2.3.1.2 Harmonin localisation in the adult murine retina

In all immunostaining experiments, the slides were removed from storage at -80°C and thawed at room temperature. Boundaries around each section were established using a PAP PEN (The Binding Site) to minimize the volume of antibody used per slide. The slides were washed in PBS for 2 minutes to remove the OCT, prior to immunolabelling.

All sections immunostained in sections 2.3.1.2, 2.3.1.3 and 2.3.2 were analysed using an epifluorescent microscope (Axioplan 2, Zeiss), and images captured using Openlab software (Improvision), before transfer to Adobe Photoshop.

2.3.1.2.1 Single antibody staining of fixed tissues

Fixed adult CD1 retinal cryosections were blocked with 4% goat serum (Santa Cruz Biotechnology Inc.) + 1% Tween 20 in PBS for 2 hours at room temperature. Sections were gently washed in PBS and then incubated at 4°C overnight, with the anti-harmonin rabbit polyclonal antibody (Kobayashi *et al* 1999) diluted 1:100 in PBS and 1% goat serum (Santa Cruz Biotechnology Inc.). After washing, sections were incubated in the dark with FITC (Fluorescein isothiocyanate) conjugated anti-rabbit IgGs antibody (Vector Laboratories) diluted to 1:50 in PBS and 1% goat serum, for 2 hours at room temperature. A nuclear counter stain was provided by 30 minutes incubation with Hoechst at 1:200 in PBS, at room temperature in the dark. Internal retina structures containing F-actin were visualized on alternative retinal sections by incubation with 1:50 Rhodamine conjugated Phalloidin (Molecular Probes) at room temperature for 20 minutes. Sections were washed and slides partly air dried before mounting with Citifluor (Citifluor Ltd) mounting media. Stained sections were stored at 4°C.

Negative control sections substituted the anti-harmonin antibody for PBS or rabbit IgGs (data not shown), but were visualized and counter stained as previously described.

2.3.1.2.2 Double antibody staining of fixed tissues

Double immunostaining with the polyclonal anti-harmonin antibody, and the photoreceptor outer segment labelling anti-rhodopsin antibody (Santa Cruz), used a 4% horse serum (Vector Laboratories) solution supplemented with 1% TWEEN 20 as blocking solution. Tissues were incubated with blocking solution at room temperature for two hours before washing and then incubating with the primary antibodies overnight at 4°C. All antibodies were diluted in blocking serum. The polyclonal anti-harmonin antibody was diluted 1:100 and the anti-rhodopsin at 1:50. The anti-harmonin antibody was detected using a biotinylated anti-rabbit IgGs antibody (1:100) (KPL) that was pre-conjugated to an avidin D- rhodamine antibody (Vector Laboratories) (1:100) at 37°C for one hour. The anti-rhodopsin antibody was detected using an anti-goat IgGs antibody conjugated to FITC (Jackson Laboratories) which was incubated at room temperature for four hours at 1:50. After immunolabelling; the cell nuclei were labelled using Hoechst nuclear stain (section 2.3.1.2.1), prior to air drying and mounting using Citifluor.

Negative control sections substituted the anti-harmonin and anti-rhodopsin antibodies for PBS.

2.3.1.3 Methodology: Investigation into the effects of fixation upon harmonin localisation

Unfixed adult CD1 retinal sections were collected and cryosectioned (section 2.3.1.1.1, 2.3.1.1.3 and 2.3.1.1.4). Sections were immunostained as described by Reiners, J et al, 2003, using polyclonal anti-harmonin (1:50), anti-myosin VIIA (1:50) (Affinity BioReagents) and anti-cadherin 23 (1:50) (Bolz, H et al, 2002). Negative controls substituted the primary antibodies for PBS. After immunolabelling; the cell nuclei were labelled using Hoechst nuclear stain (section 2.3.1.2.1), prior to air drying and mounting using Citifluor.

2.3.2 Methodology: Examination of the protein localisation of harmonin in the absence of myosin VIIA and cadherin 23

Shaker-1 and *waltzer* eyes were collected and sectioned (section 2.3.1.1), then immunostained with the polyclonal anti-harmonin antibody (section 2.3.1.2.1). Negative control sections substituted the anti-harmonin antibody for PBS.

2.3.3 Methodology: Determination of the age of onset of *Ush1c* gene expression

2.3.3.1 Harmonin localisation in the postnatal murine retina

The retinas from P2, P4, P8 & P12 CD1 mouse pups were collected, sectioned (section 2.3.1.1) and immunostained with polyclonal anti-harmonin antibody (section 2.3.1.2.1) to study the onset of harmonin expression during development.

Negative control sections substituted the anti-harmonin antibody for PBS or rabbit IgGs (data not shown). Semithin sections (2.3.1.1.5 - 2.3.1.1.6) were also collected to study the structure of the developing retina during this time period.

Immunolabelled sections were analysed using a laser scanning confocal microscope (SP2 Leica), with projection images gathered at 0.3µm throughout the whole section, using Leica Confocal Software (version 2.5), before transfer to Adobe Photoshop. Semithin sections were analysed using a light microscope (Axioplan 2, Zeiss), and images captured using Openlab software (Improvision).

2.3.3.2 *Ush1c* expression in the prenatal murine retina

2.3.3.2.1 Isolation of total RNA

All RNA isolation techniques used RNase free solutions (including DEPC H₂O (Appendix 3) and equipment. Freshly dissected tissue (section 2.3.1.1.1) was incubated overnight at -20°C/-70°C in 0.5ml TRIZOL per 10mg tissue. Once thawed, tissue was homogenized in a falcon tube using a hand-held homogeniser (Kontes). A further 0.5ml TRIZOL/10mg tissue was added, before incubation at room temperature for 5 minutes. 0.2ml chloroform/1ml TRIZOL was then added to the tissue sample and mixed by shaking the tubes by hand for 15 seconds, before incubation at 15-30°C for a further 2-3 minutes. Tubes were centrifuged in a bench top centrifuge (Jencons PLC) at 12000g/10000rpm for 30 minutes at 4°C to separate the coloured organic layer containing DNA and protein, from the upper colourless layer containing the RNA. The aqueous phase was added to another

RNase free tube and another chloroform separation was performed as previously described, using 0.2ml chloroform/1ml TRIZOL. The aqueous layer was again removed to a new tube and 0.5ml isopropyl alcohol/1ml TRIZOL was added, vortexed and then the RNA was precipitated out of solution overnight at -20°C. Tubes were centrifuged at 12000g/10000rpm for 10 minutes at 4°C, then the supernatant was removed and the RNA pellet washed with cold 75% ethanol, 1ml/1ml TRIZOL. The tube was again vortexed and centrifuged at 7500g/6000rpm for 5 minutes at 4°C. The pellet was partially air dried and then re-dissolved in RNase free water by incubating the tube at 55-60°C for 10 minutes. Total RNA concentration was measured by UV spectroscopy (section 2.5.1.2.3) and the RNA stored at -20°C.

2.3.3.2.2 Two-step Reverse Transcription Polymerase Chain Reaction (RT-PCR)

To produce cDNA, 1µg of total RNA was incubated with 1µl DNase 1 enzyme, 1µl 10x buffer and RNase free ddiH₂O to a total volume of 13µl at room temperature for 15 minutes. DNase 1 was deactivated by the addition of 2.5µl 25mM EDTA (pH8), and then incubated for 10 minutes at 65°C. 1µl of both an oligo dT primer and a random nonamer primer were added and the solution incubated for a further 10 minutes at 70°C. The tube was rapidly chilled on ice, then 4µl 5x First Strand Buffer, 1µl 0.1M DTT, 2µl 10mM dNTP (deoxyribonucleotide triphosphates) and 1µl RNase Inhibitor were added, pulse spun on a bench top centrifuge, and heated for 2 minutes at 42°C. After which, 1µl Superscript III RT enzyme was added and the enzyme mixture incubated for 5 minutes at 25°C and then for 50 minutes at 42°C.

The enzymes were deactivated by heating for 15 minutes at 70°C and the resulting cDNA stored at -20°C. The quality of the cDNA was examined by Touchdown PCR (section 2.5.1.2.6) for a total of 35 cycles, using primers to the housekeeping gene *Gapdh* (Appendix 13).

The age of onset of *Ush1c* expression was examined in the second stage of the RT-PCR reaction, using *Ush1c* specific primers (Appendix 13). A standard 25µl PCR reaction using Hot star *taq* (Qiagen) instead of Bioline *taq*, with a Touchdown thermocycler program of 40 cycles was used to produce an amplimer at all ages tested (section 2.5.1.2.6). To compare USH1 gene expression the PCR amplification step must be semi-quantitative, meaning that readings must be taken using the cycle number which first shows product production. An aliquot of PCR reaction mix was removed after cycle 25 and after each subsequent cycle. Aliquots were electrophoresed on 2% agarose gels (section 2.3.3.2.2.1), to determine the cycle number required to first detect the appearance of the PCR product. The same PCR reaction mix was used with the following thermocycler program (95°C/20 secs, 52°C/20 secs; 72°C/30 secs) and primer pairs to *Myo7a*, *Cdh23*, *Pcdh15* and *Ush1c* (Appendix 13). *Gapdh* first appeared at 28 cycles and the USH1 genes at 35 cycles.

Products were electrophoresed on 2% agarose gels and images captured on the transilluminator using the same imaging conditions for each gene. The product band intensity/mm² was calculated for each primer pair at each developmental

stage, and normalized to *Gapdh* expression. PCR amplification reactions were carried out in triplicate, using multiple cDNA preparations.

2.3.3.2.2.1 Agarose gel electrophoresis

Ultra pure agarose powder (Invitrogen) was mixed with 1XTBE buffer at a w/v concentration to produce the desired percentage gel (Appendix 6). The resulting suspension was heated in a microwave oven until the agarose was dissolved. On cooling, Ethidium bromide (0.5µl/ml) was added and the gel poured into a Hybaid gel tray with the appropriate well forming comb. Once set, 10µl of PCR product was diluted with 5µl of loading buffer (Appendix 3), loaded onto the gel and the gel electrophoresed at 75 amps for 20-40 minutes. The gel was transilluminated and photographed under UV light using the Bio-Rad Transgenomic™ Chemidoc system. The size of the amplified product was compared to DNA standards (various ladders from Invitrogen, see specific figure legends), loaded at the same time as the PCR product.

2.4 *Generation of polyclonal antibodies to harmonin isoforms*

2.4.1 Selection of the antigenic peptides for anti-harmonin antibody synthesis

The sequences of the peptides used to raise the isoform-specific anti-harmonin antibodies and their locations relative to the 3 PDZ domains of murine isoform 'a', is show in Figure 2.1A. Peptide 1 could be used to detect all three isoform classes of harmonin, whilst peptide 2 would detect only isoform classes 'a' and 'b'. Differences between the immunostaining data obtained for each antibody would highlight the specific pattern of localisation of the class 'c' isoform.

A comparison of the murine and human sequences of both peptides (Figure 2.1B) would suggest that antibodies raised to peptide 1 would be suitable for immunostaining murine or human tissue, whereas antibodies raised against peptide 2 would be more effective on murine tissue only.

Figure 2.1 Selection of Peptide 1 and 2

(A) The complete amino acid sequence of human harmonin isoform 'a' (NCBI AAG12457). The three PDZ domains are highlighted in red and the chosen peptides are underlined within the sequence. **(B)** A comparison of the human and murine amino acid sequence of the two peptides chosen by Sigma-Genosys for antibody production. The cysteine residues enclosed in square brackets are not part of the murine harmonin sequence but were added by Sigma-Genosys to enable conjugation to the carrier protein.

hours, after which it was washed four times in PBS as previously described. 50 μ l of

A

MDRKVAREFRHKVDFLIENDAEKDYLVDVLRMYHQTMDAVLVGDLKLVINEPNRPLFDAIRPLIP
LKHQVEYDQLTPRRSRKL**KEVRLDRLHPEGLGLSVRGGLEFGCGLFISHLIKGGQADSVGLQVGDE**
IVRINGYSISSCTHEEVINLIRTKKTVSIKVRHIGLIPVKSSPEESLKWQYVDQFVSESGGVRGGLGSP
GNRTTKEKKVFISLVGSRGLGCISSGPIQKPGIFVSHVKPGSLSAEVGLETGDQIVEVNGIDFTNLD
HKEAVNLKSSRSLTISIVAGAGRELFTMDRERLEEARQRELQRQELLMQKRLAMESNKILQEQQE
MERQRRKEIAQKAAEENERYRKEMEQISEEEEKFKKQWEEDWGSKEQLILPKTITAEVHPVPLRKP
KYDQGVEPADHLDGSTEEQRQQDFRKYEEGFDPYSMFSPEQIAG**KDVRLLRIKKEGSLDALEGG**
VDSPVGKVVVSAYEGGAAERHGGVKGDEIMAINGKIVTDYTLAEAEAALQKAWNQGGDWIDLV
VAVCPPKEYDDELTF

solution (p-Nitrophenyl phosphate), was added per well and incubated stationary at

B

Mouse sequence	Human sequence
LTPRRSRKL KEVRLD [C]	LTPRRSRKL KEVRLD
[C]PADHLDGSTEEQRQQ	PADDLDGGTEEQGEQ

the absorbance of the well can be read at 405nm on a Multifunction Microplate

Reader (Genios, TECAN) with XFluor[®] software (TECAN). The ELISA reading

must be 0.3 units greater than the background reading (bound antigen and buffer).

2.4.2 Methodology: Analysis of the anti-harmonin antibodies by ELISA

Peptide 1 was diluted to 20 μ g/ml in PBS. 50 μ l of this was added to enough wells

of a flat bottom 96-well plate (Nunc), to allow for examination of a variety of antibody sera concentrations for each bleed and also to allow for blank controls.

The plate was sealed with a transparent plate sealer (ABgene) and incubated at

4°C overnight. The plate was then washed four times, each time adding 300 μ l of

PBS to each well and completely emptying the wells each time before the next

wash. The wells were blocked using 300 μ l of 5% non-fat powdered milk (Marvel)

as blocking buffer, and incubated, shaking (200rpm) at room temperature for 2

hours. The plate was then washed a further four times, as above in PBS. 50 μ l of serum from each of the LTPR bleeds was diluted in blocking buffer (in the range of 1:100 – 1:10000) and added to the blocked wells. Controls substituted PBS for serum. The plate was incubated, shaking at room temperature for a further 2 hours, after which it was washed four times in PBS as previously described. 50 μ l of anti-rabbit IgG antibody conjugated to horse-radish-peroxidase (HRP) (Amersham Pharmacia) was diluted in blocking buffer, added to the wells and then incubated shaking at room temperature for 2 hours. The plate was washed again as previously described before development of the ELISA. 50 μ l of PNPP substrate solution (p-Nitrophenyl phosphate), was added per well and incubated stationary at room temperature for 40 minutes. On addition of the substrate, positive results (where peptide 1 – anti-LTPR antibody complexes have formed) turn yellow and the absorbance of the well can be read at 405nm on a Multifunction Microplate Reader (Genois, TECAN) with XFluor4 software (TECAN). The ELISA reading must be 0.3 units greater than the background reading (bound antigen and buffer only) to be valid.

The same ELISA protocol was repeated for peptide 2 using the PADH bleeds.

2.4.3 Methodology: Analysis of the anti-harmonin antibodies by immunolabelling of murine retinas

P10 CD1 murine eyes were collected, fixed and cryosectioned (section 2.3.1.1). Sections were blocked with 4% goat serum + 1% Tween 20 in PBS for 2 hours at room temperature. Sections were gently washed in PBS and then incubated at 4°C overnight; with the anti-harmonin rabbit polyclonal antibody (positive control) diluted 1:100 in PBS and 1% goat serum. After washing, sections were incubated with FITC conjugated anti-rabbit IgG secondary antibody diluted to 1:100 in PBS and 1% goat serum, for 4 hours at room temperature in the dark. Rabbit serum (Santa Cruz Biotechnology Inc.) at 1:100 was substituted for the primary antibody as a negative control, and visualized with FITC conjugated anti-rabbit IgG secondary antibody as above.

Sections were incubated with anti-LTPR or anti-PADH unpurified sera at 1:2, 1:5, 1:10, and 1:20 dilutions then incubated with FITC conjugated anti-rabbit IgG as previously described. Sections were washed in the dark, then further incubated with an anti-FITC antibody (Rockland) at 1:100 for 1 hour at room temperature to further amplify any signal. This and the following incubations were carried out in the dark. Sections were washed and then incubated again for a further 1 hour at room temperature, with anti-goat IgGs antibody conjugated to Cy5 (1:50) (Rockland) for visualization by confocal microscopy. Sections were washed, air dried and then mounted with Citifluor.

Control sections were visualized using an epifluorescent microscope (Axioplan 2), and images captured using Openlab software (Improvision). Anti-LTPR and anti-PADH labelled sections were analysed using a laser scanning confocal microscope (SP2 Leica) and single images captured using Leica Confocal Software (version 2.5), before transfer to Adobe Photoshop.

2.4.4 Methodology: Analysis of the anti-harmonin antibodies by immunoblotting analysis

2.4.4.1 Preparation of protein samples

2.4.4.1.1 Protein extraction from cells

Prior to protein extraction, cell lines had to be recovered from cryostorage, grown to confluence and then harvested (2.4.4.1.1.1 - 2.4.4.1.1.2). R28 is an adherent retinal precursor cell line derived from postnatal day 6 Sprague-Dawley rat retina immortalized with the 12S E1A gene of an adenovirus (Sun, W et al, 2002). Caco2 is also an adherent cell line, derived from an isolated primary human colonic tumor (www.sigmaaldrich.com).

2.4.4.1.1.1 Cryostorage and recovery of mammalian cell lines

R28 adherent cells were frozen in liquid nitrogen for long term storage purposes. Cells at 95%-100% confluence were harvested from the flask surface, as described for trypsinisation (section 2.4.4.1.3) Cells were pelleted by centrifugation at 410g, at

room temperature for 5 minutes (Patterson Scientific, EBA 12). Cells were resuspended in 3mls 20% fetal calf serum supplemented with 10% dimethyl sulfoxide (DMSO) (added very slowly) as a cryoprotectant. 1ml aliquots of cell suspension were added to cryogenic vials (Nalgene). All vials were placed in a polystyrene container packed with cotton wool and frozen at -80°C for 16-24 hours before transferring to the liquid nitrogen cell bank for long-term storage.

After removal from liquid nitrogen, cells were rapidly defrosted by incubation at room temperature for 1 minute and then transferred to a 37°C water bath for 1-2 minutes until thawed. The cells were immediately transferred into 12mls prewarmed growth medium and incubated under normal conditions for 16-18 hours (section 2.4.4.1.3). Growth medium was changed on the next day to remove any remaining DMSO.

2.4.4.1.1.2 Maintenance of R28 cells and trypsinisation

Cells were grown in vented medium culture flasks (Corning Incorporated) in DMEM+L-glutamine, supplemented with 10% fetal calf serum (PAA), 1% MEM vitamins (Gibco), 1% MEM non-essential amino acids (Gibco) and 0.125% Gentamicin (from an 80mg/ml stock). Cells were fed with prewarmed ~12mls media and incubate in a 37°C, 5% CO₂ incubator (Heraeus). Cells were fed or trypsinized/passaged every 2-3 days.

Media was removed from confluent flasks needing to be passaged, and cells were washed with sterile PBS, which was in turn removed. 1.5mls of prewarmed trypsin was washed over the cells and then the flask placed back in the 37°C incubator until the cells were no longer adhered to the flask surface. 10mls of medium was added to the flask to block the action of the trypsin and cell clumps were separated by pipetting. 2mls of trypsinised cells were added to 10mls of media in a fresh flask and re-incubated to maintain the cell line.

2.4.4.1.1.3 Protein extraction from cells

Media was removed from confluent cells, which were washed twice with 5mls aliquots of cold sterile PBS. Wash buffer was completely removed and then 100-300µl of freshly prepared ice cold RIPA buffer (Appendix 3) with 2µl 50x protease inhibitor cocktail (Appendix 3) per 100µl RIPA buffer was added. Flasks were incubated on ice for 5mins, and then cells were scrapped from the flask surface and collected in ice cold eppendorfs. Cell membranes were completely lysed through passage of the cell suspension through a 21G needle a few times and then centrifuged for 30mins at 13,000g. The supernatant was transferred to a fresh tube and stored at -70°C.

2.4.4.1.2 Protein extraction from tissue

The hand-held homogenizer was washed with 10mls of ddH₂O. Fresh ice cold RIPA buffer was prepared (1ml required per 50-100mg tissue) (Appendix 3) supplemented with 2µl 50x protease inhibitor cocktail (Appendix 3) per 100µl RIPA

buffer. Tissue was collected (section 2.3.1.1.1) and homogenized in the supplemented RIPA buffer in a round bottom falcon tube on ice for 2 minutes. The homogenizer was cleaned in 40mls of ddiH₂O whilst the supernatant from the homogenized tissue sample was transferred to another eppendorf and passed through a 21G needle a few times to completely lyse cell membranes. The sample was incubated on a rotator (Stuart Scientific) at 4°C for 30mins and then centrifuged at 13000rpm at 4°C for 20mins (Jencons PLC). The supernatant was transferred to a fresh eppendorf, supplemented with 10µl of PMSF (Phenylmethyl-sulfonyl fluoride) and stored at -80°C.

2.4.4.1.3 Calculation of protein concentration by the Bradford method

Two sets of BSA protein standards, concentrations 1mg/ml, 0.5mg/ml, 0.25mg/ml, 0.125mg/ml, 0.0625mg/ml, were prepared and kept on ice alongside a ddiH₂O control. A range of dilutions of the experimental protein samples was set up and added to the ice. The dye (BioRad) for the Bradford assay was diluted 1:5 with ddiH₂O and filtered through filter paper. 5µl of dye was added to 100µl of protein standard/sample, vortexed and then incubated at room temperature for 5mins – 1 hour. The absorbance of samples was measured at 595nm. The standards were used to create a calibration curve (Excel, Microsoft) from which to calculate the protein concentration of the experimental samples.

2.4.4.2 SDS-PAGE and electrotransfer of proteins onto nitrocellulose membranes

SDS-PAGE (Sodium Dodecyl Sulfate Polyacrylamide Gel Electrophoresis) mini-protein gel plates (BioRad) were cleaned with detergent and ethanol (Hayman). ~10mls resolving gel of the appropriate % (Appendix 6, Table 2.3) was poured between the plates, leaving room for ~2mls stacking gel and the exposed gel surface covered with N-butanol. Once the resolving gel had polymerized, the N-butanol was removed and the gel surface washed with ddiH₂O. The ddiH₂O was removed and the stacking gel layer pipetted on top of the resolving gel. A 10 or 15 well comb was added and the gel left to polymerize at room temperature. When both gels were set, the comb was removed and the wells washed out with running buffer (1xTGS). The gel was loaded into the gel tank (Mini-PROTEAN II cell, BioRad) and running buffer added according to the manufacturer's instructions (BioRad).

Protein samples were denatured for 20mins at 60°C in the appropriate volume of 6x Lamelli loading buffer (Appendix 6). Denatured protein samples were kept on ice until ready to load on the SDS-PAGE protein gel alongside 10µl of a pre-stained protein ladder (BioRad & Fermentas). The gel was electrophoresed at 200V for~45-75 minutes (Power Pac 200, BioRad).

Table 2.3 Separation ranges of proteins in different percentages of denaturing SDS-PAGE Gels (Sambrook, J. et al, 1989)

Protein range to be detected (kDa)	% denaturing SDS-PAGE
>250	4-5
250-120	7.5
120-50	10
70-30	13
<40	15

Whilst the gel was running, the Bio-Ice cooling unit (BioRad) was filled with ddiH₂O and frozen at -70°C. Transfer filter papers (Whatman) and fiber pads (BioRad) were equilibrated in Transfer buffer (Appendix 3) for 30mins at 4°C. Once electrophoresis was complete, the layer of stacking gel was cut from the SDS-PAGE gel. This was placed in the transfer sandwich as follows: fiber pad, 2x filter papers, SDS-PAGE gel, nitrocellulose membrane (Hybond ECL, Amersham), 2x filter papers and a fiber pad. The sandwich was positioned in the Electrode module of the Mini Trans-Blot® Electrophoretic Transfer Cell (BioRad) in order to transfer the protein from the gel to the membrane using electric current. The electrode module was placed within the transfer cell according to the manufacturer's instructions, the frozen Bio-Ice cooling unit added, and then the cell filled with cold transfer buffer and electrophoresed at 100V for 1hr.

Once transfer was complete as witnessed by the transfer of the pre-stained protein standards from the gel to the membrane, the membrane was removed from the sandwich and washed in PBS (Appendix 3), keeping the protein side, face up. Any excess membrane was removed and the top left-hand corner marked to determine orientation.

2.4.4.3 Western blotting with monoclonal and polyclonal anti-harmonin

~100mg R28 cell lysate (~24 mg/ml), ~80mg Caco2 cell lysate (~22 mg/ml) (kindly donated to this work by Dr Blaydon of this lab), ~100mg whole eye homogenate (~25 mg/ml) and 2µL USH1C IVT (section 2.5.6.1.1) using a PDZ 73 construct with a Sp6 promoter (kindly donated to this work by Dr Blaydon of this lab) as template with the Sp6 TNT[®] IVT Kit), were run on a 15% SDS-PAGE gel (Appendix 6) and electrotransferred (section 2.4.4.2). The membrane was blocked for 1 hour at room temperature on a rotator (Stuart Scientific), in 5% Marvel milk + 0.1% TWEEN 20 in PBS to minimize non-specific binding of antibodies used to visualize proteins on the membrane. The membrane was then washed (3x 5mins and 1x 15mins rotating incubation with PBS-T (Appendix 6)). In a fresh falcon tube, one half of the membrane was incubated with monoclonal anti-harmonin diluted to 1:1000 in PBS-T, overnight at 4° C. After which it was washed again as above, before incubating for one hour at room temperature with biotinylated anti mouse IgGs (KPL) diluted to 1:500, washed and finally, with Streptavidin conjugated to alkaline phosphatase (AP) (Promega) diluted to 1:2500, at room temperature for a further one hour. The other half of the membrane was incubated with polyclonal anti-harmonin at 4° over

night, diluted to 1:500. After which it was washed, incubated for one hour at room temperature with biotinylated anti rabbit IgGs (KPL) at 1:750, washed again and then with incubated for a further 1 hour at room temperature with the streptavidin-AP antibody, diluted to 1:2500. Membranes were washed 2x 1min in PBS and then 1x 2min in ddiH₂O. Western blots were developed using the ProtoBlot® Western Blue® Stabalised Substrate (Promega) at room temperature until the required colour developed. The reaction was stopped by washing in tap water.

2.4.4.4 Western blotting with anti-LTPR serum

2 μ L USH1C IVT and ~100mg whole eye homogenate were run on a 15% SDS-PAGE gel and electrotransferred (section 2.4.4.2). Immunoblotting on one half of the membrane was carried out exactly as described in section 2.4.4.2, with the polyclonal anti-harmonin antibody as a control. The other half of the membrane was immunoblotted using the following antibodies: anti-LTPR sera diluted to 1:100 and incubated overnight at 4° C, followed by biotinylated anti rabbit IgGs diluted to 1: 1000 for one hour at room temperature, and finally with streptavidin-AP diluted to 1:2500 at room temperature for a further one hour.

2.4.4.5 Protein purification from serum

2.4.4.5.1 Isolation of immunoglobulins from serum

Immunoglobulins (IgGs) were isolated from anti-LTPR whole serum according to the manufacturer's instructions (KPL) as summarized below. 40ml of

Wash/Binding Buffer (final 1x concentration, 0.1M Sodium Phosphate, 0.15M NaCl, pH 7.4) was diluted to 1x in ddH₂O. A minimum buffer volume of 30x the quantity of agarose used for purification was required. Elution Buffer (final 1x concentration, 0.2M Glycine, pH 3± 1.85) was diluted to 1x in ddH₂O, to achieve a final volume of 4x the quantity of agarose used. The column was prepared according to the manufacturers instructions, using 20% ethanol to force all air from the frit that was inserted into the bottom of the column barrel. The end of the column was clipped to allow liquid to flow through, and the frit was washed five times using a column volume (CV) of 1x Wash/Binding Buffer per wash. The column volume was calculated according to the amount of resin used in the purification process (1ml resin = 1ml CV). 1ml of resin per 500µl serum was suspended in 1x Wash/Binding Buffer at a 1:1 ratio. The slurry was poured into the column and buffer allowed to flow out by gravity. The resin was equilibrated with ten CV of the 1x wash/binding buffer. The absorbance of the eluate at 280nm was measured to calculate the background level.

500µl of serum was diluted 1:1 with binding buffer to insure proper ionic strength and pH for optimal binding to the beads. Any particulate matter was removed by filtration through a 0.8µm filter. The sample was layered onto the top of the resin, without disturbing the bed surface itself. The column was washed with ten CV of 1x Wash/Binding buffer (or until the absorbance of the eluate at 280nm approached the background level). Eight eppendorfs were set up to catch the eluted IgGs in 500µl aliquots. 120µl 5X Wash/Binding Buffer was first added to each collection tube. Then the anti-LTPR IgGs were eluted using 1ml of 1x Elution buffer at a time,

collecting the flow-through until a total of four CV passed through the column. Elution of bound IgGs was monitored by absorbance at 280nm.

2.4.4.5.2 Column regeneration

Once the sample had been eluted, the column was regenerated according to the manufacturer's instructions. The resin was washed with two CV of Elution buffer, then re-equilibrated with at least ten CV of 1x Wash/Binding Buffer. To confirm that equilibration was successful, the pH of both eluate and Wash/Binding Buffer were taken and found to be the same. The resin was stored in storage buffer in the sealed column at 2-8°C.

2.4.4.6 Western blotting with purified anti-LTPR IgGs and unpurified anti-LTPR serum

2 μ L USH1C IVT, ~100mg R28 cell lysate (~24 mg/ml) and ~80mg Caco2 cell lysate (~22 mg/ml) were run on a 15% SDS-PAGE gel and electrotransferred (section 2.4.4.2). Immunoblotting on one third of the membrane was carried out exactly as described in section 2.4.4.3, with the monoclonal anti-harmonin antibody as a control. The next third of the membrane was immunoblotted using the following antibodies: unpurified anti-LTPR serum diluted to 1:100 and incubated overnight at 4° C, followed by biotinylated anti rabbit IgGs diluted to 1: 1000 for one hour at room temperature, and finally with streptavidin-AP diluted to 1:2500 at room temperature for a further one hour. The last third used purified anti-LTPR

IgG (aliquot 2) diluted to 1:100 and incubated overnight at 4° C, followed by biotinylated anti rabbit IgGs diluted to 1:1000 for one hour at room temperature, and finally with streptavidin-AP diluted to 1:2500 at room temperature for a further one hour.

2.4.4.7 Western blotting with pre-absorbed purified anti-LTPR IgGs and unpurified anti-LTPR serum

To ensure that any bands seen on the blot are specific for harmonin, aliquots of the unpurified and purified anti LTPR antibody were incubated with an excess of peptide 1 (1mg/ml), at room temperature for 1 hour. Peptide 1 acts to pre-absorbed the antibody and therefore when incubated with the blots, it prevents the antibody from complexing with the harmonin protein. Therefore if identical experiments were performed using the standard development methods, harmonin should be detected on the standard blot but the band should be missing on the pre-absorbed blot if anti LTPR is truly detecting the harmonin protein. 2µL USH1C IVT, ~100mg whole eye homogenate and ~80mg Caco2 cell lysate (~22 mg/ml) were run on a 15% SDS-PAGE gel and electrotransferred (section 2.4.3). Sections of membrane were probed with normal anti-LTPR serum (section 2.4.4.4), pre-absorbed anti-LTPR serum (section 2.4.4.6), normal anti-LTPR IgGs (section 2.4.4.6) and pre-absorbed anti-LTPR IgGs (section 2.4.4.6).

2.4.5 Methodology: Analysis of antigenic peptide hydrophobicity

Kyte-Doolittle plots were issued for each peptide using a window size of 7. The complete harmonin protein was also examined, using both hydrophilicity scales and a window size of 20.

2.4.6 Methodology: Investigation into the presence of anti-harmonin IgGs in the anti-LTPR antibody sera

Antigenic proteins/immunoglobulins are able to diffuse in a 360° formation through agarose. If the antigen and antibody come into physical contact under these conditions, they will form a visible precipitate arc equidistant between the two wells. This principle was used in an Ouchterlony test, to examine whether the serum from the rabbits used to make the polyclonal antibodies against harmonin, actually does contain IgGs and whether they are against harmonin.

1% agarose was poured into a petri dish and six wells holding 20 μ l of solution each, were bored at a 1cm radius around a larger central well (holding 50 μ l), using the 'wrong' end of a 20 μ l pipette tip for the peripheral ring of wells and the 'wrong' end of a 1000 μ l pipette tip for the larger central well. An initial control Ouchterlony plate was set up, with the central well filled with neat anti-LTPR serum, whilst each surrounding well was filled with varying dilutions of anti-rabbit IgGs solutions (made in goat), with PBS buffer and undiluted anti-goat IgGs solution (made in donkey) as

negative controls. The plate was sealed and incubated face up at room temperature in a humid environment for 120 hours.

An experimental plate was then set up, using 0.5% agarose and with the wells spaced closer together to reduce the incubation time required to form a precipitate. The central well was filled with neat anti-LTPR serum, whilst each surrounding well contained undiluted anti-rabbit IgGs antibody as a positive control, PBS buffer as a negative control and a variety of different sources of harmonin protein, including the IVT USH1C protein (section 2.5.6.1.1; diluted 1:10), whole eye homogenate (~80mg/ml) and the R28 cell line (~80mg/ml). The remaining well contained a solution of peptide 1 of the same concentration used in the ELISA reaction (20mg/ml). Plates were then sealed and incubated face up at room temperature in a humid environment, for 24-48 hours. Precipitates could be visualized by eye and images captured using the gel imaging system (Chemidoc, BioRad).

2.5 *Investigation into candidate harmonin-interacting proteins within the normal eye*

2.5.1 *Methodology: A Yeast Two-hybrid screen of a bovine retinal library to find harmonin-interacting proteins*

2.5.1.1 Confirmation of yeast strain phenotypes

2.5.1.1.1 Long term storage of yeast

An isolated colony was scraped from the agar plate to inoculate 200-500µl of Yeast Peptone Difco agar supplemented with adenine (YPDA) medium (or the appropriate synthetic dropout (SD) medium (Clontech; Appendix 2). The tube was vortexed vigorously to thoroughly disperse the cells. Sterile glycerol was added to give a final concentration of 25%. The tube was vortexed to spread the cells evenly in the tube, and stored at -80°C.

2.5.1.1.2 Recovery of yeast from frozen stocks

Yeast from frozen stocks was streaked onto YPDA (or appropriate SD) agar plates using a sterile inoculating loop stick. The plate was incubated at 30°C until the yeast colonies reached 2 mm in diameter and then sealed with parafilm. Both Y187 and AH109 can produce pink colonies of >2mm diameter under conditions of limited adenine which are useable in later reactions. Small white colonies also formed as a result of spontaneous mutations and were avoided for all techniques

used in the yeast two-hybrid screen. The plate was stored at 4°C for up to two months.

2.5.1.1.3 Preparation of liquid yeast cultures

YPDA (or appropriate SD) medium was inoculated with a single colony (less than 2 months old) from the working stock plate (section 2.5.1.1.2) and vigorously vortexed for 1 minute to thoroughly disperse the cells. The culture was incubated at 30°C for 16-18 hours with shaking at 230 rpm. For most strains, this yields a stationary phase culture, with $OD_{600} > 1.5$

If a mid-log phase culture was needed, sufficient stationary phase culture was transferred into fresh YPDA (or appropriate SD) to produce an OD_{600} between 0.2-0.3. The medium was incubated at 30°C for 3-5 hours with constant shaking at 230 rpm or until the OD_{600} was between 0.4 and 0.6.

2.5.1.1.4 Confirmation of the phenotype of the yeast strains

Eight large pink colonies from working stock plates of AH109 and Y187 (section 2.5.1.1.2; kindly donated by Drs J. Achermann & L. Lin) were individually streaked onto SD selective plates (SD/-Ade; SD/-His; SD/-Leu; SD/-Trp; SD/-Met; SD/-Ura; YPD and YPDA) to simulate a range of nutritional selections. The plates were incubated at 30°C for 3-5 days. Colonies which expressed the correct phenotype

were made into frozen stocks (2.5.1.1.1) and used for subsequent yeast two-hybrid steps.

2.5.1.2 Generation of bait and control fusion proteins

DNA cloning: construction of yeast two-hybrid fusion proteins

All enzymes used in the following sections were from New England Biolabs, with specific storage, activation and deactivation protocols (see appropriate accompanying information provided by the manufacturer).

2.5.1.2.1 Digestion of DNA with restriction endonucleases

Sfi1 and *Xma1* sites were within the multiple cloning site (MCS) of both bait and prey vectors (Appendix 15). *Sfi1* and *Xma1* sites were added to the 5' and 3' ends respectively, of the bait and control insert sequences (PDZ1, PDZ2, PDZ3, C-terminus of cadherin 23, and the complete sequence of *USH1C* minus the first seven codons [due to primer requirements/secondary structure]) in the primers used for PCR amplification (Appendix 13). PCR amplification was performed for 35 cycles (95°C/20secs; 61°C/20secs; 72°C/2.5mins) using *taq* (Bioline) in a standard 25µl PCR reaction (section 2.5.1.2.6) with 0.017ug of template. The template used for the bait inserts was a pGEX4T-1-*USH1C* #12 clone donated by Dr D Blaydon (Blaydon, D 2004) whilst foetal ear cDNA was used to generate the control prey insert. The fidelity of the PCR was confirmed by the absence of bands in the

control lanes. PCR products were resolved by 2% agarose gel electrophoresis (section 2.3.3.2.2.1)

The insert DNA was purified from the components of the PCR reaction by gel extraction (section 2.5.1.2.2) and the resulting concentrations calculated (section 2.5.1.2.3). Full length *USH1C* (~10µg), PDZ1 (~4.5µg), PDZ2 (~4.5µg), PDZ3 (~7.5µg), pGBKT7 (~0.3µg), *cdh23* (~10µg) and pACT2 (~10µg) were each incubated with 1µl *Sfi1*, 1µl *Xma1* 2µl 10X NEB buffer 4, 0.2µl 100X NEB BSA and 12.8µl ddiH₂O, at 37°C for 1 hour to activate *Xma1* and then at 50°C to deactivate *Xma1* and *Sfi1* activate. Samples were run on 1% agarose (Appendix 6, section 2.3.3.2.2.1) to deactivate *Sfi1* and then gel purified (section 2.5.1.2.2). Samples were stored at –20°C.

2.5.1.2.2 Isolation of DNA from agarose gels

Under low intensity UV illumination, agarose gel slices containing the DNA product of interest were excised using a sterile scalpel. Slices were weighed and purified using a QIAquick Gel Extraction kit (Qiagen), according to the manufacturer's instructions.

Three volumes of Buffer QG was added to one volume of gel (100mg=~100µl) in an eppendorf. This was incubated at 50°C for 10min in a water bath, with intermittent vortexing, until the gel slice had completely dissolved. Once dissolved, one gel volume of isopropanol was added to the sample to increase the yield of DNA

fragments <500 bp and >4 kb. This step was omitted for DNA fragments outside this range. To isolate the DNA fragment, the sample was loaded onto a QIAquick spin column in a collecting tube and centrifuged at 13,000 rpm (~ 17,900 x g) in a table-top microcentrifuge (Biofuge PICO, Jencons PLC) for 60secs. The flow-through was discarded and the sample washed with 0.5ml of Buffer QG, with centrifugation as before. The flow-through was discarded and the sample washed again with 0.75ml of Buffer PE followed by centrifugation. The flow-through was again discarded and the column centrifuged again as previously to remove all traces of ethanol. The purified DNA was eluted from the column into a new 1.5ml eppendorf by incubating the column with 30-50 μ l of ddiH₂O, followed by centrifugation. The eluate was stored at -20°C.

2.5.1.2.3 Spectrophotometric quantification of DNA concentration

DNA concentration was calculated using an ultraviolet (UV) spectrophotometer (BioPhotometer, Eppendorf) to measure a solutions absorbance at 260nm (A₂₆₀), with A₂₆₀ = 1 being equivalent to 50 μ g/ml of double stranded DNA or 40 μ g/ml of RNA. DNA purity was calculated using the ratio of A₂₆₀/A₂₈₀, where pure DNA has a ratio \geq 1.7 (Sambrook, J. et al, 1989).

2.5.1.2.4 Ligation of DNA into plasmid vectors

The DNA concentration of each insert and vector aliquot was measured (section 2.5.1.2.3). It was decided to carry out at 2:1 and 5:1, insert:vector ratio ligation.

The amount of each insert and vector for each ligation was calculated (Equation 2.1) and the DNA quantities listed in Table 2.4. Vector and insert were incubated with ddiH₂O to a total final volume of 10μl, for 5 min at 45°C. The separate ligation reactions were incubated on ice, then 1μl T4 DNA ligase and 1μl of 10x ligation buffer were added and the reactions incubated for 1hr at 25°C. Ligations were stored at -20°C.

Equation 2.1 Calculation of the appropriate concentrations of insert and vector DNA required for 'sticky ended' ligation reactions.

$$x \text{ ng insert} = \frac{\alpha \text{ (bp of insert)} \times (y \text{ ng linearised vector})}{\text{bp of vector}}$$

Where α represents the ratio of insert:vector i.e. for a 2:1 ratio, $\alpha = 2$.

Table 2.4 Calculation of the ng of vector and insert DNA required for a 2:1 and 5:1 insert:vector ligation reaction

The ~ng of insert DNA (x) were calculated using Equation 2.1 with $y=100\text{ng}$ for both pGBKT7 (8000bp) and pACT2 (8100bp).

	x (ng) of insert required when $\alpha = 2$	x (ng) of insert required when $\alpha = 5$
USH1C (2060bp)	56	140
PDZ1 (390bp)	10	26
PDZ2 (255bp)	7	16.5
PDZ3 (300bp)	8	20
Cadherin 23 (800bp)	23	40

2.5.1.2.5 Transformation of DNA into bacterial cells

The bait and control prey constructs were transformed into TOP10-One shot cells (Invitrogen), whilst the vectors themselves were amplified using 1 μ l of plasmid DNA in the TOP10-One shot cells only.

2.5.1.2.5.1 Preparation of liquid cultures

A single *E.coli* colony (less than 1 month old) from a working stock plate was used to inoculate appropriate medium (LB broth with/without selective antibiotics for plasmid selection; Appendix 2 & 4) and the culture was incubated at 37°C for 16-18 hours with shaking at 230 rpm (Stuart Scientific). For most strains, this yielded a stationary phase culture.

2.5.1.2.5.2 Long term storage of *E.coli* and recovery of frozen stocks

400 μ l of 30% glycerol was added to 600 μ l of stationary phase culture to produce a glycerol stock. The culture was frozen immediately and stored at -80°C. Cells were recovered by scraping the surface of the frozen stock with an inoculating loop (NUNC), and restreaking on a LB agar plate supplemented with the appropriate antibiotic. The plate was incubated upside down at 37°C for 16-18 hours and sealed with parafilm. The plate was stored at 4°C for up to one month.

2.5.1.2.5.3 Preparation of chemically competent *E.coli*

DH5α *E.coli* were recovered on LB agar at 37°C overnight. A single colony was used to inoculate 10ml of LB broth and was incubated at 37°C overnight, in a shaking incubator at 225rpm. This culture was then used to inoculate 200ml pre-warmed LB broth which was then incubated at 37°C 225rpm, until the absorbance reached 0.45 at 550nm. Pipette tips and eppendorfs were prechilled and the following steps were carried out at 4°C. The culture was divided into four 50ml Falcon tubes and incubated on ice for 5mins, before pelleting at 2500rpm for 15 min at 4°C in a Legend RT centrifuge (Sorval). Cells were gently resuspended in 2ml TFB1 (Appendix 3), then a further 10ml of TFB1 was added and the cells left on ice for 15mins. The cells were pelleted as previously at 2500rpm for 15 min at 4°C. The pellet was resuspended in 1.6ml TFB2 (Appendix 3) and left on ice for 15mins. Competent cells were then divided into 200μl aliquots for immediate use or storage at -70°C. The transformation efficiency was examined through transformation with the control plasmid pUC19 (Appendix 10).

2.5.1.2.5.4 Transformation of plasmid DNA into chemically competent *E.coli*

The following method used to transform Max Efficiency DH5α (Invitrogen), One Shot® TOP10 Chemically Competent Cells, KC8 cells (Clontech) and the DH5α cells created (section 2.5.1.2.5.3) was modified from that provided by the manufacturer. Appendix 8 lists the genotype data for each bacterial strain

Chemically competent cells were thawed on ice and 4µl of a ligation reaction was added to 50µl, mixed by flicking and incubated on ice for 20min. Cells were then heat shocked in a 42°C water bath for 45secs, then returned to the ice for a further 2mins. 250µl of sterile pre-warmed SOC (37°C) was added to each tube and then the cells were allowed to recover at 37°C for 1hr in a shaking incubator at 200rpm. 100-200µl of cells were plated out at dilutions 1:10, 1:100 and 1:1000 on pre-dried LB-amp plates for pACT2-cdh23 or on LB-kan plates for the remaining four bait constructs (section 2.5.1.2.1) at 37°C overnight.

2.5.1.2.6 Polymerase Chain Reaction (PCR)

The standard PCR employed throughout the following chapters uses Bioline *Taq* and its provided buffers, in a 25µl total reaction volume (Table 2.5). Reactions were prepared on ice and added to a pre-heated PCR Thermocycler block (Mastercycler, Eppendorf) at 95°C. Oligonucleotide primers were designed using Primer 3 (Appendix 12) and synthesized by MWG. A negative control reaction, minus the DNA template, was included for every PCR reaction to monitor fidelity. The standard thermocycler program employed throughout these chapters unless otherwise stated is listed in Table 2.5.

Table 2.5 Definitions of the PCR reaction and thermocycler program used in PCR reactions throughout the following chapters.

Standard Bioline PCR reaction components		Standard Thermocycler program	
Primer (100pmol/μl)	0.1μl of each	95°C	2 mins
Buffer (10x)	2.5μl	<u>95°C</u>	<u>30 secs</u>
dNTPs	2.5μl	<u>Annealing temp.</u>	<u>10 secs</u>
Mg ²⁺ (50mM)	0.75μl	<u>72°C</u>	<u>20 secs</u>
<i>Taq</i>	0.1μl	Repeat ____ steps for 35 cycles	
Template	Xμl	72°C	10 mins
H ₂ O	18.95μl – Xμl	End	

In reactions where Bioline *Taq* is substituted for Hot Star *Taq* (Qiagen), the following 25μl PCR reaction mix was used:

Standard Hot Star PCR reaction components		Standard Thermocycler program	
Primer (100pmol/μl)	0.1μl of each	95°C	5 mins
Buffer (10x)	2.5μl	<u>95°C</u>	<u>30 secs</u>
dNTPs	2.5μl	<u>Annealing temp.</u>	<u>10 secs</u>
<i>Taq</i>	0.1μl	<u>72°C</u>	<u>20 secs</u>
Template	Xμl	Repeat ____ steps for 35 cycles	
H ₂ O	19.7μl – Xμl	72°C	10 mins
		End	

Single samples of the four DNA bases (Bioline) were combined to form a stock 2mM dNTP (Deoxyribonucleotide triphosphates) solution.

2.5.1.2.6.1 Identification of positive recombinants

Positive recombinants were identified through PCR amplification performed directly on individual bacterial colonies, using primers to the flanking regions of the MCS (multiple cloning site; pACT2FB & R for control, T7 & pGBKT7R for bait vector primers; Appendix 13). Single colonies were picked and dipped in the PCR mix to act as template and then dipped in 5ml of LB-antibody broth. PCR amplification was carried out (section 2.5.1.2.6) with the following thermocycler programs: (pACT2FB & R) 95°C/15secs; 57°C/15secs; 72°C/2.5min for 35 cycles and (T7 & pGBKT7R) 95°C/20secs; 61°C/20secs; 72°C/1.5min for 35 cycles. Products were analysed on a 1% agarose gel (section 2.3.3.2.2.1). Those colonies containing plasmids with insert were grown overnight in the 5ml broth at 37°C 200rpm (section 2.5.1.2.5.1), with glycerol stocks created from the overnight cultures (section 2.5.1.2.5.2). At least five recombinants were selected for each bait construct and the construct DNA purified using Qiagen Miniprep kits (section 2.5.1.2.8.1).

2.5.1.2.7 DNA sequencing

Prior to sequencing, PCR products were cleaned to remove ssDNA and free dNTPs. For PCR with volumes of up to 25µl; 1µl *Exonuclease1*, 2µl *Shrimp Alkaline Phosphatase* (SAP; USB), 0.5µl SAP Dilution Buffer and 1.5µl ddiH₂O was added to each PCR reaction and incubated for 30mins at 37°C. The enzymes were deactivated by heating at 80°C for 15 mins and the solution stored at 4°C.

Sequencing of the cleaned PCR products was carried out in two ways (Table 2.6). The Big Dye (PE) protocol adapted from the manufacture's instructions was used throughout the following chapters. The DYEnamic ET terminator protocol was used to try and increase sequence data yields in section 5.1.5.

Table 2.6 A comparison of the sequencing reaction components and thermocycler programs employed by the Big Dye and DYEnamic ET terminator sequencing systems.

Big Dye v3.1	DYEnamic ET terminator
For a 20 μ l sequencing reaction:	For a 20 μ l sequencing reaction:
Single Primer (5pmol/ μ l) 1.3 μ l	Single Primer (5pmol/ μ l) 1.3 μ l
Big Dye v3.1 2.7 μ l	DYEnamic ET terminator 8 μ l
5x Seq Buffer 2.7 μ l	Template (0.15pmol) X μ l
Template (~50-100ng) X μ l	ddiH ₂ O 9.3-X μ l
ddiH ₂ O 13.3-X μ l	
Thermocycler Program	Thermocycler Program
95°C 2mins	95°C 1mins
<u>95°C</u> <u>20secs</u>	<u>95°C</u> <u>20secs</u>
<u>50°C</u> <u>10secs</u>	<u>50°C</u> <u>15secs</u>
<u>60°C</u> <u>3mins</u>	<u>60°C</u> <u>1mins</u>
Repeat ___ steps for 35 cycles	Repeat ___ steps for 25 cycles
Store at 4°C	Store at 4°C

Sequencing reactions were cleaned using Sephadex G50 (Sigma) and run on a MegaBase 1000 DNA Analysis system (Amersham Bioscience) (Injection time: 3kV for 40sec, Run conditions: 9kV 100min) by Ms K Pearce (in-house sequencing service). Sequences were analysed using CHROMAS (Appendix 12).

2.5.1.2.7.1 Sequencing of positive recombinants

The success of the cloning was further verified by DNA sequencing of PCR products (generated in 2.5.1.2.6.1) but using the extracted DNA as template (sequencing primers: T7, pGBK7R, pGBK7-PDZ1 F/R, pGBK7-PDZ2 F/R and pGBK7-PDZ3 F/R). PCR products were cleaned (section 2.5.1.2.7) and ~80ng of the product was sequenced using Big Dye v3.1 (ABI; section 2.5.1.2.7) with the T7 primer (Appendix 13).

2.5.1.2.8 Isolation and purification of plasmid DNA

DNA was purified from overnight cultures of *E. coli* in LB broth using Qiagen Miniprep kits for cultures of 1-5ml with an expected yield of 20 μ g of plasmid DNA, and Qiagen Maxiprep kits (QIAGEN-tip 500 columns) for cultures of 100-500ml with an expected yield of 300-500 μ g plasmid DNA. The Qiagen purification protocols are summarized in sections 2.5.1.2.8.1 & 2.5.1.2.8.2 (Appendix 3).

2.5.1.2.8.1 Small scale plasmid purification

The overnight culture was centrifuged at 13000rpm for 10mins and the supernatant discarded. The bacterial pellet was resuspended in 250 μ l Resuspension Buffer P1 and transfer to an eppendorf tube. To this, 250 μ l of Lysis Buffer P2 was added and inverted 4-6 times to mix. The lysis reaction was allowed to continue for up to 5mins until the solution became viscous and slightly clear. 350 μ l of Precipitation Buffer N3 was added and the tube immediately inverted 4-6 times, followed by

centrifugation for 10min at 13000rpm in a tabletop microcentrifuge (Jencons PLC). The supernatant was applied to the QIAprep column and the white pellet discarded. The column was centrifuged at 13000rpm for 60secs and the flow-through discarded. The column was washed with 0.5 ml Wash Buffer PB followed by centrifugation as above. The flow-through was discarded and the column washed again with 0.75 ml Buffer PE, followed by centrifugation as above. The flow-through was discarded and the column centrifuged again as previously, to remove residual wash buffer. DNA was eluted by incubation of the column with 30-50µl of ddH₂O for 1min and then centrifuged as previously. The eluate was stored at -20°C.

2.5.1.2.8.2 Large scale plasmid purification

Bacterial cells were harvested by centrifugation at 6000g for 15 min at 4°C using a 6K15 Laboratory Centrifuge (Philip Harris). The supernatant was removed and the pellet resuspended in 10ml of Buffer P1 with vortexing to remove all cell clumps. 10ml of Buffer P2 was added, mixed gently by inverting 4-6 times and incubated at room temperature for 5mins. 10ml of pre-chilled Buffer P3 was mixed immediately upon addition to the resuspended cells by inverting the tube 4-6 times, and then incubated on ice for 20mins to precipitate out the genomic DNA, proteins, cell debris, and detergents. The tubes were centrifuged at >20,000g/12,000 rpm for 30min at 4°C and the supernatant moved to a new tube. The supernatant was centrifuged again at >20,000 x g for 15 min at 4°C and the new supernatant collected. A QIAGEN-tip 500 was equilibrated by applying 10ml Buffer QBT, and

the column emptied by gravity flow. The supernatant was added to the top of the drained column and allowed to enter the resin by gravity flow. The QIAGEN-tip was washed with 2 x 30ml Buffer QC by gravity flow. The DNA was eluted using 15ml Buffer QF to which 10.5ml of room-temperature isopropanol was added to precipitate out the DNA. Eluate was centrifuged immediately at >15,000g for 30mins at 4°C. The supernatant was discarded and the pellet washed with 5ml of room-temperature 70% ethanol, and centrifuged at > 15,000g for 10mins. The supernatant was again discarded and the pellet air-dried for 5-10min, then redissolved in ddH₂O.

2.5.1.2.9 Transformation of yeast cells with cloned DNA plasmid

A 50ml stationary phase culture for each yeast strain to be transformed was grown, and used to produce a 300ml mid-log phase culture (section 2.5.1.1.3). The mid-log phase culture was aliquoted into 50ml falcons and centrifuged at 1,000 xg for 5min at room temperature. The supernatants were discarded and the pellet resuspended in sterile 1x TE. Cells were pooled for each strain separately, to give a final volume of 25–50ml. The cells were pelleted as above, the supernatant discarded and the pellet resuspended in 1.5ml of fresh sterile 1x TE: 1x LiAc (Appendix 3).

0.1µg of plasmid DNA to be transformed and 0.1mg of herring testes carrier DNA (provided with MATCHMAKER system, Clontech) was denatured in a boiling water bath for 20mins. 0.1ml of yeast competent cells was added to each denatured

plasmid/carrier DNA mix to be transformed and mixed well by vortexing. 0.6ml of sterile PEG/LiAc solution (Appendix 3) was added to each cell suspension and vortexed at high speed for 10sec. Cells were incubated at 30°C for 30min, shaking at 200 rpm. 70µl of DMSO was then added and mixed carefully by inversion before heat shocking the cells at 42°C for 15mins in a water bath. Tubes were chilled on ice for 2mins, and then centrifuged for 5sec at 14,000rpm at room temperature. The pellet was resuspended in 0.5 ml of sterile 1x TE buffer and 100µl aliquots at several dilutions was plated on the appropriate SD agar plate that selected for the desired transformants. Plates were incubated upside down, at 30°C for 4 days, sealed with parafilm and stored at 4°C for up to one month.

2.5.2 Validation of bait and control proteins

2.5.2.1 Plasmid extraction from yeast

A single yeast colony was spread over ~2cm² patch of the appropriate SD agar medium and the plate incubated at 30°C for 3–4 days. A portion of the patch (~1cm²) was scraped up using an inoculating loop and resuspended in 50µl of sterile 1X TE in a 1.5-ml eppendorf. 10µl of lyticase solution (5units/ml in 1X TE buffer) was added to the yeast suspension and vortexed. Tubes were incubated at 37°C for 30–60min with shaking at 200-250 rpm, before 10µl of 20% SDS was added and tubes were vortexed again. Samples were put through one freeze/thaw cycle (at -20°C) and vortexed again to ensure complete lysis of the cells. The entire contents of the tube was poured onto a prespun CHROMA SPIN-1000

Column (Clontech) and centrifuged for 5min at 700g according to the manufacturer's instructions, to elute the purified plasmid DNA.

Alternatively, plasmid DNA was purified by phenol: chloroform extraction. After the freeze-thaw cycle, sample volumes were brought up to 200 μ l with 1x TE, to which 200 μ l of phenol:chloroform:isoamyl alcohol (25:24:1) was added. Samples were vortexed at the highest speed for 5mins and then centrifuged at 14,000 rpm for 10mins. The upper aqueous phase was transferred to a new eppendorf to which an equal volume of chloroform:isoamyl alcohol (24:1) was added. Samples were vortexed and centrifuged as above and then the new aqueous layer underwent another chloroform:isoamyl alcohol extraction step. The new aqueous phase was transferred to a fresh tube, 8 μ l of 10 M ammonium acetate and 500 μ l of 95–100% ethanol was added. Samples were incubated at –70°C for 1 hr, then centrifuge at 14,000rpm for 10mins. The supernatant was discarded and the pellet air dried, then resuspended in 20 μ l of ddH₂O. Samples were stored at –20°C.

2.5.2.1.1 Bait sequence analysis

3 μ l of plasmid DNA extracted from pGBKT7-USH1C, pGBKT7-PDZ1, pGBKT7-PDZ2, pGBKT7-PDZ3 and pACT2-cdh23 transformed yeast was used as template in a PCR amplification (section 2.5.1.2.6) for sequencing (section 2.5.1.2.7). PCR products were produced with the primers from section 2.5.1.2.1. The same primers were used for sequencing, with the PDZ domain construct primers (Appendix 13) used to sequence the centre of pGBKT7-USH1C.

2.5.2.2 Protein extraction from yeast

For each transformed yeast strain from which protein was required, a 5ml overnight culture in appropriate SD selection medium, was prepared using a single isolated colony 1–2mm in diameter and no more than 4 days old. A 10ml culture of an untransformed yeast colony in YPD was also prepared as a negative control for Western blotting analysis. The entire overnight culture was used to inoculate 50ml aliquots of YPD medium, which were then incubated at 30°C with shaking (220–250 rpm) until they reached mid-log phase (section 2.5.1.1.3). The OD₆₀₀ reading for 1ml of culture at this point, was multiplied by the culture volume to obtain the total number of OD₆₀₀ units e.g. 0.6 x 55 ml = 33 total OD₆₀₀ units. The culture was quickly chilled in two pre-chilled 50ml falcon tubes per sample, with the tubes half full with ice. These were immediately centrifuged in a pre-chilled rotor (Legend RT, Sorval) at 1000xg for 5min at 4°C. The supernatant was discarded and the pellet resuspended in 50ml of ice-cold ddiH₂O. The pellet was recovered by centrifugation at 1000 xg for 5min at 4°C.

Each cell pellet was resuspended in 100µl of ice-cold TCA buffer (Appendix 3), per 7.5 OD₆₀₀ units of cells on ice, and then transferred to 1.5ml screw-top eppendorfs containing glass beads (425–600µm) and ice-cold 20% TCA, (100µl of beads and 100µl of 20% TCA per 7.5 OD₆₀₀ units of cells). Tubes were vortexed vigorously for 4 x 1min, to disrupt the cells, with incubation on ice for 30sec in between each vortexing. The supernatant above the settled glass beads was transferred to another tube also on ice. The glass beads were washed with 500 µl of ice-cold 1:1

20% TCA:TCA buffer and vortexed as above. The liquid above the beads was added to the previously isolated aliquot of supernatant on ice. Any carryover glass beads in the combined supernatant extracts were allowed to settle and then the liquid above these beads was transferred to another eppendorf and the protein pelleted at 14,000rpm for 10min at 4°C. The supernatant was discarded and the pellet resuspended in TCA-Laemmli loading buffer (Appendix 3), using 10µl of loading buffer per OD₆₀₀ unit of cells. The protein samples were denatured by boiling in a water bath for 10min before centrifugation at 14,000rpm for 10min at room temperature. The supernatant was collected and loaded directly onto SDS-PAGE gels (Appendix 6; section 2.4.4.2) or stored at -70°C.

2.5.2.2.1 Confirmation of fusion protein identity

The total protein content of [AH109]pGBKT7-USH1C (7&12), [AH109]pGBKT7-PDZ1, [AH109]pGBKT7-PDZ2, [AH109]pGBKT7-PDZ3 and [Y187]pACT2-CDH23, with [AH109]pGBKT7, [Y187]pACT2, AH109 and Y187 (used as positive and negative controls respectively) were isolated (section 2.5.2.2). 15µl aliquots from the PDZ domain fusion proteins, [Y187]pACT2 and controls underwent electrophoresis on a 15% SDS-PAGE gel, whilst [AH109]pGBKT7-USH1C (7&12) and AH109 were run on a 10% SDS-PAGE gel (Appendix 6; section 2.4.4.2). Separated proteins were transferred to membranes and immunoblotted (section 2.4.4.3) using the following antibodies:

- pGBK7 based constructs expressing the c-Myc tag were visualised using monoclonal anti c-Myc primary antibody (1:500 dilution, Invitrogen) overnight at 4°C, followed by biotinylated anti-mouse IgG secondary antibody (1:500 dilution, KPL) for 1 hour at room temperature and a Streptavidin-AP antibody (1:2500 dilution) for a further hour at room temperature.
- pACT2 based constructs expressing the influenza hemagglutinin (HA) tag were visualised using a mouse monoclonal anti HA primary antibody (1:200 dilution, Santa Cruz Biotechnology) overnight at 4°C, followed by the same biotinylated anti-mouse IgG secondary antibody as above (1:200 dilution) for 1 hour at room temperature and a Streptavidin-AP antibody (1:2500 dilution) for a further hour at room temperature.

To further confirm that the main bait fusion protein was actually harmonin, not just a protein of a similar size, pGBK7-USH1C(12) underwent *In Vitro* Translation (IVT) (section 2.5.6.1.1). The c-Myc/USH1C tagged product was run on a 12% SDS-PAGE gel alongside a 'No DNA' lysate control. The membrane was divided and immunoblotted (section 2.4.4.3), with either anti c-Myc-AP (1:400 dilution incubated overnight at 4°C, Invitrogen); monoclonal anti-harmonin (1:400 dilution) followed by biotinylated anti-mouse IgG secondary antibody (1:1000 dilution for 1 hour at room temperature) and the Streptavidin-AP antibody (1:2500 dilution); or polyclonal anti-harmonin (1:400 dilution) with biotinylated anti rabbit IgGs-AP (1:1000 dilution for 1 hour at room temperature, KPL) and a Streptavidin-AP antibody (1:2500 dilution).

2.5.2.3 Toxicity effects of the fusion proteins on the host yeast cells

To investigate the effects of the bait fusion proteins on yeast growth, their rate of growth was compared to that of yeast transformed with the 'empty' vectors for the GAL4-BD or GAL4-AD proteins alone. Growth rates were also compared to the Clontech control fusion proteins. Isolated yeast colonies were added to single DO (drop out) SD liquid media to be incubated to mid log phase (section 2.5.1.1.3).

2.5.2.4 Autonomous activation of the reporter genes

As yeast two-hybrid selection is based on the nutritional and colourmetric selection of the reporter genes (ability to grow on SD/-His/-Ade and positive for β -galactosidase), it is important to know that none of the baits or controls are capable of activating the transcription and expression of the reporter genes.

2.5.2.4.1 Nutritional reporter gene activation

Eight colonies from the transformation plates (section 2.5.1.2.9) were streaked on SD media lacking various combinations of amino acids (SD/-Ade; SD/-His; SD/-Leu; SD/-Trp; SD/-Met; SD/-Ura; YPD and YPDA). Transformants able to autoactivate *HIS3* were re-streaked on SD-Trp supplemented with the His3p inhibitor, 3-amino-1,2,4-triazole (3-AT). Colonies were grown on 5mM, 10mM, 15mM, 50mM, 100mM and 500mM 3-AT supplemented plates.

2.5.2.4.2 β -galactosidase assay

Lac Z activation was examined by Colony Filter Lift assay as it is relatively sensitive, especially for cells that contain one or only a few copies of the *lac Z* reporter gene. It is convenient for large-scale experiments and inexpensive but is only qualitative.

Z buffer/X-gal solution was prepared (Appendix 3). For each plate of transformants to be assayed, a #5 filter paper (Whatman) was saturated with *Z* buffer/X-gal solution and placed in a clean empty Petri dish. A clean dry #5 filter paper was placed over fresh colonies 1–3mm in diameter grown on the appropriate SD selection medium appropriate for the system and plasmids. Filters were pressed down to ensure that colonies clung to the paper, which was orientated with respect to the original agar plate by poking holes in the agar at three asymmetric points. The filter was quickly snatched from the agar plate using forceps and submerged colony face up in liquid nitrogen for 10secs. Filters were allowed to thaw and then submerged in liquid nitrogen again to permeabilise the thick yeast cell walls. Once thawed, this filter was placed colony face up on the *Z* buffer/X-gal pre-wetted filter, bubbles between them eliminated, and then incubated covered in a fume hood for up to 8hours, checking periodically for the appearance of blue colonies. The β -galactosidase-producing colonies were identified by aligning the filter to the agar plate using the orienting marks. The corresponding positive colonies from the original plates were streaked onto fresh medium for further analysis.

2.5.2.5 Yeast mating

Yeast mating is an alternative method to co-transformation for introducing two different plasmids into the same host cells and is convenient for confirming interactions. Yeast transformants in MAT α (AH109) and MAT α (Y187) mating cassette types (Appendix 9) were grown on appropriate SD agar plates. One large fresh colony of each mating cassette was resuspended in 0.5ml YPDA in a 1.5ml eppendorf. Cell suspensions were incubated at 30°C overnight with shaking at 200 rpm. 100ml aliquots of the mating culture were plated on SD-Leu/-Trp to select for diploids, confirming that mating had been successful and on SD-Leu/-Trp/-His/-Ade+12mM 3-AT to select for diploids in which a positive two-hybrid interaction was occurring. Plates were incubated at 30°C for 5-10 days or until colonies appeared and then tested for β -galactosidase activity (section 2.5.2.4.2).

2.5.2.5.1 Control mating experiments

As the interaction between murine p53 protein and SV40 large T-antigen is well characterised (Li, B et al, 1993), AH109[pGBKT7-53] and Y187[pGADT7-T] were used as positive controls for the system. The bait AH109[pGBKT7-USH1C] was mated with Y187[pACT2-CDH23], a known interactor, to act as a positive control for the bait protein. AH109[pGBKT7] was mated with Y187[pACT2] to ensure that there was no activation of the selectable markers through the vector(s) alone. AH109[pGBKT7-USH1C], AH109[pGBKT7-PDZ1], AH109[pGBKT7-PDZ2] and AH109[pGBKT7-PDZ3] were also mated with Y187[pACT2] for the same reason. [AH109]pGBKT7-Lam, which encodes a fusion of the DNA-BD with human laminin

C and acts as a control for any fortuitous interactions between the bait and an unrelated prey protein (Bartel, P et al, 1993), was mated with Y187[pACT2] and also with Y187[pGADT7-T]. A prey protein that interacts with the bait and also with Laminin C is likely to be a false positive result. The mated yeast were plated onto nutritionally deficient media, any colonies that grew underwent a colony filter lift β -galactosidase assays (section 2.5.2.4.2) to confirm the phenotype.

2.5.3 Bovine retinal library screening by sequential transformation into AH109 yeast

2.5.3.1 Amplification of the retinal cDNA library

The retinal cDNA library (Tai, A W et al, 1999), was amplified using electrocompetent *E.coli*. In this method, the uptake of DNA is facilitated by the application of a large electric field to the cells and is a modification of the method provided by the manufacturer (Invitrogen).

ElectroMAX DH10B cells (Invitrogen) were thawed on wet ice. 25 μ l of electrocompetent cells was added to ~40ng of bovine retinal library cDNA (~10ng/ μ l) in a pre-chilled eppendorf. Unused cells were quickly refrozen and stored at -80°C. The solution was carefully pipetted into a pre-chilled 0.1cm cuvette (Eppendorf), avoiding any bubbles and ensuring that the solution made-contact all the way across the bottom of the cuvette chamber. Samples were electroporated using the EC1 program (1.8kV for 5msec) of a Micropulser electroporator (Biorad) in 1mm cuvettes (Molecular Bioproducts). 1ml of SOC medium (Appendix 2) was added to the cells in the cuvette and the whole solution transferred to 3ml of 2xYT

(Appendix 2) (double strength to be extra nutrient rich to increase DNA uptake and cell survival) in a 250ml sterile flask. The whole process was repeated again for a second aliquot of cells and once electroporated, was combined with the first cell aliquot in the 3ml of 2xYT broth. The cells were incubated at 37°C for 1 hour, with shaking at 225rpm. A serial dilution in LB-amp of the transformation mix was plated out on LB-amp plates at 1:10, 1:100 and 1:1000. Plates were incubated upside-down at 37°C overnight, to assess the transformation efficiency and library titre. The 1hour culture was then split over four 250ml LB-amp cultures in 1L flasks for excellent aeration and incubated at 37°C for overnight, with shaking at 225rpm. The plasmid cDNA was harvested using two maxiprep columns (Qiagen) (section 2.5.1.2.8.2) per 250ml culture and the resulting elution combined and aliquoted for storage at -20°C.

To check for representative amplification of different cDNAs within the library, individual colonies from the transformation efficiency plates underwent a 25µl standard PCR (section 2.5.1.2.6) as follows (95°C/15secs; 57°C/15secs; 72°C/2.5mins for 35 cycles), using the pACT2FB & R vector primers (Appendix 13). Two library aliquots also underwent restriction enzyme digestion (2µl library DNA; 5µl ddH2O; 1µl 10xNEB Buffer 2; 1µl *EcoR1*; 1µl *Xho1* were incubated at 37°C for 2 hours and then the enzymes deactivated by incubation at 65°C for 15mins) and were electrophoresed on 1% agarose gels (section 2.3.3.2.2.1), against uncut library DNA.

2.5.3.2 Sequential co-transformation of baits and preys

The pGBK7-USH1C(12) bait was streaked on SD-Trp agar and a 2-3mm colony <3 weeks old was used to produce a 1L YPDA mid-log phase culture (section 2.5.1.1.3). Cells were pelleted in 50ml aliquots by centrifugation (Legend RT, Sorval) at 1000xg for 5mins at room temperature. The pellets were resuspended in 500ml per transformant, of sterile 1x TE by vortexing, pooled and centrifuged as above. The pellet was resuspended in 8mls fresh sterile 1x TE/LiAc (Appendix 3). 0.47mg of retina library cDNA was denatured alongside 20mg herring testes carrier DNA at 100°C for 20mins. 8ml of competent yeast cells was added to the denatured DNA mix and vortexed. 60ml of sterile PEG/LiAc solution was next added and vortexed to mix. Yeast cells were incubated at 30°C for 30min with 200rpm shaking. Cell walls were permeabilised with 7ml of DMSO and gently inverted, followed by heat shocking at 42°C for 15mins, swirling occasionally to mix. Cells were chilled on ice for 1–2min and centrifuged for 5min at room temperature at 1,000xg. The supernatant was discarded and the cell pellet resuspended in 10ml of 1xTE.

To calculate cotransformation efficiency and library titre, serially diluted (1:20; 1:100; 1:1000) transformed cells were plated on SD-Trp/-Leu agar and incubated at 30°C for 3-5 days.

2.5.3.3 Library screening

Transformants can be selected for using high-, medium-, or low-stringency media. Less stringent screens increase the number of false positives, while more stringent screens may result in false negatives. Therefore the entire screening volume of transformed cells was plated out over ten 10cmx10cm SD-Trp/-Leu/-His/-Ade+12mM 3-AT agar plates and incubated at 30°C for 7-10 days. Prey were screened at high levels of stringency but a longer incubation time was used to try and catch low-affinity protein interactions.

Colony filter lift β -galactosidase assays (section 2.5.2.4.2) were carried out on all plates using 10cmx10cm filters which were unwieldy and left much of the colonies still on the plate. The results were poor, with most of the plate turning blue, giving a positive result after 7-8 hours of incubation with the substrate. The ten agar plates were re-incubated for a further two days to recover the colonies. The filter lift assay was repeated on the 10cmx10cm screening plates with replica plates produced simultaneously and incubated for three days at 30°C. Replica plating left most of the colony was on the replica plate and not on the filter so the β -galactosidase assay proved poor again. Therefore the large colonies from the replica plates and those that obviously activated *Lac Z* on the filter lift assay and could be clearly identified were labelled and streaked out on smaller SD-Trp/-Leu/-His/-Ade+12mM 3-AT agar plates which were incubated at 30°C for 3-4 days for further analysis.

2.5.3.4 Segregation of multiple library plasmids with a diploid and repeat analysis of activation of reporter genes

The initial library co-transformants may contain more than one AD/library plasmid, which can complicate the analysis of possible positive clones. Therefore positive interacting colonies were restreaked on SD–Leu/–Trp plates and incubated at 30°C for 4-6 days. This process was repeated once more to allow loss of some of the AD/library plasmids while maintaining selective pressure on both the DNA-BD and AD vectors. The full nutritional phenotype was then re-examined, with colonies streaked onto SD–Leu/–Trp/ –His/ Ade + 12mM 3-AT plates and incubated at 30°C for 5-8 days. They were then re-examined for β -galactosidase activity (section 2.5.2.4.2), with the incubation period required to produce a positive result by the different bait-prey combinations, compared to the incubation time required by the positive control plasmid, pCL1. Colonies that turned blue within 2-4 hours are said to involve stronger protein-protein interactions than those that take 6-8 hours (Yeast Protocols, Clontech). Glycerol stocks of colonies passing nutritional and colourimetric selection procedures were produced (section 2.5.1.1.1).

2.5.4 Characterisation of candidate interactors

2.5.4.1 PCR amplification of library inserts

PCRs were set up (section 2.5.1.2.6), using the yeast colony directly as template and performed for 35 cycles (95°C/15secs; 56°C/15secs; 72°C/2mins) using primers to the MCS of the vector (pACT2FB and pACT2R; Appendix 13) in 96 well

plates (ABgene). The initial enzyme activation step of 95°C/5mins for Bioline *taq* was lengthened to 15mins to permeabilise the yeast's thick outer cell wall. Use of the yeast colonies themselves as templates proved successful for a number of interactors. The remaining interactors underwent PCR as above but were supplemented with 1M Betaine (final concentration) to increase yield by minimizing inhibitory secondary structure formation by the template which would prevent the primer from annealing. Where this alone failed, 3µl of yeast glycerol stock rather than the yeast streak was used as template. The total PCR volume was increased to 50µl whilst maintaining relative component concentrations, to minimize any inhibitory effect the glycerol may have on the reaction. 5µl of each product was electrophoresed on 1% agarose gels (section 2.3.3.2.2.1).

Those preys that would not PCR amplify directly from either the yeast glycerol stock or directly from a yeast colony itself, underwent plasmid extraction using phenol:chloroform or CHROMA SPIN 1000 columns (section 2.5.2.1). 1-3µl of extracted plasmid was then used as template in the above PCR.

2.5.4.2 Transformation of library inserts in DH5 α and KC8 cells

In order to generate sufficient cDNA template for sequencing, yeast plasmid DNA for those preys not amplifying by PCR were transformed into *E.coli*. When transforming *E. coli* with plasmids isolated from yeast, it is best to use chemically competent *E. coli* cells that have a transformation efficiency of at least 10^7 cfu/mg (of pUC19 DNA). A large quantity of competent cells was produced (section

2.5.1.2.5.3), from a stock of DH5 α cells (Invitrogen; Appendix 8). Their competency was checked through transformation with the control plasmid pUC19 (Appendix 10).

10 μ l of yeast plasmid was added to 100 μ l of chemically competent cells synthesized in section 2.5.1.2.5.3 or to 100 μ l KC8 cells (Appendix 8, Invitrogen), thawed on ice and then the cell suspensions were incubated on ice for 30min. Cells were heat shocked at 42°C for exactly 45secs and then returned to the ice for a further 2min, before 1ml of SOC (pre-warmed to 37°C) was added. Cells were allowed to recover at 37°C for 1 hour in a shaking incubator. Cell suspensions were then pelleted by centrifugation at 2500rpm for 5min. The supernatant was discarded and the pellet resuspended in the residual liquid. 50 μ l aliquots of cells were plated on pre-dried LB-amp plates (Appendix 2). Plates were incubated overnight at 37°C but no obvious growth was seen so incubation was increased to 20 hours. Transformants were examined for the presence of the insert by PCR (sections 2.5.1.2.6 & 2.5.1.2.7). If positive for the presence of an insert, the colony was used to produce a 5ml overnight culture (sections 2.5.1.1.3) from which the plasmid DNA was isolated (section 2.5.1.2.8.1) for sequencing.

Transformation failure may be a result of a decreased amount of yeast plasmid DNA in the samples for transformation. Therefore plasmid extraction was repeated (section 2.5.2.1) but with growth of liquid colonies in 15ml falcons rather than eppendorfs and extra lyticase used during the cell lysis step. Transformation into bacteria was then repeated as above.

2.5.4.3 DNA sequence analysis of library inserts

Amplified products were analysed on 1% agarose gels, and colonies displaying multiple bands had these isolated by gel extraction (Qiaquick gel extraction kit; section 2.5.1.2.2; Qiagen). Colonies with single bands were cleaned (section 2.5.1.2.7). Sequencing was carried out (section 2.5.1.2.7) using ~80ng of template with the primer pACT2R. In an attempt to increase sequence data yield, the extension temperature on the sequencing thermocycler program was increased from 60°C to 64°C; Big Dye reaction mix was used at greater concentration with no dilution buffer; sequencing reactions were supplemented with Betaine at 1M final concentration and an alternative DYEnamic ET terminator sequencing kit was employed (section 2.5.1.2.7).

2.5.5 Confirmation and further characterization of positive interacting preys

2.5.5.1 Confirmation of prey-harmonin interaction by yeast mating

In order to confirm the protein-protein interactions *in vivo*, prey plasmids were isolated in AH109 whilst the bait and control constructs were transformed into Y187, allowing for confirmation through yeast mating.

2.5.5.1.1 Segregation of yeast plasmids

3ml of SD-Leu/+amp media (Appendix 2) was inoculated with one prey colony and incubated at 30°C for 1-2 days, shaking at 230-250rpm. 1:10 and 1:100 dilutions

were plated on SD-Leu/+amp agar and incubated for a further 2-3 days at 30°C or until colonies appeared. Several colonies from the SD-Leu/+amp plates were transferred in a grid fashion to both SD-Leu (selecting for the prey plasmid thus colonies should grow again), and SD-Trp plates (selecting for the bait plasmid thus colonies should not grow). The isolated prey plasmids that only grew on SD-Leu could then be extracted in the normal way (section 2.5.2.1), and glycerol stocks made (section 2.5.1.1.1).

2.5.5.1.2 Transformation of bait and control plasmids into strain Y187

Y187 yeast was transformed as described previously (section 2.5.1.2.9), with pGBKT7, pGBKT7-USH1C, pGBKT7-PDZ1, pGBKT7-PDZ2, pGBKT7-PDZ3 and pGBKT7-Lam.

2.5.5.1.3 Yeast mating

For each candidate prey plasmid to be tested, mating reactions were set up (section 2.5.2.5.1), between prey and each of the following: pGBKT7, pGBKT7-USH1C and pGBKT7-Lam.

2.5.5.2 Further characterization of prey-harmonin interaction through yeast mating with the PDZ domain baits

For each remaining candidate prey plasmid to be tested, mating reactions were set up (section 2.5.2.5.1), between prey and each of the following: pGBKT7-PDZ1, pGBKT7-PDZ2 and pGBKT7-PDZ3.

2.5.5.3 Futher analysis of the candidate interactor – Phosducin

2.5.5.3.1 Identification of the ORF of phosducin and confirmation of its interaction with harmonin by mating analysis

The complete DNA sequence of the prey inserts for interactors #1.3, 1.7 and 1.9 were produced using the glycerol stock as template and the reaction mix supplemented with Betaine (section 2.5.4.1 & 2.5.4.3). Mating analysis was carried out (sections 2.5.5.1.3 & 2.5.5.2).

2.5.5.3.2 Analysis of Phosducin protein sequence

Phosducin sequences from different species listed by NCBI were aligned using CLUSTALW (Appendix 12) to search for regions of homology. This was in order to determine whether the interaction seen here between a human harmonin protein and a bovine/mouse phosducin protein, could occur between both human proteins and that the interaction was not a species-dependent false positive.

2.5.6 Methodology: Confirmation of an interaction between harmonin and phosducin by co-immunoprecipitation (CO-IP)

2.5.6.1 Synthesis of c-myc tagged harmonin and identification of phosducin in whole eye homogenate

2.5.6.1.1 Protein synthesis by *in vitro* transcription and translation

pGBKT7-USH1C contained an in-frame T7 promoter sequence, so harmonin could be generated directly from the insert DNA sequence by *in vitro* transcription (IVT). Upon removal from storage at -70°C, the TNT® Quick Master Mix (Promega) was rapidly thawed by hand and placed on ice. All other components were thawed at room temperature and stored on ice. The reaction components were assembled in an RNase free 0.5ml eppendorf tube. 40µl TNT® T7 Quick Master Mix, 1µl 1mM methionine, 0.5µg DNA Template and Nuclease-Free water to a final volume of 50µl was mixed gently by pipetting and briefly pulse centrifuged. The template should be free of ethanol, calcium, RNase and salt. The reaction was incubated at 30°C for 90minutes and stored at -20°C.

MATCHMAKER control plasmids (Clontech) underwent IVT, replacing 2µl of nuclear-free water with Transcend™ Biotin-Lysyl-tRNA (Promega) to biotin-label the resulting protein and by-pass the need for the anti-HA antibody during Western blotting (section 2.4.4.3).

The IVT USH1C protein used in section 4.3 was generated as above from a PDZ73 construct produced by Dr Blaydon of this lab, with the PDZ73 sequence positioned downstream of the Sp6 promoter sequence and using the Sp6 TNT[®] IVT Kit (Promega).

2.5.6.1.1.1 Introduction of the HA tag and the T7 promoter sequence to the MCC2 positive control

The CO-IP positive control for harmonin interactions, MCC2, lacked both a T7 promoter and an HA tag for detection. These were introduced in-frame upstream of the DNA sequence, in the primers HAT7MCC2F & MCC2R (Appendix 13). A standard 25µl PCR reaction was used (section 2.5.1.2.6), but Mg²⁺ ion concentrations were increased to 0.9µl/25µl reaction volume, since the primers used were very long and would decrease Mg²⁺ ions rapidly. 1µl pGEX-4T-1-MCC2 #12 (Blaydon, D. 2004) was used as template. A 'Touchdown' thermocycler program (section 2.5.1.2.6) of 40 cycles with an extension time of 30secs was employed as the annealing temperature of the primers would vary as the reaction progressed. Initially only the 3' region specific for MCC2 would anneal but as more tagged product was formed and used as template in later cycles, the whole of the long primer would anneal to the template, altering the annealing temperature.

The PCR product was purified from PCR reaction mix components (section 2.5.6.1.1.2) and then used to synthesise HA-tagged MCC2 by IVT (section 2.5.6.1.1).

2.5.6.1.1.2 Purification of PCR products

This protocol is summarized from the manufacturer's (Qiagen) protocol. 5 volumes of Buffer PB (Appendix 3) was added to 1 volume of the PCR sample, mixed and added to a QIAquick (Qiagen) spin column in a 2ml collection tube. Columns were centrifuged (Jencons PLC) at 13,000rpm/~17,000xg for 60sec at room temperature, to bind DNA to the column. The flow-through was discarded and the column washed with 0.75ml Buffer PE. The column was centrifuged as above, the flow through discarded and centrifuged again to remove any residual buffer. The DNA was eluted from the column into a clean 1.5ml eppendorf by incubating the column with 30-50 μ l ddiH₂O followed by centrifugation as above.

2.5.6.1.2 Simultaneous detection of phosducin and harmonin on Western blots

The expression of native phosducin was examined in whole eye homogenate from SV129 adult mice (section 2.4.4.1.2). 1 μ l of eye homogenate was run on a 15% SDS-PAGE gel (section 2.4.4.2) alongside 1 μ l of IVT USH1C (section 2.5.6.1.1). Proteins were transferred to a nitrocellulose membrane for Western blotting (sections 2.4.4.3), using the following antibody combinations:

- Antibody set A – overnight incubation at 4°C with anti-c-Myc -AP (1:2000) and anti-phosducin (1:2000) (Sokolov, M et al, 2004), followed by anti-sheep IgG-AP (1:2000, Serotec) at room temperature for 1 hour.
- Antibody set B – overnight incubation at 4°C with anti-c-Myc -AP (1:2000) and anti-phosducin (1:2000), followed by anti-sheep IgG-AP (1:1000) at room temperature for 1 hour. The membrane was developed then re-probed

to achieve a stronger harmonin band using monoclonal anti-harmonin (1:500) simultaneously incubated with the secondary antibody anti-mouse-AP (1:500) for 1hr at room temperature.

- Antibody set C – overnight incubation at 4°C with anti-c-Myc -AP (1:2000) and anti-phosducin (1:2000), followed by anti-sheep IgG-AP (1:1000) at room temperature for 1 hour. The membrane was developed then re-probed to achieve a stronger harmonin band using the secondary antibody anti-mouse-AP (1:500) for 1hr at room temperature.
- Antibody set D – 1 hour incubation at room temperature with anti-c-Myc -AP (1:1000) and anti-phosducin (1:2000), followed by anti-sheep IgG-AP (1:1000) at room temperature for 1 hour.
- Antibody set E – overnight incubation at 4°C with anti-phosducin (1:2000), followed by anti-sheep IgG-AP (1:1000) and anti-c-Myc -AP (1:500) at room temperature for 1 hour

2.5.6.2 CO-IP assay

2.5.6.2.1 Assay and bait control CO-IP reactions

5µl of IVT pGADT7-T and 5µl of IVT pGBK7-53 (produced in section 2.5.6.1.1), were incubated with 30µl of 25mM Tris-buffered saline (TBS) pH7.2 in the stoppered columns for 4 hours at room temperature on a rotator (Stuart Scientific).

The controls listed in Table 2.7 were set up and incubated in the same way.

To each column, a further 30 μ l TBS and 5 μ g anti-c-Myc antibody bound to agarose beads (ProfoundTM c-Myc Tag IP/CO-IP kit, Pierce) was added, all of which was then incubated on a rotator, overnight at 4°C. The column was then placed in a collecting tube, the cap loosened and the plug removed for a 10sec pulse spin at maximum centrifugation in a bench top centrifuge. The column was washed with 0.5ml TBS-T (TBS pH 7.2 + 0.05% Tween 20); inverting each column 3 times to mix, then pulse spinning at maximum for 10seconds. The flow through was discarded and the column washed a further two times. The bound proteins were eluted by adding 20 μ l of 2x non-reducing sample buffer (made from 5x concentrate and provided with the kit), incubating both column and new collecting tube at 95-100°C for 5mins, and then pulse spun as above.

8 μ l of each eluate was loaded on a 15% SDS-PAGE gel and transferred to a nitrocellulose membrane for Western blotting (sections 2.4.4.2 & 2.4.4.3). Proteins were detected by incubating the membrane with Streptavidin-AP antibody at 1:2500 for 1 hour at room temperature.

Table 2.7 Pull down assay control reactions

<i>Incubation mix</i>	<i>Reason</i>	<i>Expected outcome</i>
'no DNA' IVT reaction and TBS buffer	Tests for non-specific binding of proteins from the reticulocyte lysate	Blank
pGKKT7-53 protein (expressing c-myc tag) and TBS buffer	Checks the specificity of anti-c-myc antibodies for the c-myc tag (+ve control)	Single band of p53 protein
pGADT7-T protein (expressing HA tag) and TBS buffer	Checks the specificity of anti-c-myc antibodies for the c-myc tag (-ve control).	Blank
TBS buffer only	Identifies any contaminants in the buffer that result in bands on the blot.	Blank
pGKKT7-53 protein and pGADT7-T protein	Checks that the system functions correctly (+ve control)	Two bands – p53 & T
The above incubations were repeated, substituting anti-c-myc beads for anti-HA beads to confirm the above points and that the proteins were not binding to the beads themselves.		
pGKKT7-USH1C protein (expressing c-myc tag) and pACT2-MCC2 protein	Checks that the system functions correctly with respect to the bait – harmonin is able to interact with a known interactor (+ve control)	Two bands – harmonin & MCC2
pACT2-MCC2 protein (expressing HA tag) and TBS buffer	Checks that the system functions correctly with respect to the bait – harmonin is able to interact with a known interactor (-ve control)	Blank

2.5.6.2.2 pGBK7-USH1C and phosphducin

15µl IVT USH1C (section 2.5.6.1.1) was incubated with ~100µg whole eye homogenate (section 2.4.4.1.2) and 20µl 25mM TBS pH7.2 at 37°C overnight. This was then placed in an elution column (provided with Profound™ c-Myc Tag IP/CO-IP kit), with 30µl TBS and 5µg anti-c-Myc antibody bound to agarose beads (Profound™ c-Myc Tag IP/CO-IP kit, Pierce) and then incubated on a rotator (Stuart Scientific) at room temperature for 35mins. The column was then placed in a collecting tube, the cap loosened, the plug removed and pulse spun for 10 seconds at maximum centrifugation in a bench top centrifuge. This initial flow through was kept on ice for immediate use or stored at -20°C for later analysis. The column was washed with 0.5ml TBS-T (TBS pH 7.2 + 0.05% Tween 20); inverting each column 3 times to mix, then pulse spun at maximum for 10seconds. The flow through was discarded and the column washed a further two times as above. The bound proteins were eluted by adding 20µl of 2X non-reducing sample buffer (made from 5x concentrate and provided with the kit), incubating both column and new collecting tube at 95-100°C for 5mins, and then pulse spun as above. The eluate was kept on ice for immediate use or stored at -20°C for later analysis. A negative control was performed alongside, as above, substituting the IVT USH1C protein for buffer.

2µl β-mercaptoethanol was added to each eluate sample and the whole volume of eluate was loaded onto a 15% SDS-PAGE gel (Appendix 6 & 2.4.4.2) alongside aliquots of IVT USH1C alone and eye homogenate alone. A 10µl aliquot of initial flow through was denatured at 95°C for 3mins with 6xLlamelli loading buffer

(Appendix 3) and loaded alongside the eluate. The separated proteins on the SDS-PAGE gel were transferred to nitrocellulose membrane for Western blotting and the membrane blocked. The membrane was immunoblotted with anti-Phosducin 1:4000 and anti-sheep IgG-AP 1:1000 for 1hour at room temperature. The membrane was washed and then immunoblotted with monoclonal anti-harmonin 1:500 and anti-mouse IgG-AP conjugated antibody 1:1000 for 1hour at room temperature (section 2.4.4.3).

2.5.7 Methodology: Validation of candidate interactor through protein localisation and gene expression analysis

2.5.7.1 Comparison of Phd and harmonin protein localisation in the normal adult retina

Fixed adult SV129 eyes were collected and sectioned (section 2.3.1.1). Sections were stained for the presence of Phosducin as described by Sokolov, M et al, 2004. Controls substituted anti-Phosducin antibody for PBS. The primary antibody was detected using anti-sheep IgG-Cy3 (Jackson Laboratories) at 1:50 for 1 hour at room temperature. A nuclear counter stain was provided by 30 minutes incubation with Hoescht at 1:200 in PBS, at room temperature in the dark. Sections were washed and slides partly air dried before mounting with Citifluor (Citifluor Ltd) mounting media.

Stained sections were stored at 4°C. Immunolabelled sections were analysed using a light microscope (Axioplan 2, Zeiss), and images captured using Openlab software (Improvision). Stained sections were compared to adult unfixed retinal sections labelled with anti-harmonin (2.3.1.3).

2.5.7.2 Comparison of Phd and harmonin protein localisation in the normal developing retina

Fixed postnatal CD1 eyes were collected and sectioned (section 2.3.1.1). Sections were stained for the presence of Phosducin (section 2.5.7.1) and compared to harmonin labelled (2.3.3.1) and semithin sections (2.3.3.1).

Immunolabelled sections were analysed using a laser scanning confocal microscope (SP2 Leica), with projection images gathered at 0.3µm throughout the whole section using Leica Confocal Software (version 2.5), before transfer to Adobe Photoshop.

2.5.7.3 Comparison of Pdc and Ush1c gene expression in the adult and developing ear

1µg of total RNA (0.1µg/µl) from an isolated adult murine cochlea and a P7 bulla, and 1µg of total murine adult eye RNA (~ 0.2µg/µl) (used in section 3.3.2), were used in a two step RT-PCR reaction (section 2.3.3.2.2). The success of cDNA

production was examined using primers to the housekeeping gene *Gapdh* (Appendix 13) in a 25µl PCR amplification reaction (section 2.5.1.2.6) for 35 cycles (95°C/15s; 55°C/15s; 72°C/30s). The expression of *Pdc* in the ear used the same PCR reaction as the housekeeping gene and the following thermocycler program, (35 or 40 cycles at 95°C/15s; 55°C/15s; 72°C/30s), with maPhdF and maPhdR primers (Appendix 13). The adult eye cDNA was used as a positive control.

3 RESULTS CHAPTER: Identification of the temporal and spatial expression of *Ush1c* and harmonin within the normal murine eye.

In order to help understand its role in the pathology of Usher syndrome, the pattern of protein localisation and *Ush1c* gene expression was examined in the normal murine eye. Immunostaining analysis had already localised harmonin to the six sensory areas of the inner ear, restricted to the hair cells within these areas (Verpy, E et al, 2000). Due to the structural similarities between auditory hair cells and visual photoreceptor cells (sections 1.2.1.1 & 1.2.2.1), it is reasonable to hypothesise that harmonin could be localised within the retinal photoreceptors. This hypothesis is further supported by the demonstration of *USH1C* expression in the outer neuroblastic layer of the retina by Bitner-Glindzicz et al (2000), which is rich in newborn rod and cone photoreceptors.

Research Objectives:

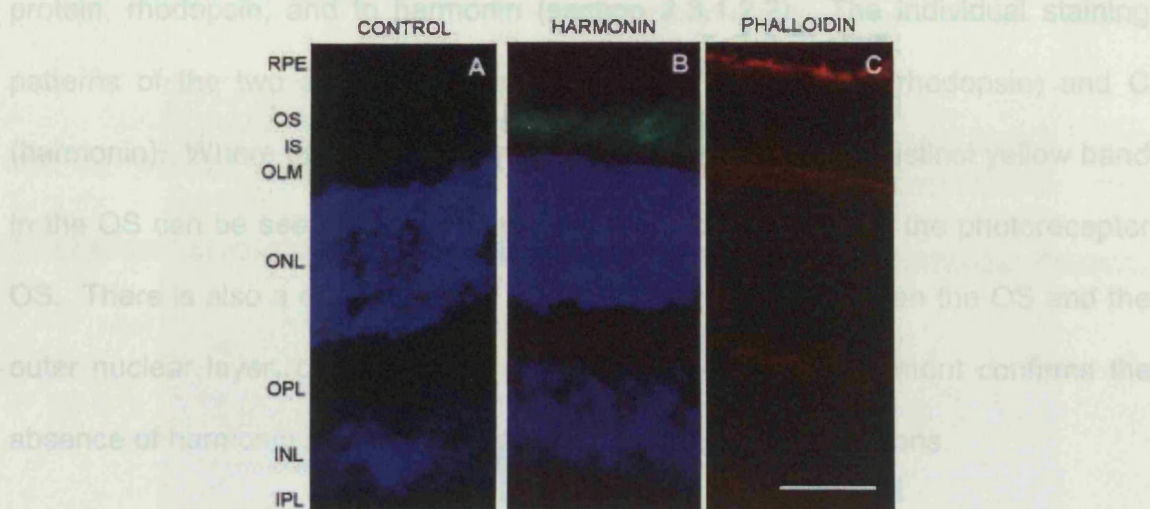
- To investigate the pattern of protein localisation of harmonin in the adult murine retina.
- To investigate the hypothesis that the type 1 Usher proteins interact, by examining the protein localisation of harmonin in the absence of myosin VIIA and cadherin 23.
- To explore possible functions of harmonin by determination of the age of onset of *Ush1c* gene expression.

3.1 *Identification of the pattern of protein localisation of harmonin in the adult murine retina*

3.1.1 *Harmonin localisation in the adult murine retina*

Adult murine retinal tissues were immunostained for the presence of harmonin (section 2.3.1.2.1). High levels of harmonin immunoreactivity were seen in the OS of the adult murine retina (Figure 3.1B). This staining was not seen when PBS was substituted for the anti-harmonin antibody (Figure 3.1A). Comparison of harmonin staining and phalloidin labelling (Figure 3.1C.), clearly demonstrates the absence of harmonin in the RPE, and also demonstrates a gap in staining between the green harmonin (B) in the OS and the blue of the Hoechst in the ONL (A), edged with the red of the OLM (C), suggesting that harmonin is not localised to the IS in fixed adult retinal tissue sections.

Figure 3.1 Localisation of harmonin in the adult murine retina

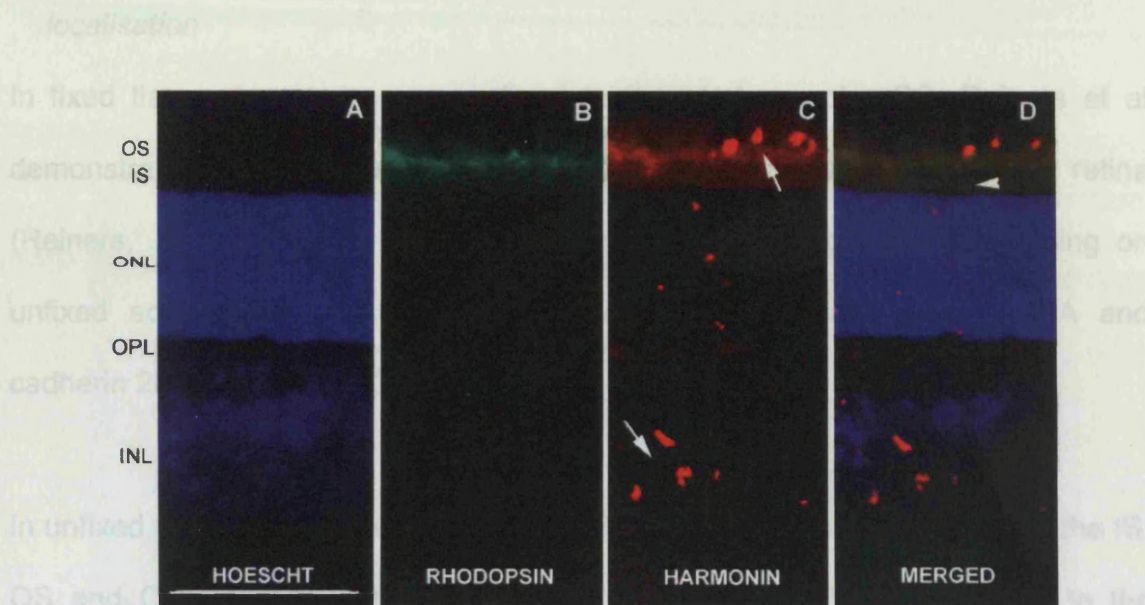


(A) Replacement of the anti-harmonin antibody with PBS. A nuclear counter-stain is provided with Hoechst (blue). (B) Harmonin (green) is clearly localised as a discrete band within the OS of the photoreceptor. No harmonin immunostaining was detected in the inner retina or RPE (compare the lack of staining in B in the region of the RPE highlighted in C). Note the absence of harmonin immunoreactivity at the photoreceptor IS. (C) The RPE, OLM and parts of the OPL, were visualised using rhodamine conjugated phalloidin to label the F-actin found in these structures.

GCL, ganglion cell layer. IPL, inner plexiform layer. INL, inner nuclear layer. OPL, outer plexiform layer. ONL, outer nuclear layer. OLM, outer limiting membrane. IS, photoreceptor inner segments. OS, photoreceptor outer segments. RPE, retinal pigmented epithelium. Scale bars 50 μ m.

Retinal sections were double immunostained with antibodies to the OS-specific protein, rhodopsin, and to harmonin (section 2.3.1.2.2). The individual staining patterns of the two antibodies can be seen in Figure 3.2B. (rhodopsin) and C (harmonin). Where these images are overlaid (Figure 3.2D), a distinct yellow band in the OS can be seen, confirming the presence of harmonin in the photoreceptor OS. There is also a distinct lack of staining in the region between the OS and the outer nuclear layer, corresponding to the IS. Thus this experiment confirms the absence of harmonin in the photoreceptor IS in fixed retinal sections.

Figure 3.2 Colocalisation of harmonin and rhodopsin in the photoreceptor outer segments



Retinal sections were stained for the presence of (B) rhodopsin (green), (C) harmonin (red) and counter stained with (A) Hoechst (blue). Punctate background staining from the secondary antibodies used is shown in C (white arrow). When the three images are overlaid in D, a yellow band is seen in the OS showing that the two proteins colocalise in this region and no staining is seen in the photoreceptor IS (white arrowhead), or any other region of the neural retina.

INL, inner nuclear layer. OPL, outer plexiform layer. ONL, outer nuclear layer. IS, photoreceptor inner segments. OS, photoreceptor outer segments. Scale bars 50 μ m.

Figure 3.2 and 3.3 support the findings of Fleitens *et al.* showing all three USH1 proteins to colocalise in the photoreceptor IS and OPL (Figure 3.3C-E), and would suggest that paraformaldehyde fixation can mask the harmonin antigens and reduce the ability of the antibody to detect the protein.

3.1.2 The effects of fixation upon harmonin, myosin VIIA and cadherin 23

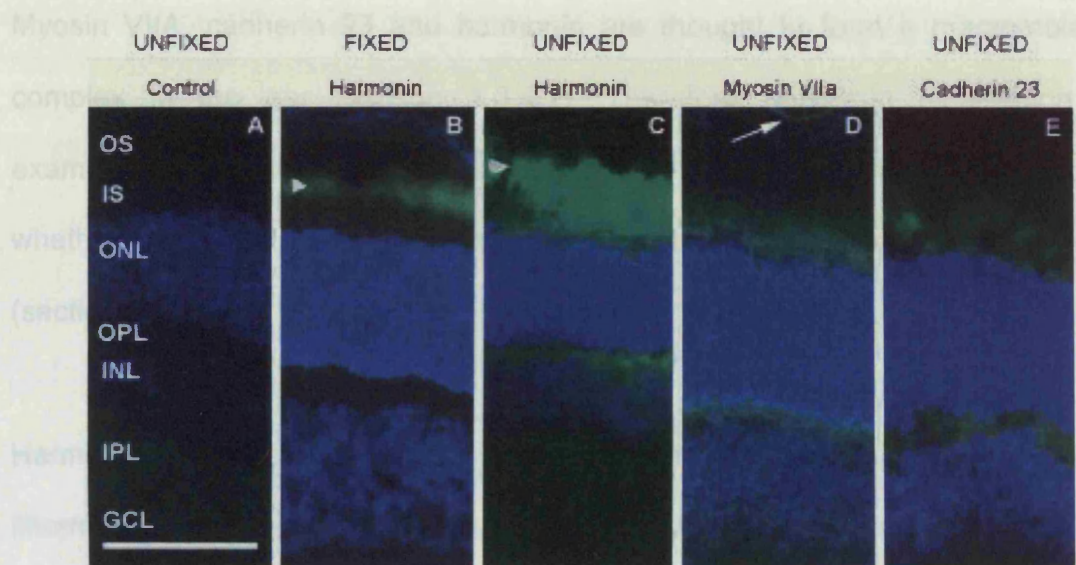
localisation

In fixed tissue, harmonin was confined to the photoreceptor OS. Reiners et al demonstrated further areas of harmonin immunoreactivity in the unfixed retina (Reiners, J et al, 2003). In order to confirm their findings, immunostaining on unfixed adult murine tissues was performed for harmonin, myosin VIIA and cadherin 23 (section 2.3.1.3).

In unfixed tissue, harmonin showed additional immunostaining, localising to the IS, OS and OPL (Figure 3.3C). In unfixed tissue, myosin VIIA is localised to the photoreceptor IS and OPL and to the RPE (Figure 3.3D); previously in fixed tissue, it was localised to the RPE and the photoreceptor connecting cilium only (Liu, X et al, 1997). Cadherin 23 was confined to the IS and OPL of the photoreceptor only (Figure 3.3E). No staining was seen in the photoreceptors in the negative controls for any of the primary antibodies (Figure 3.3A). In unfixed tissue, levels of immunostaining were generally higher throughout the retina, compared to fixed tissue (Figure 3.3C and B). These results support the findings of Reiners et al, showing all three USH1 proteins to colocalise in the photoreceptor IS and OPL (Figure 3.3C-E), and would suggest that paraformaldehyde fixation can mask the harmonin antigens and reduce the ability of the antibody to detect the protein.

3.2 Examination of harmonin localisation in fixed retinal tissue in the absence of myosin VIIa or cadherin 23

Figure 3.3 Immunolocalisation of USH1 proteins in unfixed and fixed murine retinas



3.4B&C), indicating that the loss of one or both myosin VIIa alleles results in the absence

(A) Example of a negative control section, substituting PBS for the primary antibody. Low level background is visible throughout the inner neural retina (INL, IPL & GCL). (B) Harmonin (green) is localised to the photoreceptor OS (white arrowhead) in fixed tissue. (C) Immunostaining on unfixed tissue (shown in green) for harmonin (D), myosin VIIA and (E) cadherin 23, shows all three to be present in photoreceptor IS and the OPL.

GCL, ganglion cell layer. IPL, inner plexiform layer. INL, inner nuclear layer. OPL, outer plexiform layer. ONL, outer nuclear layer. IS, photoreceptor IS. OS, photoreceptor OS. Scale bars 50 μ m.

3.2 *Examination of harmonin localisation in fixed retinal tissue in the absence of myosin VIIA or cadherin 23*

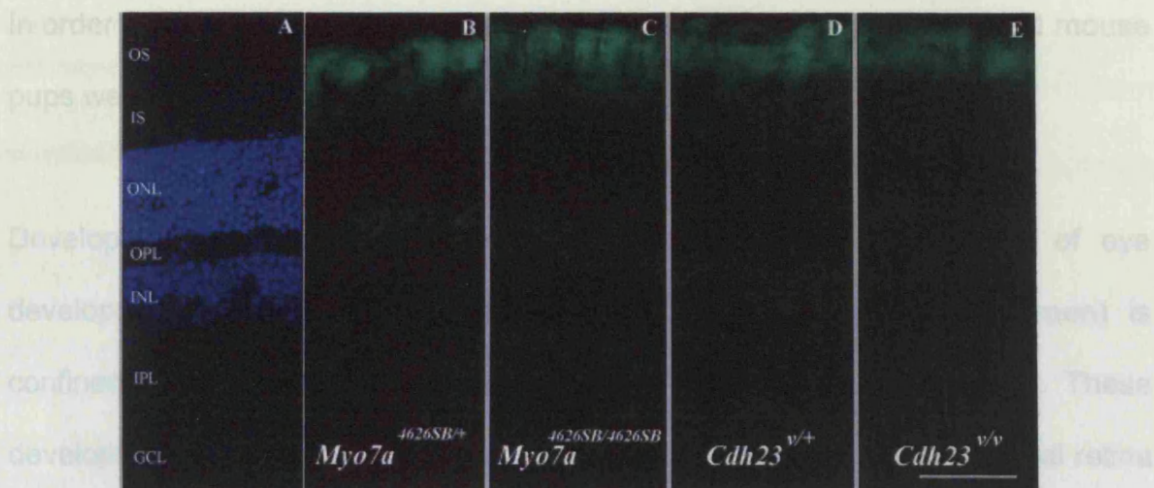
Myosin VIIA, cadherin 23 and harmonin are thought to form a macromolecular complex in the ear (section 1.3.4.1). Therefore harmonin localisation was examined in the retina of null mouse models for USH1B and USH1D, to determine whether its spatial positioning was maintained in the absence of either protein (section 2.3.2).

Harmonin was localised in the photoreceptor OS in both the heterozygous littermate control and in the homozygous null *Myo7a*^{4626SB} mutant retina (Figure 3.4B&C), indicating that the loss of one or both myosin VIIA alleles has no effect on harmonin localisation in the OS. In the retina of the *Cdh23*^v heterozygote and homozygote mice (Figure 3.4D&E), harmonin was also maintained in the photoreceptor OS, showing that cadherin 23 is not required for the localisation of harmonin to the photoreceptor OS either. Fixed tissue was used in this study as increased masking of harmonin by fixation had not been demonstrated at this time.

3.3 Determination of the age of onset of *Uahr* gene expression

Figure 3.4 Immunolocalisation of harmonin in normal and mutant murine retinas

3.3.1 Harmonin localisation in the postnatal murine retina



Harmonin was visualised by FITC (green) with Hoechst nuclear staining (blue). (A) Negative control. (B) In the heterozygote *shaker-1* ($Myo7a^{+/-}$) (C) and the homozygote *shaker-1* ($Myo7a^{4626SB/4626SB}$), harmonin localised to the photoreceptor OS. In the heterozygote *waltzer* mouse ($Cdh23^{v/+}$) (D), and the homozygote *waltzer* ($Cdh23^{v/v}$) (E), harmonin localisation in the photoreceptor OS was also maintained.

GCL, ganglion cell layer. IPL, inner plexiform layer. INL, inner nuclear layer. OPL, outer plexiform layer. ONL, outer nuclear layer. OLM, outer limiting membrane. IS, photoreceptor inner segments. OS, photoreceptor outer segments. Scale bar 50 μ m.

3.3 Determination of the age of onset of *Ush1c* gene expression

3.3.1 Harmonin localisation in the postnatal murine retina

In order to study the temporal expression of harmonin, the retinas from CD1 mouse pups were immunostained (section 2.3.3.1).

Development was examined from P2-P12, (covering the final stages of eye development, section 1.2.2.2). In Figure 3.5, at P2-P4, harmonin (green) is confined to the outermost layer of progenitor cells in the outer retina. These developmental stages are comparable to the 12 week stage in human foetal retina development, and these results are consistent with the findings from human expression studies, where harmonin was confined to the outer neuroblastic layer at 12 weeks (Bitner-Glindzicz, M et al, 2000). At P8, harmonin staining is seen as a discreet layer above the ONL, in the location of the developing IS and OS. By P12, it is clear that in fixed tissue, harmonin is localised to the OS. No harmonin immunostaining was detected in the RPE or inner retina throughout development.

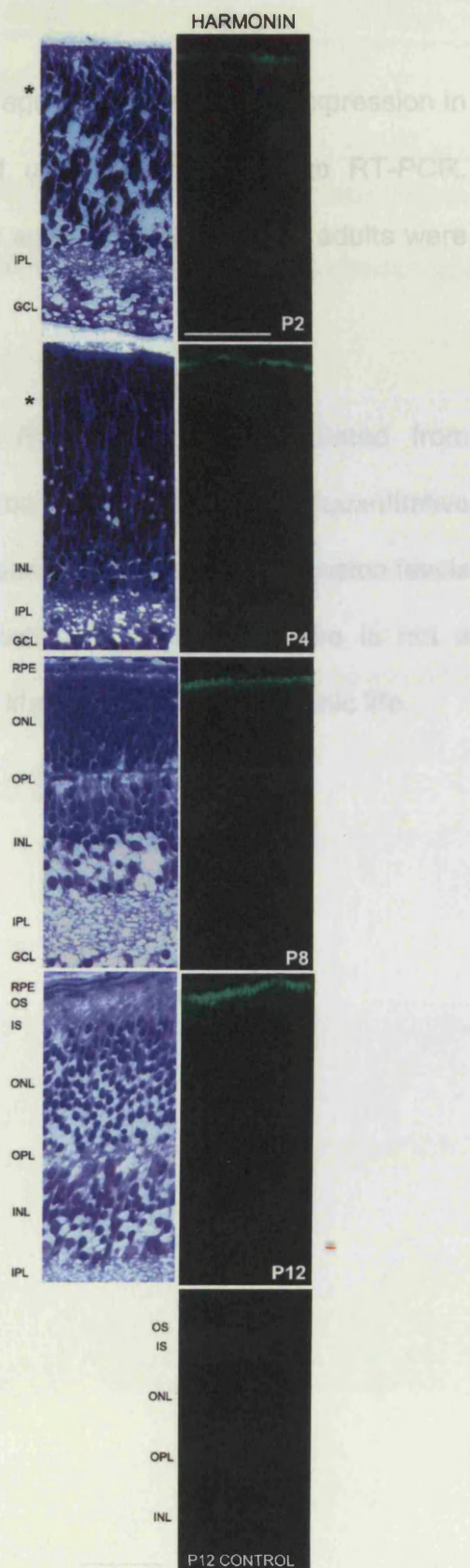
Unfixed tissue from developing eyes proved too unstable to examine, losing all discernable tissue architecture during the immunostaining procedure.

Figure 3.5 Harmonin localisation in the developing (P2-P12) murine retina

Development of retinal photoreceptors from P2-P12 is shown using semithin sections (blue), simultaneous to analysis of the expression of harmonin by immunofluorescence (green) in CD1 wildtype mouse retina.

At P2 and P4, harmonin is localised to the newborn photoreceptors (*) of the outer retina and later confined to the developing photoreceptor segments by P8. At P12, harmonin is clearly localised to the OS in fixed tissue. Replacement of the anti-harmonin antibody with PBS (bottom, P12 control panel) showed minimal non-specific background staining throughout the neural retina in fixed tissue. No harmonin immunostaining was detected in the RPE or inner retina at any developmental stage.

GCL, ganglion cell layer. IPL, inner plexiform layer. INL, inner nuclear layer. OPL, outer plexiform layer. ONL, outer nuclear layer. IS, photoreceptor inner segments. OS, photoreceptor outer segments. * Newborn photoreceptor layer. Scale bars 50 μ m.



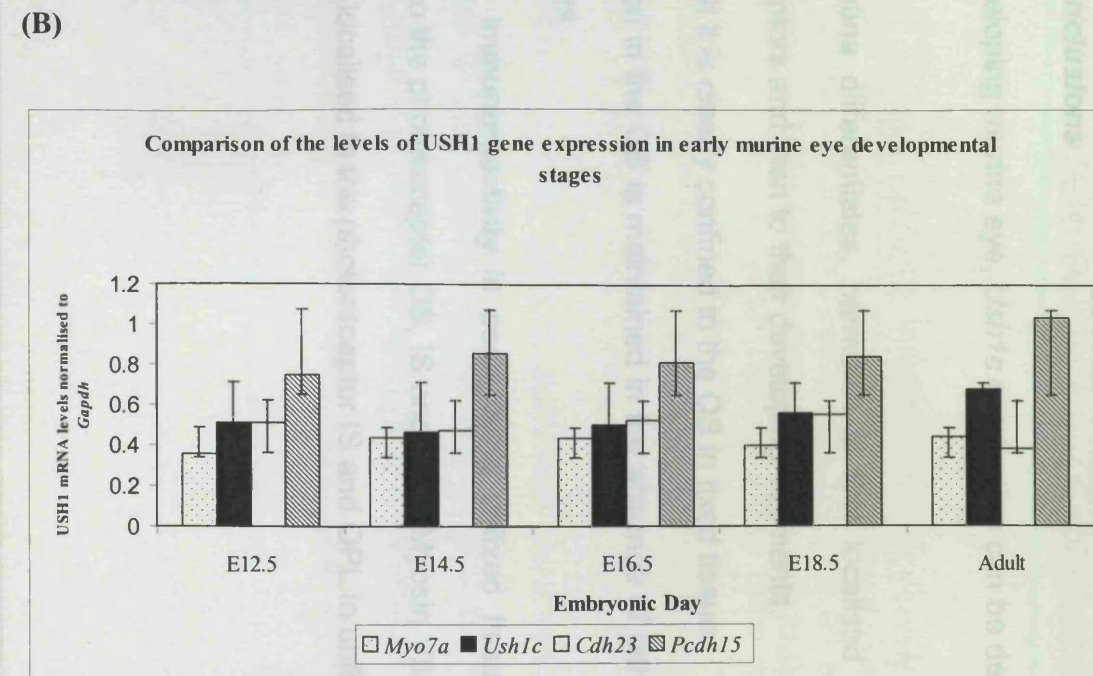
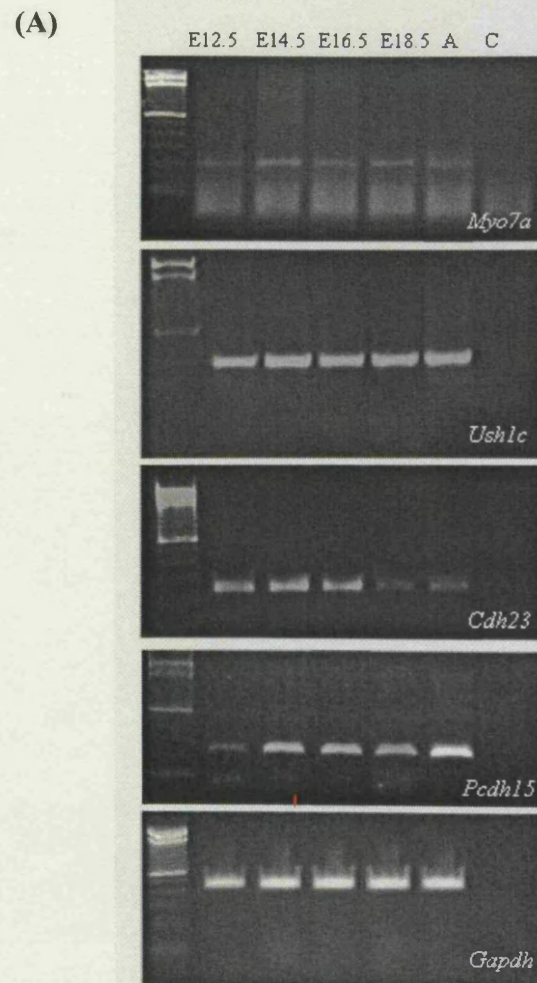
3.3.2 *Ush1c* expression in the prenatal murine retina

As harmonin was detected as early as P2, the age of onset of *Ush1c* expression in embryonic murine eyes was then examined using semi-quantitative RT-PCR. Whole eye extracts from CD1 mouse embryos aged E12.5-E18.5 and adults were used (section 2.3.3.2).

Expression of *Ush1c*, *Myo7a*, *Cdh23* and *Pcdh15* was demonstrated from embryonic day E12.5 to E18.5 and into adulthood (Figure 3.6A). Semiquantitative PCR analysis of the expression of the USH1 genes, showed their expression levels to be fairly similar (Figure 3.6B). It is interesting to note, that there is not a significant alteration in transcript levels in adult life compared to embryonic life.

Figure 3.6 Usher type 1 gene expression during prenatal murine eye development

(A) Semi-quantitative RT-PCR analysis of USH1 gene expression during early murine eye development. The developmental stages examined are indicated above each lane. (100bp DNA size standard. A, Adult. C, Negative control.). (B) A comparison of the expression levels of the USH1 genes by semi-quantitative PCR (Raw data can be found in Appendix 14). Error bars represent 2 standard deviations.



3.4 *Conclusions*

- In the developing murine eye, *Ush1c* expression can be detected as early as E12.5.
- As the retina differentiates, harmonin is first localised to the new born photoreceptors and then to their developing segments.
- In the adult it is clearly confined to the OS in fixed tissue.
- Localisation in the OS is maintained in the absence of either myosin VIIA or cadherin 23.
- Additional immunoreactivity is seen using unfixed tissue, with harmonin localised to the photoreceptor OS, IS and OPL. Myosin VIIA and cadherin 23 were also localised to the photoreceptor IS and OPL in unfixed tissue.

4 RESULTS CHAPTER: Generation of polyclonal antibodies to harmonin isoforms

Harmonin has multiple isoforms (section 1.3.3.2) which vary in protein localisation (Reiners, J et al, 2003) and binding partners (Boeda, B et al, 2002). Production of isoform specific antibodies will allow harmonin isoform-protein expression patterns to be investigated. Since the expression and localisation work has revolved around mice, it was decided to produce the antibodies against the murine harmonin isoforms. Antibodies were selected and raised by Sigma-Genosys (section 2.4.1), against peptide 1 (LTPRRSRKLKEVRLD – detecting all harmonin isoform classes) and peptide 2 (PADHLDGSTEEQRQQ – detecting isoform classes 'a' and 'b' only). Subsequent analysis is described in this chapter.

Research Objective:

- To validate two new polyclonal antibodies to the different harmonin isoforms.

Henceforth, the antibodies produced against peptide 1 are referred to as 'anti-LTPR sera' or 'anti-LTPR IgGs' if purified, whilst antibodies produced against peptide 2 are known as 'anti-PADH sera' or 'anti-PADH IgGs' if purified. The antibody produced by Dr Scanlan (Scanlan, M J et al, 1999) is known as the 'monoclonal anti-harmonin antibody' and the antibody produced by Dr Kobayashi (Kobayashi, I et al, 1999) is known as the 'polyclonal anti-harmonin antibody'. Analysis involving the native harmonin protein is listed by its tissue source, and IVT-produced harmonin protein is named IVT USH1C.

4.1 *Analysis of the anti-harmonin antibodies by ELISA*

ELISA analysis (section 2.4.2) examined whether the host organism had raised IgGs against the antigenic peptides and is summarized in Table 4.1 and 4.2 for peptides 1 and 2 respectively. For both peptides there was an initial surge of antibody production between the preimmune and test bleed 1, due to the primary immune response on initial presentation of the antigen. This then fell slightly for test bleeds 2 and 3 as IgG levels plateaued and then declined. IgG levels rose again for the harvest bleed due to the secondary immune response to the antigen, reaching levels equal to or greater than those seen for test bleed 1. Test bleed 3 for peptide 2, failed to produce a satisfactory result at the dilutions tested for unknown reasons but was successful for the harvest bleed.

A comparison of the antigenicity of each peptide at different stages during the immunization protocol is seen in Figure 4.1. An initial surge in antibody production was seen for both peptides after the initial antigen inoculation, noted by a steep rise in IgGs levels between the preimmune bleed and test bleed 1. Levels dipped during test bleeds 2 and 3, but rose again after the fifth inoculation (as seen by the harvest bleed levels). IgG levels for peptide 2 did not recover as well as was seen for peptide 1. At all stages examined, peptide 2 appeared to produce only 50% of the immune response seen from peptide 1. This maybe due to differences in the immune systems of the two host animals or the result of the different biochemistry of the two peptides. As a result, anti-LTPR serum raised against peptide 1 was chosen for further analysis.

Table 4.1 Examination of the antigenicity of peptide 1 by ELISA.

A positive ELISA result is where the absorbance reading is 0.3 units greater than that of the value determined for the blank/negative control and is highlighted here in bold.

Pep1		Dilution									
		Blank	1:100	1:500	1:1000	1:5000	1:10000	1:50000	1:100000	1:500000	1:500000
Absorbance @ 405nm	Pre-immune	0.0639	0.0977	0.0662	0.0643	0.0658	0.0680				
	Test bleed 1	0.0639		2.2781	1.4255	0.4810	0.2658				
	Test bleed 2	0.0847			1.0223	0.3386	0.1693	0.1011	0.0790	0.0719	
	Test bleed 3	0.0847				0.2924	0.1819	0.1929	0.0862	0.0742	
	Harvest bleed	0.0612	2.4447	1.6154	1.2945	0.4681	0.2867	0.1373	0.1098	0.1113	

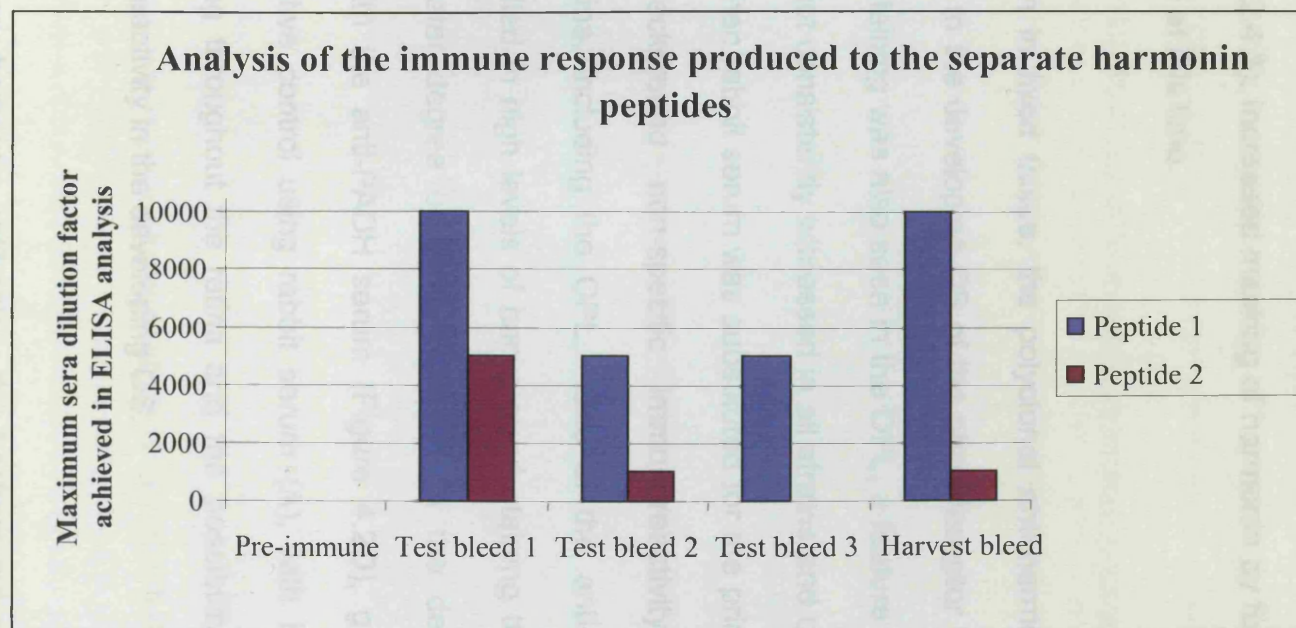
Table 4.2 Examination of the antigenicity of peptide 2 by ELISA.

A positive ELISA result is where the absorbance reading is 0.3 units greater than that of the value determined for the blank/negative control and is highlighted here in bold.

Pep2		Dilution									
		Blank	1:100	1:500	1:1000	1:5000	1:10000	1:50000	1:100000	1:500000	
Absorbance @ 405nm	Pre-immune	0.0646	0.0821	0.0695	0.0660	0.0711	0.0665				
	Test bleed 1	0.0639			0.8543	0.3236	0.1640	0.0813	0.0758		
	Test bleed 2	0.0696			0.3427	0.0923	0.0918	0.0649	0.0694	0.0647	
	Test bleed 3	0.0847				0.1230	0.0850	0.0671	0.0681	0.0662	
	Harvest bleed	0.0675	1.9840	0.6655	0.4205	0.1798	0.1597	0.1089	0.0949	0.0856	

Figure 4.1 Analysis of the immune response produced to the separate harmonin peptides

A comparison of the levels of IgGs raised against peptides 1 and 2, at the various stages of the immunisation procedure. Peptide 1 produced a greater immune response at all stages of the antibody production process.



4.2 *Analysis of the anti-harmonin antibodies by immunolabelling of murine retinas*

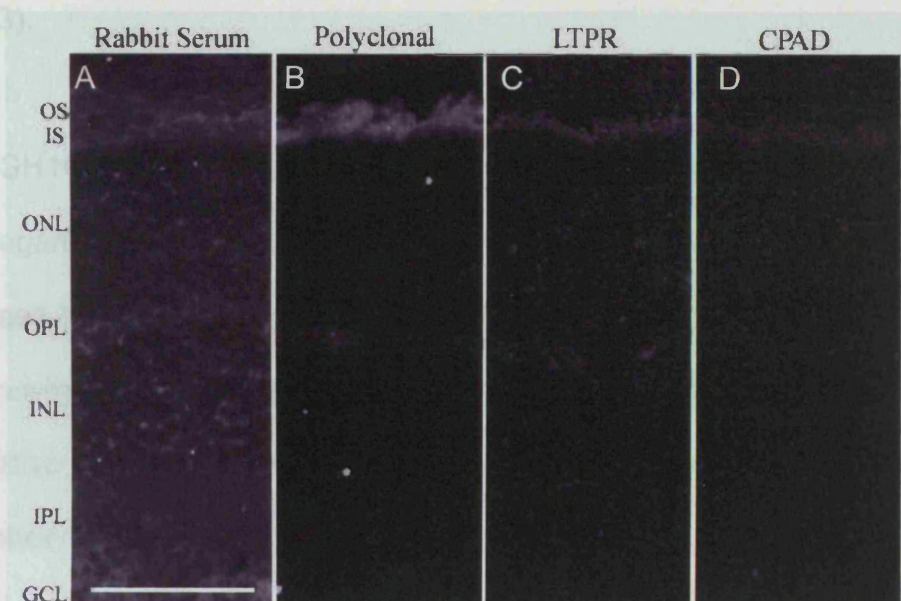
Anti-LTPR and anti-PADH sera were used on fixed retinal sections from P10 CD1 mice (section 2.4.3). Increased masking of harmonin by fixation had not been demonstrated at this time.

As previously seen in fixed tissue, the polyclonal anti-harmonin antibody localised harmonin to the developing OS of the photoreceptor (Figure 4.2B). Low level immunostaining was also seen in the OPL, a feature seen in some fixed sections but not consistently witnessed in all strains and developmental ages examined. When rabbit serum was substituted for the primary antibody (Figure 4.2A), background non-specific immunoreactivity was seen throughout the retina, including the OPL. Use of the anti-LTPR serum (Figure 4.2C) resulted in high levels of background staining throughout the retina, with a greater degree of immunostaining in the developing OS. Immunostaining with the anti-PADH serum (Figure 4.2D), gave a similar result to the negative control using rabbit serum (A), with high levels of background staining throughout the retina and the possibility of a limited degree of immunoreactivity in the developing OS.

With both of the new harmonin antibodies, the background staining levels were very high, similar to the rabbit serum negative control and both required further amplification for visualization, compared to the polyclonal anti-harmonin antibody. The high background levels may be the result of other IgGs present in the sera that were produced in response to the carrier

proteins or other antigens the host was exposed to during the antibody synthesis protocol. This would suggest that although anti-LTPR serum produces better results than the anti-PADH serum, neither of the new anti-harmonin antibodies are suitable for immunostaining.

Figure 4.2 Comparative immunolocalisation of harmonin using the polyclonal anti-harmonin antibody, the anti-LTPR sera and the anti-PADH sera



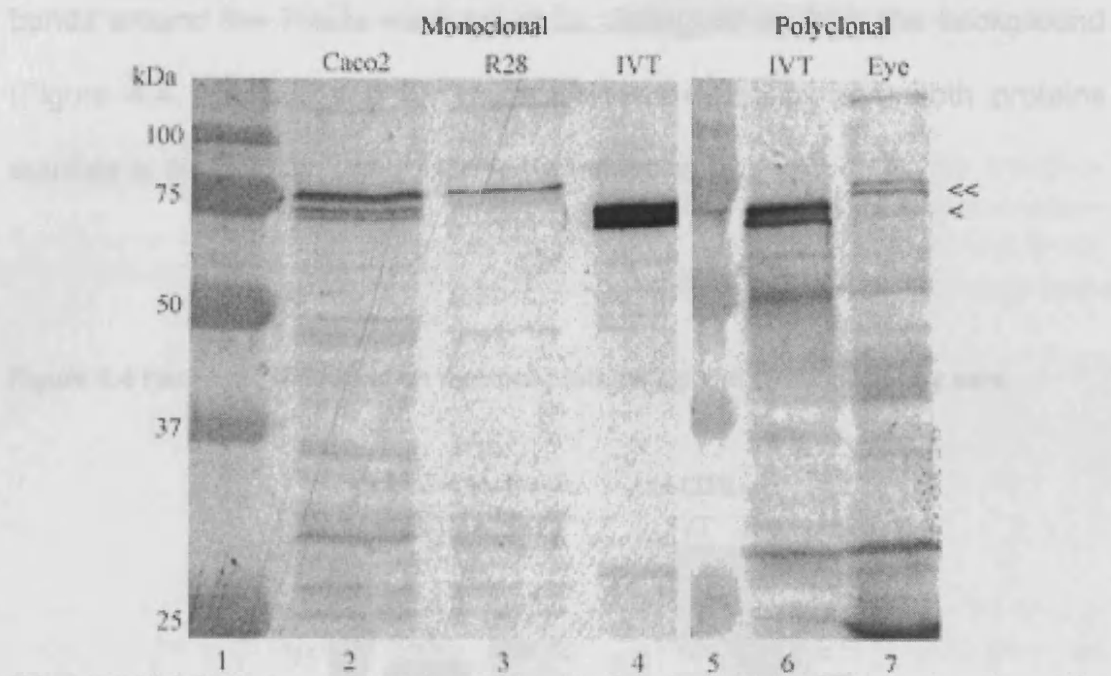
Fixed retinal sections from P10 CD1 mouse immunolabelled with polyclonal anti-harmonin antibody (B; positive control), anti-LTPR sera (C) and anti-PADH antibody sera (D). Rabbit serum was used as a negative control (A). Immunostaining for harmonin was visualised using FITC in the positive and negative controls. Further amplification was necessary for the anti-LTPR and anti-PADH sera. Single images were collected by confocal microscopy.

GCL, ganglion cell layer. IPL, inner plexiform layer. INL, inner nuclear layer. OPL, outer plexiform layer. ONL, outer nuclear layer. * developing photoreceptor inner and outer segments. Scale bar 50 μ m.

4.3 *Analysis of the anti-harmonin antibodies by immunoblotting analysis*

Anti-LTPR serum was used on a Western blot to visualize harmonin from various protein sources (sections 2.4.4.1 - 2.4.4.2 & 2.5.6.1.1). These tissues were first validated as sources of the harmonin protein by immunoblotting with either the monoclonal (Scanlan, M J et al, 1999) or polyclonal (Kobayashi, I et al, 1999) anti-harmonin antibodies (section 2.4.4.3).

IVT USH1C or harmonin can clearly be seen in their respective lanes (Figure 4.3) regardless of which antibody is used for detection. Three close bands are seen in lanes four and six containing the bound IVT protein. It is not known why three bands exist or why the IVT protein runs slightly smaller than the native protein (compare lanes 2 and 3). An alteration in glycosylation or phosphorylation of the protein in the IVT form has been suggested and investigated by Blaydon, D, 2004. Three bands can also be seen in the Caco2 cell line and two bands for whole eye homogenate samples, in lanes two and seven respectively.

Figure 4.3 Validation of protein aliquots as sources of the harmonin protein

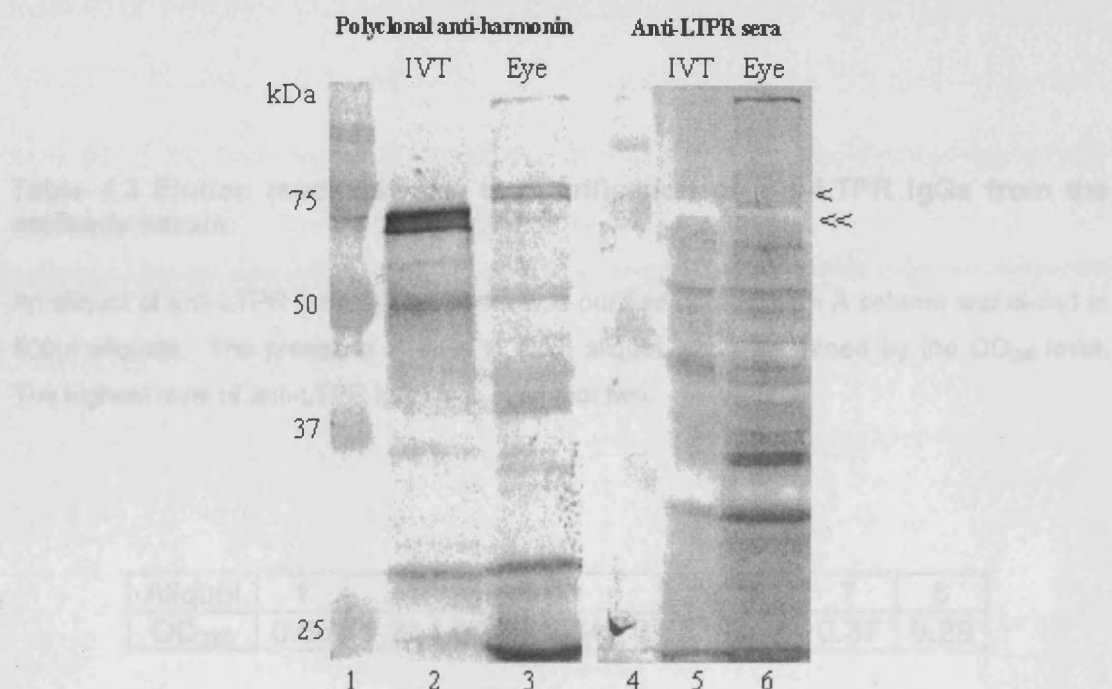
Cell lines R28 & Caco2, whole eye homogenate and IVT USH1C were probed for the presence of harmonin using the anti-harmonin monoclonal and polyclonal antibodies. Lane 1, protein standards. Lane 2, Caco2 cell lysate. Lane 3, R28 cell lysate. Lane 4, IVT USH1C. Lane 5, protein standards. Lane 6, IVT USH1C. Lane 7, whole eye homogenate. Lanes 1 to 4 were incubated with monoclonal anti-harmonin. Lanes 5 to 7 were incubated with polyclonal anti-harmonin.

The presence of the slightly smaller IVT USH1C protein in lanes four and six, is denoted by <. The native protein appears slightly larger than the 75 kDa protein standard mark and is denoted by <<. The polyclonal anti-harmonin antibody appears to produce higher background levels than the monoclonal (compare the extra non-specific bands in lanes four and six).

Lanes 1, protein standards. Lane 2, IVT USH1C. Lane 3, whole eye homogenate. Lanes 4, protein standards. Lanes 5, IVT USH1C. Lane 6, whole eye homogenate. Lanes 1-3 were probed with polyclonal anti-harmonin antibody, whilst lanes 4-6 were probed with anti-USH1C antibody sera.

The same experiment was repeated using the anti-LTPR serum on IVT USH1C protein and whole eye homogenate (section 2.4.4.4), but no clear bands around the 75kDa mark could be distinguished from the background (Figure 4.4, lanes 5 and 6). Harmonin was detected from both proteins sources in the positive control lanes (lanes 2 and 3).

Figure 4.4 Harmonin detection on western blots using anti-LTPR antibody sera



The presence of the slightly smaller IVT USH1C protein in lane two, is denoted by << and the native protein in lane three is denoted by <.

Lanes 1, protein standards. Lane 2, IVT USH1C. Lane 3, whole eye homogenate. Lanes 4, protein standards. Lane 5, IVT USH1C. Lane 6, whole eye homogenate. Lanes 1-3 were probed with polyclonal anti-harmonin antibody, whilst lanes 4-6 were probes with anti-LTPR antibody sera.

In order to try and improve immunoblotting results using anti-LTPR serum by reducing background/non-specific binding, affinity column purification of the IgGs from the sera was performed (section 2.4.4.5). Eight aliquots of ~500 μ l each were collected and absorbance taken at 280nm to monitor the elution of the IgGs from the beads (Table 4.3). Sample 2 was then used at 1:100 on western blots. Higher concentrations produced unusable background levels (data not shown).

Table 4.3 Elution readings from the purification of anti-LTPR IgGs from the antibody serum

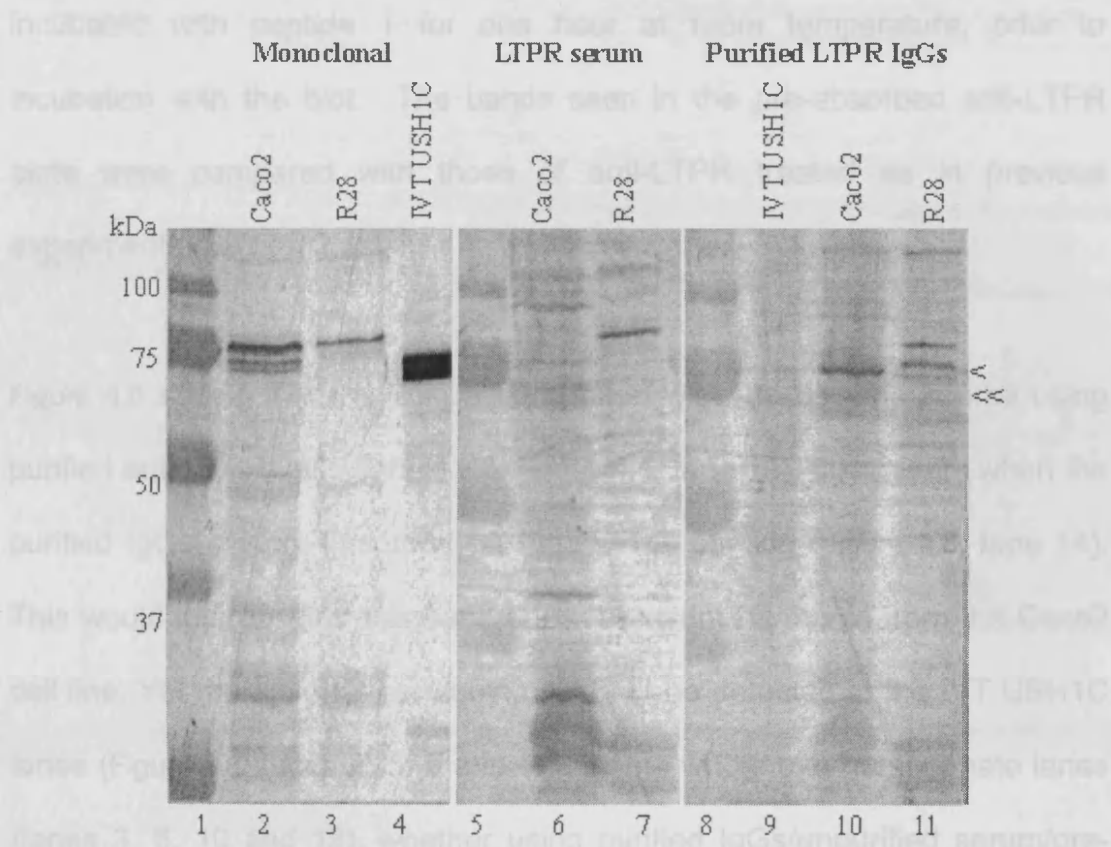
An aliquot of anti-LTPR harvest bleed sera was purified on a Protein A column and eluted in 500 μ l aliquots. The presence of IgGs in each aliquot was determined by the OD₂₈₀ level. The highest level of anti-LTPR IgGs was in aliquot two.

Aliquot	1	2	3	4	5	6	7	8
OD ₂₈₀	0.66	1.21	0.97	1.14	0.85	0.57	0.37	0.29

The ability of purified anti-LTPR IgGs to detect harmonin from the IVT reaction, Caco2 cell lysate and R28 cell lysate, was compared to that of unpurified anti-LTPR serum and the monoclonal anti-harmonin antibody (section 2.4.4.6).

Figure 4.5 shows that harmonin can be detected using the monoclonal anti-harmonin antibody (lanes 2, 3 and 4) but no strong band can be seen at 75kDa with the unpurified serum in either Caco2 or R28 cells (lanes 6 and 7). A band at exactly 75 kDa is seen in the Caco2 and R28 lanes (lanes 10 and 11) using purified anti-LTPR IgGs, yet this not seen in the IVT USH1C protein lane (lane 9). This would suggest that the purified antibody could be cross-reacting with a protein of similar size to harmonin.

Figure 4.5 A comparison of the ability of purified anti-LTPR IgGs to recognise harmonin, compared to that of the unpurified anti-LTPR antibody sera



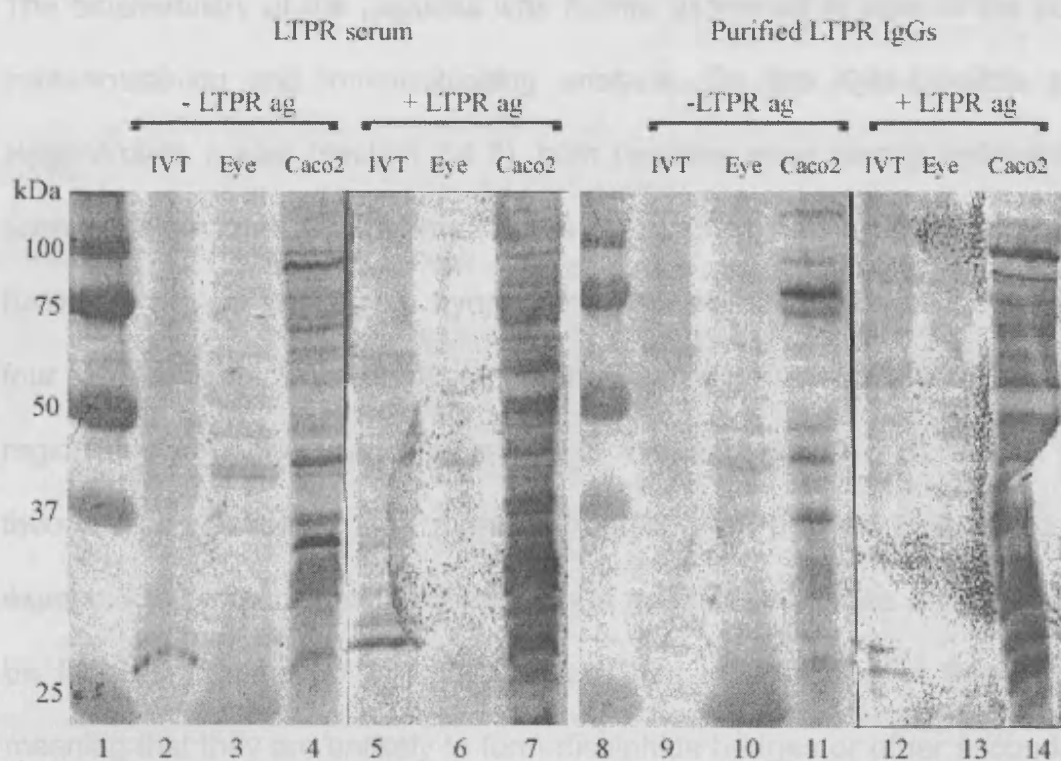
The monoclonal anti-harmonin antibody detects the harmonin protein from all three tissue sources in lanes 2-4. Unpurified anti-LTPR antibody sera does not detect a 75 kDa band in lane six and seven with the cell lines, although there is a distinct darker band for the R28 cell line in lane seven, greater than 75 kDa. Purified anti-LTPR IgGs show a strong band at 75 kDa which is also seen in the Caco 2 cell line in lane 10. Purified anti-LTPR IgGs is unable to detect the IVT USH1C protein, lane nine.

Lanes 1,5&8, protein standards. Lane 2,6&10, Caco2 cell lysate. Lane 3,7&11, R28 cell lysate. Lane 4&9, IVT USH1C. The presence of the slightly smaller IVT USH1C protein is denoted by << and the native protein by <.

To confirm whether the dark band seen in lanes 10 and 11 of Figure 4.5 is actually harmonin, samples of purified and unpurified antibody were incubated with peptide 1 for one hour at room temperature, prior to incubation with the blot. The bands seen in the pre-absorbed anti-LTPR blots were compared with those of anti-LTPR treated as in previous experiments (section 2.4.4.7.).

Figure 4.6 shows that the 75kDa band seen with the cell line source using purified anti-LTPR IgGs (lane 11 & Figure 4.5, lane 10), disappears when the purified IgGs are pre-absorbed with the LTPR peptide (Figure 4.6, lane 14). This would indicate that this band does represent harmonin from the Caco2 cell line. Yet the fact that harmonin could not be detected in the IVT USH1C lanes (Figure 4.6, lanes 2, 5, 9 and 12), or the whole eye homogenate lanes (lanes 3, 6, 10 and 13), whether using purified IgGs/unpurified serum/pre-absorbed samples, supports the results of Figure 4.5, suggesting that the anti-LTPR antibody is picking up a non-specific band in the Caco2 cell line that is coincidentally the same size as harmonin.

Figure 4.6 Examination of the specificity of the anti-LTPR antibody sera and purified anti-LTPR IgGs for harmonin



Aliquots of the unpurified sera (lanes 5-7) and purified anti-LTPR IgGs (lanes 12-14) were preabsorbed with an excess of peptide 1.

There is very little difference in the banding pattern between the pre-absorbed and non pre-absorbed unpurified anti-LTPR sera or purified anti-LTPR IgGs. At no point are any bands detected in the IVT USH1C or whole eye homogenate protein source.

Lanes 1&8, protein standards. Lanes 2,5,9&12, IVT USH1C. Lane 3,6,10&13 whole eye homogenate. Lane 4,7,11&14 Caco2 cell lysate.

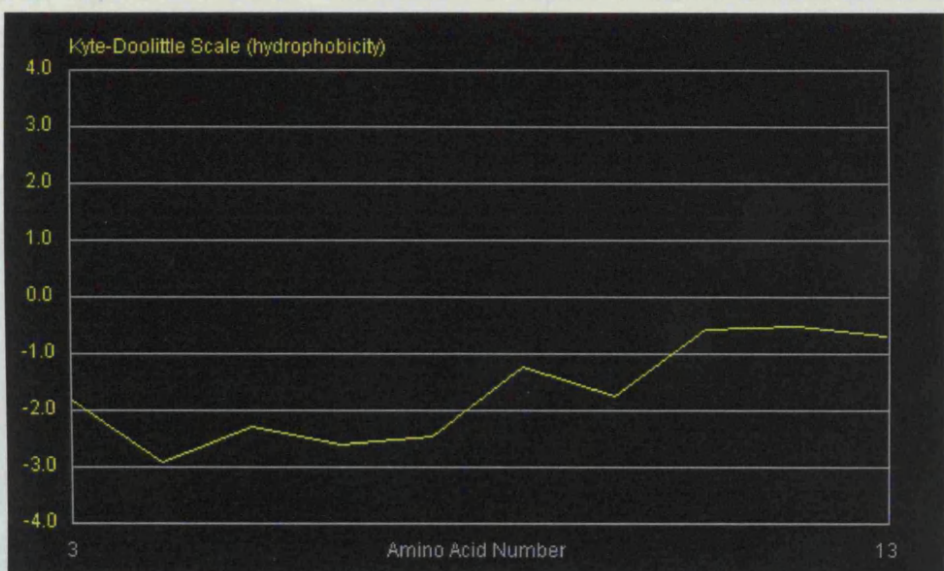
4.4 *Analysis of antigenic peptide hydrophobicity*

The biochemistry of the peptides was further examined in view of the poor immunostaining and immunoblotting analysis. On the Kyte-Doolittle and Hopp-Woods scales (section 2.4.5), both peptides were clearly hydrophilic, scoring below zero at all points (Figure 4.7). Examination of the complete harmonin protein using both hydrophilicity scales, showed that there were four clear regions of hydrophilicity, and that peptide 1 was located in the first region of hydrophilicity and peptide 2, in the third region (Figure 4.8). In theory, since peptide 2 was more hydrophilic than peptide 1, it would be expected to be more antigenic although in practice, this does not appear to be the case. Neither of the peptides are rich in cysteines or threonines, meaning that they are unlikely to form disulphide bridges or other secondary structures. This data would suggest that both peptides have no biochemical properties that would prevent their success during antibody synthesis protocols.

Figure 4.7 Kyte-Doolittle analysis of the hydrophobicity of the peptides

(A) The complete amino acid sequence of peptide 1 was plotted on a Kyte-Doolittle hydrophobicity plot, using a window size of 7 to promote clear detection of hydrophobic regions. Peptide 1 was seen to be hydrophilic throughout. **(B)** The complete amino acid sequence of peptide 2 was plotted on a Kyte-Doolittle hydrophobicity plot, also using a window size of 7. None of the amino acids of peptide 2 were hydrophobic in fact the C-terminal amino acids were particularly hydrophilic, suggesting that this peptide would be a good candidate for use in antibody synthesis.

A



B

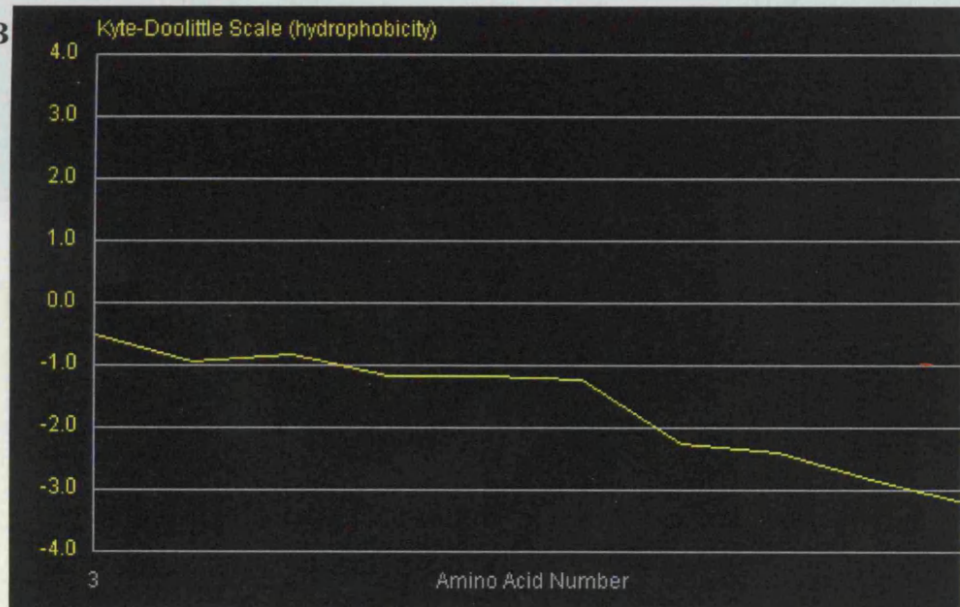
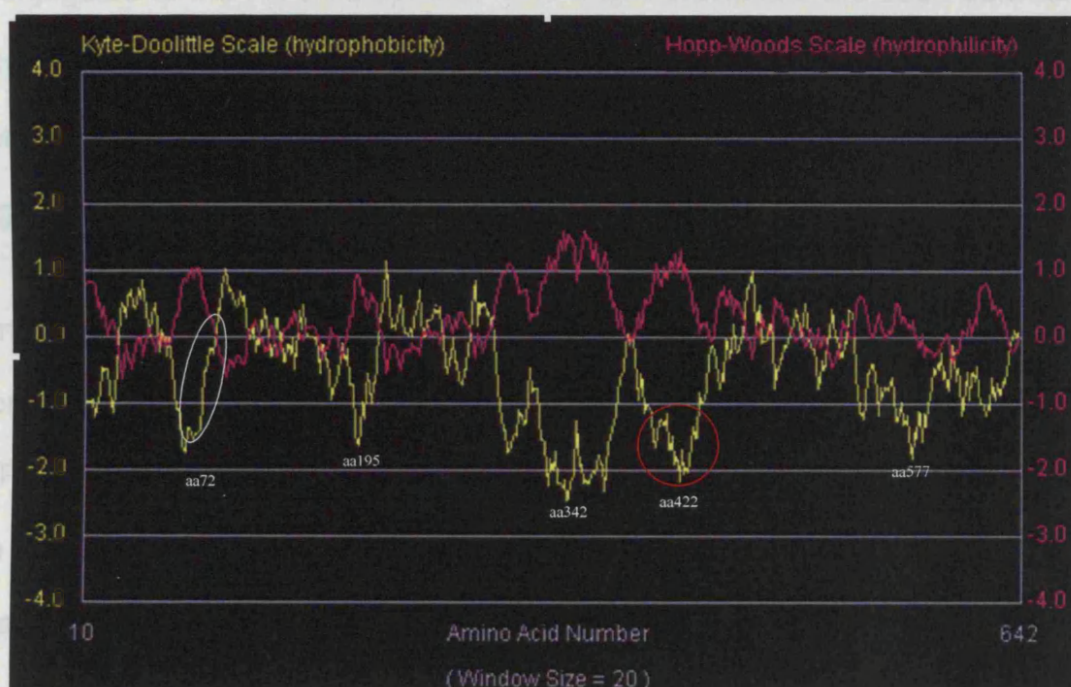


Figure 4.8 A hydrophobicity plot of the complete murine harmonin isoform amino acid sequence

Kyte-Doolittle and Hopp-Woods hydrophobicity plots were produced for the complete harmonin protein sequence. A window size of 20 was used to distinguish hydrophobic regions that would not be suitable as peptides to raise an antibody against. Amino acids scoring less than 0 on a Kyte-Doolittle plot are hydrophilic and those scoring more than 0 on a Hopp-Woods plot are also deemed hydrophilic.

There are four clear regions where the plots are polar, rich in hydrophilic amino acids. The most hydrophilic amino acids in these regions are listed in white on the plots, denoted the hydrophilic regions on the plot. The position of peptide 1 relative to these amino acids is denoted by the white circle of the plot, and peptide 2 by the red circle. Both are within highly hydrophilic regions of the harmonin protein.



4.5 *Investigation into the presence of anti-harmonin IgGs in the anti-LTPR antibody sera*

An initial control Ouchterlony plate was set up (section 2.4.6), to determine whether any anti-rabbit IgGs were present in the anti-LTPR serum. A distinct precipitate arc was formed between the anti-LTPR antibody sera and the undiluted anti-rabbit IgGs solution (Figure 4.9). The anti-rabbit IgG antibody (made in goat) and the anti-goat IgG antibody (made in donkey) are both conjugated to the FITC fluorophore. The bright precipitate arc seen between the anti-rabbit IgG and anti-LTPR antibodies is not an artifact due to the presence of the fluorophore, as no illumination is seen around the anti-goat IgG well.

In order to investigate whether the host animal inoculated with peptide 1 had produced IgGs against harmonin, another Ouchterlony plate was set up (Figure 4.10), using a variety of harmonin protein sources. Once again, only a precipitate formed between the anti-LTPR serum and the undiluted anti-rabbit IgGs solution. This indicates that the anti-LTPR serum contains rabbit IgGs, but that these are not necessarily raised against peptide 1, and that they will not bind to the IVT USH1C or native harmonin protein.

Figure 4.9 Ouchterlony analysis investigating the presence of anti-rabbit IgGs in the sera collected from the peptide 1 host.

A distinct precipitate arc was formed between the anti-LTPR antibody sera and the undiluted anti-rabbit IgGs solution.

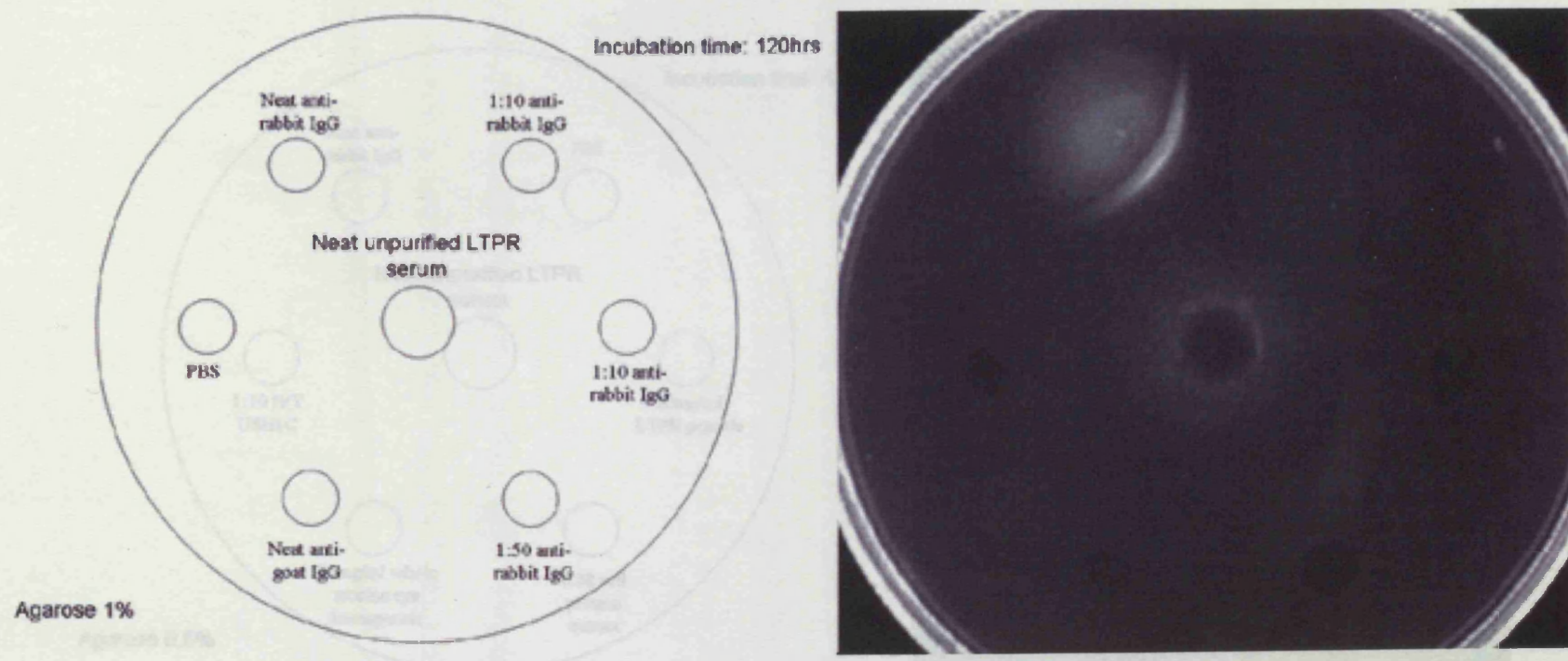
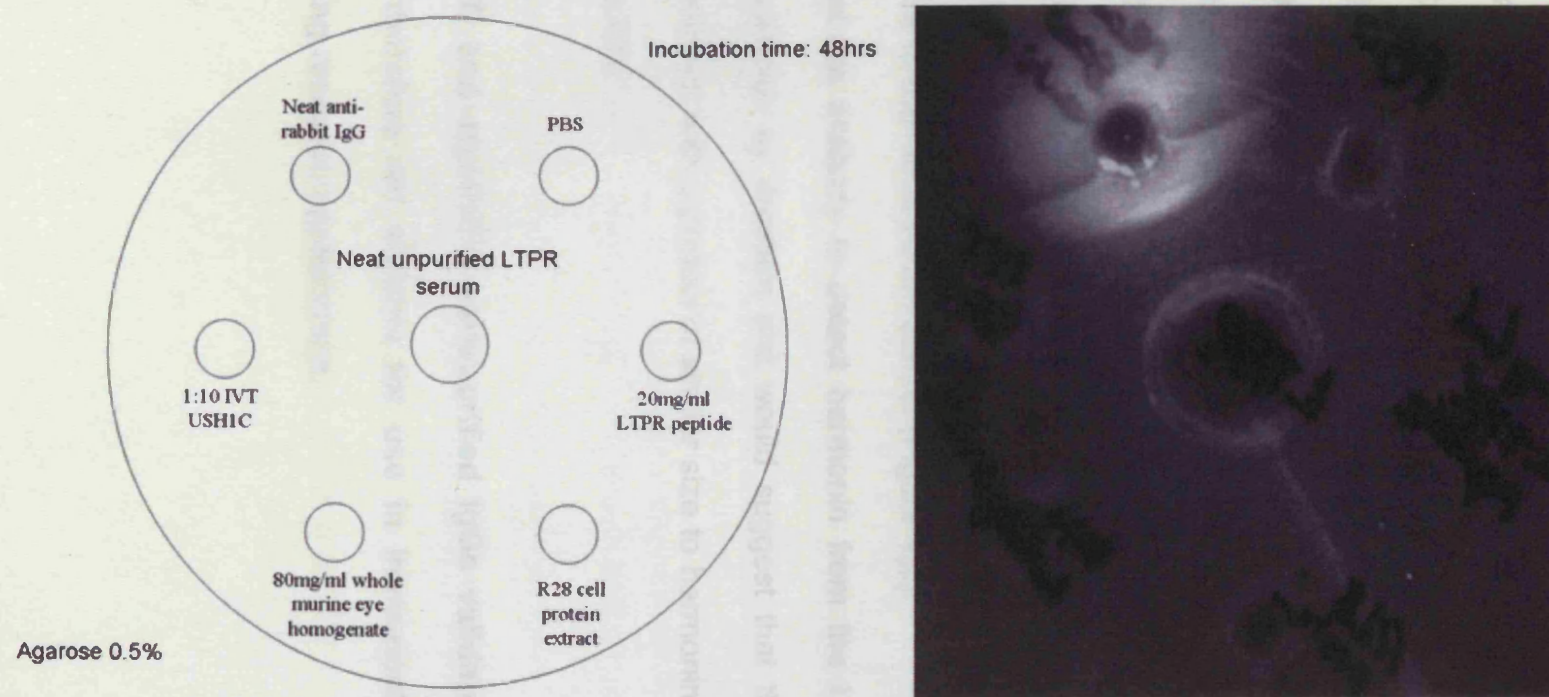


Figure 4.10 Ouchterlony analysis investigating the presence of anti-harmonin IgGs in the sera collected from the peptide 1 host.

A distinct protein precipitate could only be seen between the anti-LTPR serum and the undiluted anti-rabbit IgG antibody. The anti-LTPR serum did not recognise/precipitate with harmonin or with peptide 1 which it was raised against. Incubation for a further 24hrs did not lead to further precipitate formation.



4.6 *Conclusions*

- It is likely that the antibody synthesis protocol has resulted in the production of antibodies to peptides 1 & 2, as seen by the ELISA results (section 4.1), but these are not specific for harmonin.
- The other IgGs in the sera could be due to the carrier protein or other antigens the host was exposed to during or before the anti-harmonin antibody synthesis period (section 1.5.1.2.1.2). It is likely that these are being detected in the Ouchterlony tests (section 4.10).
- A low ratio of anti-harmonin IgGs:anti-rabbit IgGs in the sera would account for the poor immunostaining results, where background staining was high, similar to the rabbit serum control (Figure 4.2).
- The inability of the antibody to detect harmonin from the IVT or eye homogenate samples by Western blot would suggest that the purified antibody cross-reacts with a protein of similar size to harmonin in the cell lysates (Figure 4.6).
- **The anti-LTPR and anti-PADH sera/purified IgGs validated in this chapter are therefore not suitable for use in immunostaining or immunoblotting research applications.**

5 RESULTS CHAPTER: Identification of candidate harmonin-interacting proteins in the eye.

Harmonin isoform 'b' has been shown to interact with myosin VIIA and cadherin 23 in the ear (Boeda, B et al, 2002). Since harmonin colocalised with myosin VIIA and cadherin 23 in the IS and OPL of the retinal photoreceptors, it is possible that similar interactions occur in the eye. Yet harmonin is also localised to the photoreceptor OS, where neither myosin VIIa nor cadherin 23 are localised, suggesting that harmonin may interact with other retinal proteins.

Aims:

- To carry out a Yeast Two-hybrid screen of a bovine retinal library in order to identify candidate proteins that may interact with harmonin.
- To confirm any interactions discovered by alternative *in vitro* methods.

5.1 A Yeast Two-hybrid screen of a bovine retinal library to find *harmonin-interacting proteins*

5.1.1 Confirmation of yeast strain phenotypes

The yeast strain phenotype was analysed (section 2.5.1.1), with Y187 displaying the correct phenotype (Table 5.1; Y187 1-8), whilst the AH109 strain grew on medium lacking histidine (AH109 A-H). Repeat streaking from the frozen stock on fresh plates resulted in the correct phenotype for all 1-8 AH109 colonies.

Table 5.1 Analysis of the phenotype of the yeast host strains

The ability of the yeast strains to grow on minimal SD media lacking different amino acids is denoted alongside their predicted phenotype.

+ = growth - = no growth

Strain		Clone Identity	SD/-Ade	SD/-His	SD/-Leu	SD/-Trp	SD/-Met	SD/-Ura	YPD	YPDA
Y187	Expected phenotype		-	-	-	-	-	+	-	+
	Tested phenotype	1,2,3,4,5,6,7,8	-	-	-	-	-	+	-	+
AH109	Expected phenotype		-	-	-	-	+	+	-	+
	Tested phenotype	A,B,C,D,E,F,G, H	-	+	-	-	+	+	-	+
	Retested phenotype	1,2,3,4,5,6,7,8	-	-	-	-	+	+	-	+

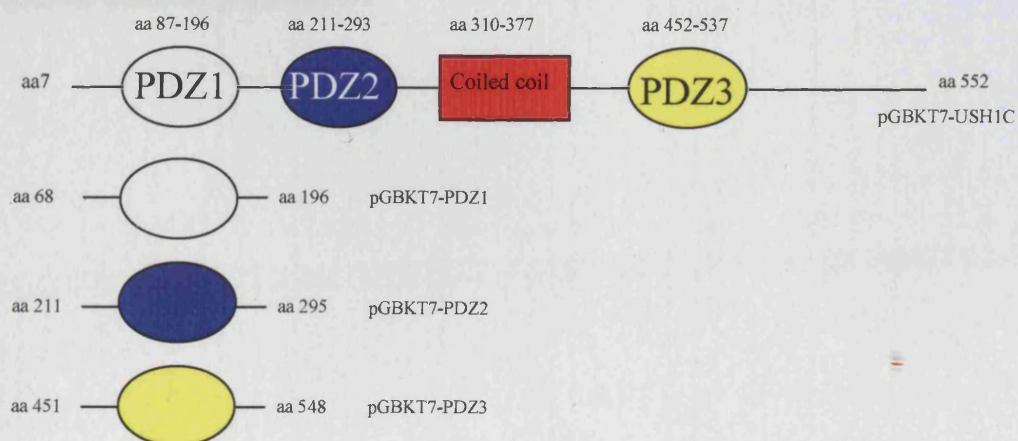
5.1.2 Generation of bait and control fusion proteins

5.1.2.1 Production of bait and control fusion protein constructs

A 'bait' corresponding to the amino acid sequence of human *USH1C* isoform 'a' (NCBI accession number NP_005700) fused to the GAL4-BD, was constructed in the pGBK7 vector (Clontech; sequence under submission to NBCI; Appendix 15). Smaller baits corresponding to the individual PDZ domains were also constructed (section 2.5.1.2; Figure 5.1).

Figure 5.1 Schematic showing the structure of harmonin isoform 'a' and the peptides used to construct the bait fusion proteins.

The amino acids encompassing the region fused to the GAL4 domain and the individual structural domains have been labelled on pGBK7-USH1C. The regions used to construct the PDZ domain baits are also labelled on the relevant schematic.



Constructs from this point on have been labelled as pGBK7-USH1C which expresses the GAL4BD-harmonin fusion protein; pGBK7-PDZ1 which expresses the GAL4BD-PDZ1 domain fusion protein; pGBK7-PDZ2 which expresses the GAL4BD-PDZ2 and pGBK7-PDZ3 which expresses the GAL4BD-PDZ3. Harmonin is known to interact with the C-terminus of cadherin 23 (Siemens, J et al, 2002), so this region was used as a positive control – pACT2-cdh23 (Appendix 15; pACT2 NCBI accession number U29899).

5.1.2.2 Transformation of bait and control constructs into yeast

The individual vectors, bait constructs and control prey constructs were transformed into yeast (section 2.5.1.2.9). The transformation efficiencies (Table 5.2), were generally optimal, with only a slight decrease in efficiency for pGBK7, pGBK7-53 and pGBK7-PDZ2, probably a reflection of a suboptimal plasmid preparation.

Table 5.2 Calculation of the transformation efficiency of control and bait plasmids into the host yeast strains

Individual transformation efficiencies were calculated for the following, using Equation 5.1. Optimal transformation efficiency is $\geq 1 \times 10^4$ cfu/ μ g.

Strain[plasmid]	Transformation efficiency (cfu/ μ g DNA)
AH109[pGBKT7]	9×10^3
AH109[pGBKT7-USH1C (7)]	2×10^4
AH109[pGBKT7-USH1C (12)]	7.4×10^4
AH109[pGBKT7-PDZ1]	2.54×10^4
AH109[pGBKT7-PDZ2]	8.9×10^3
AH109[pGBKT7-PDZ3]	1.35×10^4
AH109[pGBKT7-53]	8.5×10^3
AH109[pGBKT7-Lam]	5×10^4
Y187[pACT2]	1.9×10^4
Y187[pACT2-CDH23]	1.7×10^4
Y187[pGADT7-T]	2.5×10^4

Equation 5.1 Transformation efficiency formula

$$\frac{\text{cfu} \times \text{total suspension volume } (\mu\text{l})}{\text{DNA} \times \text{Volume plated } (\mu\text{l}) \times \text{dilution factor} \times \text{amount of DNA used } (\mu\text{l})} = \text{cfu}/\mu\text{g}$$

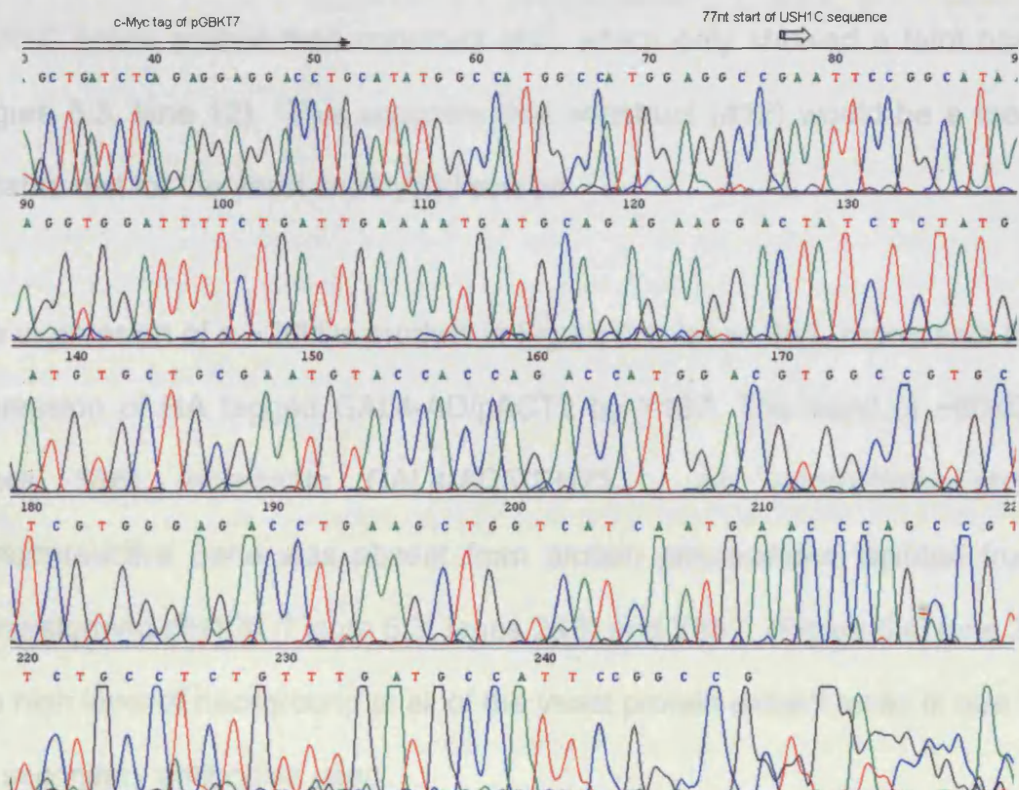
5.1.3 Validation of bait and control fusion proteins

5.1.3.1 Analysis of the DNA sequence of the baits

The complete DNA sequence for all of the bait constructs was analysed (section 2.5.2.1). No sequence variations were apparent, whilst the correct orientation and reading frame seen in the bacterial transformants was maintained in the yeast transformants (Figure 5.2).

Figure 5.2 The sequencing electropherogram of pGBKT7-USH1C(12)

The 3' end of the c-Myc epitope tag can clearly be seen (→) leading into the initial part of the MCS of the vector. The sequence continues in frame into *USH1C* at 77nt on the electropherogram (block arrow) at the *Sfi*1 site.



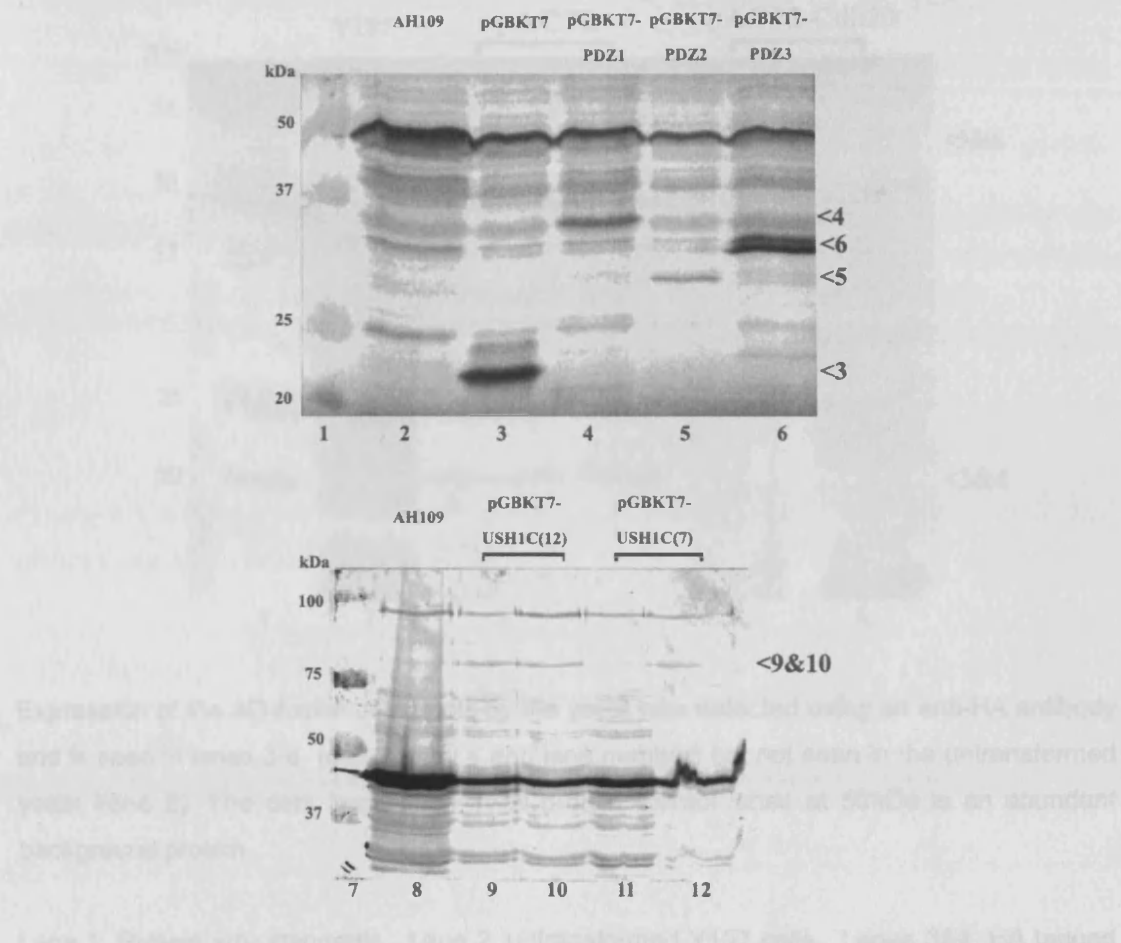
5.1.3.2 Confirmation that the bait fusion protein is harmonin

The protein content of both baits and controls was examined (section 2.5.2.2) by antibody staining of yeast protein extracts on Western blots.

In-frame stable expression of the correct fusion proteins was seen in Figure 5.3. The expression of c-myc tagged ~23kDa GAL4-BD/pGBKT7 by AH109 is seen in lane 3. The bands of ~96kDa (lanes 9&10), ~36kDa (lane 4), ~30kDa (lane 5) and ~32kDa (lane 6) represent the tagged fusion bait proteins, GAL4-BD/USH1C (~73kDa+GAL4-BD), GAL4-BD/PDZ1, GAL4-BD/PDZ2 and GAL4-BD/PDZ3 respectively. A comparison of pGBKT7-USH1C (12) (Figure 5.3, lanes 9&10) with pGBKT7-USH1C (7) (lanes 11&12), showed that construct (#12) produced greater amounts of the BD-USH1C fusion protein than construct (#7), which only showed a faint band (Figure 5.3, lane 12). This suggests that construct (#12) would be a more suitable bait for the yeast two-hybrid screen.

The expression of a ~20kDa product in Figure 5.4; lanes 3&4, represents the expression of HA tagged GAL4-AD/pACT2 by Y187. The band of ~60kDa (lanes 5&6) represents GAL4-AD/CDH23. An appropriate sized immunoreactive band was absent from protein preparations isolated from untransformed AH109 (Figure 5.3, lanes 2&8) and Y187, (Figure 5.4, lane 2). The high level of background in all of the yeast protein extract lanes is due to the secondary antibodies used.

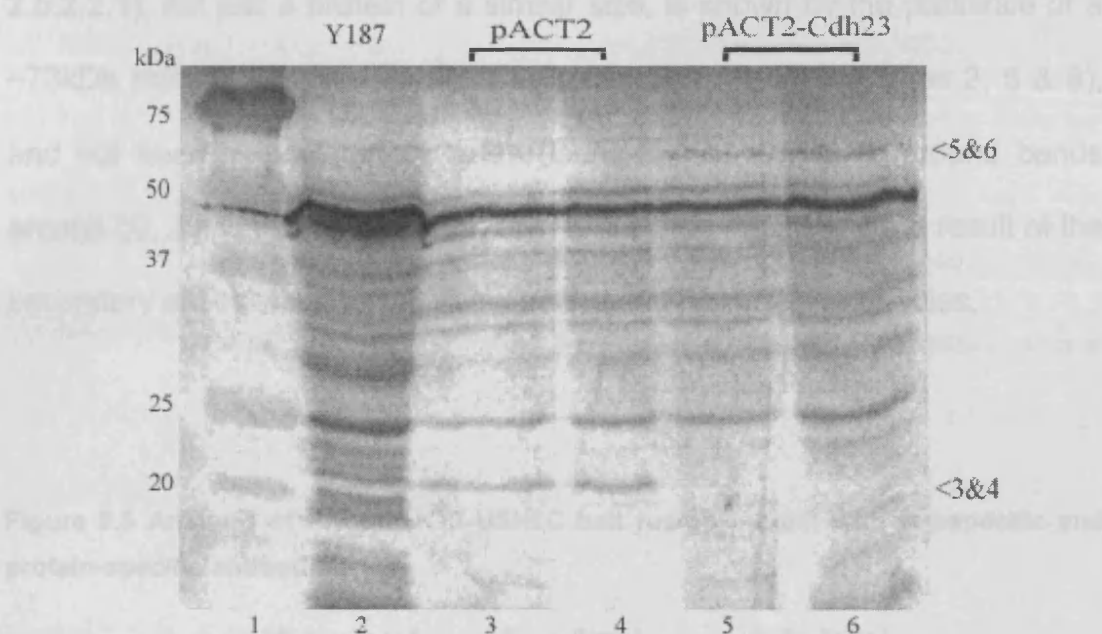
Figure 5.3 Expression of the GAL4BD-bait fusion proteins from the pGBKT7-bait constructs by transformed AH109 yeast cells.



Expression of the c-Myc tagged BD-fusion constructs by the yeast was detected using an anti-c-Myc antibody and is seen by the appropriately sized bands in lanes 3-6 or 9-12, denoted by < and lane number. None of these bands are seen in any other lane or in the untransformed yeast (lanes 2&8). The dark band seen in all protein extract lanes at 50kDa is an abundant background protein.

Lanes 1&7, Protein size standards. Lanes 2&8, untransformed AH109 cells. Lane 3, GAL4BD expressed by yeast transformed with pGBKT7. Lane 4, GAL4BD-PDZ1 expressed by yeast transformed with pGBKT7-PDZ1. Lane 5, GAL4BD-PDZ2 expressed by yeast transformed with pGBKT7-PDZ2. Lane 6, GAL4BD-PDZ3 expressed by yeast transformed with pGBKT7-PDZ3. Lanes 9&10, GAL4BD-USH1C expressed by yeast transformed with pGBKT7-USH1C(12). Lanes 11&12, AL4BD-USH1C expressed by yeast transformed with pGBKT7-USH1C(7).

Figure 5.4 Expression of the GAL4AD-bait fusion proteins from the pACT2-positive control constructs by transformed Y187 yeast cells.



Expression of the AD-fusion constructs by the yeast was detected using an anti-HA antibody and is seen in lanes 3-6, (denoted by < and lane number) but not seen in the untransformed yeast (lane 2). The dark band seen in all protein extract lanes at 50kDa is an abundant background protein

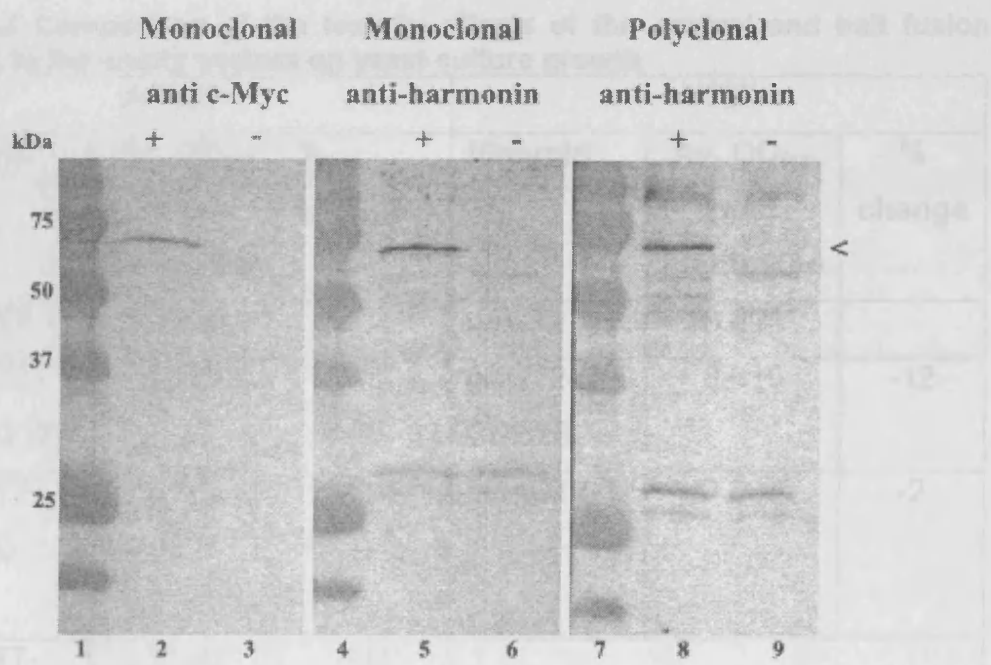
Lane 1, Protein size standards. Lane 2, untransformed Y187 cells. Lanes 3&4, HA tagged GAL4AD expressed by yeast transformed with pACT2. Lanes 5&6, HA tagged GAL4AD-CDH23 expressed by yeast transformed with pACT2-Cdh23.

Expression of the USH1C bait vector produced by C71 from the pGEX17-USH1C(12) is detected by the presence of a band ~73kDa (labeled by <).

Lanes 1-4: Protein size standards. Lanes 2-5: 35S-³⁵S-Myc/USH1C. Lanes 3,5&9: No C71 vector control with no protein bands. Lanes 1-3 were probed with the anti- α -Myc antibody. Lanes 4-6 were probed with the monoclonal anti-hemagglutinin antibody. Lanes 7-9 were probed with the polyclonal anti-hemagglutinin antibody.

Confirmation that the fusion protein produced is actually harmonin (section 2.5.2.2.1), not just a protein of a similar size, is shown by the presence of a ~73kDa protein identified by all three antibodies (Figure 5.5 lanes 2, 5 & 8), and not seen in any control lanes (lanes 3, 6 & 9). Background bands around 50, 25kDa (lanes 5,6,8&9) and 100kDa (lanes 8&9) are a result of the secondary antibodies used to visualise the anti-harmonin antibodies.

Figure 5.5 Analysis of the pGBKT7-USH1C bait fusion protein with tag-specific and protein-specific antibodies



Expression of the USH1C bait protein produced by IVT from the pGBKT7-USH1C(12) is denoted by the presence of a band ~73kDa (labelled by <).

Lanes 1,4&7 Protein size standards. Lanes 2,5&8 IVT c-Myc/USH1C. Lanes 3,6&9 'No DNA' lysate control with no protein bands. Lanes 1-3 were probed with the anti-c-Myc antibody. Lanes 4-6 were probed with the monoclonal anti-harmonin antibody. Lanes 7-9 were probed with the polyclonal anti-harmonin antibody.

5.1.3.3 Toxicity effects of the bait fusion protein on host yeast cells

All of the transformed yeast grew well (section 2.5.2.3), with both Clontech control fusion proteins (pGBKT7-53 and pGADT7-T) showing a very minimal drop in growth rate compared to the 'empty' vectors (Table 5.3). There was ~10% drop in growth rate for the main bait construct (pGBKT7-USH1C), pACT2-CDH23 and pGBKT7-PDZ3 but in terms of OD₆₀₀ (<0.1 units), this is not significant. The growth rate appeared to increase for yeast transformed with pGBKT7-PDZ2 and pGBKT7- PDZ1.

Table 5.3 Comparison of the toxicity effects of the control and bait fusion proteins to the empty vectors on yeast culture growth

AH109			Y187		
Plasmid	Av. OD ₆₀₀ post incubation	% change	Plasmid	Av. OD ₆₀₀ post incubation	% change
pGBKT7	0.848		pACT2	0.694	
pGBKT7- USH1C (7)	0.747	-12	pACT2- CDH23	0.610	-12
pGBKT7- USH1C (12)	0.733	-13.5	pGADT7-T	0.680	-2
pGBKT7- PDZ1	1.114	+31			
pGBKT7- PDZ2	0.862	+2			-
pGBKT7- PDZ3	0.929	-10			
pGBKT7-53	0.835	-1.5			

5.1.3.4 Verification that neither the bait fusion protein nor the DNA-BD alone is able to autonomously activate the reporter genes

All transformants bar pGBKT7-USH1C displayed the correct nutritional phenotype (section 2.5.2.4) and did not autoactivate either *HIS3* or *ADE2* (Table 5.4). pGBKT7-USH1C (7) and (12) colonies able to grow in the absence of adenine were immediately eliminated from further use. Colonies #6 and #8 of pGBKT7-USH1C(12) that showed minimal growth in the absence of histidine, were grown on media supplemented with 3-AT (section 1.5.2.1; Table 5.5). None of the remaining transformants were able to autoactivate the *LacZ* reporter gene (section 2.5.2.4.2; Table 5.6).

Table 5.4 Comparison of the ability of the bait and control proteins to autonomously activate transcription of nutritional reporter genes.

Multiple colonies from the stock plates were streaked onto the following SD media and incubated at 30°C for 10 days.

+ = growth

- = no growth

* = minimal growth/very small colonies

Strain	Plasmid	Selection marker	SD/-Trp	SD/-Trp/-Ade	SD/-Trp/-His	SD/-Leu	SD/-Leu/-Ade	SD/-Leu/-His
Y187	pCL1	LEU2	-	-	-	+	-	-
	pACT2	LEU2	-	-	-	+	-	-
	pACT2-CDH23 (9)	LEU2	-	-	-	+	-	-
	pGK7	TRP1	+	-	-	-	-	-
	pGDAT7-T	LEU2	-	-	-	+	-	-
AH109	pGK7-p53	TRP1	+	-	-	-	-	-
	pGK7-Lam	TRP1	+	-	-	-	-	-
	pGK7	TRP1	+	-	-	-	-	-
	pGK7-USH1C (7)	TRP1	+1-8	*6,7&8	+1-4,6&7 *5&8	-	-	-
	pGK7-USH1C (12)	TRP1	+1-8	*3&4	+1-5&7 *6&8	-	-	-
	pGK7-PDZ1	TRP1	+	-	-	-	-	-
	pGK7-PDZ2	TRP1	+	-	-	-	-	-
	pGK7-PDZ3	TRP1	+	-	-	-	-	-

Table 5.5 Determination of the concentration of 3-AT required to inhibit the ability of baits pGBK7-USH1C (12-6&8) to autonomously activate transcription of the HIS3 and LacZ reporter genes

Any colonies that grew underwent a colony filter lift β -galactosidase assay.

+ = growth

- = no growth

Blue = β -galactosidase production

White = no β -galactosidase production

		SD-Trp/-His supplemented with 3-AT							
	SD-Trp/-His	5mM	10mM	12mM	15mM	50mM	100mM	500mM	
pGBK7-USH1C (12-6)	+	+ >5 colonies White/Blue	+ <5 colonies White/Blue	-	-	-	-	-	
pGBK7-USH1C (12-8)	+	+ >5 colonies White	+ <3 colonies White	-	-	-	-	-	

Table 5.6 Comparison of the ability of the bait and control proteins to autonomously activate transcription of the *Lac Z* reporter gene.

The ability of bait and control transformants to activate *Lac Z* was compared to pCL1 which endogenously expresses β -galactosidase. One of the pGBKT7-USH1C (7) bait colonies produced β -galactosidase, whilst the remaining seven stayed white.

+ = β -galactosidase production (cells turn blue) - = no β -galactosidase production (cells remain white)

pGBKT7	pGBKT7-USH1C (12)	pGBKT7- PDZ1	pGBKT7- PDZ2	pGBKT7- PDZ3	pGBKT7- 53	pGBKT7- Lam	pACT2	pACT2- CDH23	pGADT7- T	pCL1
-	-	-	-	-	-	-	-	-	-	+

5.1.3.5 Control yeast mating experiments

The compatibility of the yeast strains and vectors were checked through control mating (section 2.5.2.5.1). Growth on SD-Leu/-Trp/-His/-Ade media was only seen for matings between the system positive controls and the bait positive controls (Table 5.7). These matings also resulted in activation of the *Lac Z* reporter gene.

Table 5.7 Results of Control Mating Analysis

+ = growth - = no growth

Mating reactions		SD Minimal Medium	Growth	β -gal assay
Y187 [Plasmid]	AH109 [Plasmid]			
[pGADT7-T]	[pGBKT7-53]	-Leu/-Trp	+	Blue
		-Leu/-Trp/-His/-Ade	+	Blue
[pGADT7-T]	[pGBKT7-Lam]	-Leu/-Trp	+	White
		-Leu/-Trp/-His/-Ade	-	
[pACT2]	[pGBKT7]	-Leu/-Trp	+	White
		-Leu/-Trp/-His/-Ade	-	
[pACT2]	[pGBKT7-Lam]	-Leu/-Trp	+	White
		-Leu/-Trp/-His/-Ade	-	
[pACT2]	[pGBKT7-USH1C]	-Leu/-Trp	+	White
		-Leu/-Trp/-His/-Ade	-	
[pACT2]	[pGBKT7-PDZ1]	-Leu/-Trp	+	White
		-Leu/-Trp/-His/-Ade	-	
[pACT2]	[pGBKT7-PDZ2]	-Leu/-Trp	+	White
		-Leu/-Trp/-His/-Ade	-	
[pACT2]	[pGBKT7-PDZ3]	-Leu/-Trp	+	White
		-Leu/-Trp/-His/-Ade	-	
[pACT2-CDH23]	[pGBKT7-USH1C]	-Leu/-Trp	+	Blue
		-Leu/-Trp/-His/-Ade	+	Blue

5.1.4 Bovine retinal library screening by sequential transformation into AH109 yeast

5.1.4.1 Prey library amplification

Amplification of the bovine retinal cDNA library aliquot, (Tai, A W et al, 1999), (section 2.5.3.1), resulted in an acceptable transformation efficiency of 4.25×10^8 cfu/ μ g (Equation 5.2). The average concentration of amplified library aliquots was 0.6 μ g/ μ l, with a total amount of ~7.5mg of library DNA.

Equation 5.2 Calculation of the transformation efficiency during library amplification

$$\frac{\text{CFU on control plate}}{\text{pg plasmid DNA}} \times \frac{1 \times 10^6 \text{ pg}}{\mu\text{g}} \times \frac{\text{volume of transformants}}{\mu\text{g}} \times \frac{\text{dilution factor}}{\text{volume plated}}$$

$$\frac{3400 \text{ CFU}}{80000 \text{ pg}} \times \frac{1 \times 10^6 \text{ pg}}{\mu\text{g}} \times \frac{1 \text{ ml}}{0.1 \text{ ml}} \times 10^3 = 4.25 \times 10^8 \text{ cfu}/\mu\text{g}$$

The continued representation of the library contents post-amplification, was shown by the presence of a bright band on the gel around 8kb consisting of the vector backbone (Figure 5.6, lanes 3 and 4). This was followed by a spread of paler bands, ranging in size from 500bp-4kb in the same lanes, suggesting a representational amplification of the library and thus its suitability for the yeast two-hybrid screen.

Figure 5.6 Examination of the bovine retinal library post-amplification amplification

Library inserts were digested from the vector backbone of amplified library aliquots. Lane 1, uncut amplified library - aliquot A. Lane 2, uncut amplified library - aliquot B. Lane 3, digested amplified library aliquot - A. Lane 4, digested amplified library aliquot - B. Lane 5, DNA size standards.

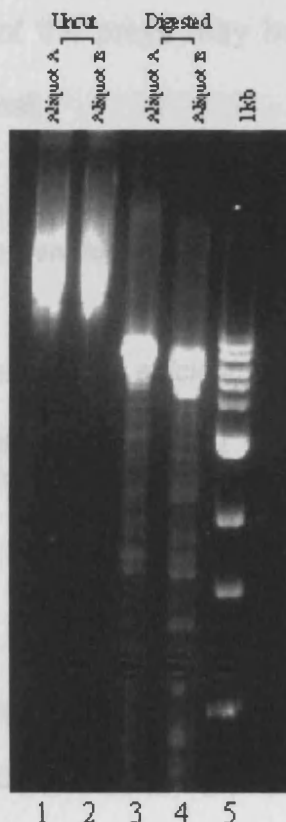


Figure 5.6 Examination of the bovine retinal library post-amplification amplification

Figure 5.7 Calculation of the bovine retinal library titre and number of library colonies screened

Concentration of library DNA used = $23.5 \times 10^6 \times 10^3 \text{ cfu/ml}$
Volume plated for inclusion = $100 \mu\text{l} \times 0.01 \times 470 \text{ ng}$
= $4.35 \times 10^3 \text{ cfu/ml}$
Number of library colonies screened = $4.35 \times 10^3 \times 470$
= 2.0×10^6

The library titre was calculated using Equation 5.3 and at $3.4 \times 10^9 \text{ cfu/ml}$, further showed that the library was acceptable for screening.

Equation 5.3 Calculation of the bovine retinal library titre

$$\begin{aligned} \text{Library titre (cfu/ml)} &= \# \text{ of colonies} \times \text{dilution factor} \times 10^3 \\ &= 3400 \times 1000 \times 1000 \\ &= 3.4 \times 10^9 \text{ cfu/ml} \end{aligned}$$

on the calculations in Figure 5.7 and Figure 5.8, it was decided to continue

5.1.4.2 Sequential co-transformation of bait and preys

The transformation efficiency (Figure 5.7) of the sequential transformation of the bait and library of preys transformed into AH109 yeast (section 2.5.3.2 - 2.5.3.3) was poor. The bait is not toxic to the yeast (section 5.1.3.3) which would suggest that some of the preys may be, or that aeration of the log phase culture was not optimal.

Figure 5.7 Calculation of the co-transformation efficiency and number of library clones screened

Cotransformation efficiency (cfu/µg DNA)

$$\frac{\text{cfu} \times \text{total suspension volume (µl)}}{\text{Volume plated (µl)} \times \text{dilution factor} \times \text{amount of DNA used (µg)}} = \frac{23 \times (10\text{ml} \times 10^3 \text{ µl/ml})}{100 \text{ µl} \times 0.01 \times 470 \text{ µg}} = 4.89 \times 10^2$$

Number of clones screened

$$\frac{\text{cfu/µg} \times \text{µg of library plasmid used}}{4.89 \times 10^2 \times 470} = 2.3 \times 10^5$$

The recommended number of clones to screen is $\sim 10^6$ but this co-transformation screened only 10^5 (Figure 5.7), probably due to the reduced transformation efficiency. A repeat screen of 10^6 clones would require 2mg of library cDNA (Figure 5.8), which is fourfold greater than the upper limits for a library scale transformation (0.1-0.5mg) and therefore impossible. Based on the calculations in Figure 5.7 and Figure 5.8, it was decided to continue

the screen and examine the possible interactors within the 10^5 library inserts that were screened. Furthermore, interactions were examined between bovine and human proteins, which may also reduce the number of possible interacting proteins picked up by the screen.

Figure 5.8 The amount of library cDNA required to screen 10^6 independent clones.

$$\begin{aligned} \text{mg DNA needed} &= \frac{10^6 \text{ clones}}{(\# \text{ of clones screened} / \mu\text{g DNA used})} \\ &= \frac{10^6}{(2.3 \times 10^5) / 470} = 2.05 \text{ mg} \end{aligned}$$

5.1.4.3 Library screening

The number of large colonies per screening plate was counted after seven days incubation (Table 5.8). The plates were incubated for a further four days to try and catch slow growing colonies which would represent weak interactors. Unfortunately during this period, colony numbers multiplied massively making it difficult to identify the colonies in Table 5.8 and the colony filter lift assay was poor. Therefore to ensure that no possible interactors were missed, all large colonies and those that could easily be identified as positives (blue) on the β -galactosidase assay filters were collected for further analysis (section 2.5.3.3; Appendix 16).

Table 5.8 Initial colony numbers resulting from the Yeast Two-hybrid screen after seven days incubation at 30°C.

The number of large (2-4mm in diameter) colonies of the correct colour resulting from the screen were identified per plate.

<i>Plate ID</i>	<i>Number of colonies that grew after seven days at 30°C</i>
1	12
2	5
3	12
4	8
5	3
6	11
7	8
8	12
9	5
10	8

5.1.4.4 Segregation of multiple library plasmids with a diploid and repeat analysis of activation of reporter genes

The behaviour of each of the 337 colonies selected (Appendix 16), was further examined by: growth on SD-Trp/-Leu to eliminate diploids; growth on SD-Trp/-Leu/-His/-Ade+ 12mM 3-AT to reconfirm the interaction by nutritional selection; and examination of their ability to activate *LacZ* (section 2.5.3.4). Results for each colony can be found in Appendix 16 and are summarised in Table 5.9.

128 of these colonies failed to grow past the initial streak site and were eliminated from further investigation. Of those colonies that did grow on SD-Trp/-Leu/-His/-Ade+ 12mM 3-AT, a further 63 were eliminated as they failed to activate *Lac Z*, leaving 145 colonies for further investigation.

Of those colonies producing β galactosidase, 10 did so at a comparable rate to the positive control which turned blue within 2 hours of introduction of the substrate (Table 5.10). A further 47 turned blue within four hours of introduction of the substrate, suggesting that these were physically strong interactions and unlikely to be false positives.

Table 5.9 Summary of Appendix 16, showing the elimination of diploid and false positive colonies from further analysis.

No. of colonies originally isolated from the yeast two-hybrid screen	337
No. of interacting colonies failing to grow on SD-Trp/-Leu	1/337
No. of interacting colonies failing to grow on SD-Trp/-Leu/-His/-Ade+ 12mM 3-AT	128/336
No. of interacting colonies failing the β galactosidase assay	63/208
No. of interacting colonies for further investigation	145

Table 5.10 Examination of the strength of bait-prey interactions as a measure of the speed of their activation of *LacZ* in comparison to pCL1

No. of hours of incubation for a positive result (colonies turned blue)	2	3.5	4	4.5	5	5.5	6.5	7	7.5	8
No. of interacting colonies	10	46	1	33	3	33	2	10	6	1

5.1.5 Characterisation of candidate interactors

145 colonies underwent further analysis by sequencing and/or yeast mating.

5.1.5.1 DNA sequence analysis of library inserts

A full detailed list of the sequence identity (section 2.5.4) of each interactor can be found in Appendix 19, but has been summarized in Table 5.11. 115 interactors have been sequenced to date, whilst the remaining interactors failed to either PCR amplify or sequence.

Of the 115 sequenced interactors, 6 were sections of UTR (untranslated regions), 45 were known false positives (including ribosomal & mitochondrial proteins), whilst 29 were out of frame transcripts. 9 of the interactors were in-frame, making them high priority for further investigation.

Table 5.11 A summary of the sequence data produced from the sequenced preys listed in Appendix 19.

Insert type	# of colonies
Ribosomal proteins	19
Mitochondrial proteins	25
Sequence known but failed mating controls	9
5' or 3'UTR	6
Clones	11
Out of frame transcripts	29
Vector only	5
Known false positives	2
In-frame transcripts	9

5.1.6 Confirmation and further characterization of positive interacting preys

5.1.6.1 Confirmation of prey-harmonin interaction by yeast mating

Table 5.12 shows the results of yeast mating experiments (section 2.5.5.1.3) between segregated prey plasmids (section 2.5.5.1.1) and Y187[pGBKT7-USH1C] or controls (section 2.5.5.1.2; transformation efficiencies are listed in Appendix 17).

A number of interactors were excluded from further analysis because they activated the reporter genes when mated with controls. Positive results confirmed the initial screening result, showing that the preys interacted with harmonin (Table 5.12, highlighted in yellow). 32 of these interactors were subsequently excluded from further investigation through sequence analysis, with most of these interactors being ribosomal proteins (Appendix 18 and Appendix 19)

Table 5.12 Confirmation of interactions between prey proteins and harmonin *in vivo* by yeast mating analysis

✓=Growth of yeast colonies on selective media

✗=Failure to grow on selective media

=Prey proteins that did not interact with control prey(s)

+=Positive β -galactosidase assay

Colony ID #	pGBT7			all USH1C			Lam		
	Growth on SD-2DO	Growth on SD-4DO	Lac Z activity	Growth on SD-2DO	Growth on SD-4DO	Lac Z activity	Growth on SD-2DO	Growth on SD-4DO	Lac Z activity
pACT2-cdh23	✓	✗		✓	✓	+	✓	✗	
1.3	✓	✗		✓	✓	+	✓	✗	
1.4	✓	✗		✓	✓	+	✓	✗	
1.7	✓	✗		✓	✓	+	✓	✗	
1.9	✓	✗		✓	✓	+	✓	✗	
1.11	✓	✗		✓	✓	+	✓	✗	
1.13	✓	✗		✓	✓	+	✓	✗	
1.22	✓	✗		✓	✓	+	✓	✗	
1.35	✓	✗		✓	✓	+	✓	✗	
1.41	✓	✗		✓	✓	+	✓	✗	
2.1	✓	✗		✓	✓	+	✓	✓	+
2.3	✓	✗		✓	✓	+	✓	✓	+
2.15	✓	✗		✓	✓	+	✓	✗	
2.18	✓	✗		✓	✓	+	✓	✗	
2.32	✓	✗		✓	✓	+	✓	✓	+
3.5	✓	✗		✓	✓	+	✓	✗	
3.7	✓	✗		✓	✓	+	✓	✗	
3.10	✓	✗		✓	✓	+	✓	✗	
3.33	✓	✗		✓	✓	+	✓	✗	
4.1	✓	✗		✓	✓	+	✓	✗	
4.14	✓	✗		✓	✓	+	✓	✓	+
4.23	✓	✗		✓	✓	+	✓	✓	+
5.4	✓	✗		✓	✓	+	✓	✓	+
5.6	✓	✗		✓	✓	+	✓	✓	+
5.17	✓	✗		✓	✓	+	✓	✗	
5.18	✓	✗		✓	✓	+	✓	✓	+
6.3	✓	✗		✓	✓	+	✓	✗	
6.5	✓	✗		✓	✓	+	✓	✗	
6.9	✓	✓	+	✓	✓	+	✓	✓	+
6.11	✓	✓	+	✓	✓	+	✓	✓	+
6.12	✓	✗		✓	✓	+	✓	✗	
6.29	✓	✗		✓	✓	+	✓	✓	+
7.1	✓	✗		✓	✓	+	✓	✗	
7.12	✓	✗		✓	✓	+	✓	✗	
7.14	✓	✗		✓	✓	+	✓	✓	+
7.20	✓	✗		✓	✓	+	✓	✗	
7.23	✓	✗		✓	✓	+	✓	✗	
8.3	✓	✗		✓	✓	+	✓	✗	
8.4	✓	✗		✓	✓	+	✓	✗	
8.6	✓	✓		✓	✓	+	✓	✗	
8.15	✓	✓	+	✓	✓	+	✓	✓	+
8.21	✓	✗		✓	✓	+	✓	✗	
8.28	✓	✗		✓	✓	+	✓	✗	
10.25	✓	✓	+	✓	✓	+	✓	✗	
10.41	✓	✗		✓	✓	+	✓	✓	+

Of the interactors eliminated from further study by sequence or mating analysis (Appendix 18 summarized in Table 5.13), 12 encoded clones with no known open reading frame (ORF) and were therefore low priority for further investigation. The same 9 interactors from Table 5.11 were confirmed here as high priority candidates for further investigation (#1.3, #1.7, #1.9, #1.22' #2.15, #6.12, #7.1, #7.23 & #8.3).

Table 5.13 A summary of the reasons for excluding individual interactors from further analysis.

Interacting colonies were excluded from further investigation for the following reasons on the basis of sequence and mating analysis.

	No. of colonies
No sequence data available	30
Failed mating controls	15
Excluded on basis of sequence analysis (known false interactors, out of frame, UTR etc)	80
Low priority sequenced interactors	11
High priority sequenced interactors	9
	Total =145

Table 5.14 briefly describes the 6 different proteins encoded by the 9 high priority sequenced interactors from Table 5.13.

Table 5.14 A brief description of the six high priority sequenced interacting proteins

Colony ID #	Protein (NCBI accession number)	Published data
1.3; 1.7; 1.9	Phosducin (M33529)	<ul style="list-style-type: none"> ▪ Small cytosolic protein that undergoes site-specific phosphorylation. ▪ Known to interact with G protein subunits and 14-3-3 proteins.
1.22	NICE 3 (NM_138740)	<ul style="list-style-type: none"> ▪ Member of the Epidermal Differentiation Complex family of proteins. ▪ Expressed in a variety of tissues, including the ear and eye.
2.15	Retbindin (NM_001024961)	<ul style="list-style-type: none"> ▪ Highly retina-preferred protein. ▪ Significantly similar to riboflavin binding proteins.
6.12	TUBB (Beta tubulin) (NM_001003900)	<ul style="list-style-type: none"> ▪ Component of the microtubule cytoskeleton.
7.1	IK cytokine (NM_006083)	<ul style="list-style-type: none"> ▪ Small secretory molecule involved in the immune system.
7.23; 8.3	Hypothetical Protein LOC83640 (NM_031452)	<ul style="list-style-type: none"> ▪ No published data at present.

5.1.6.2 Further characterization of prey-harmonin interaction through yeast

mating with the PDZ domain baits

No preys were found to interact with PDZ3 or with PDZ2 (Table 5.15) through yeast mating analysis (section 2.5.5.2), whilst 4 preys interacted with PDZ1. Prey #7.23 and gave a single colony that was positive for *Lac Z* expression when mated with pGBKT7-PDZ1. This is most likely to be a spontaneous mutation rather than a true interaction since #7.23 and #8.3 are the same cDNA clone, and #8.3 did not interact with any of the PDZ domains. The remaining 8 preys that passed the mating controls and interacted with pGBKT7-USH1C did not interact with any of the individual PDZ domains (Table 5.15).

Table 5.15 Characterisation of the interactions between pGBKT7-USH1C and the prey proteins through yeast mating with PDZ domain bait constructs.

✓=Growth of yeast colonies on selective media ✗=Failure to grow on selective media

+=Yeast turned blue, positive *LacZ* assay ★= 1 *LacZ* positive colony only

■=Preys for which sequence data is unavailable/BLAST searches failed

Colony ID #	PDZ1			PDZ2			PDZ3		
	Mated	Grew on SD-4DO	<i>Lac Z</i> activity	Mated	Grew on SD-4DO	<i>Lac Z</i> activity	Mated	Grew on SD-4DO	<i>Lac Z</i> activity
1.3	✓	✗		✓	✗		✓	✗	
1.4	✓	✓	+	✓	✗		✓	✗	
1.7	✓	✗		✓	✗		✓	✗	
1.9	✓	✗		✓	✗		✓	✗	
1.22	✓	✓	+	✓	✗		✓	✗	
2.15	✓	✗		✓	✗		✓	✗	
3.33	✓	✗		✓	✗		✓	✗	
6.5	✓	✗		✓	✗		✓	✗	
6.12	✓	✗		✓	✗		✓	✗	
7.1	✓	✓	+	✓	✗		✓	✗	
7.23	✓	✓★	+	✓	✗		✓	✗	
8.3	✓	✗		✓	✗		✓	✗	

5.1.6.3 Analysis of possible PBI sequences within prey protein sequences

Analysis of the protein sequence of the 6 candidate interacting proteins, showed the presence of class 1 C terminal PBIs in Retbindin (#2.15) and NICE-3 (#1.22) and a class 3 terminal PBI in TUBB (#6.12) (Figure 5.9) when compared to the C terminal region of cadherin 23. Both Retbindin and NICE-3 also contained multiple internal class 1 PBIs as defined by Siemens, J et al, 2002 and Adato, A et al, 2005b (Figure 5.9 in yellow).

Figure 5.9 CLUSTALW alignments of possible harmonin interacting proteins against the PBI region of cadherin 23

Protein sequence (human) comparison (Appendix 12) between Cadherin 23 (NM_022124) and (A) Nice 3, (B) IK cytokine, (C) Phosducin, (D) LOC83640, (E) Retbindin and (F) TUBB.

*** means that the residues in that column are identical in all aligned sequences; ":" means that conserved substitutions have been observed for amino acids of similar character [Small (small+ hydrophobic (incl.aromatic -Y)); Acidic; Basic; (Hydroxyl + Amine + Basic - Q)]; ":" means that semi-conserved substitutions are observed.  Boxed regions are C terminal class 1 PBIs whilst internal class 1 PBIs are shaded yellow.

(A) Cadherin 23 and Nice 3 (NM_138740)

CDH23	-----RYLRAAIQEYDNIAKLGQIIREGPIKGSLLKV	32
NICE-3	MASGSNWLGVNVVLMAYGS L FVLLFIFVKRQIMRFAMKSRRGPHPVGHNAPKDLKE	60
	:: * .. : :: * : * - **	
CDH23	VLEDYLR-----LKKLFA Q RMV Q KASSCHSSIS--ELI Q TELDEEPGDHSP	76
NICE-3	EIDIR L SRV Q DIKYEP Q LLADDDARLLQLETQGNQSCYNYLYRMKALDAIRTSEIPFHSE	120
	:: * . : * .. * . * : : : .. * * **	
CDH23	GQG--SLRFRHKPPVELKGPDGIHVVHGSTGTLLATDLNSLPEE-----DQKGLGRSL	127
NICE-3	GRH P RS L MGK N FRSYLLDLRNTSTPKGV R KALIDTLLDGYETARYGTGV F FGQNEYLYQ	180
	*: ** :: . * . : .. * : * : * .. . * : *	
CDH23	ETLTAAEATAFERNARTESAKSTPLH K LR--DVIMETPLE I TEL-----	169
NICE-3	EALSELATAVKARI G SSQRHHQSAAKDLTQSPEVSP T IQV T YLPSSQ K S K RAKH F LELK	240
	*: * : :: . * . : .. * : * .. : * . * : *	
CDH23	-----	
NICE-3	SFKDN N YNT L EST L	253

(B) Cadherin 23 and IK cytokine (NM_006083)

CDH23	-----RYLRAAIQEYDNIAKLGQIIREGPIKG-----	27
IK	MPERDSEPSNPLAPDGH D VDDPHSFHQSKLTNEDFRKLLMTPRAAPTSAPP S KS R HH E	60
	: : : : :: ** * . * ..	
CDH23	-----SLKV V LEDY I RLKKLFA Q RMV Q KASSCHSSIS-----ELI	63
IK	PREYNEDEDPAARRRK K KKSY Y AKLRQQEIERERELAEKYR D RAKERRDG V N K DYEETELI	120
	* : : : .. : : * : : * .. : .. . ***	
CDH23	QTELDE-----EPGDHSPGQGS L RFRHKPPVELKGPDGIHVVHGSTGTLLAT---DLNS	114
IK	STTANYRAVGPTAEADK S AAE K R R Q L Q E SK F GGDMEHTH L V K G L D F ALLQ K VR L EIAS	180
	* : .. * : .. : : .. . : * : * : * : ** . : * : *	
CDH23	LPEEDQKGLGRS I LET L TAAEAT-----AFERNARTESAKSTPL	152
IK	KDKEEEELMEKP Q KET K KDEDPENKIEFKTR L GRNV Y MLFK S KAYERNEL F LP G RMAYV	240
	*: * : : .. : . * . * : * : *** .. : : :	
CDH23	HKLRDVIMETPLE I TEL-----	
169		
IK	V D LDEYADTD I PTTLIRSKADCP T MEA Q TT L TTNDIV I S K L T QILSYLRQ G TRN K KL K KK	300
	* * : * : * : *	

CDH23	DKDGKLEEKKPPEADMNIFEDIGDYVPSTTKTPRDKERERYRERERDRERDRDRDRERER	360
CDH23	ERDRERERERDREREKKRHSYFEKPKV DDEPMDVDKGPGSTKELIKSINEKFAGSAGW	420
CDH23	EGTESLKKPEDKKQLGDFFGMSNSYAE CYPATMDDMAVDSDEEVDYSKMDQGNKKGPLGR	480
CDH23	WDFDTQEYSEYMMNKEALPKAAFQYGIKMSEGRKTRRFKETNDKAELDRQWKKISAIIE	540
CDH23	KRKMEADGVEVKRPKY	557

(C) Cadherin 23 and Phosducin (M33478)

(D) Cadherin 23 and LOC83640 (NM_031452)

CDH23 LOC83640	REPAAVPKDDDRYLRAAIQEYDNIAKLQGIIREGPIKGSLLKVLEDYLR -----MTDTAEAVPK	50 10 : . . * :
CDH23 LOC83640	LKKLFAQRMVQKASSCHSSISELIQTELDEEPGDHSPGQGSLRFRHKPPV FEEMFASRFTENDKEYQEYLRKRPPESPPIVEEWSNRAG-GNQRNRGNRLQ	100 59 : : : * * . : : . . : . : * : . * . * * :
CDH23 LOC83640	ELKGPDGIHVVHGSGTGLLATDLNSLPEEDQKGLGRSLETLTAAEATAFE DNRQFRGRDNRGWPSDNRSNQWHGRSGWNNYQPHR-QEPYYPPQYGHYG	150 108 : : * . * .. : : : . : : * * . . : :
CDH23 LOC83640	RNARTESAKSTPLHKL RDVIMETPLE[ITAL] 180 YNQRPPYYGYY----- 118 * *	

(E) Cadherin 23 and Retbindin (NM_031429)

CDH23 Retbindin	-REPAAVKPD DRY LA AI QEYD N IAKLGQ I IREG-----PIKGSLLKVV 44 MDEALETQ L KTSRGRFSATESL P T L ELL S QVDMDCRVHMRPIGLT W V L Q L 50
CDH23 Retbindin	LEDY L R L KKLFA Q RMVQKASSCHS-----SIS E LIQTEL 78 T L W A ILLEAC G GS R PL Q ARS S Q H HGLA D LGK G KL H LAG P CC P SEMDTTE 100
CDH23 Retbindin	DEEP G DH-----SPGQGS L R F R H K P VELKG P DG I H V VHG S TGT L LAT D L 123 T S GP G NH P ER C GV P S P ECES F LE H L Q R A L R S R F R L R LLG V R Q A Q PL C EEL 150
CDH23 Retbindin	NS-----L P EE D Q K G-----LG 135 CQ A WF A NCE D DI T CG P T W L P SE K R G C E P S CL T Y Q T F AD G T D L C R S AL G 200
CDH23 Retbindin	RSLET L TAAEATAF E R-----NARTESAKSTPLHKL R D V IM E PL 175 HAL P VAA P GAR H CFN I SI A V P R P R P G R R G REAP S R S R S P R T S I L D A AG 250
CDH23 Retbindin	E I TEL-----180 SGSGSGS G SGP 261

(F) Cadherin 23 and TUBB (NM_001003900)

CDH23	TUBB	-----REPAAVKPPDDDRYLRRAAIQEY 21
		MREIVHIQAGQCGNQIGAKFWEVISDEHGIDPTGSYHGDSLQLERINVY 50
		: * : . * . * : *
CDH23	TUBB	DNIAK-----LGQIIRE----- 33
		YNEAAGNKYVPRAILVDLEPGTMDSVRSQGPGQQIFRPDNFVFGQSGAGNN 100
		* * : * * : * : *
CDH23	TUBB	-----GPIKGSSLKVVLLEDYLRLKKLFAQRMVQKASS-CHSSISEL 73
		WAKGHYTEGAELVDSVLDVVRKESESCDCDLCQGFQLTHSLGGGTGSGMGT 150
		. : * : * . * : : * . : * : : . . * . : * . : * .
CDH23	TUBB	IQTTELDEEPGDHSPGQGSRLRFRHKPPVELKGPD---GIHVVHGSTGTLL 119
		LISKIREEYPDRIIMNTFSVMPSPKVSDTVVEPYNATLSVHQLVENTDETY 200
		: : : : * * : . * : * . : * : * . : * : . * . : * .
CDH23	TUBB	ATDLNSLPEEDQKGLRS-----LETILTAAEATAFERNARTESAKSTPL 163
		SHDNEALYDICFRTLKLTPTYGDLNHLVSATMSGVTTCLRFPGQLNADL 250
		: * : : * : : * : * : * : * . : * : . : * . : * . : * .
CDH23	TUBB	HKL RDVIMETP-----LE[TEL]----- 180
		RKLAVNMVPFPRVHFFMPGFAPLTSRGSQQYRALTVPELTQQMFDSKNMM 300
		: * * : : * * : * : * : * . : * . : * .
CDH23	TUBB	-----
		AAACDPRHGRYLTVAIIFRGRMSMKEVDEQMLNVQNKNSSYFVEWIPNNVK 350
CDH23	TUBB	-----
		TAVCDIPPRGLKMSATFIGNSTAIQELFKRISEQFTAMFRKAFLHWYTG 400
CDH23	TUBB	-----
		EGMDEMEFTEAEESNMNDLVSEYQQYQDADAEQGEFEEEEEDEA 445

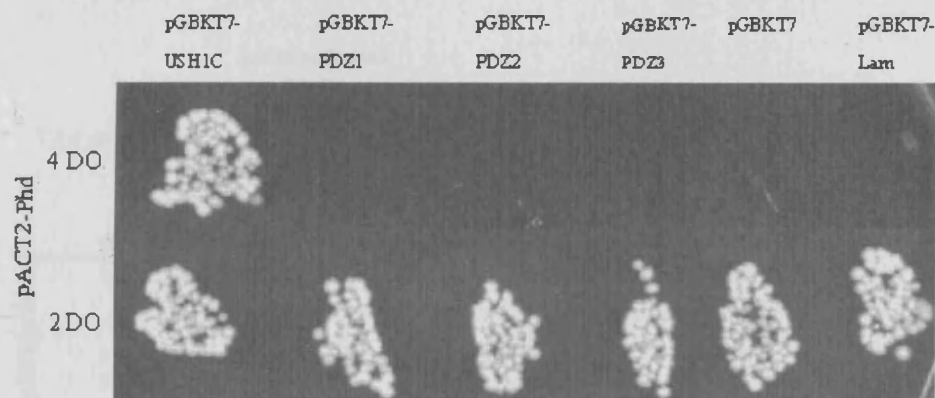
5.1.6.4 Further analysis of the candidate interactor – phosducin

5.1.6.4.1 Identification of the ORF of phosducin and confirmation of its interaction with harmonin by mating analysis.

Figure 5.10 shows that phosducin interacts with the whole harmonin bait but not with any of the individual PDZ domains (sections 2.5.5.2 & 2.5.5.3), suggesting that phosducin interacts with a region of harmonin other than the classical PDZ binding motifs i.e. the coiled coil region.

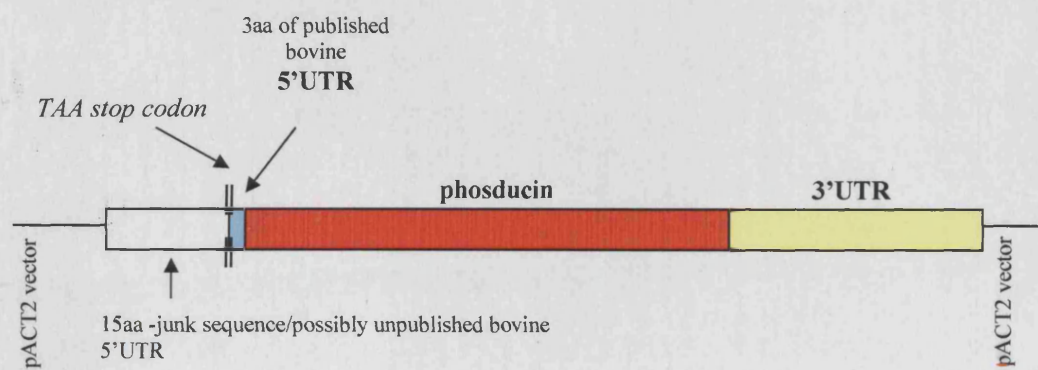
Figure 5.10 Results of the direct mating analysis between phosducin and bait/control constructs.

Successful interaction with only the whole USH1C protein activated the nutritional selection reporter genes and allowed growth on SD-Trp/-Leu/-His/-Ade+12mM 3-AT (4DO) drop out media.



Phosducin was identified as a possible interactor with harmonin on three separate occasions during the library screen (Appendix 19 - #1.3, #1.7 and #1.9), and each colony was found to contain the same cDNA clone (Figure 5.11). The insert sequence starts with 15 amino acids in frame with the GAL4BD of the pACT2 vector, which have shown no homology to other sequences in NCBI databases but may be part of the 5'UTR of phosducin which has not yet been published. There then followed the whole of the coding region (245 amino acids) and a large region of the 3'UTR, with no further ORFs apparent. Four amino acids upstream of phosducin's start codon is a stop codon but as stated in section 5.1.5.1, yeast can read through the stop codon and produce the prey fusion protein.

Figure 5.11 Schematic of the library cDNA clone extracted from yeast colonies #1.3/1.7/1.9, containing the open reading frame of phosducin



5.1.6.4.2 Analysis of phosducin protein sequence

Figure 5.12 shows the complete protein sequence of phosducin is highly conserved between species. The human sequence shares 89% amino acid homology with the bovine sequence, 87% with the murine sequence, 77% with the avian sequence and 17% with the invertebrate *c.elegans* sequence. The C terminal 150-200 amino acids in particular are highly conserved between all species. This supports the hypothesis of an interaction between phosducin and harmonin in bovine, murine and human tissues and that it was not a false positive due to species compatibility problems.

Figure 5.12 An alignment of the protein sequence of phosducin from various species to examine protein homology and areas of conservation.

ClustalW protein sequence alignment (Appendix 12) of phosducin amino acid sequence from multiple species, denoting the degree of conservation of each amino acid. "==" means that the residues in that column are identical in all aligned sequences; ":" means that conserved substitutions have been observed for amino acids of similar character [Small (small+ hydrophobic (incl.aromatic -Y)); Acidic; Basic; (Hydroxyl + Amine + Basic -Q)]; ":" means that semi-conserved substitutions are observed.

Human	(A35422)	SIQEYELIHKEKEDENCLRKYRRQCMQDMHQKLSFGPRYGFVYLETGKQFLETIEKELKITTIVVHIYEDGIKGCDALNSSLTCCLAAE	89
Chimp	(XP_524997)	SIQEYELIHKEKEDENCLRKYRRQCMQDMHQKLSFGPRYGFVYLETGQFLETIEKELKITTIVVHIYEDGIKGCDALNSSLTCCLAAE	89
Dog	(NP_001003076)	SIQEYELIHRDKEDENCLRKYRRQCMQDMHQKLSFGPRYGFVYLETGQFLETIEKEQKITTIVVHIYEDGVKGCDALNSSLTCCLAAE	89
Cat	(S52096)	SIQEYELIHRDKEDENCLRKYRRQCMQDMHQKLSFGPRYGFVYLETGQFLETIEKEQKITTIVVHIYEDGIKGCDALNSSLTCCLAAE	89
Cow	(A38379)	SVQEYELIHDKEDENCLRKYRRQCMQDMHQKLSFGPRYGFVYLESGEQFLETIEKEQKITTIVVHIYEDGIKGCDALNSSLICLAAE	89
Horse	(AAD26865)	SIQEYELIHQDKEDENCLRKYRRQCMQDMHQKLSFGPRYGFVYLETGQFLETIEKEQKITTIVVHIYEDGIKGCDALNSSLACLAAE	89
Rat	(NP_037004)	SIQEYELIHQDKEDEGCLRKYRRQCMQDMHQKLSFGPRYGFVYLETGQFLETIEKEQKVTIVVVNIYEDGVRGCDALNSSLICLAAE	89
Mouse	(NP_077778)	SIQEYELIHQDKEDESCLRKYRRQCMQDMHQKLSFGPRYGFVYLETGQFLETIEKEQKVTIVVVNIYEDGVRGCDALNSSLACLAAE	89
Red Fowl	(XP_426634)	SMQEYELINDEKEDESCLQKYRKRCMQDMHQRLSFGPKYGYLCELQNQEQLFLEAIERKRTTIVVHIYEDGIKGCNALNSSLTCCLAAE	89
C.elegans	(NP_502574)	KEEREKAQREDDEDEDFEMTLEGLKAKRRLREMRKIAANR--VIEMTDKKQYSDAVDGS-SSYLLCVLIYEPESDCEYLTRIVKILAAD	86
		.. : . : . : **. . . : : : . . . : : : : : : . . : * : ** * : * . . * . : . . .	
Human	(A35422)	YPIVKFCKIKASNTGAGDRFSLDVLPTLIIYKGELISNFISVAEQAEEFFAGDVESFLNEYGLLPEREVHVLEHTKIEEDVE	174
Chimp	(XP_524997)	YPIVKFCKIKASNTGAGDRFSLDVLPTLIIYKGELISNFISVAEQAEEFFAGDVESFLNEYGLLPEREVHAEHTKIEEDVE	174
Dog	(NP_001003076)	YPMVKFCKIKASNTGAGDRFSSDVLPTLIIYKGELISNFISVSEQFAEEFFAGDVESFLNEYGLLPEREIHALDQTNME-EDTE	173
Cat	(S52096)	YPMVKFCKIKASNTGARDRFSSDVLPTLIIYKGELISNFISVSEQFAEEFFAGDVESFLNEYGLLPEREIHALDQTNME-EDIE	173
Cow	(A38379)	YPMVKFCKIKASNTGAGDRFSSDVLPTLIIYKGELISNFISVTEQLAEEFFTGDVESFLNEYGLLPKEKMHVLEQSNME-EDME	173
Horse	(AAD26865)	YPMVKFCKIKASNTGAGDRFSSDVLPTLIIYKGELISNFISVAEQAEEFFAGDVESFLNEYGLLPEREIHALEQTSME-EDVE	173
Rat	(NP_037004)	YPMVKFCKIKASNTGAGDRFSSDVLPTLIIYKGELISNFISVAEQAEDFFAADVESFLNEYGLLPEREIHDLGQTNTEDDEDIE	174
Mouse	(NP_077778)	YPMVKFCKIKASNTGAGDRFSTDVLPTLIIYKGELISNFISVAEQAEEFFAVDVESFLNEYGLLPEREIHDLEQTNMEDEDIE	174
Red Fowl	(XP_426634)	YTTVKFCKIKASNTGAGDRFSDEVLPTLIIYKGELISNFISVSEOFNEEFFAVDVESFLNEYGLLPEREIPLGNVNTDEQDVE	174
C.elegans	(NP_502574)	CPKTKFVRATSTLLEMSRAFRNGVPCLQFYSGNLIGNFVKISAILGQDYDCKKLTKFIRGQHIDLMAGGYASDSDNESEDD- 170	
		.. . ** : : : * : : * . . . : * : : * : : : . . : : : . . . : . . : * . . . : . . : * .	

5.2 Confirmation of an interaction between harmonin and phosducin by co-immunoprecipitation (CO-IP)

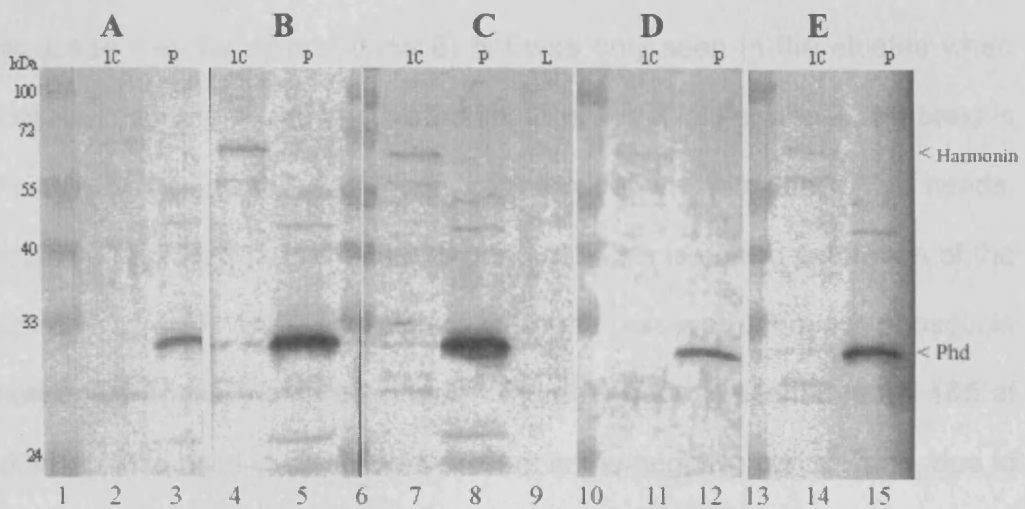
5.2.1 Synthesis of c-myc tagged harmonin and identification of phosducin in whole eye homogenate

To confirm the interaction between harmonin and phosducin, proteins had to be synthesised (section 2.5.6.1.1) or a suitable tissue source found (section 2.4.4.1.2). Figure 5.13 clearly shows Phosducin in the murine eye homogenate as a dark band on the western blot under all immunoblotting conditions. Previous western blots conducted during this research have also detected harmonin in whole eye homogenate (data not shown), but these used much higher concentrations of eye homogenate than used here to detect phosducin.

In vitro translated c-Myc tagged harmonin can be detected in the IVT USH1C lanes and is not affected by the antibodies used to visualize Phosducin (Figure 5.13). The harmonin band appears darker when using the monoclonal anti-harmonin antibody (lane 4) than the anti-c-Myc antibody (lane 2). Use of the anti-harmonin antibody and its AP conjugated secondary antibody resulted in additional pale bands at ~25 and 50kDa in the eye homogenate lanes (lane 5&8). These are not the correct size to be alternative harmonin protein isoforms from the eye homogenate and are most likely to be background from the use of mouse eye tissue with an anti-mouse IgG secondary antibody. Multiple faint bands can also be seen in the IVT USH1C (lanes 4, 7 and 14) and also in the 'no DNA' lysate control lane (lane

9). Neither harmonin nor phosducin can be detected in the control lane, suggesting that these background bands are a byproduct of the antibodies used.

Figure 5.13 Western blots showing the presence of phosducin in murine retinal homogenate



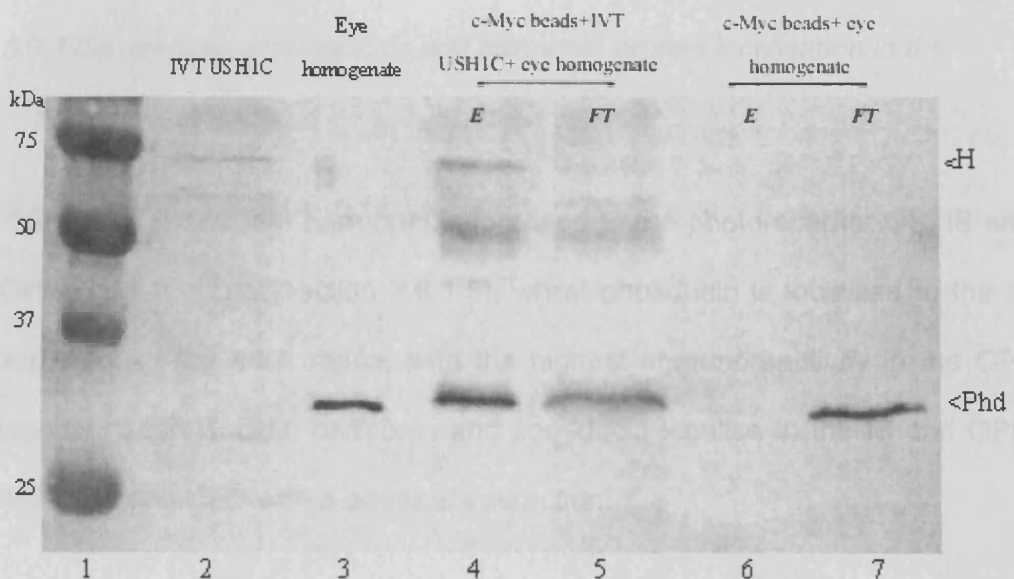
Western blots of the native phosducin protein from mouse whole eye homogenate (P) alongside IVT c-Myc tagged harmonin (IC) were probed simultaneously with an antibody to phosducin and either an antibody to the c-Myc tag (A, C-E) or to harmonin (B), to determine the optimal detection method of both proteins. Immunoblotting conditions for A-E are described in section 2.5.6.1.2.

Harmonin and phosducin (Phd) proteins are denoted by < at ~72kDa and ~33kDa respectively. Protein size standards are shown in lanes 1, 6, 10 & 13. Neither protein is seen in the control 'No DNA lysate' lane (L).

5.2.2 CO-IP assay

The reliability of the CO-IP/ pull down assay was first confirmed using known interactors (Appendix 20) and then repeated with harmonin and phosducin (section 2.5.6.2.2). Phosducin was pulled out in the presence of harmonin (Figure 5.14, lane 4) but not in controls with the coated beads alone (lane 6), confirming the interaction of harmonin and phosducin. The presence of phosducin in the negative control flow-through (lane 7) proves that phosducin was present in the control (lane 6) but was only seen in the eluates when incubated with the beads and harmonin (lane 4). A fainter phosducin band is detected in the initial flow-through from incubations with the c-Myc beads, harmonin and the eye homogenate (lane 5). This is due to saturation of the harmonin protein with phosducin, with the excess unbound phosducin showing up in this flow-through lane. A further band is seen in lanes 4&5 at ~50kDa. This band is sometimes present in the negative control lane, due to a protein from the eye homogenate binding to the beads that is detected by the secondary antibodies used (see section 5.2.1 and Figure 5.13).

Figure 5.14 Interaction of harmonin and phosducin confirmed *in vitro* through pull down analysis.



Phosducin was isolated from whole murine eye homogenate through CO-IP with c-Myc tagged harmonin using immobilized antibodies to the c-Myc. Western blots of pulled-down proteins were probed simultaneously with antibodies to harmonin and phosducin.

Lane 1, Protein size standards. Lane 2, c-myc tagged harmonin detected by anti-harmonin antibody. Lane 3, phosducin protein detected by anti-phosducin antibody. Lane 4, phosducin and harmonin detected from c-Myc pull down of eye homogenate and c-Myc tagged harmonin. Lane 5, phosducin detected in the initial flow through solution of proteins unbound to the c-Myc beads in lane 4. Lane 6, neither phosducin nor harmonin was detected from c-Myc pull down in the absence of harmonin. Lane 7, an intense band of phosducin protein detected in the initial flow through solution of proteins unbound to the c-Myc beads in the absence of harmonin from lane 6.

E: Eluate FT: Column flow through H: Harmonin

GCL: gentamicin cassette; IVD: vector containing IVT mRNA; IVT: in vitro transcription; LPA: linear polyacrylamide; OMA: outer nuclear layer; OS: outer segment; SDS: sodium dodecyl sulfate; SDS-PAGE: sodium dodecyl sulfate-polyacrylamide gel electrophoresis; SDS-PAGE: sodium dodecyl sulfate-polyacrylamide gel electrophoresis.

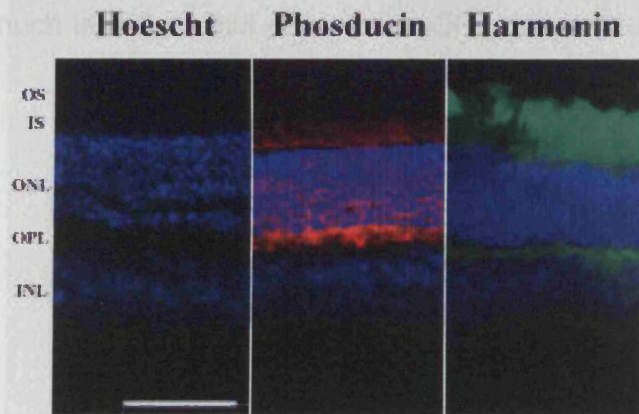
5.3 Validation of candidate interactor through protein localisation and gene expression analysis

5.3.1 Comparison of phosducin and harmonin protein localisation in the normal adult retina

Figure 5.15 shows that harmonin is localised to the photoreceptor OS, IS and OPL in adult retina (section 2.3.1.3), whilst phosducin is localised to the IS and ONL of the adult retina, with the highest immunoreactivity in the OPL (section 2.5.7.1). Both harmonin and phosducin localise to the IS and OPL, which is consistent with a physical interaction.

Figure 5.15 Immunolocalisation of phosducin and harmonin in the adult murine retina

Harmonin is labeled in green and phosducin in red. Replacement of the anti-phosducin antibody with PBS showed no non-specific background staining in the neural retina in fixed tissue (Hoescht control lane).



GCL, ganglion cell layer. IPL, inner plexiform layer. INL, inner nuclear layer. OPL, outer plexiform layer. ONL, outer nuclear layer. IS, photoreceptor inner segments. OS, photoreceptor outer segments. Scale bars 10 μ m.

5.3.2 Comparison of phosducin and harmonin protein localisation in the normal developing retina

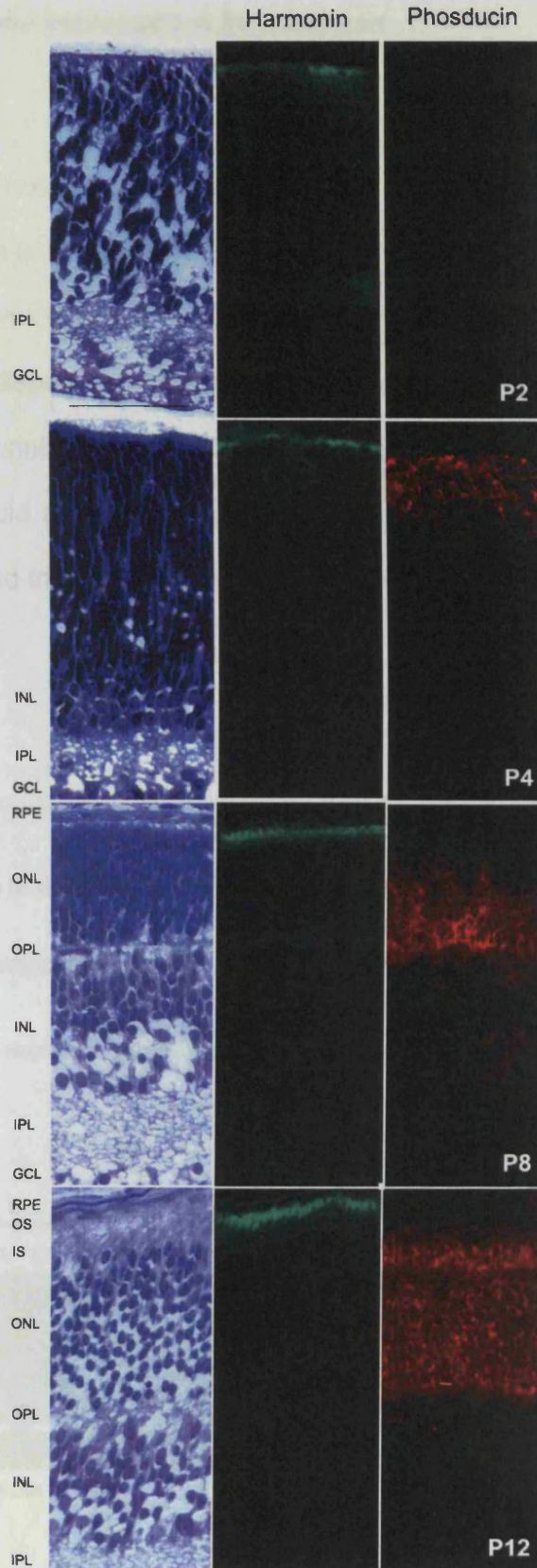
Figure 5.16 shows that *Pdc* (encoding Phosducin) expression is initiated between P2 and P4, with phosducin localised to the perinuclear region within the developing photoreceptor (section 2.5.7.2). *Ush1c* expression starts earlier than *Pdc*, with harmonin detectable at P2. During the very early developmental stages (P2-P4), *Ush1c* looks to be expressed by far fewer cells than *Pdc*, with harmonin specifically localised to cells of the outermost edge of the developing photoreceptor layer. By P8, immunolabelling of harmonin is restricted to the developing segments, whilst phosducin is seen throughout the newly formed ONL. At P12, the strongest harmonin immunoreactivity was seen in the photoreceptor OS layer of fixed tissue. In contrast, phosducin immunoreactivity was highest in the IS but also seen strongly throughout the ONL. As the retina develops, the levels of phosducin at the developing OPL increases but immunoreactivity at these stages examined is much less than that seen in the OPL of the adult retina (Figure 5.15).

Figure 5.16 Localisation of phosducin and harmonin in the developing retina.

Semithin sections (stained with methyl blue) are shown for comparison to demonstrate development of retinal layers from P2-P12 (section 1.2.1.2).

Harmonin (green) is present in the newborn photoreceptors prior to phosducin (red). As development proceeds, phosducin is clearly labelled in the ONL and IS (P8 and P12).

GCL, ganglion cell layer. IPL, inner plexiform layer. INL, inner nuclear layer. OPL, outer plexiform layer. ONL, outer nuclear layer. IS, photoreceptor inner segments. OS, photoreceptor outer segments.
Scale bars 10 μ m.



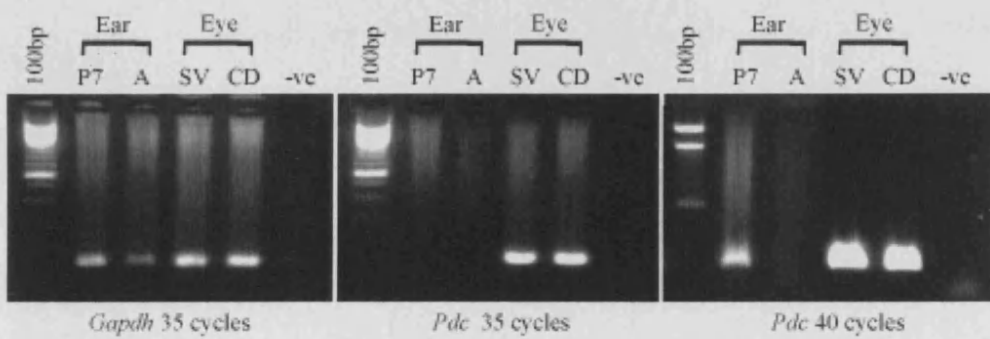
5.3.3 Comparison of *Pdc* and *Ush1c* gene expression in the adult and developing ear by RT-PCR

RT-PCR showing *Pdc* expression was noted in the adult murine eye (section 2.5.7.3 & Figure 3.6), but was not seen in the adult or developing ear (Figure 5.17, 35 cycles). Production of cDNA was successful as positive results were obtained for the housekeeping gene, *Gapdh*. Increasing the cycle number to 40 produced a band in the P7 ear sample but still nothing in the adult ear. Although the data is qualitative, it would suggest that phosducin expression in the ear is far less than in the eye, and that the gene is not expressed in the adult ear.

Figure 5.17 Investigation of *Pdc* expression in developing and adult murine ear

Pdc expression was examined in a P7 developing inner ear (P7), an isolated adult cochlea (A), and in CD1(CD) & SV129 (SV) adult eyes

100bp: DNA size standards -ve: control reaction substituting ddiH₂O for DNA as template.



5.4 *Conclusions*

- Six candidate harmonin-interacting proteins were isolated: all were seen to interact with full length harmonin, whilst two also interacted with PDZ1 and the remaining four with a region other than the three PDZ domains.
- Phosducin was demonstrated by yeast mating and a pull down assay to interact with full length harmonin but not through direct binding with any of the three PDZ domains. Its interaction with harmonin was confirmed by CO-IP analysis.
- Phosducin's pattern of localisation in the adult and developing retina was similar to that of harmonin, with both proteins localised to the photoreceptor IS and OPL.
- *Pdc* expression was also seen in the developing ear (in the bulla that contained cochlear and vestibular tissue), but not in the adult cochlea.

6 DISCUSSION

This study examined the localisation of the *Ush1c* protein, harmonin, both in normal murine eyes and in models of Usher syndrome types 1B and 1D. Harmonin was localised to the photoreceptor OS of fixed retinal tissue, with further protein expression seen in the IS and OPL of unfixed retina. Maintenance of harmonin localisation in the OS of fixed tissue from both murine models resulted in a Yeast Two-Hybrid assay to investigate alternative harmonin-interacting proteins. Six candidate proteins were identified. Interaction of one of these proteins, Phosducin, was confirmed by a pull-down assay and shown by immunofluorescence staining to colocalise with harmonin in the photoreceptor IS and OPL. These findings and the further insights they have provided into the possible pathogenic mechanisms of Usher syndrome, are discussed in the following chapter.

6.1 *Determination of the temporal and spatial expression of *Ush1c* and harmonin within the normal murine eye*

- In the developing murine eye, *Ush1c* expression can be detected as early as E12.5 by RT-PCR.

The fact that all the USH1 genes examined here are expressed simultaneously in the retina from E12.5, would support the hypothesis that in

the retina, all the USH1 proteins are involved in the same functional pathway or directly interact to form a macromolecular complex. Expression of *Ush1c* at such an early stage of development would suggest that it was essential for correct eye development, as seen in the ear, where it plays a role in organising the developing stereocilia bundle on the auditory hair cells. Yet although Usher patients have profound congenital deafness, they have normal vision at birth; therefore harmonin is unlikely to play a role in correctly organizing the developing photoreceptor.

- As the retina differentiates, harmonin is first localised to the new born photoreceptors and then to their developing segments. In the adult it is clearly confined to the OS in fixed tissue.

The localisation of harmonin to the photoreceptor OS could implicate it in phototransduction. Harmonin may be embedded in the OS disks where it may anchor the photopigments ready for phototransduction. Colocalisation of harmonin and rhodopsin, and the fact that rhodopsin has a C terminal PBI, supports this hypothesis. Other PDZ-domain-containing proteins involved in phototransduction include INAD, which acts not only as a 'transducisome' but has been postulated to have a direct role in termination of the photoresponse whilst also contributing to the rapidity of the activation response (Sheng, M. *Annu Rev Neurosci*, 2001). However, comparative mRNA expression studies have shown that visual transduction protein expression in vertebrates, is initiated alongside outer segment disk emergence (or slightly prior to disk

emergence, in cones) (Timmers *et al* 1993; Johnson, P T *et al*, 2001). In humans this is around 5½ months gestation but in the mouse this occurs as late as P6. The fact that *Ush1c* is expressed prior to this reduces the likelihood of a role for harmonin in phototransduction.

- Additional immunoreactivity is seen using unfixed tissue, with harmonin localised to the photoreceptor OS, IS and OPL.

A comparison of harmonin localisation in fixed and unfixed tissue saw the protein confined to the OS in fixed tissue but further immunoreactivity noted in the IS and the OPL. It has been hypothesized that the discrepancy between immunostaining results in different fixation states may be due to antigen masking by fixation of the retinal tissue (Reiners, J *et al*, 2003), resulting in lower levels of staining generally. The work here supports this hypothesis since consistently higher levels of harmonin staining were seen in all parts of the photoreceptor using unfixed tissue. Furthermore, myosin VIIA could only be detected in the RPE and connecting cilium in fixed tissue (Liu, X *et al*, 1997), but could also be seen in the OPL and IS of unfixed tissue. The additional myosin VIIA staining in the OPL published by Reiners *et al*, was claimed by others to be an artifact of the antibody used (Williams, D S *et al*, 2004). Yet the work carried out here with an alternative commercially available antibody to myosin VIIA disputes this statement, also finding myosin VIIA in the IS and OPL.

The colocalisation of harmonin, myosin VIIA and cadherin 23 to the IS and OPL in unfixed tissue (Figure 3.3 and Wolfrum, U et al, 2004), would suggest that the USH1 proteins could form a complex in the eye, similar to that seen in the ear. In the OPL, the ribbon synapses are formed between the photoreceptors and the second order neurons. PDZ proteins are known to be important in structurally organizing the synaptic apparatus at the pre and post synaptic densities (Garner, C C et al, 2000) and so this could be a potential function for harmonin. Alternatively, the co-localisation of the three proteins to the IS would suggest that the Usher proteins could have a function relating to disk formation/organization. In both the OPL and IS, the function of harmonin and the other Usher proteins must not be essential for developing normal vision as patients can see at birth.

- Localisation in the OS is maintained in the absence of either myosin VIIA or cadherin 23.

The localisation of harmonin to the photoreceptor OS using fixed tissue was maintained in the retinas of *shaker-1* and *waltzer* mice that are null mutants for myosin VIIA and cadherin 23 respectively (Figure 3.5). In the ear, myosin VIIA is thought to be essential for the correct localisation of harmonin isoform 'b', which in turn is postulated to link cadherin 23 in the hair cell stereocilia, to the actin cytoskeleton during development (Boeda, B et al, 2002). It is interesting to note that Reiners *et al* (2003) saw differences in harmonin isoform localisation in the retina, with isoform 'b' restricted to the OS whilst

isoforms 'a' and 'c' were found in the OS, IS and OPL. Whilst here immunostaining data on the mutant mice does show that at least one harmonin isoform does not require myosin VIIA or cadherin 23 for localisation to the OS, the possibility that one or more isoforms of harmonin are mislocalised cannot be excluded without the use of isoform-specific antibodies. Furthermore, the possibility that one or more isoforms are mislocalised in the OPL or IS cannot be excluded since visualisation of harmonin labelling in these regions was not possible with fixed tissues.

Since harmonin has been postulated to interact with cadherin 23 in the ear (Boeda, B et al, 2002; section 1.3.4.1), it would have been interesting to investigate the localisation of cadherin 23 in the absence of harmonin, using the mutant mouse for *Ush1c, deaf circler* (Johnson, K R et al, 2003), to see if its expression is maintained in the IS and OPL. Furthermore it would be interesting to compare cadherin 23 staining in the *deaf circler* mouse (which is null for all forms of harmonin), to cadherin 23 staining in the *deaf circler 2 Jackson* mouse. Although this mouse also has mutations in *Ush1c*, these effect the alternatively spliced exons of isoform 'b' but allow correct expression of harmonin isoforms 'a' and 'c', resulting in nonsyndromic deafness (Johnson, K R et al, 2003). Furthermore, cadherin 23 isoforms have different expression patterns in the ear and eye (Siemens, J et al, 2002), thus different cadherin 23-harmonin complexes may form in both the two tissues. This would be a further interesting aspect to investigate, both in wild type and in the Usher mutant mice *waltzer* and *deaf circler*.

6.2 *Investigation into candidate harmonin-interacting proteins*

within the normal eye

- Six candidate harmonin-interacting proteins were isolated: all were seen to interact with full length harmonin, whilst two also interacted with PDZ1 and the remaining four with a region other than the three PDZ domains.

Of the six candidate harmonin-interacting proteins identified in the yeast two-hybrid screen, NICE-3 was isolated from two different clones, one encoding the N-terminal half (#6.29) and the other, the C-Terminal half (#1.22). NICE-3 is one of the five family members of the NICE proteins that are part of the epidermal differentiation complex, localised to chromosome 1. *NICE-3* is alternatively spliced, with one of its three transcripts corresponding to the predicted human protein HSPCO12 (Zhang, Q H et al, 2000), expressed in CD34+ hematopoietic stem/progenitor cells. *NICE-3* is widely expressed at low levels in many tissues, including the blood, brain, prostate, lungs, ovary and the ear and eye. The protein is predicted to contain an N-4 cytosine-specific DNA methylase signature, although the functional significance of this is unknown (Marenholz, I et al, 2001). The mating analysis, following the initial yeast two-hybrid screen, showed the N-terminal clone to be a false positive, interacting with the pGBKT7-Lam control protein. The C-terminal region, which contains a class 1 PBI at the carboxyl end of the protein, interacted with the whole pGBKT7-USH1C fusion protein and with the PDZ1 construct. The mating with the PDZ1 construct produced multiple blue colonies but could not be repeated on further mating experiments: the reason

for this is unknown but may be due to spontaneous mutations within the fusion protein during storage. Although a large proportion of clone #1.22 was successfully sequenced, a portion of the 3' insert sequence most likely containing the 3'UTR of *NICE-3*, remains unanalyzed despite the use of a variety of sequencing reaction conditions and supplements. *NICE-3* also proved difficult to synthesise by IVT and since no known antibody to the protein is available, confirmation of its interaction with harmonin has not been possible.

Another possible candidate protein with a C-terminal class 1 PBI was Retbindin (#2.15). The Retbindin gene is located at 19p13 and predicted to have multiple promoters producing a highly retina-preferred protein. Retbindin has a weak but significant similarity to riboflavin binding proteins, with distant similarity to mammalian folate receptors. It is rich in cysteines and conserved glycosylation sites, suggesting that this protein is secreted and post translationally modified. Its predicted ligands include carotenoids, suggesting it may play a role in sequestering flavinoids and protecting the retina from free radical damage (Wistow, G et al, 2002). Although Retbindin possesses a class 1 PBI, it only interacted with the pGBK7-USH1C construct and its predicted role does not fit into that postulated for harmonin in the retina. Furthermore, the identified sequence was canine which could lead to false positives (section 1.5.2.1). There was also a stop codon in the insert sequence upstream from the coding region of Retbindin, such that harmonin may have been acting with a fusion protein produced from the upstream insert sequence and not interacting directly with Retbindin. These

factors when combined reduce the likelihood of Retbindin being a candidate for a harmonin-interacting protein.

An IK cytokine (#7.1) was also identified from the initial screen and was shown to interact with both pGBKT7-USH1C and pGBKT7-PDZ1, yet it did not have a PBI. The fact that this is a small secretory molecule involved in the immune system reduces the likelihood of this being a binding partner central to harmonin's function. The hypothetical protein LOC83640 was identified twice (#7.23 and #8.3) from the same cDNA clone and was shown to interact with the full length harmonin protein only.

Beta tubulin, a component of the microtubule cytoskeleton with a class 3 PBI, interacts with pGBKT7-USH1C but none of the PDZ domains directly. In the developing retina, beta tubulin is localised to virtually all cell types but is especially strong in the OPL and IPL. In the adult retina, staining was seen in the OPL and IPL but was also present in the photoreceptor OS (Sharma, R K et al, 2003). It is interesting to uncover another component of the cytoskeleton as a potential interactor of harmonin, since harmonin is already known to interact with the actin cytoskeleton in the developing stereocilia. The connecting cilium of the photoreceptor is rich in microtubules: although harmonin has been seen in the photoreceptor IS and OS (Figure 3.6), definitive proof of its presence in the connecting cilium has not yet been determined by high resolution analysis. However the identification of a protein highly expressed in the connecting cilium as a potential interactor of

harmonin would support the argument of harmonin localisation in the connecting cilium.

- Phosducin was demonstrated by yeast mating and a pull down assay to interact with full length harmonin but not through direct binding of any of the three PDZ domains. Its interaction with harmonin was confirmed by CO-IP analysis.

Phosducin is a small acidic cytosolic protein, which undergoes site specific phosphorylation at many of its serine residues. The protein's phosphorylation state is altered by cAMP and Ca^{2+} levels which are controlled in a light-dependent manner and ultimately affect phosducin's ability to bind to certain binding partners (Lee, B Y et al, 2004). Structurally similar proteins, thought to be family members, are the phosducin-like proteins (PhdLPs) and phosducin-like orphan proteins (PhdLOP). PhdLPs are localised throughout the inner retinal layers and can bind $\beta\gamma$ subunits of G proteins (Schulz, R, 2001 and references therein). A novel germ line specific PhLP has been found in mice and exerts a function in germ cell maturation (Lopez, P et al, 2003). PhdLOPs are localised to the cell nucleus (phosducin and PhdLPs are cytosolic) and are missing the amino terminus seen in phosducin and PhdLPs. They are thought to play a role in transcriptional activation, interacting with SUG1 (Zhu, X et al, 1998) and the retinal and pineal gland-specific transcription factor, CRX (Zhu, X et al, 2000).

Phosducin does not interact with harmonin via any of the PDZ domains but instead may bind to the very end of the C terminus, the coiled coil domain or the linker regions between the structural domains. The use of alternative binding sites on PDZ proteins has been seen in the case of INAD, the *Drosophila* 5-PDZ-domain-containing protein. INAD uses its linking region between PDZ1 and PDZ2 to bind calmodulin, bringing it into close proximity with other participants of the phototransduction cascade (Huber, A, 2001).

- Phosducin's pattern of localisation in the adult and developing retina was similar to that of harmonin, with both proteins localised to the photoreceptor IS and OPL.

Although phosducin protein synthesis is initiated after harmonin, the localization of the proteins during development in the newborn photoreceptors is similar. In addition, their appearance in the developing photoreceptor projections occurs simultaneously (as these structures develop), further supporting the theory of a functional interaction between these proteins. Phosducin was shown to be localised to the IS, ONL and OPL, with phosducin staining in the OPL reaching its peak, at a time when the ribbon synapses have fully developed (P12-P15) (Grun, G, 1982), supporting the hypothesis that phosducin and harmonin are localised to these particular structures within the OPL (Reiners, J et al, 2003; Chen, J et al, 2005).

Phosducin has also been shown to be expressed in the OS of the photoreceptors by serial tangential sectioning (Sokolov, M et al, 2004). Here it was hypothesized to have a role in phototransduction through its interaction with the $\beta\gamma$ subunits of Transducin, a photoreceptor specific heterotrimeric G-protein, acting as an antagonist to the α subunit and facilitating light driven Transducin translocation. Yet phosducin protein levels are relatively low in the OS compared to what would be expected for a protein with this proposed function (Sokolov, M et al, 2004) and is in fact expressed at seven-fold higher levels in the OPL than in the OS (Chen, J et al, 2005). Thus phosducin has been suggested to have alternative/multiple roles including: acting as a phosphorylation-dependent switch in signalling cascades involved in light adaptation; involvement in transcriptional activation (Schulz, R, 2001); and in shielding G-proteins from proteosome degradation (Sokolov, M et al, 2004; Chen, J et al, 2005).

- *Pdc* expression was also seen in the developing ear (in the bulla that contained cochlear and vestibular tissue), but not in the adult cochlea.

Pdc (the gene encoding phosducin), expression was detected in the developing murine ear but absent from the adult cochlea. This may mean that phosducin plays a role during ear development but does not have a function in ear maintenance/homeostasis and thus is not required in the adult ear. Alternatively *Pdc* may in fact be expressed in the vestibular system rather than in the cochlea, since the tissue from the developing mouse ear consisted of developing cochlear and vestibular tissue, whilst in the adult, an

isolated cochlea was used. Immunostaining for phosducin on ear tissue sections would clarify this point. Phosducin has also been observed in other tissues that have been seen to show pathology in some cases of Usher syndrome, including the olfactory system (Danner *et al* 1996) where it is found at comparable levels to that in the brain (levels in the brain are higher than in most tissues but significantly lower than that found in the retina (Schulz, R, 2001)).

It is interesting to note that in auditory transduction unlike in phototransduction (section 1.2.1.2 & 1.2.2.3), a second messenger cascade system (including G proteins) is not used to amplify and transmit the signal but instead employs direct gating of the transducer channel (Alessandro Martini, 1996). Therefore G-proteins and their binding partners (including phosducin which is able to interact with a whole range of G-proteins (Bauer, P H *et al*, 1998)) are not necessary in the cochlea ribbon synapses.

6.3 *Possible pathogenic mechanisms in Usher syndrome.*

Harmonin and phosducin

Phosducin is known to bind to the photoreceptor inner segment and synaptic protein 14-3-3 in its phosphorylated form (Nakano, K *et al*, 2001). Decreases in intracellular Ca^{2+} levels blocked this interaction by inhibiting phosphorylation at two specific serines (54 and 73). This led to the supposition that phosducin may be involved in Ca^{2+} dependent light

adaptation (Thulin, C D et al, 2001). In the fly photoreceptor cell, calcium homeostasis is maintained through light-induced Ca^{2+} ion influx through designated Ca^{2+} ion channels (of the TRP family which is correctly localised through interactions with the PDZ containing INAD protein (Huber, A, 2001), with extrusion by $\text{Na}^+/\text{Ca}^{2+}$ exchange. The influx results in two separate Ca^{2+} signals: the global rise that mediates light adaptation; and the rapid transient amplitude that shapes quantum bumps into all or nothing signals (Oberwinkler, J, 2002). Free 14-3-3 has been postulated to potentiate the release of glutamate at retina synapses and be involved in light adaptation (Nakano, K et al, 2001).

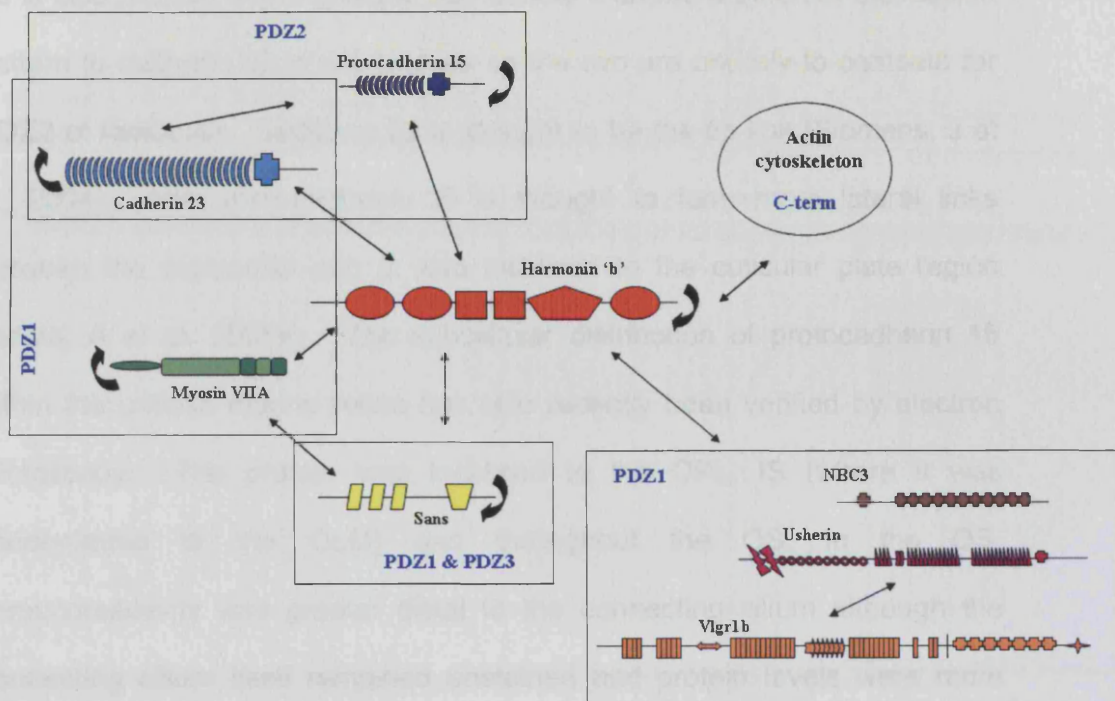
Furthermore, since phosducin can interact with alternative G-proteins to Transducin, it has been suggested that it could interact with the G protein associated with the group III metabotropic glutamate receptor, since both are localised to the rod IS, (Nakano, K et al, 2001). This particular glutamate receptor acts as an autoreceptor, down regulating intracellular Ca^{2+} to control light-regulated release of glutamate from the photoreceptor synapses. This provides a negative feedback system that is thought to aid in fine adjustment of the light-regulated release of glutamate from the synapses and to act as a safety device against excitotoxic glutamate levels that would damage the photoreceptor (Koulen, P et al, 1999). Harmonin may compete with 14-3-3 or the G protein subunits for the same binding site within phosducin, or it may alternatively bind to the C terminus. It is also unclear whether harmonin has a preference for binding to the phosphorylated or dephosphorylated form of phosducin.

Pdc has been investigated as a candidate gene for Usher syndrome and other retinal disease (Nishiguchi, K M et al, 2004; Ara-Iwata, F et al, 1996). In dogs, a sequence variant close to the region of the protein that directly interacts with the G-protein subunits, was associated with photoreceptor dysplasia but did not account entirely for the genetics of inherited retinal degeneration in the breed (Zhang, Q et al, 1998). Human patients with retinitis pigmentosa, dominant RP, recessive RP, Leber Congenital Amaurosis, or cone-rod degeneration, were screened for mutations in *Pdc*. Single cases of a polymorphism in the 5' untranslated region or a rare single-base sequence variant (only three variants ever noted), were seen in separate heterozygous patients but none were interpreted as pathogenic (Nishiguchi, K M et al, 2004b; Nishiguchi, K M et al, 2004a). Two different heterozygous mutations in highly conserved amino acids were individually seen in an USH2 and an Acute Zonal Occult Outer Retinopathy (AZOOR) patient. Yet a lack of further patients with mutations in *Pdc*, did not support a relationship between *Pdc* with either of these ocular disorders (Ara-Iwata, F et al, 1996). It has been suggested that the addition of a heterozygous mutation in particular cases of AZOOR could be the reason for the increase in severity of the phenotype seen in these patients (Ara-Iwata, F et al, 1996): it would therefore not be unreasonable to suggest that *Pdc* could be a modifier gene in both AZOOR and Usher syndrome.

Harmonin and the USH1 proteins

Harmonin, cadherin 23 and myosin VIIA have been shown to interact and now a direct binding link has been established between the SAM domain of sans with both PDZ1 and PDZ3 of harmonin (Figure 6.1), thereby recruiting Sans to the actin filaments. It is localised to the cuticular plate where it contributes to hair bundle cohesion via an activity exerted from underneath the hair cell bundle (Adato, A et al, 2005b). Interactions have also been established between sans and myosin VIIA via the central region of sans and the tail of myosin VIIA. Sans also uses this region for homodimerisation and is unable to bind to harmonin or myosin VIIA as a single protein. At the apical region of the hair cells it is expected to form homodimers allowing it to interact with either harmonin or myosin VIIA but never both simultaneously or in situations where harmonin and myosin VIIA have already formed a complex (Adato, A et al, 2005b). This would indicate a very specific role for both Sans-based protein complexes and for the separate harmonin-myosin VIIA complex in the hair cell. Whether similar interactions are seen in the retina has yet to be established.

Figure 6.1 Interaction of the USH1 and USH2 proteins via harmonin



A schematic summarizing the protein interaction data discussed above and in section 1.3.4 (references are included therein).

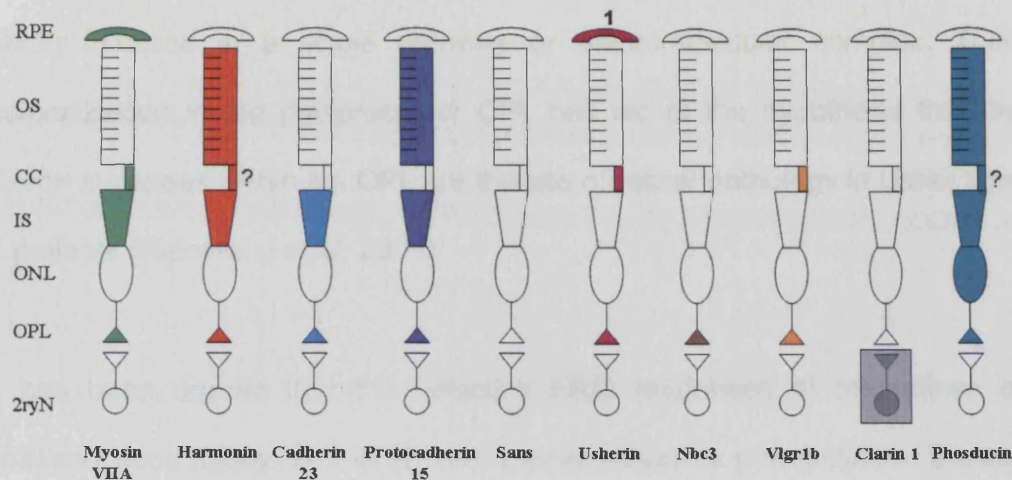
The proteins are collated into labelled boxed groups according to the region of harmonin with which they interact. Proven interactions are denoted with a double headed arrow. The ability of certain proteins to dimerise is denoted with a curved arrow.

Harmonin was also shown to interact with the C terminal PBI of protocadherin 15 via its PDZ2 domain (Figure 6.1). Although protocadherin 15 is also present in the growing hair bundle it shows a different expression pattern to cadherin 23 in the cochlea so the two are unlikely to compete for PDZ2 of harmonin. Cadherin 23 is thought to be the tip link (Siemens, J et al, 2004), whilst protocadherin 15 is thought to form more lateral links between the stereocilia and is also localised to the cuticular plate region (Adato, A et al, 2005b). The subcellular distribution of protocadherin 15 within the unfixed murine retina has also recently been verified by electron microscopy. The protein was localised to the OPL, IS (where it was concentrated to the OLM) and throughout the OS. In the OS, immunoreactivity was greater distal to the connecting cilium although the connecting cilium itself remained unstained and protein levels were more abundant in cone photoreceptor OS than in rod OS. It has therefore been hypothesised that since only protocadherin 15 and harmonin have been localised to the photoreceptor OS, that harmonin isoform 'b' links protocadherin 15 at the OS disk membranes to the actin cytoskeleton (Boeda, B et al, 2002), thereby rigidly organizes the newly synthesized disks starting at the connecting cilium with respect to the actin cytoskeleton (Reiners, J et al, 2005a). Figure 6.2 summarises the recent developments in the understanding of Usher protein localisation in the retina.

Since harmonin is a multidomain protein and likely to be able to bind to multiple proteins simultaneously, it is possible that harmonin may interact with protocadherin 15 and phosducin at the IS/OS, thus fulfilling the role

postulated by Reiners *et al* (2005) in organising the newly synthesized OS disks. Yet, as discussed previously, it is unlikely that the USH1 proteins are involved in correct sensory cell development in the retina, in contrast to their role in the ear (section 1.3.4.1), since patients have normal vision at birth. Therefore although harmonin/protocadherin 15 and harmonin/phosducin may indeed interact within the IS or OS, it is unlikely to be the site of pathology for Usher syndrome type 1.

Figure 6.2 A summary of the localisation of phosducin and the Usher proteins in the murine retina



The majority of the Usher proteins and phosducin colocalise to the OPL. Clarin-1 is also postulated to colocalise to the OPL but may function on the post synaptic membrane of the ribbon synapses of OPL, since it is expressed by the horizontal and Müller cells and not the photoreceptors. The patterns of protein expression of the Usher proteins support the argument that the OPL and more likely the ribbon synapses is the site of Usher pathology within the retina.

1= Usherin is localised to the Bruch's membrane above the RPE rather than the RPE itself.

?- Due to the presence of the protein in both the OS and IS, it is possible that it also localises to the CC but this has not yet been proved/disproved.

2ryN, second order retinal neurons. OPL, outer plexiform layer. ONL, outer nuclear layer. IS, photoreceptor inner segments. CC, connecting cilium. OS, photoreceptor outer segments. RPE, retinal pigmented epithelium.

The homogeneous nature of the clinical phenotype of Usher type 1, and the overlapping expression patterns of the USH1 genes and proteins: both temporally (Figure 3.6) and spatially (Figure 3.3), point to the USH1 proteins being involved in a single pathway or macromolecular complex. Their colocalisation in the photoreceptor OPL has led to the hypothesis that the ribbon synapses within the OPL are the site of retinal pathology in Usher type 1 patients (Reiners, J et al, 2003).

It has been argued that the defective ERG responses of the retinas of *shaker-1* mice (Libby, R T et al, 2001), where there is a reduction in b-wave amplitude, is indicative of a synaptic dysfunction (Wolfrum, U et al, 2004), supporting the hypothesis of Reiners et al. However, others argue that the *shaker-1* ERGs did not show the same abnormalities of b:a wave ratio observed in mice with proven synaptic defects (Williams, D S et al, 2004). Examples of such mice include the *Bsn*, *nrc* and *Lamb2* mice, all of whom have floating ribbons at the presynaptic membrane of the photoreceptor synapse (Libby, R T et al, 2004 and references therein). But as stated earlier, the murine models for Usher syndrome type 1 do not have a clinically significant degree of retinal dystrophy, and therefore findings in these mice must be viewed with that in mind.

However, some 'proven' synaptic defects display a more subtle decrease in b-wave and a-wave amplitude on an ERG (Libby, R T et al, 2004), more in keeping with the ERG data for certain *waltzer* alleles (Libby, R T et al, 2003). For example, myosin Va has been shown to be unnecessary for anchoring

the ribbon but may be important in recycling or replenishing the synaptic vesicles (Libby, R T et al, 2004). In the myosin Va mutant, this decrease may be as a consequence of feedback from post synaptic activity upon the photoreceptor or alternatively may be due to defects in the IS where myosin Va is also expressed (a similar pattern of expression seen for four of the USH1 proteins to date). This leaves the question as to whether any of the USH1 proteins play a similar role to myosin Va in the photoreceptor ribbon synapses, in replenishing the synaptic vesicles, or whether they play a more structural/organisational role in keeping with their function in the ear.

In addition, many members of the cadherin/protocadherin superfamily are expressed in the CNS synapses, where they are involved in segregation of neuronal precursor populations, in axonal outgrowth and in synapse formation. Many cadherins are localised to the synaptic junctions where they modulate synaptic structure and transmission properties e.g. N-cadherin or protocadherin 7 (Frank, M et al, 2002).

Furthermore, it is relevant to note that the Shank protein, a proline-rich multidomain protein consisting of SH3, PDZ and SAM domains, binds the metabotropic glutamate receptor interacting protein, Homer 1a, at synapses to help link it to the cytoskeleton (Garner, C C et al, 2000). Sans also contains a SAM domain and so could potentially be involved in a structural complex involving harmonin, phosducin and glutamate receptors at retinal synapses, although its individual expression pattern within the retina has not yet been determined. All this would support the hypothesis of a role for the

USH1 proteins in the modulation of retinal ribbon synapse structure and transmission, further supported by the new found interaction of an USH1 protein with phosducin.

Harmonin, phosducin and the USH2 & USH3 proteins

The interaction of harmonin and phosducin would argue a role for harmonin and maybe other Usher proteins in synaptic transmission/control of vesicle release. This is also supported by the proposed roles of the USH2 proteins, which have also been shown to interact with harmonin via PDZ1 (Figure 6.1) and be expressed in the photoreceptor OPL (Figure 6.2) (Reiners, J et al, 2005b). NBC3 has been postulated to interact with PMCA Ca^{2+} -ATPase plasma membrane channels, which are also suggested to complex with PSD-95 (a PDZ domain containing protein), in the photoreceptor synaptic terminals. NBC3 could therefore interact with harmonin indirectly through the PMCA ion channels or directly, using its C terminal PBI. Studies have shown that the function of L-type voltage gated Ca^{2+} channels in the photoreceptor synaptic terminal is very sensitive to changes in pH thus NBC3 could play a role in buffering H^+ loads for these channels (Bok, D et al, 2003 and references therein).

As discussed in section 1.3.3.8, Vlgr1b may act as an extracellular Ca^{2+} sink, as a Ca^{2+} dependent cell adhesion molecule or to monitor intra- and extracellular Ca^{2+} trafficking. Disruption of Ca^{2+} metabolism is known to affect both hearing and vision as has been shown with the *deaf waddler*

mouse, which has mutations in *PMCA2* (note the postulated interaction between PMCA channels and NBC3 discussed above) (Weston, M D et al, 2004). It would be interesting to determine whether the USH2B and USH2C proteins are involved in Ca^{2+} and H^+ ion level regulation for correct photoreceptor synaptic function, and whether their behaviour is influenced by an interaction with harmonin.

The long isoform of usherin has now been localised to the OPL and connecting cilium of the photoreceptors, in addition to the Bruch's membrane where the small isoform is also expressed. It is interesting to note that as well as complexing with harmonin, usherin can form dimmers with *Vlgr1b*. The interaction of these two very large proteins is thought to help stabilise Usher protein complexes formed in the ear and may do so in the retina also. No interactions have been noted between the USH2 proteins and any of the other USH1 proteins aside from harmonin (Reiners, J et al, 2005b).

Clarin-1 shows protein sequence homology to Stargazin: which has been shown to play a key role in the shaping and maintenance of cerebellar synapses. It is also involved in control of expression and mobilisation of particular glutamate receptors in the post-synaptic cleft in cerebellar granular cells, as well as possibly playing a role in forming protein-protein contacts across the synaptic cleft (Chen, L et al, 2000; Ottersen, O P et al, 1998). Although Clarin-1 has been found near both pre- and post- synaptic membranes, it is not clear whether it has a PBI (Adato, A et al, 2002) and the ability to complex with harmonin directly. Instead it may also be involved in

controlling synaptic transmission via the glutamate receptors and Ca^{2+} as has been postulated above for harmonin, phosducin and the USH2 proteins.

In conclusion, the subcellular localisation of the USH1 proteins and putative localisation data on the USH2 proteins reveals co-localisation of all these Usher proteins within the OPL of the retinal photoreceptors (Figure 6.2). It has been postulated that the site of retinal pathology in Usher type 1 patients is in the photoreceptor ribbon synapses, with harmonin acting as a scaffold to organise the proteins at the synapse membranes (Reiners, J et al, 2003). This may also be the site of pathology in Usher types 2 and 3, due to the overlapping protein localisation patterns of all the Usher proteins. In this case the defect may be in control mechanisms of vesicle release rather than structural/organisational (Reiners, J et al, 2005a) as postulated for type 1. However, it is not known whether the USH1, 2 & 3 proteins complex altogether or whether separate USH1 and USH2 complexes are formed, with harmonin being the link within and maybe between these complexes. Yet dysfunction of any of the USH complex proteins would result in synaptic dysfunction causing the retinal phenotype of Usher syndrome. This argument is further supported by the finding of an interaction between harmonin and phosducin, suggesting that the OPL and more specifically the ribbon synapses are the site of Usher pathology within the retina.

REFERENCES

Adato, A., Kalinski, H., Weil, D., Chaib, H., Korostishevsky, M., and Bonne-Tamir, B. (1999) Possible interaction between USH1B and USH3 gene products as implied by apparent digenic deafness inheritance. *Am J Hum Genet.* 65, 261-5.

Adato, A., Lefevre, G., Delprat, B., Michel, V., Michalski, N., Chardenoux, S., Weil, D., El Amraoui, A., and Petit, C. (2005a) Usherin, the defective protein in Usher syndrome type IIA, is likely to be a component of interstereocilia ankle links in the inner ear sensory cells. *Hum.Mol.Genet.*

Adato, A., Michel, V., Kikkawa, Y., Reiners, J., Alagramam, K. N., Weil, D., Yonekawa, H., Wolfrum, U., El Amraoui, A., and Petit, C. (2005b) Interactions in the network of Usher syndrome type 1 proteins. *Hum.Mol.Genet.* 14, 347-356.

Adato, A., Vreugde, S., Joensuu, T., Avidan, N., Hamalainen, R., Belenkiy, O., Olander, T., Bonne-Tamir, B., Ben-Asher, E., Espinos, C., Millan, J. M., Lehesjoki, A. E., Flannery, J. G., Avraham, K. B., Pietrokowski, S., Sankila, E. M., Beckmann, J. S., and Lancet, D. (2002) USH3A transcripts encode clarin-1, a four-transmembrane-domain protein with a possible role in sensory synapses. *Eur J Hum Genet.* 10, 339-50.

Ahmed, Z. M., Riazuddin, S., Ahmad, J., Bernstein, S. L., Guo, Y., Sabar, M. F., Sieving, P., Riazuddin, S., Griffith, A. J., Friedman, T. B., Belyantseva, I. A., and Wilcox, E. R. (2003) PCDH15 is expressed in the neurosensory epithelium of the eye and ear and mutant alleles are responsible for both USH1F and DFNB23. *Hum.Mol.Genet.* 12, 3215-3223.

Ahmed, Z. M., Riazuddin, S., Bernstein, S. L., Ahmed, Z., Khan, S., Griffith, A. J., Morell, R. J., Friedman, T. B., and Wilcox, E. R. (2001) Mutations of the protocadherin gene PCDH15 cause Usher syndrome type 1F. *Am J Hum Genet.* 69, 25-34.

Ahmed, Z. M., Smith, T. N., Riazuddin, S., Makishima, T., Ghosh, M., Bokhari, S., Menon, P. S., Deshmukh, D., Griffith, A. J., Friedman, T. B., and Wilcox, E. R. (2002) Nonsyndromic recessive deafness DFNB18 and Usher syndrome type IC are allelic mutations of USHIC. *Hum Genet.* 110, 527-31.

Alagramam, K. N., Murcia, C. L., Kwon, H. Y., Pawlowski, K. S., Wright, C. G., and Woychik, R. P. (2001a) The mouse Ames waltzer hearing-loss mutant is caused by mutation of Pcdh15, a novel protocadherin gene. *Nat Genet.* 27, 99-102.

Alagramam, K. N., Yuan, H., Kuehn, M. H., Murcia, C. L., Wayne, S., Srisailpathy, C. R., Lowry, R. B., Knaus, R., Van Laer, L., Bernier, F. P., Schwartz, S., Lee, C., Morton, C. C., Mullins, R. F., Ramesh, A., Van Camp, G., Hagemen, G. S., Woychik, R. P., and Smith, R. J. (2001b) Mutations in the novel protocadherin PCDH15 cause Usher syndrome type 1F. *Hum Mol Genet.* 10, 1709-18.

Ara-Iwata, F., Jacobson, S. G., Gass, J. D., Hotta, Y., Fujiki, K., Hayakawa, M., and Inana, G. (1996) Analysis of phosducin as a candidate gene for retinopathies. *Ophthalmic Genet.* 17, 3-14.

Ball, S. L., Bardenstein, D., and Alagramam, K. N. (2003) Assessment of retinal structure and function in Ames waltzer mice. *Invest Ophthalmol Vis Sci.* 44, 3986-3992.

Barrong, S. D., Chaitin, M. H., Fliesler, S. J., Possin, D. E., Jacobson, S. G., and Milam, A. H. (1992) Ultrastructure of connecting cilia in different forms of retinitis pigmentosa. *Arch.Ophthalmol.* 110, 706-710.

Bartel, P., Chien, C. T., Sternglanz, R., and Fields, S. (1993) Elimination of false positives that arise in using the two-hybrid system. *Biotechniques.* 14, 920-924.

Bauer, P. H., Bluml, K., Schroder, S., Hegler, J., Dees, C., and Lohse, M. J. (1998) Interactions of phosducin with the subunits of G-proteins. Binding to the alpha as well as the betagamma subunits. *J.Biol.Chem.*273, 9465-9471.

Began, D. M., Hanke, C., Hood, A. F., Sechrist, K. D., and Moores, W. B. (2001) Plaques on the face of a 26-year-old woman with Usher syndrome. *Arch Dermatol.*137, 219-24.

Berne R.M. and Levy M.N. 1998 *Physiology*. 4th edition Mosby Inc, Missouri

Besharse, J. C., Baker, S. A., Luby-Phelps, K., and Pazour, G. J. (2003) Photoreceptor intersegmental transport and retinal degeneration: a conserved pathway common to motile and sensory cilia. *Adv.Exp.Med.Biol.*533, 157-164.

Bhattacharya, G., Miller, C., Kimberling, W. J., Jablonski, M. M., and Cosgrove, D. (2002) Localization and expression of usherin: a novel basement membrane protein defective in people with Usher's syndrome type Ila. *Hear Res.*163, 1-11.

Bitner-Glindzicz, M., Lindley, K. J., Rutland, P., Blaydon, D., Smith, V. V., Milla, P. J., Hussain, K., Furth-Lavi, J., Cosgrove, K. E., Shepherd, R. M., Barnes, P. D., O'Brien, R. E., Farndon, P. A., Sowden, J., Liu, X. Z., Scanlan, M. J., Malcolm, S., Dunne, M. J., Aynsley-Green, A., and Glaser, B. (2000) A recessive contiguous gene deletion causing infantile hyperinsulinism, enteropathy and deafness identifies the Usher type 1C gene. *Nat Genet.*26, 56-60.

Blaydon, Diana. (2004) PhD thesis: Molecular genetics of usher syndrome type 1C. University College London.

Boeda, B., El-Amraoui, A., Bahloul, A., Goodyear, R., Daviet, L., Blanchard, S., Perfettini, I., Fath, K. R., Shorte, S., Reiners, J., Houdusse, A., Legrain, P., Wolfrum, U., Richardson, G., and Petit, C. (2002) Myosin VIIa, harmonin and cadherin 23, three Usher I gene products that cooperate to shape the sensory hair cell bundle. *Embo J.*21, 6689-99.

Bok, D., Galbraith, G., Lopez, I., Woodruff, M., Nusinowitz, S., BeltrandelRio, H., Huang, W., Zhao, S., Geske, R., Montgomery, C., Van, Sligtenhorst, I., Friddle, C., Platt, K., Sparks, M. J., Pushkin, A., Abuladze, N., Ishiyama, A., Dukkipati, R., Liu, W., and Kurtz, I. (2003) Blindness and auditory impairment caused by loss of the sodium bicarbonate cotransporter NBC3. *Nat.Genet.*34, 313-319.

Bolz, H., Bolz, S. S., Schade, G., Kothe, C., Mohrmann, G., Hess, M., and Gal, A. (2004) Impaired calmodulin binding of myosin-7A causes autosomal dominant hearing loss (DFNA11). *Hum.Mutat.*24, 274-275.

Bolz, H., Reiners, J., Wolfrum, U., and Gal, A. (2002) Role of cadherins in Ca²⁺-mediated cell adhesion and inherited photoreceptor degeneration. *Adv.Exp.Med.Biol.*514, 399-410.

Bolz, H., von Brederlow, B., Ramirez, A., Bryda, E. C., Kutsche, K., Nothwang, H. G., Seeliger, M., del, C. Salcedo Cabrera M., Vila, M. C., Molina, O. P., Gal, A., and Kubisch, C. (2001) Mutation of CDH23, encoding a new member of the cadherin gene family, causes Usher syndrome type 1D. *Nat Genet.*27, 108-12.

Bonneau, D., Raymond, F., Kremer, C., Klossek, J. M., Kaplan, J., and Patte, F. (1993) Usher syndrome type I associated with bronchiectasis and immotile nasal cilia in two brothers. *J.Med.Genet.*30, 253-254.

Bork, J. M., Peters, L. M., Riazuddin, S., Bernstein, S. L., Ahmed, Z. M., Ness, S. L., Polomeno, R., Ramesh, A., Schloss, M., Srisailpathy, C. R., Wayne, S., Bellman, S., Desmukh, D., Ahmed, Z., Khan, S. N., Kaloustian, V. M., Li, X. C., Lalwani, A., Bitner-Glindzicz, M., Nance, W. E., Liu, X. Z., Wistow, G., Smith, R. J., Griffith, A. J., Wilcox, E. R., Friedman, T. B., and Morell, R. J. (2001) Usher syndrome 1D and nonsyndromic autosomal

recessive deafness DFNB12 are caused by allelic mutations of the novel cadherin-like gene CDH23. *Am J Hum Genet.*68, 26-37.

Boughman, J. A., Conneally, P. M., and Nance, W. E. (1980) Population genetic studies of retinitis pigmentosa. *Am.J.Hum.Genet.*32, 223-235.

Boughman, J. A., Vernon, M., and Shaver, K. A. (1983) Usher syndrome: definition and estimate of prevalence from two high-risk populations. *J.Chronic.Dis.*36, 595-603.

Bowes, C., van Veen, T., and Farber, D. B. (1988) Opsin, G-protein and 48-kDa protein in normal and rd mouse retinas: developmental expression of mRNAs and proteins and light/dark cycling of mRNAs. *Exp.Eye Res.*47, 369-390.

Bustin, S. A. (2000) Absolute quantification of mRNA using real-time reverse transcription polymerase chain reaction assays. *J.Mol.Endocrinol.*25, 169-193.

Chaib, H., Kaplan, J., Gerber, S., Vincent, C., Ayadi, H., Slim, R., Munnich, A., Weissenbach, J., and Petit, C. (1997) A newly identified locus for Usher syndrome type I, USH1E, maps to chromosome 21q21. *Hum Mol Genet.*6, 27-31.

Chen, J., Simon, M. I., Matthes, M. T., Yasumura, D., and LaVail, M. M. (1999) Increased susceptibility to light damage in an arrestin knockout mouse model of Oguchi disease (stationary night blindness). *Invest Ophthalmol.Vis.Sci.*40, 2978-2982.

Chen, J., Yoshida, T., Nakano, K., and Bitensky, M. W. (2005) Subcellular localization of phosducin in rod photoreceptors. *Vis.Neurosci.*22, 19-25.

Chen, L., Chetkovich, D. M., Petralia, R. S., Sweeney, N. T., Kawasaki, Y., Wenthold, R. J., Bredt, D. S., and Nicoll, R. A. (2000) Stargazin regulates synaptic targeting of AMPA receptors by two distinct mechanisms. *Nature.*408, 936-943.

Di Palma, F., Holme, R. H., Bryda, E. C., Belyantseva, I. A., Pellegrino, R., Kachar, B., Steel, K. P., and Noben-Trauth, K. (2001) Mutations in Cdh23, encoding a new type of cadherin, cause stereocilia disorganization in waltzer, the mouse model for Usher syndrome type 1D. *Nat Genet.*27, 103-7.

Dryja, T. P. (2001) Retinitis Pigmentosa and Stationary Night Blindness. 5903-5933.

El-Amraoui, A., Sahly, I., Picaud, S., Sahel, J., Abitbol, M., and Petit, C. (1996) Human Usher 1B/mouse shaker-1: the retinal phenotype discrepancy explained by the presence/absence of myosin VIIA in the photoreceptor cells. *Hum Mol Genet.*5, 1171-8.

Eudy, J. D., Weston, M. D., Yao, S., Hoover, D. M., Rehm, H. L., Ma-Edmonds, M., Yan, D., Ahmad, I., Cheng, J. J., Ayuso, C., Cremers, C., Davenport, S., Moller, C., Talmadge, C. B., Beisel, K. W., Tamayo, M., Morton, C. C., Swaroop, A., Kimberling, W. J., and Sumegi, J. (1998a) Mutation of a gene encoding a protein with extracellular matrix motifs in Usher syndrome type Ila. *Science.*280, 1753-7.

Eudy, J. D., Yao, S., Weston, M. D., Ma-Edmonds, M., Talmadge, C. B., Cheng, J. J., Kimberling, W. J., and Sumegi, J. (1998b) Isolation of a gene encoding a novel member of the nuclear receptor superfamily from the critical region of Usher syndrome type Ila at 1q41. *Genomics.*50, 382-4.

Fields, R. R., Zhou, G., Huang, D., Davis, J. R., Moller, C., Jacobson, S. G., Kimberling, W. J., and Sumegi, J. (2002) Usher Syndrome Type III: Revised Genomic Structure of the USH3 Gene and Identification of Novel Mutations. *Am J Hum Genet.*71, 607-17.

Fiore, Mariano, Mancini, Robert, and De Robertis, Eduardo. 1974 *Atlas of Histology.* 3rd edition. Lea and Febiger, Philadelphia

Frank, M. and Kemler, R. (2002) Protocadherins. *Curr.Opin.Cell Biol.*14, 557-562.

Friedman, T., Battey, J., Kachar, B., Riazuddin, S., Noben-Trauth, K., Griffith, A., and Wilcox, E. (2000) Modifier genes of hereditary hearing loss. *Curr Opin Neurobiol.*10, 487-93.

Garner, C. C., Nash, J., and Huganir, R. L. (2000) PDZ domains in synapse assembly and signalling. *Trends Cell Biol.*10, 274-280.

Geller, S. F., Isosomppi, J., Makela, H., Sankila, E. M., Johnson, P. T., and Flannery, J. G. 2004 Vision loss in Usher syndrome type III is caused by mutations in Clarin-1, an inner retinal protein

Gibson, F., Walsh, J., Mburu, P., Varela, A., Brown, K. A., Antonio, M., Beisel, K. W., Steel, K. P., and Brown, S. D. (1995) A type VII myosin encoded by the mouse deafness gene shaker-1. *Nature.*374, 62-4.

Gilbert, P. 2000 A-Z of syndromes and Inherited Disorders. 3rd edition Stanley Thorne, UK

Glowatzki, E. and Fuchs, P. A. (2002) Transmitter release at the hair cell ribbon synapse. *Nat.Neurosci.*5, 147-154.

Gorlin, R. J., Tilsner, T. J., Feinstein, S., and Duvall, A. J., III. (1979) Usher's syndrome type III. *Arch.Otolaryngol.*105, 353-354.

Grun, G. (1982) The development of the vertebrate retina: a comparative survey. *Adv.Anat.Embryol.Cell Biol.*78, 1-85.

Harris, B. Z., Hillier, B. J., and Lim, W. A. (2001a) Energetic determinants of internal motif recognition by PDZ domains. *Biochemistry.*40, 5921-30.

Harris, B. Z. and Lim, W. A. (2001b) Mechanism and role of PDZ domains in signaling complex assembly. *J Cell Sci.*114, 3219-31.

Hasson, T., Heintzelman, M. B., Santos-Sacchi, J., Corey, D. P., and Mooseker, M. S. (1995) Expression in cochlea and retina of myosin VIIa, the gene product defective in Usher syndrome type 1B. *Proc Natl Acad Sci U S A.*92, 9815-9.

Hirai, A., Tada, M., Furuuchi, K., Ishikawa, S., Makiyama, K., Hamada, J., Okada, F., Kobayashi, I., Fukuda, H., and Moriuchi, T. (2004) Expression of AIE-75 PDZ-domain protein induces G2/M cell cycle arrest in human colorectal adenocarcinoma SW480 cells. *Cancer Lett.*211, 209-218.

Hope, C. I., Bunney, S., Proops, D., and Fielder, A. R. (1997) Usher syndrome in the city of Birmingham--prevalence and clinical classification. *Br.J.Ophthalmol.*81, 46-53.

Huber, A. (2001) Scaffolding proteins organize multimolecular protein complexes for sensory signal transduction. *Eur.J.Neurosci.*14, 769-776.

Humphries, P., Kenna, P., and Farrar, G. J. (1992) On the molecular genetics of retinitis pigmentosa. *Science.*256, 804-8.

Hung, A. Y. and Sheng, M. (2002) PDZ domains: structural modules for protein complex assembly. *J Biol Chem.*277, 5699-702.

Hunter, D. G., Fishman, G. A., Mehta, R. S., and Kretzer, F. L. (1986) Abnormal sperm and photoreceptor axonemes in Usher's syndrome. *Arch.Ophthalmol.*104, 385-389.

Ishikawa, S., Kobayashi, I., Hamada, J., Tada, M., Hirai, A., Furuuchi, K., Takahashi, Y., Ba, Y., and Moriuchi, T. (2001) Interaction of MCC2, a novel homologue of MCC tumor suppressor, with PDZ-domain Protein AIE-75. *Gene.*267, 101-10.

Jeon, C. J., Pyun, J. K., and Yang, H. W. (1998) Calretinin and calbindin D28K immunoreactivity in the superficial layers of the rabbit superior colliculus. *Neuroreport*.9, 3847-3852.

Joensuu, T., Hamalainen, R., Yuan, B., Johnson, C., Tegelberg, S., Gasparini, P., Zelante, L., Pivola, U., Pakarinen, L., Lehesjoki, A. E., de la Chapelle, A., and Sankila, E. M. (2001) Mutations in a novel gene with transmembrane domains underlie Usher syndrome type 3. *Am J Hum Genet*.69, 673-84.

Johnson, K. R., Gagnon, L. H., Webb, L. S., Peters, L. L., Hawes, N. L., Chang, B., and Zheng, Q. Y. (2003) Mouse models of USH1C and DFNB18: phenotypic and molecular analyses of two new spontaneous mutations of the Ush1c gene. *Hum.Mol.Genet*.12, 3075-3086.

Johnson, K. R., Zheng, Q. Y., Weston, M. D., Ptacek, L. J., and Noben-Trauth, K. (2005) The Mass1frings mutation underlies early onset hearing impairment in BUB/BnJ mice, a model for the auditory pathology of Usher syndrome IIC. *Genomics*.85, 582-590.

Johnson, P. T., Williams, R. R., and Reese, B. E. (2001) Developmental patterns of protein expression in photoreceptors implicate distinct environmental versus cell-intrinsic mechanisms. *Vis.Neurosci*.18, 157-168.

Johnston, A. M., Naselli, G., Niwa, H., Brodnicki, T., Harrison, L. C., and Gomez, L. J. (2004) Harp (harmonin-interacting, ankyrin repeat-containing protein), a novel protein that interacts with harmonin in epithelial tissues. *Genes Cells*.9, 967-982.

Kaplan, J., Gerber, S., Bonneau, D., Rozet, J. M., Delrieu, O., Briard, M. L., Dollfus, H., Ghazi, I., Dufier, J. L., Frezal, J., and et al. (1992) A gene for Usher syndrome type I (USH1A) maps to chromosome 14q. *Genomics*.14, 979-87.

Keats, B. J. and Corey, D. P. (1999) The Usher Syndromes. *American Journal of Medical Genetics*.89, 158-166.

Kikkawa, Y., Shitara, H., Wakana, S., Kohara, Y., Takada, T., Okamoto, M., Taya, C., Kamiya, K., Yoshikawa, Y., Tokano, H., Kitamura, K., Shimizu, K., Wakabayashi, Y., Shiroishi, T., Kominami, R., and Yonekawa, H. (2003) Mutations in a new scaffold protein Sans cause deafness in Jackson shaker mice. *Hum Mol Genet*.12, 453-461.

Kimberling, W. J., Moller, C. G., Davenport, S., Priluck, I. A., Beighton, P. H., Greenberg, J., Reardon, W., Weston, M. D., Kenyon, J. B., Grunkemeyer, J. A., and et al. (1992) Linkage of Usher syndrome type I gene (USH1B) to the long arm of chromosome 11. *Genomics*.14, 988-94.

Kobayashi, I., Imamura, K., Kubota, M., Ishikawa, S., Yamada, M., Tonoki, H., Okano, M., Storch, W. B., Moriuchi, T., Sakiyama, Y., and Kobayashi, K. (1999) Identification of an autoimmune enteropathy-related 75-kilodalton antigen. *Gastroenterology*.117, 823-30.

Koulen, P., Kuhn, R., Wassle, H., and Brandstatter, J. H. (1999) Modulation of the intracellular calcium concentration in photoreceptor terminals by a presynaptic metabotropic glutamate receptor. *Proc.Natl.Acad.Sci.U.S.A*.96, 9909-9914.

Kros, C. J., Marcotti, W., van Netten, S. M., Self, T. J., Libby, R. T., Brown, S. D., Richardson, G. P., and Steel, K. P. (2002) Reduced climbing and increased slipping adaptation in cochlear hair cells of mice with Myo7a mutations. *Nat Neurosci*.5, 41-47.

Lagziel, A., Ahmed, Z. M., Schultz, J. M., Morell, R. J., Belyantseva, I. A., and Friedman, T. B. (2005) Spatiotemporal pattern and isoforms of cadherin 23 in wild type and waltzer mice during inner ear hair cell development. *Dev.Biol*.280, 295-306.

Larsen, William J. 17-7-2001 Human Embryology. 3rd edition. Churchill Livingstone,

Lee, B. Y., Thulin, C. D., and Willardson, B. M. (2004) Site-specific phosphorylation of phosducin in intact retina. Dynamics of phosphorylation and effects on G protein beta gamma dimer binding. *J.Biol.Chem.*279, 54008-54017.

Li, B. and Fields, S. (1993) Identification of mutations in p53 that affect its binding to SV40 large T antigen by using the yeast two-hybrid system. *FASEB J.*7, 957-963.

Libby, R. T., Kitamoto, J., Holme, R. H., Williams, D. S., and Steel, K. P. (2003) Cdh23 mutations in the mouse are associated with retinal dysfunction but not retinal degeneration. *Exp.Eye Res.*77, 731-739.

Libby, R. T., Lillo, C., Kitamoto, J., Williams, D. S., and Steel, K. P. (2004) Myosin Va is required for normal photoreceptor synaptic activity. *J.Cell Sci.*117, 4509-4515.

Libby, R. T. and Steel, K. P. (2001) Electoretinographic anomalies in mice with mutations in Myo7a, the gene involved in human Usher syndrome type 1B. *Invest Ophthalmol Vis Sci.*42, 770-8.

Liu, X., Ondek, B., and Williams, D. S. (1998) Mutant myosin VIIa causes defective melanosome distribution in the RPE of shaker-1 mice. *Nat Genet.*19, 117-8.

Liu, X., Udovichenko, I. P., Brown, S. D., Steel, K. P., and Williams, D. S. (1999) Myosin VIIa participates in opsin transport through the photoreceptor cilium. *J Neurosci.*19, 6267-74.

Liu, X., Vasant, G., Udovichenko, I. P., Wolfrum, U., and Williams, D. S. (1997) Myosin VIIa, the product of the Usher 1B syndrome gene, is concentrated in the connecting cilia of photoreceptor cells. *Cell Motil Cytoskeleton.*37, 240-52.

Lopez, P., Yaman, R., Lopez-Fernandez, L. A., Vidal, F., Puel, D., Clertant, P., Cuzin, F., and Rassoulzadegan, M. (2003) A novel germ line-specific gene of the phosducin-like protein (PhLP) family. A meiotic function conserved from yeast to mice. *J.Biol.Chem.*278, 1751-1757.

Marenholz, I., Zirra, M., Fischer, D. F., Backendorf, C., Ziegler, A., and Mischke, D. (2001) Identification of human epidermal differentiation complex (EDC)-encoded genes by subtractive hybridization of entire YACs to a gridded keratinocyte cDNA library. *Genome Res.*11, 341-355.

Marietta, J., Walters, K. S., Burgess, R., Ni, L., Fukushima, K., Moore, K. C., Hejtmancik, J. F., and Smith, R. J. (1997) Usher's syndrome type IC: clinical studies and fine-mapping the disease locus. *Ann.Otol.Rhinol.Laryngol.*106, 123-128.

Martini, Alessandro, Read, Andrew, and Stephens, Dafydd. 1996 Genetics and hearing impairment . 1st edition Whurr Publishers Ltd, London, England

Maubaret, C., Griffoin, J. M., Arnaud, B., and Hamel, C. (2005) Novel mutations in MYO7A and USH2A in Usher syndrome. *Ophthalmic Genet.*26, 25-29.

Maude, M. B., Anderson, E. O., and Anderson, R. E. (1998) Polyunsaturated fatty acids are lower in blood lipids of Usher's type I but not Usher's type II. *Invest Ophthalmol Vis Sci.*39, 2164-6.

McMillan, D. R., Kayes-Wandover, K. M., Richardson, J. A., and White, P. C. (2002) Very large G protein-coupled receptor-1, the largest known cell surface protein, is highly expressed in the developing central nervous system. *J.Biol.Chem.*277, 785-792.

McMillan, D. R. and White, P. C. (2004) Loss of the transmembrane and cytoplasmic domains of the very large G-protein-coupled receptor-1 (VLGR1 or Mass1) causes audiogenic seizures in mice. *Mol.Cell Neurosci.*26, 322-329.

Mustapha, M., Chouery, E., Torchard-Pagnez, D., Nouaille, S., Khrais, A., Sayegh, F., Megarbane, A., Loiselet, J., Lathrop, M., Petit, C., and Weil, D. (2002) A novel locus for Usher syndrome type 1, USH1G, maps to chromosome 17q24-25. *Human Genetics*.110, 348-350.

Nakano, K., Chen, J., Tarr, G. E., Yoshida, T., Flynn, J. M., and Bitensky, M. W. (2001) Rethinking the role of phosducin: light-regulated binding of phosducin to 14-3-3 in rod inner segments. *Proc.Natl.Acad.Sci.U.S.A.*98, 4693-4698.

Ness, S. L., Ben Yosef, T., Bar-Lev, A., Madeo, A. C., Brewer, C. C., Avraham, K. B., Kornreich, R., Desnick, R. J., Willner, J. P., Friedman, T. B., and Griffith, A. J. (2003) Genetic homogeneity and phenotypic variability among Ashkenazi Jews with Usher syndrome type III. *J.Med.Genet.*40, 767-772.

Nishiguchi, K. M., Berson, E. L., and Dryja, T. P. (2004a) Mutation screening of the phosducin gene PDC in patients with retinitis pigmentosa and allied diseases. *Mol.Vis.*10, 62-64.

Nishiguchi, K. M., Sandberg, M. A., Kooijman, A. C., Martemyanov, K. A., Pott, J. W., Hagstrom, S. A., Arshavsky, V. Y., Berson, E. L., and Dryja, T. P. (2004b) Defects in RGS9 or its anchor protein R9AP in patients with slow photoreceptor deactivation. *Nature*.427, 75-78.

Oberwinkler, J. (2002) Calcium homeostasis in fly photoreceptor cells. *Adv.Exp.Med.Biol.*514, 539-583.

Ottersen, O. P., Takumi, Y., Matsubara, A., Landsend, A. S., Laake, J. H., and Usami, S. (1998) Molecular organization of a type of peripheral glutamate synapse: the afferent synapses of hair cells in the inner ear. *Prog.Neurobiol.*54, 127-148.

Otterstedde, C. R., Spandau, U., Blankenagel, A., Kimberling, W. J., and Reisser, C. (2001) A new clinical classification for Usher's syndrome based on a new subtype of Usher's syndrome type I. *Laryngoscope*.111, 84-6.

Ouyang, X. M., Xia, X. J., Verpy, E., Du, L. L., Pandya, A., Petit, C., Balkany, T., Nance, W. E., and Liu, X. Z. (2002) Mutations in the alternatively spliced exons of USH1C cause non-syndromic recessive deafness. *Hum Genet.*111, 26-30.

Petit, C. (2001) USHER SYNDROME: From Genetics to Pathogenesis. *Annu Rev Genomics Hum Genet.*2, 271-97.

Petit, C., Levilliers, J., and Hardelin, J. P. (2001) Molecular genetics of hearing loss. *Annu Rev Genet.*35, 589-645.

Pieke-Dahl, S., Moller, C. G., Kelley, P. M., Astuto, L. M., Cremers, C. W., Gorin, M. B., and Kimberling, W. J. (2000) Genetic heterogeneity of Usher syndrome type II: localisation to chromosome 5q. *J Med Genet.*37, 256-62.

Plantinga, R. F., Kleemola, L., Huygen, P. L., Joensuu, T., Sankila, E. M., Pennings, R. J., and Cremers, C. W. (2005) Serial audiometry and speech recognition findings in Finnish Usher syndrome type III patients. *Audiol.Neurotol.*10, 79-89.

Pushkin, A., Abuladze, N., Lee, I., Newman, D., Hwang, J., and Kurtz, I. (1999) Cloning, tissue distribution, genomic organization, and functional characterization of NBC3, a new member of the sodium bicarbonate cotransporter family. *J.Biol.Chem.*274, 16569-16575.

Rattner, A., Sun, H., and Nathans, J. (1999) Molecular genetics of human retinal disease. *Annu Rev Genet.*33, 89-131.

Redowicz, M. J. (2002) Myosins and pathology: genetics and biology. *Acta Biochim.Pol.*49, 789-804.

Reiners, J., Marker, T., Jurgens, K., Reidel, B., and Wolfrum, U. (2005a) Photoreceptor expression of the Usher syndrome type 1 protein protocadherin 15 (USH1F) and its interaction with the scaffold protein harmonin (USH1C). *Mol.Vis.*11, 347-355.

Reiners, J., Reidel, B., El Amraoui, A., Boeda, B., Huber, I., Petit, C., and Wolfrum, U. (2003) Differential distribution of harmonin isoforms and their possible role in Usher-1 protein complexes in mammalian photoreceptor cells. *Invest Ophthalmol Vis Sci.*44, 5006-5015.

Reiners, J., Van Wijk, E., Marker, T., Zimmermann, U., Jurgens, K., Te, Brinke H., Overlack, N., Roepman, R., Knipper, M., Kremer, H., and Wolfrum, U. (2005b) The scaffold protein harmonin (USH1C) provides molecular links between Usher syndrome type 1 and type 2. *Hum.Mol.Genet.*

Resendes, B. L., Williamson, R. E., and Morton, C. C. (2001) At the speed of sound: gene discovery in the auditory system. *Am J Hum Genet.*69, 923-35.

Roitt, I., Brostoff, J., and Male, D. 2001 Immunology. 6th edition

Sahly, I., El-Amraoui, A., Abitbol, M., Petit, C., and Dufier, J. L. (1997) Expression of myosin VIIA during mouse embryogenesis. *Anat Embryol (Berl).*196, 159-70.

Sambrook, J., Fritsch, E. F., and Maniatis, T. 1989 Molecular Cloning - A Laboratory Manual. 2nd edition Cold Spring Harbor Laboratory Press, USA

Saouda, M., Mansour, A., Bou Moglabey, Y., el Zir, E., Mustapha, M., Chaib, H., Nehme, A., Megarbane, A., Loiselet, J., Petit, C., and Slim, R. (1998) The Usher syndrome in the Lebanese population and further refinement of the USH2A candidate region. *Hum Genet.*103, 193-8.

Scanlan, M. J., Williamson, B., Jungbluth, A., Stockert, E., Arden, K. C., Viars, C. S., Gure, A. O., Gordan, J. D., Chen, Y. T., and Old, L. J. (1999) Isoforms of the human PDZ-73 protein exhibit differential tissue expression. *Biochim Biophys Acta.*1445, 39-52.

Schulz, R. (2001) The pharmacology of phosducin. *Pharmacol.Res.*43, 1-10.

Schwartz, E. A., Leonard, M. L., Bizios, R., and Bowser, S. S. (1997) Analysis and modeling of the primary cilium bending response to fluid shear. *Am.J.Physiol.*272, F132-F138.

Schwartz, S. B., Aleman, T. S., Cideciyan, A. V., Windsor, E. A., Sumaroka, A., Roman, A. J., Rane, T., Smilko, E. E., Bennett, J., Stone, E. M., Kimberling, W. J., Liu, X. Z., and Jacobson, S. G. (2005) Disease expression in Usher syndrome caused by VLGR1 gene mutation (USH2C) and comparison with USH2A phenotype. *Invest Ophthalmol Vis Sci.*46, 734-743.

Seeliger, M. W., Zrenner, E., Apfelstedt-Sylla, E., and Jaissle, G. B. (2001) Identification of Usher syndrome subtypes by ERG implicit time. *Invest Ophthalmol Vis Sci.*42, 3066-71.

Seiler, C., Finger-Baier, K. C., Rinner, O., Makhankov, Y. V., Schwarz, H., Neuhauss, S. C., and Nicolson, T. (2005) Duplicated genes with split functions: independent roles of protocadherin15 orthologues in zebrafish hearing and vision. *Development.*132, 615-623.

Self, T., Mahony, M., Fleming, J., Walsh, J., Brown, S. D., and Steel, K. P. (1998) Shaker-1 mutations reveal roles for myosin VIIA in both development and function of cochlear hair cells. *Development.*125, 557-66.

Seyedahmadi, B. J., Rivolta, C., Keene, J. A., Berson, E. L., and Dryja, T. P. (2004) Comprehensive screening of the USH2A gene in Usher syndrome type II and non-syndromic recessive retinitis pigmentosa. *Exp.Eye Res.*79, 167-173.

Sharma, R. K., O'Leary, T. E., Fields, C. M., and Johnson, D. A. (2003) Development of the outer retina in the mouse. *Brain Res.Dev.Brain Res.*145, 93-105.

Sheng, M. and Sala, C. (2001) PDZ domains and the organization of supramolecular complexes. *Annu Rev Neurosci.*24, 1-29.

Siemens, J., Kazmierczak, P., Reynolds, A., Sticker, M., Littlewood-Evans, A., and Muller, U. (2002) The Usher syndrome proteins cadherin 23 and harmonin form a complex by means of PDZ-domain interactions. *Proc Natl Acad Sci U S A.*29, 29-

Siemens, J., Lillo, C., Dumont, R. A., Reynolds, A., Williams, D. S., Gillespie, P. G., and Muller, U. (2004) Cadherin 23 is a component of the tip link in hair-cell stereocilia. *Nature.*428, 950-955.

Smith, R. J., Berlin, C. I., Hejtmancik, J. F., Keats, B. J., Kimberling, W. J., Lewis, R. A., Moller, C. G., Pelias, M. Z., and Tranebjaerg, L. (1994) Clinical diagnosis of the Usher syndromes. Usher Syndrome Consortium. *Am.J.Med.Genet.*50, 32-38.

Smith, R. J., Lee, E. C., Kimberling, W. J., Daiger, S. P., Pelias, M. Z., Keats, B. J., Jay, M., Bird, A., Reardon, W., Guest, M., and et al. (1992) Localization of two genes for Usher syndrome type I to chromosome 11. *Genomics.*14, 995-1002.

Smits, B. M., Peters, T. A., Mul, J. D., Croes, H. J., Fransen, J. A., Beynon, A. J., Guryev, V., Plasterk, R. H., and Cuppen, E. (2005) Identification of a rat model for Usher syndrome type 1B by ENU mutagenesis-driven forward genetics. *Genetics.*

Sokolov, M., Strissel, K. J., Leskov, I. B., Michaud, N. A., Govardovskii, V. I., and Arshavsky, V. Y. (2004) Phosducin facilitates light-driven transducin translocation in rod photoreceptors. Evidence from the phosducin knockout mouse. *J.Biol.Chem.*279, 19149-19156.

Sterling, P. and Matthews, G. (2005) Structure and function of ribbon synapses. *Trends Neurosci.*28, 20-29.

Strachan, T and Read, AP. 1999 Human Molecular Genetics 2. 2nd edition. BIOS Scientific Publishers Ltd, Oxford, UK

Sun, W., Seigel, G. M., and Salvi, R. J. (2002) Retinal precursor cells express functional ionotropic glutamate and GABA receptors. *Neuroreport.*13, 2421-2424.

Tai, A. W., Chuang, J. Z., Bode, C., Wolfrum, U., and Sung, C. H. (1999) Rhodopsin's carboxy-terminal cytoplasmic tail acts as a membrane receptor for cytoplasmic dynein by binding to the dynein light chain Tctex-1. *Cell.*97, 877-887.

Takasaki, K., Balaban, C. D., and Sando, I. (2000) Histopathologic findings of the inner ears with Alport, Usher and Waardenburg syndromes. *Adv.Otorhinolaryngol.*56, 218-232.

Thulin, C. D., Savage, J. R., McLaughlin, J. N., Truscott, S. M., Old, W. M., Ahn, N. G., Resing, K. A., Hamm, H. E., Bitensky, M. W., and Willardson, B. M. (2001) Modulation of the G protein regulator phosducin by Ca2+/calmodulin-dependent protein kinase II phosphorylation and 14-3-3 protein binding. *J.Biol.Chem.*276, 23805-23815.

Toby, G. G. and Golemis, E. A. (2001) Using the yeast interaction trap and other two-hybrid-based approaches to study protein-protein interactions. *Methods.*24, 201-17.

Todi, S. V., Franke, J. D., Kiehart, D. P., and Eberl, D. F. (2005) Myosin VIIA defects, which underlie the Usher 1B syndrome in humans, lead to deafness in *Drosophila*. *Curr.Biol.*15, 862-868.

Traboulsi, Elias. I. 1999 *Genetic Disease of the Eye*. 1st edition. Oxford University Press Inc, USA

Usher CH. (1914) On the inheritance of retinitis pigmentosa, with notes of cases. *R.Lond.Ophthalmol.Hosp.Rep.*19, 130-236.

Van Wijk, E., Pennings, R. J., Te, Brinke H., Claassen, A., Yntema, H. G., Hoefsloot, L. H., Cremers, F. P., Cremers, C. W., and Kremer, H. (2004) Identification of 51 Novel Exons of the Usher Syndrome Type 2A (USH2A) Gene That Encode Multiple Conserved Functional Domains and That Are Mutated in Patients with Usher Syndrome Type II. *Am.J.Hum.Genet.*74,

Vernon, M. (1969) Usher's syndrome--deafness and progressive blindness. Clinical cases, prevention, theory and literature survey. *J.Chronic.Dis.*22, 133-151.

Verpy, E., Leibovici, M., Zwaenepoel, I., Liu, X. Z., Gal, A., Salem, N., Mansour, A., Blanchard, S., Kobayashi, I., Keats, B. J., Slim, R., and Petit, C. (2000) A defect in harmonin, a PDZ domain-containing protein expressed in the inner ear sensory hair cells, underlies Usher syndrome type 1C. *Nat Genet.*26, 51-5.

Weil, D., El-Amraoui, A., Masmoudi, S., Mustapha, M., Kikkawa, Y., Laine, S., Delmaghani, S., Adato, A., Nadifi, S., Zina, Z. B., Hamel, C., Gal, A., Ayadi, H., Yonekawa, H., and Petit, C. (2003) Usher syndrome type I G (USH1G) is caused by mutations in the gene encoding SANS, a protein that associates with the USH1C protein, harmonin. *Hum Mol Genet.*12, 463-471.

Weil, D., Kussel, P., Blanchard, S., Levy, G., Levi-Acobas, F., Drira, M., Ayadi, H., and Petit, C. (1997) The autosomal recessive isolated deafness, DFNB2, and the Usher 1B syndrome are allelic defects of the myosin-VIIA gene. *Nat Genet.*16, 191-3.

Weil, D., Levy, G., Sahly, I., Levi-Acobas, F., Blanchard, S., El-Amraoui, A., Crozet, F., Philippe, H., Abitbol, M., and Petit, C. (1996) Human myosin VIIA responsible for the Usher 1B syndrome: a predicted membrane-associated motor protein expressed in developing sensory epithelia. *Proc Natl Acad Sci U S A.*93, 3232-7.

Weston, M. D., Eudy, J. D., Fujita, S., Yao, S., Usami, S., Cremers, C., Greenberg, J., Ramesar, R., Martini, A., Moller, C., Smith, R. J., Sumegi, J., Kimberling, W. J., and Greenburg, J. (2000) Genomic structure and identification of novel mutations in usherin, the gene responsible for Usher syndrome type Ila. *Am J Hum Genet.*66, 1199-210.

Weston, M. D., Luijendijk, M. W., Humphrey, K. D., Moller, C., and Kimberling, W. J. (2004) Mutations in the VLGR1 gene implicate G-protein signaling in the pathogenesis of Usher syndrome type II. *Am.J.Hum.Genet.*74, 357-366.

Willems, P. J. (2000) Genetic causes of hearing loss. *N Engl J Med.*342, 1101-1109.

Williams, D. S. and Gibbs, D. (2004) Usher 1 Protein Complexes in the Retina (e-letter <http://intl.iovs.org/cgi/eletters/44/11/5006>). *Invest Ophthalmol Vis Sci.*

Wistow, G., Bernstein, S. L., Wyatt, M. K., Ray, S., Behal, A., Touchman, J. W., Bouffard, G., Smith, D., and Peterson, K. (2002) Expressed sequence tag analysis of human retina for the NEIBank Project: retbindin, an abundant, novel retinal cDNA and alternative splicing of other retina-preferred gene transcripts. *Mol Vis.*8, 196-204.

Wolfrum, U., Liu, X., Schmitt, A., Udovichenko, I. P., and Williams, D. S. (1998) Myosin VIIa as a common component of cilia and microvilli. *Cell Motil Cytoskeleton.*40, 261-71.

Wolfrum, U. and Reiners, J. (2004) Myosin VIIa in Photoreceptor Cell Synapses May Contribute to an Usher 1 Protein Complex in the Retina (e-letter <http://intl.iovs.org/cgi/eletters/44/11/5006>). *Invest Ophthalmol Vis Sci.*

Wolfrum, U. and Schmitt, A. (2000) Rhodopsin transport in the membrane of the connecting cilium of mammalian photoreceptor cells. *Cell Motil Cytoskeleton.*46, 95-107.

Yagi, H., Takamura, Y., Yoneda, T., Konno, D., Akagi, Y., Yoshida, K., and Sato, M. (2005) Vlgr1 knockout mice show audiogenic seizure susceptibility. *J.Neurochem.*92, 191-202.

Zhang, Q., Acland, G. M., Parshall, C. J., Haskell, J., Ray, K., and Aguirre, G. D. (1998) Characterization of canine photoreceptor phosducin cDNA and identification of a sequence variant in dogs with photoreceptor dysplasia. *Gene.*215, 231-239.

Zhang, Q. H., Ye, M., Wu, X. Y., Ren, S. X., Zhao, M., Zhao, C. J., Fu, G., Shen, Y., Fan, H. Y., Lu, G., Zhong, M., Xu, X. R., Han, Z. G., Zhang, J. W., Tao, J., Huang, Q. H., Zhou, J., Hu, G. X., Gu, J., Chen, S. J., and Chen, Z. (2000) Cloning and functional analysis of cDNAs with open reading frames for 300 previously undefined genes expressed in CD34+ hematopoietic stem/progenitor cells. *Genome Res.*10, 1546-1560.

Zheng, Q. Y., Yan, D., Ouyang, X. M., Du, L. L., Yu, H., Chang, B., Johnson, K. R., and Liu, X. Z. (2005) Digenic inheritance of deafness caused by mutations in genes encoding cadherin 23 and protocadherin 15 in mice and humans. *Hum.Mol.Genet.*14, 103-111.

Zhu, X. and Craft, C. M. (1998) Interaction of phosducin and phosducin isoforms with a 26S proteasomal subunit, SUG1. *Mol.Vis.*4, 13-

Zhu, X. and Craft, C. M. (2000) The carboxyl terminal domain of phosducin functions as a transcriptional activator. *Biochem.Biophys.Res.Commun.*270, 504-509.

APPENDICES

Appendix 1 Suppliers

Chemicals were obtained from the following suppliers. Those not listed here but discussed in this work were of reagent grade from Sigma.

Name of company	Reagent
AB gene	Plate sealers
	96-well PCR plates
Agar Scientific	LR gold
Amersham Pharmacia Biotech	Hybond ECL nitrocellulose membrane
	ET terminator sequencing kit
Amresco	5xTBE
Athene	200nm nickel mesh grids
BBInternational	Biomount
BDH	Formaldehyde
	Sucrose
	Tris
	HCl
	Glycerol
	β -mercaptoethanol
	Na ₂ HPO ₄
	KCl
	MgSO ₄
	Acetone
	Superfrost uncoated glass slides
	Methanol
	MOPS
	MES
	KOH
	RbCl ₂
	CaCl ₂
	MnCl ₂
	NaCl
Bioline	dNTPs

	Taq polymerase, 10x buffer & 50 mM MgCl ₂
Bio-Rad	10x TGS buffer
	Gel Doc™ 2000 imaging system
	Precision plus protein™ standards
	Protein assay dye
	SDS PAGE gel preparation apparatus and electrophoresis system (Mini-PROTEAN II cell)
Bright	B1009DR solid knife
Citifluor Ltd	Glycerol/PBS mounting solution
Clontech	YPD
	SD drop out medium supplements
	SD minimal base media
CLP	50ml Falcon tubes
Corning Incorporated	72cm ² cell culture flask/vented cap
Diatome	2.7mm Diamond Knife
Eppendorf AG	PCR film
	Spectrophotometer cuvette
Fermentas	PageRuler™ Prestained Protein Ladder
FLUKA	PMSF
GIBCO	MEM vitamins
	MEM non-essential amino acids
Hayman	Absolute Ethanol
International Biotechnologies	Bromophenol Blue
Invitrogen™	100bp ladder
	Agarose
	Dnase I
	DMEM with L-Glutamate
	Hind III DNA fragments
	LB broth
	1kb DNA ladder

	One Shot® TOP10 competent cells
	S.O.C. medium
	Superscript™ II Reverse transcriptase
	5x First Strand Buffer
	T4 DNA Ligase
	Trizol™
KPL	Protein A kit
Kontes	Pellet Pestle® Motor Homogeniser
Marvel	5% non-fat powdered milk
MWG	Oligonucleotides
National Diagnostics	37:5:1 Acrylamide/Bis-acrylamide (Protogel)
	Histoclear
New England Biolabs (NEB)	Restriction endonuclease enzymes
NUNC	96-well flat bottom ELISA plates
	Inoculating Loops
PAA	Fetal Calf Serum
Perkin Elmer (PE) Applied Biosystems	BigDye™ cycle-sequencing kit
Pierce	ProFound™ c-Myc Tag IP/C0-IP kit and amplification set
Promega	TNT® Quick Coupled Transcription/Translation system
	Transcend™ Biotin-Lysyl-tRNA
	ProtoBlot® Western Blue® Stabilized Substrate
Qiagen	HotStarTaq™ DNA polymerase
	QIAprep spin miniprep kit
	QIAprep spin maxiprep kit
	QIAquick PCR purification kit
	QIAquick gel extraction kit

Raymond A. Lamb	Optimal Cutting Temperature compound (OCT)
	Heamatoylin staining solution
	Eosin staining solution
Sigma	All other chemicals
The Binding Site	PAP-PEN
USB	Shrimp Alkaline Phosphatase
Whatman	Filter paper (various sizes)

Appendix 2 Media

Media were produced as follows, autoclaved at 121°C for 20 minutes and stored at 4°C.

10X Drop-out (DO) Solution

DO solutions are a mixture of specific amino acids and nucleosides used to supplement SD base to make SD medium, normally missing one or more of the nutrients required by untransformed yeast to grow on SD medium.

L-Adenine hemisulfate salt	200 mg/L
L-Arginine HCl	200 mg/L
L-Histidine HCl monohydrate	200 mg/L
L-Isoleucine	300 mg/L
L-Leucine	1000 mg/L
L-Lysine HCl	300 mg/L
L-Methionine	200 mg/L
L-Phenylalanine	500 mg/L
L-Threonine	2000 mg/L
L-Tryptophan	200 mg/L
L-Tyrosine	300 mg/L
L-Uracil	200 mg/L
L-Valine	1500 mg/L

LB broth and agar (Luria's Broth)

10g/L	Tryptone
5g/L	Yeast extract
10g/L	NaCl
	Double distilled H ₂ O
15g/L	BactoAgar (plates only)

SD medium (Synthetic Drop-out Medium)

26.7g/L	SD Minimal Base
20g/L	Agar (plates only)
100ml/L	Appropriate 10x drop-out solution
12 mM	3-AT (3-amino-1,2,4-triazole) (for pGBK7-USH1C only)

Adjust the pH to 5.8 if necessary

SOC

950ml	Double distilled H ₂ O
20g/L	Tryptone
5g/L	Yeast extract
0.5g/L	NaCl
10ml/L	250mM KCl

Adjust to pH 7 with NaOH. Make up to 1L with double distilled H₂O and autoclave.

Just prior to use, add 5ml sterile 2M MgCl₂ and 20ml sterile 1M glucose.

YPDA (Adenine-supplemented Yeast Peptone Difco)

50 g/L Yeast Peptone Difco

15 ml/L 0.2% adenine hemisulfate (final concentration is 0.003%)

20g/L Agar (plates only)

Adjust the pH to 6.5 if necessary

YT broth

950ml Double distilled H₂O

16g/L Tryptone

10g/L Yeast extract

5g/L NaCl

Adjust to pH 7 with NaOH. Make up to 1L with double distilled H₂O and autoclave.

Appendix 3 Buffers and solutions

Buffers were made up as follows. Solutions were stored at 4°C unless otherwise stated. Solutions were autoclaved 121°C for 20 minutes if stated.

DNA loading buffer

50%	Glycerol
0.05%	Orange G

DEPC water

0.1% DEPC incubated at 37 degrees for 12 hours then autoclaved.

6x Llamelli loading buffer

0.35M	Tris-HCl pH 6.8
10.28%	SDS
36%	Glycerol
5%	β-mercaptoethanol
0.012%	Bromophenol blue

10X LiAc

1 M lithium acetate Autoclave

Adjust to pH 7.5 with dilute acetic acid

1M MES (Morpholino ethane sulfonic acid)

19.5g/100ml MES

Adjust pH to 6.2 using KOH, filter-sterilize and store at 4°C

1M MOPS (3-(N-morpholino) propane sulfonic acid)

11.5 1g/50ml MOPS

Filter (0.22µm) and store at 4°C

50% PEG 3350 (Polyethylene glycol) warm solution to 50°C to help the PEG go into solution.

PBS (Phosphate buffered saline)

137mM	NaCl
2.7mM	KCl
10mM	Na ₂ HPO ₄
1.8mM	KH ₂ PO ₄

Adjust to pH7.4 using HCl

PBS-T

PBS+0.1% TWEEN 20

PEG/LiAc solution (polyethylene glycol/lithium acetate) (Prepare fresh just prior to use)

To prepare 10 ml of solution

8 ml/10ml 50% PEG

1 ml/10ml 10X TE

1 ml/10ml 10X LiAc

Protease inhibitor cocktail for protein extraction from tissue/cells

2mM AEBSF

1mM EDTA

130 μ M Bestatin

14 μ M E-64

1 μ M Leupeptin

0.3 μ M Aprotinin

Protease Inhibitor Solution for protein extraction from yeast

(concentrated) (Prepare solution fresh just prior to use on ice)

0.1 mg/ml Pepstatin A (in DMSO)

0.03 mM Leupeptin

145 mM Benzamidine

0.37 mg/ml Aprotinin

Qiagen DNA preparation buffers

Resuspension Buffer P1 50mMTris-HCl

10mM EDTA

100 μ g/ml RnaseA (store at 4°C)

Lysis Buffer P2 0.2 M NaOH

1%SDS

Neutralization Buffer P3 3.0M Potassium acetate pH5.5

Equilibration Buffer QBT 750mM NaCl
50mM MOPS, pH7.0
15% isopropanol (v/v)
0.15% Triton X-100 (v/v)

Wash Buffer QC 1.0M NaCl
50mM MOPS, pH7.0
15% isopropanol (v/v)

Elution Buffer QF 1.25M NaCl
50mM TrisCl, pH8.5
15% isopropanol (v/v)

The compositions of the remaining buffers used in these kits are not freely available.

RIPA buffer

5ml/100ml	3M NaCl
1ml/100ml	NP-40
0.5g/100ml	sodium deoxycholate
1ml/100ml	10% SDS
2ml/100ml	2.5M Tris pH8

SDS/glycerol stock solution

7.3% w/v SDS
29.1% v/v Glycerol
83.3 mM Tris-base (not pH-adjusted)
Spatula tip-full Bromophenol blue

Deionized H₂O

TBE (Tris-borate buffer) (5x stock)

54g/L Tris base
27.5g/L Boric acid
20ml/L 0.5M EDTA (pH5)

25mM TBS (Tris buffered saline)

3g/L Tris base
8g/L NaCl
0.2g/L KCl

Adjust to pH7.4 using HCl and autoclave.

TCA Buffer (Prepare solution fresh just prior to use on ice)

20 mM Tris-HCl (pH 8)
50 mM Ammonium acetate
2 mM EDTA
50 µl/ml Protease inhibitor solution
100 µl PMSF (100X stock)
Deionized H₂O

TCA-Laemmli loading buffer (Prepare fresh just prior to use)

480 μ l/ml	SDS/glycerol stock solution
400 μ l/ml	Tris/EDTA solution
50 μ l/ml	β -mercaptoethanol
20 μ l/ml	PMSF (stock solution 100X)
20 μ l/ml	Protease inhibitor solution
Deionized H ₂ O	

10X TE buffer pH 7.5 Autoclave

0.1 M Tris-HCl

10 mM EDTA

TFB1

5ml/500ml	MES 1M (pH 6.2)
6.045g/500ml	RbCl ₂
0.735g/500ml	CaCl ₂ . 2H ₂ O
4.94g/500ml	MnCl ₂ . 4H ₂ O

All salts are added as solids. Adjust pH to 5.8 with acetic acid and then filter the solution through a pre-rinsed 0.22 μ m filter. Store at 4°C.

TFB2

1.102g/100ml	CaCl ₂ . 2H ₂ O
0.120g/100ml	RbCl ₂
15ml/100ml	glycerol
1ml/100ml	1M MOPS

Bring the pH to 6.5, filter-sterilize and store at 4°C.

TGS (Running buffer)

25 mM	Tris
192 mM	Glycine
0.1% (w/v)	SDS pH8.3

Transfer buffer

48mM	Tris
39mM	Glycine
20% (v/v)	Methanol
	pH 9.2

Store at 4°C.

Tris/EDTA solution

200 mM	Tris-base (not pH-adjusted)
20 mM	EDTA
	Deionized H ₂ O

X-gal stock solution

Dissolve 5-bromo-4-chloro-3-indolyl- β -D-galactopyranoside in N,N-dimethylformamide (DMF) at a concentration of 20 mg/ml. Store in the dark at -20°C.

Z buffer

16.1 g/L $\text{Na}_2\text{HPO}_4 \cdot 7\text{H}_2\text{O}$

5.50 g/L $\text{NaH}_2\text{PO}_4 \cdot \text{H}_2\text{O}$

0.75 g/L KCl

0.246 g/L $\text{MgSO}_4 \cdot 7\text{H}_2\text{O}$

Double distilled H_2O

Adjust to pH 7.0 and autoclave. Store at room temperature for up to 1 year.

Z buffer/X-gal solution

100 ml/100ml Z buffer

0.27 ml/100ml β -mercaptoethanol

1.67 ml/100ml X-gal stock solution

Appendix 4 Antibiotics

Ampicillin 50mg/ml stock stored at -20°C.

To prepare, filter solution through a 0.2µm syringe filter

Add 1µl stock per 1ml of agar/broth

Kanamycin 10mg/ml stock stored at -20°C.

Add 2.5µl stock per 1ml of agar/broth

Appendix 5 Fixatives and cryopreservation buffers

Dissected tissues and cells were preserved through the use of fixatives. Fixatives function by cross-linking the amino groups of proteins and nucleic acids to each other, thereby rendering degradative enzymes inoperative.

4% Paraformaldehyde (PFA)

The powder is toxic so the solution is made in a fume hood. Make up to 4% using DEPC treated PBS, dissolving on a heated stirring plate at 60°C. Remove any residual cloudiness if necessary, using a drop of dilute NaCl, then aliquot into 10ml portions and freeze at -20°C.

Sucrose/PBS cryopreservation buffer

Make up a 20% sucrose solution in PBS.

Filter-sterilize and store at room temperature.

Appendix 6 Agarose and SDS-PAGE gel recipes

1% DNA agarose gel

1g Agarose/100ml TBE

0.5µl/ml Ethidium bromide

5% SDS-PAGE stacking gel

330µl/2ml 30% acrylamide mix

250µl/2ml 1.5M Tris (pH 6.8)

20µl/2ml 10% SDS

20µl/2ml 10% ammonium persulfate

2µl/2ml TEMED

1.4ml/2ml ddiH₂O

10% SDS-PAGE resolving gel

3.3ml/10ml 30% acrylamide mix

2.5ml/10ml 1.5M Tris (pH 8.8)

100µl/10ml 10% SDS

100µl/10ml 10% ammonium persulfate

4µl/10ml TEMED

4.0ml/10ml ddiH₂O

12% SDS-PAGE resolving gel

4.0ml/10ml 30% acrylamide mix
2.5ml/10ml 1.5M Tris (pH 8.8)
100µl/10ml 10% SDS
100µl/10ml 10% ammonium persulfate
4µl/10ml TEMED
3.3ml/10ml ddiH₂O

15% SDS-PAGE resolving gel

5.0ml/10ml 30% acrylamide mix
2.5ml/10ml 1.5M Tris (pH 8.8)
100µl/10ml 10% SDS
100µl/10ml 10% ammonium persulfate
4µl/10ml TEMED
2.3ml/10ml ddiH₂O

Appendix 7 Antibodies and cell labelling solutions

A list of the antibodies, the host they were raised in and their label ie FITC (and suppliers) used in this research.

Company	Antibody/Label
Affinity BioReagents	Polyclonal rabbit anti-myosin VIIA
Amersham Pharmacia	Goat anti-rabbit IgG-Horse radish peroxidase (HRP) conjugated
Invitrogen	Monoclonal mouse anti-c-Myc alkaline phosphatase (AP) conjugated
Jackson Laboratories	Donkey anti-sheep IgG – Cy3 conjugated
	Donkey anti-goat IgG-FITC conjugated
Kirkegaard and Perry Laboratories (KPL)	Biotinylated goat anti-mouse IgG
	Biotinylated goat anti-rabbit IgG
Molecular Probes	Rhodamine conjugated Phalloidin
Promega	Streptavidin-AP conjugate
Rockland	Donkey anti-goat IgG-Cy5 conjugated
	Goat anti-FITC
Santa Cruz Biotechnology Inc.	Goat anti-mouse IgG – AP conjugated
	Rabbit serum
	Goat serum
	Monoclonal mouse anti-HA
	Goat polyclonal anti-rhodopsin
Serotec	Donkey anti-sheep IgG AP conjugated
Vector Laboratories	Horse serum
	Goat anti-rabbit IgG-FITC conjugated
	Avidin-D conjugated to Rhodamine
Gift from Dr Scanlan, (Ludwig Institute for Cancer Research, NY USA)	Monoclonal mouse anti-harmonin

Gift from Dr Kobayashi, (Hokkaido University Graduate School of Medicine and University Hospital, Japan)	Polyclonal rabbit anti-harmonin
Gift from Dr Arshavsky, (Harvard Medical School and the Massachusetts Eye and Ear Infirmary, MA USA)	Polyclonal sheep anti-phosducin
Gift from Dr Müller, (Scripps Research Institute, CA USA)	Polyclonal rabbit anti-cadherin 23

Appendix 8 Genotype and phenotype details of *E.coli* strains

A variety of *E.coli* strains were used throughout this work. They are documented below alongside their genotype and use in this work.

Strain	Genotype	Company	Function
Max Efficiency DH5 α	F- ϕ 80lacZ Δ M15 Δ (lacZYA-argF) U169 recA1 endA1 hsdR17(rk-, mk+) phoA supE44 λ - thi-1 gyrA96 relA1	Invitrogen	Y2H – Isolation of preys
ElectroMAX TM DH10B TM	F- mcrA .(mrr-hsdRMS-mcrBC) ϕ 80lacZ.M15 .lacX74 recA1 endA1 araD139.(ara, leu)7697 galU galK ϵ - rpsL nupG	Invitrogen	Y2H-library amplification
One Shot [®] TOP10 Chemically Competent <i>E. coli</i> Cells	F- mcrA Δ (mrr-hsdRMS-mcrBC) ϕ 80lacZ Δ M15 Δ lacX74 recA1 araD139 Δ (ara-leu)7697 galU galK rpsL (StrR) endA1 nupG	Invitrogen	Y2H - Propagation of baits TA cloning
KC8	hsdR, leuB600, trpC9830, pyrF::Tn5, hisB463, lacDX74, strA, galU,K	Clontech	Y2H – Isolation of preys

Appendix 9 Genotypes of yeast strains used in the Yeast Two-hybrid screen

All yeast strains were a kind gift from Dr J. Achermann and Dr L. Lin (Institute of Child Health and Great Ormond Street Hospital for Sick Children, London UK) and further information can be obtained from the Yeast Strain Handbook, Clontech. AH109 was used for bait protein expression and sequential co-transformation library screening. Consequently, isolated prey proteins were then expressed in AH109, therefore Y187 was used for bait and control protein expression in yeast mating experiments.

Yeast strain	Genotype	Reporters
AH109	MAT α , trp1-901, leu2-3, 112, ura3-52, his3-200, gal4 Δ , gal80 Δ , LYS2 :: GAL1 _{UAS} -GAL1 _{TATA} -HIS3, MEL1 GAL2 UAS-GAL2 _{TATA} -ADE2, URA3::MEL1 _{UAS} -MEL1 _{TATA} -lacZ	HIS3, ADE2, lacZ, trp1, leu2, MEL1
Y187	MAT α , ura3- 52, his3- 200, ade 2- 101, trp 1- 901, leu 2- 3, 112, gal4 Δ , met-, gal80 Δ , URA3 :: GAL1 _{UAS} .GAL1 _{TATA} .lacZ, MEL1	lacZ, MEL1

Appendix 10 Plasmids used in the Yeast Two-hybrid screen and associated experiments

Prominent features and details of suppliers are shown below.

Name	Function	Features	Suppliers
pGBT7	Y2H – construction of bait fusion protein	<ul style="list-style-type: none"> Expressed in yeast only Tryptophan and kanamycin selective c-myc tagged T7 promoter for <i>in vitro</i> translation 	(Clontech) Donated by Dr J. Achermann And Dr L.Lin
pACT2	Y2H – in which prey library of fusion proteins was produced	<ul style="list-style-type: none"> Expressed in yeast and bacteria Leucine and ampicillin selective HA tagged 	(Clontech) Donated by Dr C. Sung (Tai, A W et al, 1999)
pGADT7	Y2H – in which control fusion proteins were produced	<ul style="list-style-type: none"> Expressed in yeast only Leucine and ampicillin selective HA tagged T7 promoter for <i>in vitro</i> translation 	(Clontech) Donated by Dr J. Achermann And Dr L.Lin
pCL1	Y2H – positive control for β -galactosidase assay	<ul style="list-style-type: none"> Expressed in yeast Endogenous over expression of β-galactosidase assay 	(Clontech) Donated by Dr J. Achermann and Dr L.Lin
pUC19	Positive control vector for bacterial transformation efficiency	<ul style="list-style-type: none"> Expressed in bacteria Ampicillin selective Expresses β-galactosidase allowing blue/white selection 	Invitrogen

Appendix 11 Equipment

A list of the equipment (and suppliers) used in this research is shown below.

Supplier	Equipment
Bio-Rad	Mini Trans-Blot® Electrophoretic Transfer Cell
	Mini-PROTEAN II cell
	Power Pac 200
Bio-Rad Transgenomic™	ChemiDoc, agarose gel transilluminator
Bright	Cryostat (OFT model with 5040 microtome)
Eppendorf	BioPhotometer, Spectrophotometer
Heraeus	Stationary plate incubator
	Hera Cell culture incubator
Hybaid	Agarose gel tanks
Jencons PLC	Biofuge PICO, bench top centrifuge
Jenoptik	Jenoptik ProgRes C14 Imaging Microscope Camera
Leica, Milton Keynes, UK	Confocal Microscope (SP2)
Orion	Orion 410A pH meter
Patterson Scientific	EBA 12 bench top centrifuge
Philip Harris	Laboratory Centrifuge 6K15, Sigma
Reichert	Ultracut E microtome
RMC	UV 6500 Freeze Substitution Polymerization Apparatus
Sorval	Legend RT, Centrifuge
Stuart Scientific	360° Rotator
	Shaking Incubator
TECAN	Genios Multifunction Microplate Reader
Zeiss	Axioplan 2 Imaging Microscope

Appendix 12 Software

A list of the software (and suppliers) and its use in this research is shown below.

Application	Product	Supplier
Capture of confocal microscopy images	Leica confocal software	Leica microsystems
Capture of fluorescent microscopy images	Openlab	Improvision
DNA sequence analysis	Chromas	Technelysium Pty Ltd
ELISA plate reader	XFluor4	TECAN
Hydrophobicity plots	Kyte-Doolittle and Hopp-Woods	Colombia State University http://arbl.cvmbs.colostate.edu/molkit/hydropathy/
Gel image capture	Quantity One 4.4.0.	Bio-Rad Transgenomic™
Primer design	Primer 3	http://frodo.wi.mit.edu/cgi-bin/primer3/primer3_www.cgi
Protein sequence alignments	CLUSTALW	European Bioinformatics Institute http://www.ebi.ac.uk/ClustalWw/
Storage and presentation of images	Photoshop 6.0	Adobe

Appendix 13 List of primers used/ Sequence of oligonucleotide primers

All oligonucleotide primers were synthesized by MWG. Primers used in the construction of the bait and control fusion proteins introduced restriction digest sites (*Sfi*1 and *Xma*1) to the insert sequences (section 2.5.1.2.1).

Name	Oligonucleotide Sequence (5' → 3')	Chapter
Semi-quantitative RT-PCR primers		
USH1BF	GTTCTCCGTGTTGGTCCTGT	2.3.3.2
USH1BR	GAAGCCTGACTCCTCACCAAG	
USH1CF	AAGGAACGGGTCGTGCAACG	
USH1CR	TGGGAGATGAAGAGCCCACAGC	
USH1DF	ACGAGAGTGTACCCGACCAC	
USH1DR	ATGAGACCCGTGTCCTTGTC	
USH1FF	AACCCCGCGTCAATCTTAATG	
USH1FR	TAATGGCAGCAGCAGAAATG	
GapdhF	CCCTTCATTGACCTCAACTA	
GapdhR	TTCTCCATGGTGGTGAAGAC	
Yeast two-hybrid bait and control fusion protein construction and analysis primers		
pGBK7-	CGCCATGGAGGCC GAATTCCGGCATAAGGTG	2.5.1.2.1
USH1CF		
pGBK7-	TCC CCCCGGG CAGCAATTAGAGCAGAGG	
USH1CR		
pGBK7-PDZ1F	CGCCATGGAGGCC CTGAAGCACCAAGGTGGAAT	
pGBK7-PDZ1R	TCC CCCCCGGG GCCAGATTCCGACACAAACT	
pGBK7-PDZ2	GGCCATGGAGGCC AAGGTCTTCATCAGCCTGGTA	
pGBK7-PDZ2R	TCC CCCCCGGG GCAGCTACAATGGAGATGGTC	
pGBK7-PDZ3	GGCCATGGAGGCC AAGGATGTCCGGCTCCTAC	
pGBK7-PDZ3R	TCC CCCCCGGG GCTCATCGTCATACTCCTTGG	

CDH23Y2HF	CGCCATGGAGGCCATCTACATCCTGAGGGACGA	
CDH23Y2HR	TCC CCCCCGGG AATCCTCCAGGACCACCTC	
pGBK7R	GTCACTTAAAATTGTATACACTT	
T7	GTAATACGACTCACTATAGGG	
Y2HCDH23INTE RN	TCGATGAGAACAAAGGAGCAG	
Yeast two-hybrid control fusion protein and prey identity analysis primers		
pACT2FB	GAGATGGTGCACGATGCACAGTTG	5.1.5.1
pACT2R	CTATTCGATGATGAAGATACCCCAC	
phosducin sequencing primers		
cowPHD250	TTCGTAATACCGCAGACAGTG	2.5.5.3.1
cowPHD459	GCCGAATACCCTATGGTCAA	
cowPHD689	GCAGAGCAAAATGGAAGAGG	
cowPHD932	GCAATATGTTAGTAGACAAAGAG	
CowPhosducin sequencingR	TAGGACATGCATCTCCTTTCAAGG	
Primers for production of tagged control proteins for control Co-IP experiments		
T7+HA+mcc2F	AAAATTGTAATACGACTCACTATAGGGCGAGCCGCC ACCATGTACCCATACGATGTTCCAGATTACGCTAGC AGCGGGGACGAGGAAGAGTGG	2.5.6.1.1 .1
MCC2R	AGGGGCCTACAGAAAGGTGTCCCCAAG	
Primers for the examination of <i>Pdc</i> expression in the murine ear		
maPhdF (exon3)	CAAGAAGGAAATCCTCAGACAAA	2.5.7.3
maPhdR (exon4)	TGTTTCAGCTCATACACAAACC	

Appendix 14 Semi-quantitative PCR raw data examining the expression of the USH1 genes during embryonic eye developmental stages and in the adult eye.

The intensity reading for each gene at each developmental stage was normalized to the *Gapdh* intensity of the same stage in that experiment. The average normalized intensity for each developmental stage was calculated from the results of the three experiments.

For example: Exp1: E12.5 *Myo7a* Intensity = 813.5448 Normalised intensity = $813.5448/3062.082 = 0.265684$.

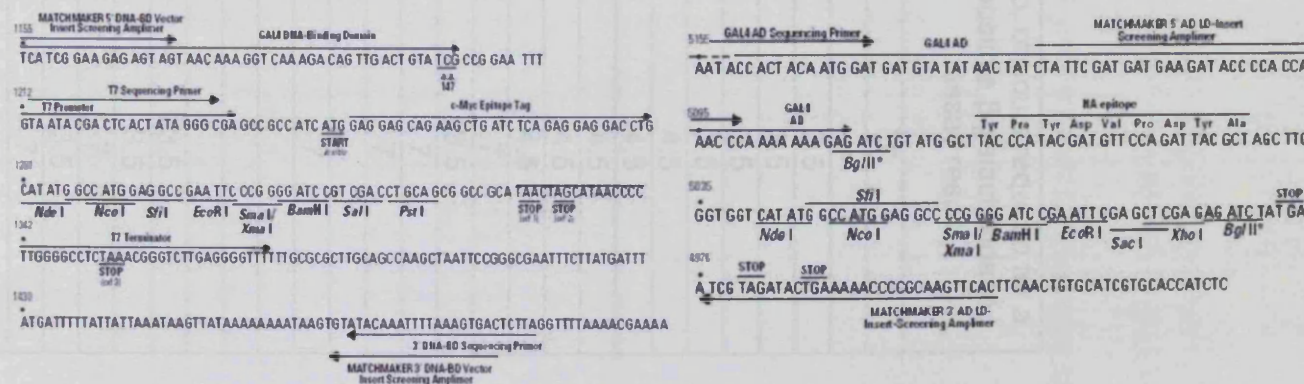
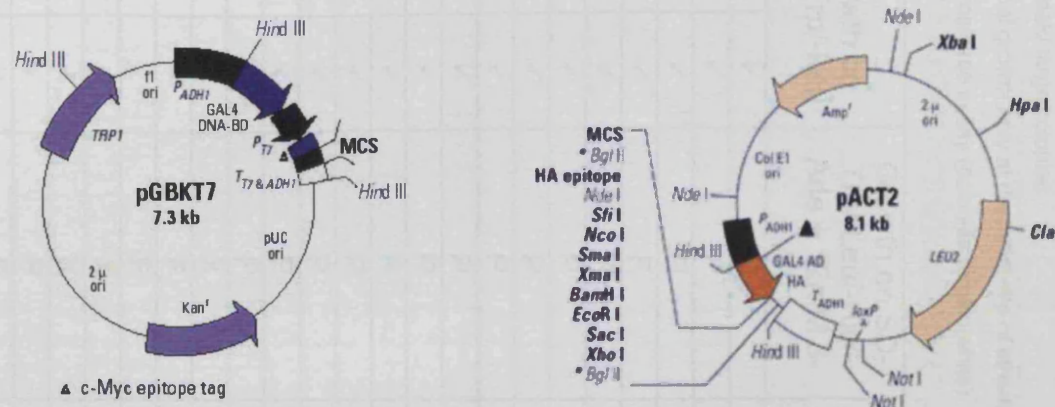
Exp1: E12.5 *Myo7a* Average = $(0.265684+0.305298+0.48794)/3 = 0.352974$

This data is represented graphically in Figure 3.6.

		<i>Myo7a</i>		<i>Ush1c</i>		<i>Cdh23</i>		<i>Pcdh15</i>		<i>Gapdh</i>	
	Developmental stage	Intensity /mm ²	Normalised Intensity to <i>Gapdh</i>	Intensity /mm ²	Normalised Intensity to <i>Gapdh</i>	Intensity /mm ²	Normalised Intensity to <i>Gapdh</i>	Intensity /mm ²	Normalised Intensity to <i>Gapdh</i>	Intensity /mm ²	Normalised Intensity to <i>Gapdh</i>
Exp 1:	E12.5	813.5448	0.265684	1401.374	0.457654	1563.509	0.510603	3395.895	1.109015	3062.082	1
	E14.5	966.7901	0.315062	1479.759	0.482231	1430.273	0.466105	3444.254	1.122431	3068.567	1
	E16.5	1010.201	0.338105	1522.434	0.509545	1734.73	0.580599	3404.465	1.139445	2987.827	1
	E18.5	791.0506	0.260524	1480.054	0.487439	1939.937	0.638897	3410.211	1.123115	3036.386	1
	Adult	799.0613	0.329689	1634.033	0.674194	980.8554	0.404696	3243.234	1.338142	2423.685	1
Exp 2:	E12.5	961.7554	0.305298	1517.722	0.481782	1499.709	0.476065	2622.272	0.832409	3150.223	1
	E14.5	1005.13	0.308016	1382.107	0.423538	1495.236	0.458206	3543.41	1.085856	3263.24	1
	E16.5	1161.5	0.334172	1504.873	0.432964	1829.98	0.526499	3290.468	0.946693	3475.748	1
	E18.5	805.2657	0.260915	1577.881	0.511251	1741.095	0.564134	3166.597	1.026012	3086.314	1
	Adult	728.1427	0.273257	1654.948	0.621067	945.5206	0.354834	3069.72	1.152001	2664.685	1
Exp 3:	E12.5	1472.48	0.48794	1784.697	0.5914	1655.096	0.548454	945.4473	0.313295	3017.751	1
	E14.5	2260.174	0.688197	1610.138	0.490269	1666.708	0.507494	1240.291	0.377655	3284.194	1
	E16.5	1895.066	0.638008	1669.831	0.562179	1411.744	0.475289	1087.795	0.366226	2970.284	1
	E18.5	2047.972	0.676915	2065.437	0.682688	1421.546	0.469863	1155.793	0.382023	3025.45	1
	Adult	1843.661	0.732329	1894.645	0.752581	1019.904	0.405121	1564.548	0.621461	2517.531	1
Average:	E12.5		0.352974		0.510279		0.511707		0.751573		
	E14.5		0.437092		0.465346		0.477268		0.861981		
	E16.5		0.436762		0.501563		0.527463		0.817455		
	E18.5		0.399451		0.560459		0.557631		0.843717		
	Adult		0.445091		0.682614		0.388217		1.037201		

Appendix 15 Yeast Two-hybrid Vector Information

Schematics of the 'bait' (pGBKT7) and 'prey' (pACT2) vectors used in the Yeast Two-hybrid screen, showing the relative positions of the GAL4BD/GAL4AD, the nutritional selection markers, the antibiotic selection markers, details of the ORF, details of the MCS and the position of the T7 promoter (if present). Data is available at <http://www.clontech.com/clontech/>



Appendix 16 Yeast 2 Hybrid Harmonin screening results

The initial colonies resulting from the sequential co-transformation of pGBK7-USH1C(12-8) and pACT2-bovine retinal library plasmids, were each examined for their continued ability to activate the nutritional and colourmetric selection markers.

P = partial growth of streak/ small individual colonies

F = full growth of streak/ large colonies

✗ = no growth/minimal growth only at the initial site of streak

- = negative β galactosidase assay (colonies remain white)

Colony ID #	Growth on SD-Trp/-Leu		Growth on SD-Trp/-Leu/-His/-Ade + 12mM 3-AT	No. of hours required for a positive β galactosidase assay result
1.1	✓	✓	P	7
1.2	✓	✓	P	-
1.3	✓	✓	P	3.5
1.4	✓	✓	F	3.5
1.5	✓	✓	P	3.5
1.6	✓	✓	P	7.5
1.7	✓	✓	P	4.5
1.8	✓	✓	P	4.5
1.9	✓	✓	P	4.5
1.10	✓	✓	P	4.5
1.11	✓	✓	P	4.5
1.12	✓	✓	P	7
1.13	✓	✓	P	3.5
1.14	✓	✓	P	7
1.15	✓	✓	P	7
1.16	✓	✓	✗	
1.17	✓	✓	F	7
1.18	✓	✓	F	-
1.19	✓	✓	✗	
1.20	✓	✓	✗	
1.21	✓	✓	P	3.5
1.22	✓	✓	F	3.5
1.23	✓	✓	F	7
1.24	✓	✓	P	3.5
1.25	✓	✓	F	7
1.26	✓	✓	F	-
1.27	✓	✓	✗	
1.28	✓	✓	✗	
1.29	✓	✓	F	3.5
1.30	✓	✓	F	4.5
1.31	✗			
1.32	✓	✓	P	3.5

1.33	✓	✓	P	5.5
1.34	✓	✓	F	3.5
1.35	✓	✓	F	7
1.36	✓	✓	P	-
1.37	✓	✓	P	3.5
1.38	✓	✓	X	
1.39	✓	✓	P	3.5
1.40	✓	✓	X	
1.41	✓	✓	F	3.5
1.42	✓	✓	P	-
2.1	✓	✓	F	4.5
2.2	✓	✓	P	5.5
2.3	✓	✓	F	5.5
2.5	✓	✓	P	-
2.6	✓	✓	P	-
2.7	✓	✓	P	-
2.8	✓	✓	P	8
2.9	✓	✓	P	-
2.10	✓	✓	X	
2.11	✓	✓	P	4.5
2.12	✓	✓	P	5.5
2.13	✓	✓	X	
2.14	✓	✓	X	
2.15	✓	✓	P	7.5
2.16	✓	✓	P	-
2.17	✓	✓	P	-
2.18	✓	✓	P	5.5
2.19	✓	✓	P	3.5
2.21	✓	✓	P	3.5
2.22	✓	✓	P	-
2.23	✓	✓	P	4.5
2.24	✓	✓	X	
2.25	✓	✓	X	
2.26	✓	✓	X	
2.27	✓	✓	P	4.5
2.28	✓	✓	P	7.5
2.29	✓	✓	X	
2.30	✓	✓	X	
2.31	✓	✓	X	
2.32	✓	✓	F	3.5
2.33	✓	✓	X	
2.34	✓	✓	X	
2.35	✓	✓	P	7.5
2.36	✓	✓	P	7.5
2.37	✓	✓	X	
2.38	✓	✓	X	
2.39	✓	✓	P	4.5
2.41	✓	✓	X	

2.42	✓	✓	P	-
2.43	✓	✓	X	
2.44	✓	✓	P	4.5
3.1	✓	✓	P	5.5
3.2	✓	✓	P	-
3.3	✓	✓	X	
3.4	✓	✓	X	
3.5	✓	✓	P	4.5
3.6	✓	✓	F	4.5
3.7	✓	✓	F	3.5
3.8	✓	✓	X	
3.9	✓	✓	P	3.5
3.10	✓	✓	F	3.5
3.11	✓	✓	X	
3.12	✓	✓	P	5.5
3.13	✓	✓	P	-
3.14	✓	✓	P	4.5
3.15	✓	✓	X	
3.16	✓	✓	P	5.5
3.17	✓	✓	P	7.5
3.18	✓	✓	X	
3.19	✓	✓	P	
3.20	✓	✓	X	
3.21	✓	✓	P	3.5
3.22	✓	✓	X	
3.23	✓	✓	X	
3.24	✓	✓	X	
3.25	✓	✓	X	
3.26	✓	✓	P	4.5
3.27	✓	✓	X	
3.28	✓	✓	X	
3.29	✓	✓	P	4.5
3.30	✓	✓	X	
3.31	✓	✓	X	
3.32	✓	✓	P	5.5
3.33	✓	✓	P	2
3.34	✓	✓	X	
3.35	✓	✓	P	4.5
3.36	✓	✓	P	3.5
3.37	✓	✓	P	5.5
3.38	✓	✓	P	3.5
3.39	✓	✓	X	
3.40	✓	✓	X	
3.41	✓	✓	F	-
3.42	✓	✓	P	5.5
3.43	✓	✓	X	
3.44	✓	✓	P	3.5
3.45	✓	✓	P	5.5

3.46	✓	✓	X	
3.47	✓	✓	P	4.5
3.48	✓	✓	P	4.5
4.1	✓	✓	F	6.5
4.2	✓	✓	P	5.5
4.3	✓	✓	P	3.5
4.4	✓	✓	P	5.5
4.5	✓	✓	P	3.5
4.6	✓	✓	F	-
4.7	✓	✓	P	3.5
4.8	✓	✓	F	7
4.9	✓	✓	X	
4.10	✓	✓	P	3.5
4.11	✓	✓	P	-
4.12	✓	✓	X	
4.13	✓	✓	P	-
4.14	✓	✓	F	3.5
4.15	✓	✓	P	-
4.16	✓	✓	P	-
4.17	✓	✓	P	-
4.18	✓	✓	P	4.5
4.19	✓	✓	X	
4.20	✓	✓	P	5.5
4.21	✓	✓	X	
4.22	✓	✓	X	
4.23	✓	✓	F	3.5
5.1	✓	✓	X	
5.2	✓	✓	P	4.5
5.3	✓	✓	F	-
5.4	✓	✓	P	3.5
5.5	✓	✓	X	
5.6	✓	✓	F	3.5
5.7	✓	✓	P	-
5.8	✓	✓	X	
5.9	✓	✓	X	
5.10	✓	✓	F	3.5
5.11	✓	✓	P	6.5
5.12	✓	✓	X	
5.13	✓	✓	P	-
5.14	✓	✓	P	6.5
5.15	✓	✓	P	-
5.16	✓	✓	X	
5.17	✓	✓	P	2
5.18	✓	✓	F	2
6.1	✓	✓	P	5.5
6.2	✓	✓	X	
6.3	✓	✓	F	3.5
6.4	✓	✓	P	-

6.5	✓	✓	F	3.5
6.6	✓	✓	P	5.5
6.7	✓	✓	X	
6.8	✓	✓	X	
6.9	✓	✓	P	3.5
6.10	✓	✓	X	
6.11	✓	✓	P	3.5
6.12	✓	✓	P	5.5
6.13	✓	✓	P	-
6.14	✓	✓	P	-
6.15	✓	✓	P	3.5
6.16	✓	✓	X	
6.17	✓	✓	X	5.5
6.18	✓	✓	P	3.5
6.19	✓	✓	P	5.5
6.21	✓	✓	P	5.5
6.22	✓	✓	P	3.5
6.23	✓	✓	X	
6.24	✓	✓	X	
6.25	✓	✓	X	
6.26	✓	✓	P	-
6.27	✓	✓	X	
6.28	✓	✓	P	-
6.29	✓	✓	F	2
6.30	✓	✓	P	-
6.31	✓	✓	X	
6.32	✓	✓	F	-
6.33	✓	✓	X	
6.34	✓	✓	F	5.5
7.1	✓	✓	F	4.5
7.2	✓	✓	F	4
7.3	✓	✓	X	
7.4	✓	✓	P	7.5
7.5	✓	✓	P	7.5
7.6	✓	✓	F	5.5
7.7	✓	✓	P	-
7.8	✓	✓	X	
7.9	✓	✓	F	4.5
7.10	✓	✓	P	-
7.11	✓	✓	P	-
7.12	✓	✓	F	3.5
7.13	✓	✓	X	
7.14	✓	✓	F	2
7.15	✓	✓	X	
7.16	✓	✓	X	
7.17	✓	✓	P	-
7.18	✓	✓	X	
7.19	✓	✓	X	

7.20	✓	✓	F	2
7.21	✓	✓	X	
7.22	✓	✓	X	
7.23	✓	✓	P	5.5
7.24	✓	✓	F	4.5
8.1	✓	✓	P	4.5
8.2	✓	✓	X	
8.3	✓	✓	P	5.5
8.4	✓	✓	F	3.5
8.5	✓	✓	X	
8.6	✓	✓	F	2
8.7	✓	✓	F	-
8.8	✓	✓	X	
8.9	✓	✓	X	
8.10	✓	✓	X	5
8.11	✓	✓	X	
8.12	✓	✓	P	5
8.13	✓	✓	P	5
8.14	✓	✓	X	
8.15	✓	✓	F	2
8.16	✓	✓	P	-
8.17	✓	✓	P	5.5
8.18	✓	✓	P	-
8.19	✓	✓	P	-
8.20	✓	✓	P	-
8.21	✓	✓	F	2
8.22	✓	✓	X	
8.23	✓	✓	P	-
8.24	✓	✓	X	
8.25	✓	✓	P	-
8.26	✓	✓	P	4.5
8.27	✓	✓	X	
8.28	✓	✓	F	2
8.29	✓	✓	X	
8.30	✓	✓	X	
8.31	✓	✓	X	
8.32	✓	✓	X	3.5
8.33	✓	✓	P	5.5
8.34	✓	✓	X	5.5
8.35	✓	✓	P	3.5
8.36	✓	✓	X	
9.2	✓	✓	F	-
9.3	✓	✓	F	-
9.4	✓	✓	X	
9.5	✓	✓	F	4.5
9.6	✓	✓	X	
9.7	✓	✓	X	
9.8	✓	✓	X	

9.9	✓	✓	P	5.5
9.10	✓	✓	P	-
9.11	✓	✓	X	
9.12	✓	✓	X	
9.13	✓	✓	P	4.5
9.14	✓	✓	F	4.5
9.15	✓	✓	X	
9.16	✓	✓	P	5.5
9.17	✓	✓	X	
9.18	✓	✓	F	5.5
9.19	✓	✓	X	
9.20	✓	✓	X	
9.21	✓	✓	X	
9.23	✓	✓	P	-
9.24	✓	✓	X	
10.1	✓	✓	P	-
10.2	✓	✓	X	
10.3	✓	✓	P	
10.4	✓	✓	X	
10.5	✓	✓	P	-
10.6	✓	✓	P	-
10.7	✓	✓	P	-
10.8	✓	✓	P	-
10.9	✓	✓	X	
10.10	✓	✓	X	
10.11	✓	✓	X	
10.12	✓	✓	F	-
10.13	✓	✓	X	
10.14	✓	✓	P	4.5
10.15	✓	✓	P	5.5
10.16	✓	✓	X	
10.17	✓	✓	X	
10.18	✓	✓	X	
10.20	✓	✓	X	
10.21	✓	✓	X	
10.22	✓	✓	P	-
10.23	✓	✓	F	5.5
10.24	✓	✓	X	
10.25	✓	✓	F	4.5
10.26	✓	✓	F	-
10.27	✓	✓	X	
10.28	✓	✓	F	4.5
10.29	✓	✓	X	
10.30	✓	✓	X	
10.31	✓	✓	X	
10.32	✓	✓	X	
10.33	✓	✓	X	
10.34	✓	✓	X	

10.35	✓	✓	X	
10.36	✓	✓	X	
10.37	✓	✓	P	3.5
10.38	✓	✓	X	
10.40	✓	✓	X	
10.41	✓	✓	P	3.5
10.42	✓	✓	X	
10.43	✓	✓	X	
10.44	✓	✓	X	

Appendix 17 Calculation of the transformation efficiency of control and bait plasmids into Y187 yeast

Individual transformation efficiencies were calculated for the following, using Equation 5.1. Optimal transformation efficiency is $\geq 1 \times 10^4$ cfu/ μ g.

Strain[plasmid]	Transformation efficiency (cfu/μg DNA)
Y187[pGBT7-USH1C]	1.5×10^4
Y187[pGBT7-PDZ1]	3.4×10^3
Y187[pGBT7-PDZ2]	1.8×10^3
Y187[pGBT7-PDZ3]	2.8×10^3
Y187[pGBT7-Lam]	1.5×10^4
Y187[pGBT7]	2×10^4

Appendix 18 Colony Exclusion Data

Interacting colonies were excluded from further investigation for the following reasons on the basis of sequence and mating analysis.

Failed mating controls	Excluded on basis of sequence analysis	Clones/ Low priority sequenced interactors	No sequence data available	No seq but passed mating	High priority sequenced interactors
2.1	1.1	4.1	1.32	1.5	1.4 <i>1.3 phosducin</i>
2.3	1.6	4.2	1.37	1.14	3.33 <i>1.7 phosducin</i>
2.32	1.8	4.4	2.11	1.21	6.3 <i>1.9 phosducin</i>
4.14	1.10	4.7	2.12	1.24	<i>1.22 NICE 3</i>
4.23	1.11	4.10	3.45	1.29	<i>2.15 Retbindin</i>
5.4	1.12	4.18	4.5	1.30	<i>6.12 TUBB</i>
5.18	1.13	4.20	6.1	1.33	<i>7.1 IK cytokine</i>
					<i>7.23 hypothetical protein</i>
6.9	1.15	5.2	6.17	1.39	<i>8.3 hypothetical protein</i>
6.11	1.17	5.6	7.2	2.19	
6.29	1.23	5.10	7.4	2.23	
7.14	1.25	5.14	8.32	2.36	
8.6	1.34	5.17		3.6	
8.15	1.35	6.5		3.12	
10.25	1.41	6.6		3.14	
10.41	2.2	6.15		3.16	
	2.8	6.18		3.21	
	2.18	6.19		4.3	
	2.21	6.21			
	2.27	6.22		8.1	
	2.28	6.34		8.10	
	2.35	7.5		8.13	
	2.39	7.6		8.34	
	2.44	7.9		8.35	
	3.1	7.12		9.9	
	3.5	7.20		9.14	
	3.7	7.24		9.18	
	3.9	8.4		10.14	
	3.10	8.12			
	3.17	8.17			
	3.26	8.21			
	3.29	8.26			
	3.32	8.28			
	3.35	8.33			
	3.36	9.5			
	3.37	9.13			
	3.38	9.16			
	3.42	10.15			
	3.44	10.23			
	3.47	10.28			
	3.48	10.37			

Appendix 19 Colony identity

The 145 colonies remaining for further analysis from the initial 377 (section 5.1.4.4) are listed below according to their colony ID number. Where possible, each colony was assessed as being a true interactor of harmonin through sequence and mating analysis, the results of which are also listed below.

✓=Activated both nutritional and colourmetric reporter genes during yeast mating analysis

✗=Failure to activated reporter genes mating during yeast mating analysis

- = Not tested

Colony ID #	Mated						Encoded protein (NCBI accession number)	In frame?
	All USH1C	PDZ1	PDZ2	PDZ3	PGBKT7	Lam		
1.1							T complex (BT006969)	NO
1.3	✓	✗	✗	✗	✗	✗	Phosducin (M33529)	YES
1.4	✓	✓ 1 colony	✗	✗	✗	✗		
1.5								
1.6							Pyruvate kinase (BCO23328)	Mitocondrial
1.7	✓	✗	✗	✗	✗	✗	Phosducin (M33529)	YES
1.8							MOB1 (NM_024761)/clones	3'UTR
1.9	✓	✗	✗	✗	✗	✗	Phosducin (M33529)	YES
1.10							S36 (NM_033281)	Ribosomal
1.11	✓	✗	✗	✗	✗	✗	Spectrin (U83867)	NO

1.12							Deltex 3 (NM-178502)	NO
1.13	✓	✗	✗	✗	✗	✗	TAFA 3 (AY325116)	NO
1.14								
1.15							NADH dehydrogenase (AF493542)	Mitochondrial
1.17							NRL (XM_547742)	-
1.21								
1.22	✓	✓ ✗	✗	✗	✗	✗	NICE 3 (NM_138740)	YES
1.23							FTH1 (NM_174062)	NO
1.24								
1.25							Hypothetical proteins (NM_138820)	NO
1.29								
1.30								
1.32							Chr16 clones (AC135782)	
1.33								
1.34							Sec 61 beta (NM_006808)	NO
1.35	✓	✗	✗	✗	✗	✗	MAP2K1 (NM_002755)	-
1.37							Chr 1 clones (AL611962)	
1.39								
1.41	✓	✓	✗	✗	✗	✗	FLJ45246 zinc finger protein (ZNF621) (NM_198484)	Poor blast match
2.1	✓	-	-	-	✗	✓	Pellino 3 alpha (BC025723)	NO
2.2							NADH dehydrogenase (AF493542)	Mitochondrial
2.3	✓	-	-	-	✗	✓	NADH dehydrogenase (AF493542)	Mitochondrial
2.8							Solute carrier (NM_006358)	Mitochondrial
2.11							Clones (AC0107065); MHC class2 (NG_004658)	Mitochondrial
2.12							Clones (AC092496); solute carrier (AY078403)	-
2.15	✓	✗	✗	✗	✗	✗	Retbindin (NM_03429)	YES

2.18	✓	x	x	x	x	x	S antigen (NM_18100); arrestin (BTU08346)	NO
2.19							70kDa heat shock protein (NM_174345)	
2.21							Vector (U29899)	
2.23								
2.27							Vector (U29899)	
2.28							UNQ431 (AY358431)	NO
2.32	✓	-	-	-	x	✓	Zinc finger protein (XM_372751)	YES
2.35							Clones (BC029876); ribosomal protein (U13369)	Ribosomal
2.36								
2.39							ROM1 (NM_174147)	NO
2.44							L9 (AY017376)	Ribosomal
3.1							ATP synthase (NM_174717)	Mitochondrial
3.5	✓	✓	x	x	x	x	FLJ45246 zinc finger protein (ZNF621) (NM_198484)	Poor blast result
3.6								
3.7	✓	x	x	x	x	x	RBM4 (BC032735); Lark (U89505)	NO
3.9							S antigen (BTANTSRI); arrestin (BTU08346)	NO
3.10	✓	✓	x	x	x	x	UNQ431 (AY358431); C type Lectin (XM542117)	x stop and no ATG
3.12								
3.14								
3.16								
3.17							GLUT3 (SHPGLUT3A)	
3.21								
3.26							NADH dehydrogenase (AF493542)	Mitochondrial
3.29							NADH dehydrogenase (AF493542)	Mitochondrial

3.32							Vecto (U29899)r	NO
3.33	✓	✗	✗	✗	✗	✗	Clone (AL713994)	
3.35							CDC10 (NM_001001168)	?
3.36							Opsin (BVOPSA)	NO
3.37							Transducin (NM_181022)	NO
3.38							NADH dehydrogenase (AF493542)	Mitochondrial
3.42							NADH dehydrogenase (AF493542)	Mitochondrial
3.44							Cofilin 1 (NM_005507)	NO
3.45							Mouse chr 2 clones (AL844903)	
3.47							Cytochrome C oxidase (BC0000187)	Mitochondrial
3.48							Cofilin 1 (NM_005507)	NO
4.1	✓	✗	✗	✗	✗	✗	14-3-3 epsilon (AF043735)	NO
4.2							P0 (AB098998)	Ribosomal
4.3								
4.4							P0 (AB098998)	Ribosomal
4.5							Clones (AC114484)	
4.7							Peripherin (NM_001003289)	3'UTR
4.8								
4.10							Peripherin (NM_001003289)	3'UTR
4.14	✓	-	-	-	✗	✓	OS9 (HSU41653)	-
4.18							ATP synthase (NM_175796)	Mitochondrial
4.20							BSMAP (AF186264)	NO
4.23	✓	-	-	-	✗	✓	Clones (AC026701)	
5.2							Hes 4 (NM_021170)	NO
5.4	✓	-	-	-	✗	✓	Cdc42 (AF502289); TRIP10 (NM_004240)	NO
5.6							Cytokine (BC051295); LDH-A (BOVPLDH9)	Mitochondrial

5.10							Ribosomal protein (D50107)	Ribosomal
5.11								
5.14							Vector (U29899)	
5.17	✓	✗	✗	✗	✗	✗	S16 (NM_001020)	Ribosomal
5.18	✓	-		-	✗	✓	S16 (NM_001020)	Ribosomal
6.1							Clones (BC069216)	
6.3	✓	✗	✗	✗	✗	✗	Very CG rich-BLAST failed	
6.5	✓	✓	✗	✗	✗	✗	L11 (NM_000975)	Ribosomal
6.6							NADH dehydrogenase (NM_175783)	Mitochondrial
6.9	✓	-	-	-	✓	✓	EBNA1 (BC009175)	-
6.11	✓	-	-	-	✓	✓	P0 (AB098998)	Ribosomal
6.12	✓	✗	✗	✗	✗	✗	Beta tubulin (TUBB) (NM001003900))	YES
6.15							Beta tubulin (chicken GGCB7TUB!)	?
6.17							Clones (AC069536)	
6.18							S15 (NM_001018)	Ribosomal
6.19							TUBB2 (NM_006088)	NO
6.22							ROM1 (NM_174174)	NO
6.29	✓	-	-	-	✗	✓	Nice 3 (BC008306)	YES
6.34							L11 (NM_000975)	Ribosomal
7.1	✓	✓ 1 colony	✗	✗	✗	✗	IK cytokine (BC051295)	YES
7.2							Chr17 (AC134407)	
7.4							cGMP phosphodiesterase (NM_174421)	Mitochondrial
7.5							NADH dehydrogenase (AF493542)	Mitochondrial
7.6							Ribosomal protein (NM_182538)	Ribosomal
7.9							ATPase (NM_001694); Proteolipid (NM_174149)	Mitochondrial

7.12	✓	✓ 1 small colony	✗	✗	✗	✗	NADH dehydrogenase (NM_005001)	Mitochondrial
7.14	✓	-	-	-	✗	✓	Mitochondrial genome seq (V00654)	Mitochondrial
7.20	✓	✓	✗	✗	✗	✗	UNC119 (NM_005148); HRG4 (U40998)	3'UTR
7.23	✓	✓ 1 colony	✗	✗	✗	✗	C6orf119 – hypothetical protein LOC83640 (NM_031452)	YES
7.24							Mitochondrial seq (V00654)	Mitochondrial
8.1								
8.3	✓	✗	✗	✗	✗	✗	C6orf119 – hypothetical protein LOC83640 (NM_031452)	YES
8.4							NADH dehydrogenase (NM_005001)	Mitochondrial
8.6	✓	-	-	-	✓	✗	NADH dehydrogenase (NM_005001)	Mitochondrial
8.10								
8.12							Mitotic apparatus (BC013023)	-
8.13								
8.15	✓	-	-	-	✗	✓	Ubiquitin D (BC012472)	
8.17							Mitotic apparatus (BC013023)	-
8.21	✓	✓	✗	✗	✗	✗	L10a (BC070216)	Ribosomal
8.26							Hypothetical MGC12972 (BC005064)	NO
8.28	✓	✓	✗	✗	✗	✗	DEAD box family of RNA helicase (NM_020865)	-/Ribosomal
8.32							Ribosomal (NM_001011)	Ribosomal
8.33							Ribosomal (NM_001011)	Ribosomal
8.34								
8.35								
9.5							Vector (U29899)	
9.9								

9.13							KIF3A (BC032599r)	-
9.14								
9.16							SCN2B (Na+ channel) (NM_004588)	3'UTR
9.18								
10.14							Ribosomal protein (NM_001011)	Ribosomal
10.15							Annexin 3 (rat/mouse)(NM_013470)	Mitocondrial
10.23							DEAD box family of RNA helicase (NM_004398)	-/Ribosomal
10.25	✓	✗	✗	✗	✓	✗	MAGE-F1 (AF320910) 1	NO
10.28							HLA-B associated transcript (BC018875)	-
10.37							HLA-B associated transcript (BC018875)	-
10.41	✓	✗	✗	✓	✗	✓	PFDN 5 (AF520958)	-

Appendix 20 Control CO-IP assay

The reliability of the CO-IP/ pull down assay was confirmed using known interactors: the SV40 T antigen (pGADT7-T) and p53 (pGBK7-53) (Clontech) (section 2.5.6.2.1).

No bands were seen in the negative controls that incubated the anti-c-Myc beads with the 'No DNA' lysate or TBS buffer only (Figure A1, lanes 7&8).

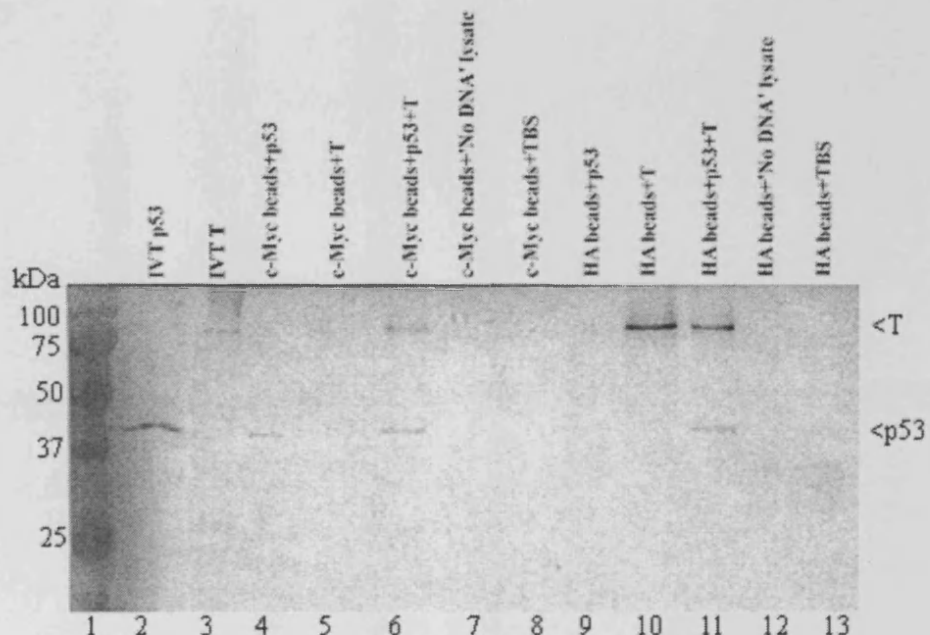
The individual IVT proteins can be seen in lanes 2&3 (denoted with an arrowhead) and the ability of the anti-c-Myc coated beads to bind the c-Myc tagged p53 protein is seen by the presence of a p53 sized band in lane 4. The anti-c-Myc coated beads are unable to bind the HA tagged T protein (no band in lane 5), therefore there is no cross-reactivity between the tags. So the presence of two bands in lane 6, where the beads have been incubated with both p53 and T, proves that the system is able to specifically bind to the tag of one protein and then successfully isolated its binding partner from a protein mix.

This was further confirmed by exchanging the anti-c-Myc coated beads that would bind p53, for anti-HA coated beads that bound T (lane 10). The anti-HA coated beads did not independently bind p53 (lane 9) nor any proteins from the controls (lanes 12&13). p53 could only be detected when incubated with both the anti-HA beads and with T (lane 11).

A further control experiment involving HA tagged MCC2 and c-myc tagged harmonin protein, was also undertaken. In the presence of c-Myc tagged

harmonin, MCC2 could be detected but not when incubated with the anti-c-Myc beads alone (data not shown as HA antibody detection was too poor to capture on the transilluminator).

Figure A1 Interaction of c-Myc tagged p53 with HA tagged SV40 T-antigen by pull down analysis.



The pull down system was checked for specificity using IVT generated p53 (c-myc tagged) and the SV40 T antigen (HA tagged) that are known to interact.

Lane 1, Protein size standards. Lane 2&3 isolated p53 and T respectively. Proteins in lanes 4-8 were pulled out of a reticulocyte lysate mix using anti-c-myc coated beads. Lane 4, p53. Lane 5, no HA tagged T detected. Lane 6, p53 and T detected. Lane 7, no protein was detected from a 'No DNA' IVT lysate control. Lane 8, no protein was detected using TBS buffer.

Proteins in lanes 9-13 were pulled out of a reticulocyte lysate mix using anti-HA coated beads. Lane 9, no c-Myc tagged p53 detected. Lane 10, T. Lane 11, p53 and T detected. Lane 12, no protein was detected from a 'No DNA' IVT lysate control. Lane 13, no protein was detected using TBS buffer.